Investigation into the effects of zinc on the anti-breast cancer properties of disulfiram

A thesis submitted for the degree of
Philosophiae Doctor in Cardiff University

by

Helen L. Wiggins

September 2015

Cardiff School of Pharmacy and Pharmaceutical
Sciences
Cardiff University

Abstract

Breast cancer is the second-leading cause of cancer related death in women and future therapies may involve the strategic use of previously developed drugs, which have established toxicity profiles and are often ex-patent. The alcohol-deterrent disulfiram has been proposed as an anti-cancer agent, based on its capacity to interact with copper-dependent processes. However, little has been done to determine the relationship between this drug and zinc, despite knowledge that disulfiram binds this metal and zinc levels are dysregulated in breast cancer. This thesis investigated whether zinc is an important factor when considering disulfiram efficacy as an anti-breast cancer agent.

Disulfiram was toxic to MCF-7 and BT474 breast cancer cell lines and produced a striking time-dependent biphasic toxicity response between 5-20 µM. Co-incubation of the drug with low-level zinc removed this effect, suggesting that the availability of extracellular zinc significantly influenced disulfiram efficacy. Structure-activity relationship studies with disulfiram analogues revealed the biphasic effect could be influenced by altering the size of chemical groups bound to the drug's nitrogen atom.

Live-cell confocal microscopy using fluorescent endocytic probes and the zinc dye Fluozin-3, coupled with the development of a complimentary Fluozin-3 flow cytometry assay found that disulfiram rapidly increased zinc levels in breast cancer cells specifically in endo-lysosomes. This indicates that the

cytotoxic effects of this drug may be due to acute zinc overload. Further investigation into disulfiram effects on lysosomes suggested that the drug disrupts lysosomal membranes and releases hydrolytic enzymes into the cytosol. Lysosomal membrane permeabilisation has been demonstrated to promote apoptosis and may be a mechanism to explain disulfiram cytotoxicity in breast cancer. This could have important clinical implications in situations of high intracellular zinc as seen in breast tumours, indicating that breast cancer cells may be more susceptible to the zinc ionophore action of disulfiram than non-cancer cells.

Acknowledgements

I would like to begin by thanking my supervisor Prof. Arwyn Jones for giving me the opportunity to undertake this project and for his invaluable guidance, enthusiasm and support which have enabled me to submit this thesis. In addition I am grateful to Dr. Kathryn Taylor and my co-supervisors Dr. Andrew Westwell and Dr. Stephen Hiscox for their helpful feedback and assistance. Antibodies in Chapter 6 were generously provided by Dr. Emyr Lloyd-Jones, to whom I wish to extend my thanks.

I am equally grateful to Cancer Research Wales for their generous funding.

I wish to thank my lab members Jen Wymant, Edd Sayers, Paul Moody, Lin He, Hope Roberts-Dalton and Noura Elissa for their kindness, encouragement and friendship. Their input in lab meetings as well as the contributions from Dr. Pete Watson has been very much appreciated.

Finally I wish extend my gratitude to the friends that I have made in the School of Pharmacy and Pharmaceutical Sciences during my time there and my family for their encouragement.
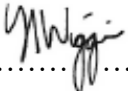
Declaration

This work has not been submitted in substance for any other degree or award at this or any other university or place of learning, nor is being submitted concurrently in candidature for any degree or other award.

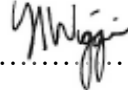Signed ……………………………… (candidate) Date: 10/03/16

STATEMENT 1

This thesis is being submitted in partial fulfillment of the requirements for the degree of PhD.

Signed ……………………………… (candidate) Date: 10/03/16

STATEMENT 2

This thesis is the result of my own independent work/ investigation, except where otherwise stated.

Other sources are acknowledged by explicit references. The views expressed are my own.

Signed ……………………………… (candidate) Date: 10/03/16

STATEMENT 3

I hereby give consent for my thesis, if accepted, to be available for photocopying and for inter-library loan, and for the title and summary to be made available to outside organisations.

Signed ……………………………… (candidate) Date: 10/03/16

Table of Contents

List of Publications, Conference Abstracts and Prizes

Publications

<u>Wiggins, H.L.</u>, Wymant, J.M., Solfa, F., Hiscox, S.E., Taylor, K.M., Westwell, A.D. and Jones, A.T. 2015. Disulfiram-induced cytotoxicity and endo-lysosomal sequestration of zinc in breast cancer cells. *Biochemical Pharmacology*. 93(3), p. 332–342. (Attached as Appendix)

Cilibrasi, V., Tsang, K., Morelli, M., Solfa, F., <u>Wiggins, H.L.</u>, Jones, A.T., and Westwell, A. 2015. Synthesis of substituted carbamo(dithioperoxo)thioates as potential BCA2-inhibitory anticancer agents. *Tetrahedron Letters*. 56(20), p. 2583–2585.

Conference abstracts

<u>Wiggins, H.L.</u>, Hiscox, S., Westwell, A., Taylor, K., and Jones, A. T. 2014. Disulfiram-induced cytotoxicity and endolysosomal sequestration of zinc in breast cancer cell models. EACR-23, Munich, Germany.

<u>Wiggins, H.L.</u>, Westwell, A., Hiscox, S., and Jones, A.T. 2013. Disulfiram increases intracellular zinc in late endosomal compartments of breast cancer models. 9th Zinc-UK meeting, UCL Institute of Opthalmology, London.

<u>Wiggins, H.L.</u>, Westwell, A., Hiscox, S., and Jones, A.T. 2013. Studies on the cytotoxicity of disulfiram in *in vitro* breast cancer models. Joint 34th EORTC-PAMM-BACR Winter Meeting.

Public engagement events

Cancer Research Wales Open Days, Velindre Hospital, Cardiff. January 2011 and 2014.

"Cabinet of Curiosities" Einstein's Garden, Greenman Festival. August 2012.

Prizes

Lecture prize at Cardiff University's School of Pharmacy and Pharmaceutical Sciences Postgraduate Research Day 2014

Oral presentation prize winner at Cardiff University's "Speaking of Science 2013"

Poster presentation prize at Cardiff University's "Speaking of Science 2012"

List of Figures

List of Tables

List of Abbreviations

AI	Aromatase inhibitors
ALDH	Aldehyde dehydrogenase
ANOVA	Analysis of variance
AO	Acridine orange
ATCC	American type culture collection
BCA	Bicinchoninic acid
BCA2	Breast cancer associated gene 2
bFGF	Basic fibroblast growth factor
BOLERO	Breast cancer trials of oral everolimus group
BRCA 1/ 2	Breast cancer gene 1/ 2
BSA	Bovine serum albumin
CSC	Cancer stem cells
$CuCl_2$	Copper chloride
DDC	Diethyldithiocarbamate
DMSO	Dimethyl sulfoxide
DNMT	Dna methyltransferase
DTT	Dithiothreitol
ECM	Extracellular matrix
EDTA	Ethylenediametetra acetic acid
EEA 1	Early endosome antigen 1
EGF	Epidermal growth factor
EGFR	Epidermal growth factor receptor
ER	Oestrogen receptor

ERE	Oestrogen response element
ERK	Extracellular signal regulated kinase
FBS	Foetal bovine serum
FRET	Fluorescence resonance energy transfer
HEPES	Na-4-(2-hydroxyethyl)-1-piperazineethanesulfonic acid
HER2	Human epidermal growth factor receptor 2
HI	Heat inactivated
HRP	Horseradish peroxidase
IF	Immunofluorescence
IκB	Inhibitor of κb
JNK	C-Jun N-terminal kinase
LAMP 1/ 2	Lysosome associated membrane proteins 1/ 2
LC3B	Microtubule associated protein 1 light chain 3 B
LMP	Lysosomal membrane permeabilisation
MAPK	Mitogen activated protein kinase
MDR	Multiple drug resistance
MMPs	Matrix metalloproteinases
mTOR	Mechanistic target of rapamycin
MTT	3-(4,5-dimethylthiazol-2-yl)-2,5-diphenyltetrazolium bromide
NaP	Sodium pyrithione
NCI: SEER	National Cancer Institute: Surveillance, Epidemiology and End Results program
NFκB	Nuclear factor κb
PARP	Poly ADP ribose polymerase
PBS	Phosphate buffered saline
PBST	Phosphate buffered saline tween
PCR	Polymerase chain reaction

PDTC	Pyrollidine dithiocarbamate
PFA	Paraformaldehyde
P-gp	P-glycoprotein
PI	Propidium iodide
PI3K	Phosphoinositide 3-kinase
PNF	Post nuclear fraction
PR	Progesterone receptor
PVDF	Polyvinylidene fluoride
RDFS	Relative disease free survival
RECK	Reversion-inducing cysteine-rich protein with Kazal motifs
ROS	Reactive oxygen species
SDS	Sodium dodecyl sulphate
SFM	Serum free media
SOD	Superoxide dismutase
TPEN	N,N,N′,N′-Tetrakis(2-pyridylmethyl)ethylenediamine
WB	Western blotting
ZIP	Zinc influx transporter
$ZnCl_2$	Zinc chloride
ZnT	Zinc transporter

1. Introduction

1.1. Clinical breast cancer

1.1.1. Breast cancer incidence and mortality worldwide

According to the most recent worldwide statistics, in 2012 there were 1.7 million cases of breast cancer diagnosed, accounting for 25% of all cancers in women (Cancer Research UK 2014a). This makes breast cancer the second most frequently diagnosed form of the disease, narrowly behind lung, and the most prevalent in the female population. Despite the high incidence, mortality due to breast cancer ranks fifth worldwide (Cancer Research UK 2014b). However it is still the second leading cause of cancer death in women, resulting in 522,000 fatalities in 2012.

According to the best available data, incidence of breast cancer is higher in less developed regions and mortality is 1.6 fold greater (Ferlay *et al.,* 2015). These figures are likely to reflect differences in early detection, treatment availability, lifestyle and life expectancy between socio-economic climates. Reducing the mortality gap between world regions remains an ongoing challenge.

1.1.2. Tumour formation and progression to metastatic disease

Breast tumours originate from cells which have acquired genetic abrogation that prime the cell for cancer growth (Figure 1.1). This process, known as initiation, can occur as a result of inherited mutations in genes such as breast
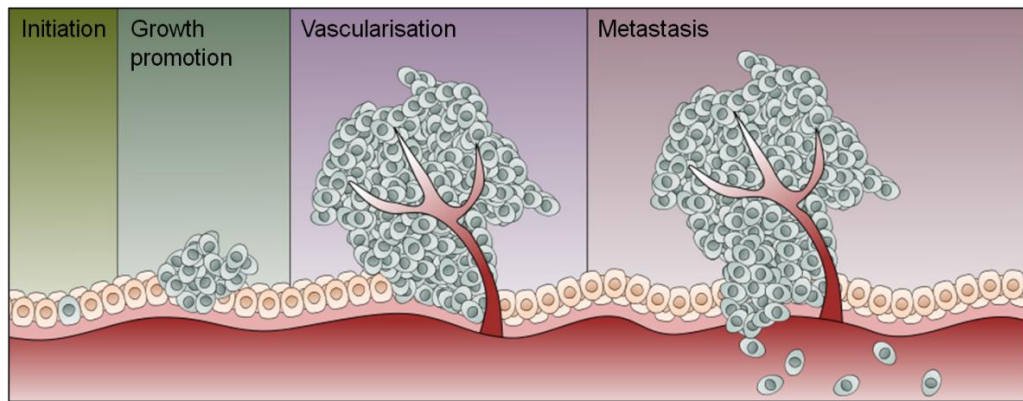
Figure 1.1. Progression of tumours from initiation to metastatic disease.

cancer genes 1 and 2 (BRCA 1 and 2), discussed in Section 1.1.4, or through exposure to environmental carcinogens such benzene (Collins *et al.,* 2015). Initiation results in loss of tumour suppressor genes which further contributes to genomic instability and activation of oncogenes which increase cell replication. Tumour growth then occurs due to increased replication rate and inhibition of cell death processes which may require growth promoting compounds, such as oestrogen which is particularly relevant to the study of breast cancer (Section 1.1.4). Here, oestrogen binds to its cytoplasmic receptor which then translocates to the nucleus and promotes expression of genes associated with replication and restricts those associated with cell death (Frasor *et al.,* 2003; Sadler *et al.,* 2009). At this stage tumour growth is limited by the diffusion barrier which prevents acquisition of nutrients and excretion of waste products. For the developing tumour to grow beyond 1-2 mm^2 in size requires the recruitment of new blood vessels (Muthukkaruppan *et al.,* 1982; Hanahan and Weinberg 2011). This processes known as angiogenesis, involves the secretion of angiogenic factors which stimulate growth and migration of
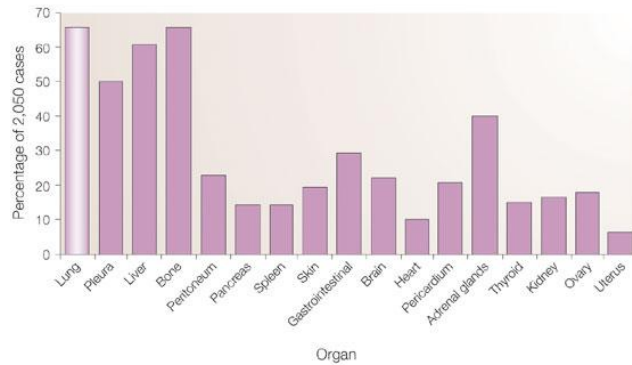
Figure 1.2. Sites of breast cancer metastases. Figure from Weigelt *et al.,* 2005.

endothelial cells lining blood vessels towards the tumour, ultimately resulting in tumour vascularisation (Hillen and Griffioen 2007). In order to become metastatic, a condition associated with significantly worse clinical outcomes as highlighted in Section 1.1.3, the tumour cells must penetrate the basement membrane and invade into either neighbouring tissues or the vasculature where they can form distal tumours. In breast cancer, common sites of local metastases are in surrounding tissues such as lymph nodes and the collar bone (Figure 1.2). However, in advanced disease, distal tumours preferentially occur in organs such as lung, liver and bone (Weigelt *et al.,* 2005).

The tumour initiating cells share many of the properties of stem cells, and are therefore frequently referred to as cancer stem cells (CSC). CSC can be characterised based on expression levels of marker proteins such as aldehyde dehydrogenase (ALDH), low expression of CD24 and high expression of CD44 (Al-Hajj *et al.,* 2003; de Beca *et al.,* 2013). They have the capacity to self renew and may differentiate to form the heterogeneous population of cancer cells observed within a tumour (Hope *et al.,* 2004; Anderson *et al.,*

3

2011). As all cells within the tumour originate from these CSC, it is their properties which govern the clinical nature of the tumour. For example in acquired chemoresistance it is hypothesised that CSC which survive chemotherapy are able to reform tumours with resistant properties (Yu *et al.,* 2007a; Vidal *et al.,* 2014).

1.1.3. Role of the oestrogen receptor and its signalling in breast cancer

An important consideration in the study of breast cancer is the role of oestrogen receptors (ERs) in tumour growth, this is the primary feature for stratifying the disease (Section 1.1.5) and optimising treatment (Section 1.2). Oestrogens are a class of steroid hormones capable of passive diffusion through the cell membrane and binding to cytoplasmic ERs, of which there are two structurally related forms: ERα and ERβ. Of these, ERα is the best characterised, predominately associated with the transcription of growth promoting genes and frequently over-expressed in breast tumours. It is ERα which is responsible for classification of ER^+ disease. In comparison the role of ERβ is less well defined, although it is noted for its tumour suppressor properties and has been associated with favourable properties such as low grade tumours and decreased lymph node involvement (Marotti *et al.,* 2010).

The classical model of ER activity involves its activation by ligand, dissociation of cytoplasmic chaperone proteins and translocation of the ligand-receptor complex to the nucleus. Here it binds to distinct regions of DNA in gene promoter regions, known as oestrogen responsive elements (ERE) and

can alter the expression of oestrogen responsive genes (O'Lone *et al.,* 2004). The activity of ER at ERE is dependent on the binding of nuclear co-regulators which may activate or repress the action of ER primarily through their ability to alter chromatin structure such that gene transcription is promoted or repressed (Green and Carroll, 2007). The distribution of these co-regulators may partially explain why ER antagonists behave differently in certain tissues (Martinkovich *et al.,* 2014).

Extensive study of ER activity, motivated by its importance in the pathology of breast cancer, has identified other mechanisms of action to modulate cell activity outside this classical framework. For example ER activation and nuclear translocation may alter the activity of other transcription factors such as nuclear factor κB (NFκB; Biswas *et al.,* 2005). In addition, ER may be phosphorylated and activated in the absence of ligand by membrane bound receptor tyrosine kinases such as epidermal growth factor receptor (EGFR; Marquez *et al.,* 2001). This observation is particularly relevant to breast cancer due to the over-expression of EGFR in this disease (Section 1.1.5).

1.1.4. Diagnosis and pathology of breast cancer

Breast cancer diagnosis relies upon biopsy of the suspected tumour and pathology reporting to confirm invasive disease. As well as this, pathology reports also include information which may be used to determine prognosis and therapeutic strategies. These factors include apparent differentiation of cancer

Table 1.1. Summary of breast cancer stages and 5 year relative disease free survival. Relative disease free survival (RDFS) is a normalised value which considers death from causes other than cancer. *indicate values for which individual sub-categories were not available. RDFS are obtained from the National Cancer Institute: Surveillance Epidemiology and End Results program (NCI: SEER) database, 2012 statistics (Howlader *et al.,* 1975-2012).

Stage	Description	RDFS
0	Carcinoma in situ	100%
I	Evidence of invasion, tumour size <2 cm and no lymph node involvement	100%
IIA	No tumour in the breast but lymph node positive OR tumour <2 cm and lymph node involvement OR tumour 2-5cm and no lymph node involvement	93%*
IIB	Tumour 2-5 cm and lymph node involvement OR tumour >5cm and no lymph node involvement	93%*
IIIA	No tumour found but gross lymph node involvement or in lymph nodes close to breastbone OR tumour (any size) and lymph node positive with evidence of structure formation	72%*
IIIB	Tumour (any size) and spread to chest wall and/ or skin AND lymph node positive with evidence of structure formation	72%*
IIIC	No tumour found or tumour any size and spread to chest wall and/or skin AND cancer spread to lymph nodes surrounding collarbone AND lymph nodes near breastbone	72%*
IV	Cancer has spread beyond breast and surrounding lymph nodes to other organs	22%

cells, tumour size, extent of lymph node involvement, and presence of therapeutic or diagnostic markers. Tumour size, number and location of positive lymph nodes combine to determine disease stage and the aggression required for treatment. Staging is prognostically ranked 0-IV with stage IV considered incurable. The features and 5 year survival rate of each stage, as determined at initial diagnosis, is shown in Table 1.1.

1.1.5. Molecular sub-types of breast cancer

Pathology reports also include information regarding the presence of therapeutic and diagnostic markers, such as ER, progesterone receptor (PR), human epidermal growth factor receptor 2 (HER2) and EGFR. These are used

Table 1.2. Molecular sub-classification of breast cancer. Table adapted from Holliday and Speirs 2011, frequency and 5 year survival data from O'Brien *et al.,* 2010 where 12% of cases were unclassified.

Sub-type	ER/ PR	HER2	Other molecular features	Frequency	5 year survival
Luminal A	+	-	Ki67 low	54%	91%
Luminal B	+	-	Ki67 high	10%	88%
HER 2[+]	-	+	Ki67 high	6%	74%
Basal-like	-	-	Ki67 high, EGFR[+]	18%	76%

to subcategorise the disease in order to optimise response to certain therapies; for this purpose the most relevant markers are ER, PR and HER2. Sub-categories include: luminal A, luminal B, HER2 over-expressing and basal-like (triple negative). The molecular features, frequency and prognosis of each sub-type are summarised in Table 1.2. Additionally "normal-like" disease is also commonly described, in which many genes associated with non-cancerous epithelial cells are expressed (Sorlie *et al.,* 2001; Liu *et al.,* 2014). This sub-category shares many of the molecular features of basal-like disease. Despite the prevalence of ER, PR and HER2 in distinguishing between sub-types, other molecular features also aid in disease categorisation. For example, relative expression of Ki67, a protein found exclusively in the nucleus of proliferating cells, is an indication of disease aggression which indicates the need for more aggressive treatment (Inwald *et al.,* 2013). This feature partially distinguishes between luminal A and B type tumours.

Although not required for identifying sub-types, there are numerous molecular features which are common to certain sub-categories of breast cancer. Of these EGFR is the best characterised due to the potential for targeted therapies and

its frequent over-expression in difficult to treat and aggressive tumours, such as ER/ PR negative, HER2$^+$ and basal-like (Rimawi *et al.,* 2010). These sub-types generally lack druggable targets and therefore anti-EGFR therapies may improve prognosis. Genetic counselling is also available in order to determine whether an individual carries a mutation which increases their risk of developing cancer. A common genetic test for breast cancer is mutation of tumour suppressor genes BRCA1 and BRCA2, which together provide the most common cause of hereditary breast cancer (Petrucelli *et al.,* 2010). These proteins are involved in preventing chromosomal abnormalities primarily due to their function in DNA double strand break repair (Venkitaraman 2002; Yao *et al.,* 2015). Loss of function mutations in these proteins increases the risk of developing breast cancer before the age of 70 from 12% to 57% with BRCA1 mutation, and 49% with BRCA2 mutation (Howlader *et al.,* 1975-2012; Chen and Parmigiani 2007).

In vitro pre-clinical studies typically use cell lines which model breast cancer sub-categories in order to predict patient response to drugs or aid further disease characterisation. Some common breast cancer lines, the disease they model and information regarding the patient from which they originate are shown in Table 1.3.

Table 1.3. Cellular models of breast cancer sub-types. Patient information and derivation site columns contain data from American Type Culture Collection (ATCC). In the cell line column, typically only the abbreviation preceding the "/" is used to identify these cell lines. *MCF-10A cells derive from a patient with benign masses in the breast tissue.

Cell line/ ATCC Ref.	Classification	Patient info.	Derivation site
MCF-7/ HTB-22	Luminal A	69 year old, Caucasian, female, adenocarcinoma	Pleural effusion metastatic site
T47D/ HTB-133	Luminal A	54 year old, female, ductal carcinoma	Pleural effusion metastatic site
BT-474/ HTB-20	Luminal B	60 year old, Caucasian, female, ductal carcinoma	Mammary duct
MDA-MB-231/ CRM-HTB-26	Basal-like	51 year old, Caucasian female, adenocarcinoma	Pleural effusion metastatic site
SK-BR-3/ HTB-30	HER2$^+$	43 year old, Caucasian, female, adenocarcinoma	Pleural effusion metastatic site
MCF-10A/ CRL-10317	Fibrocystic disease*	36 year old, Caucasian female	Mammary gland

1.2. Current breast cancer therapeutics

Breast cancer treatment typically involves a combination of surgery, radiation and drug therapy. The molecular characteristics of the tumour and stage at diagnosis dictate the nature of drug therapy, which may include chemotherapy and targeted therapeutics. Tumours which have a favourable prognosis, for example <1 cm diameter and hormone receptor positive, may not require chemotherapy and may rely on targeted therapeutics, such as tamoxifen, alone (Tryfonidis *et al.,* 2014). Drug administration can be started before (neo-adjuvant) or after (adjuvant) surgery depending on tumour size, with stage III or large stage II tumours receiving neo-adjuvant treatment. Neo-adjuvant therapies are also used to decrease size of in-operable tumours and enable further treatment options. Wherever possible, targeted therapies against

molecular drivers of the disease are administered which have a more favourable side effect profile than chemotherapy and frequently used in combination (Jackson and Chester 2015).

1.2.1. Tamoxifen

Tamoxifen binds the ER and in breast tissue acts as an antagonist by preventing the binding of co-activators and instead increasing co-repressor binding (Shiau *et al.,* 1998; Kanaujiya *et al.,* 2013). Thus, the drug prevents transcription of oestrogen regulated pro-growth and anti-apoptotic genes, and is frequently used in the treatment of ER^+ disease. The most recent follow up studies show that 5 year tamoxifen treatment can halve recurrence rates (Davies *et al.,* 2011). However there is conflicting evidence suggesting that the benefits of tamoxifen may extend beyond the treatment period; recurrence rates decrease by 32% in the 4 years following cessation of treatment, but there is no benefit in overall survival.

Tamoxifen exhibits partial ER agonist activity in some tissues including bone and uterus, which provides both favourable and adverse off target effects. Studies using tamoxifen as a preventative medicine have shown that it can reduce fracture rate in post-menopausal patients with ER^+ tumours, but also produces a small increase in rates of endometrial cancer and cardiac abnormalities (Fisher *et al.,* 2005). Despite this, the adverse effect profile of tamoxifen is considered favourable as only 0.6% of patients taking tamoxifen die from these combined complications (Davies *et al.,* 2011).

These benefits have led to tamoxifen being used as a preventative medicine in individuals with high risk of developing breast cancer. Here, it has been shown that 5 year treatment can decrease overall breast cancer incidence by 28% and ER^+ incidence by 33% (Cuzick *et al.,* 2015).

1.2.2. Fulvestrant

Fulvestrant (ICI 182, 780, Faslodex^{TM}) is another ER antagonist with a different mechanism of action to tamoxifen, which avoids the partial agonistic effects and may be favourable to some patients. It inhibits receptor dimerisation, up-regulates receptor degradation, and has been shown to inhibit nuclear ER content to a similar extent as tamoxifen (Robertson *et al.,* 2001). Clinically, fulvestrant is equally as effective as tamoxifen at decreasing progression and increasing overall survival in patients with advanced disease (Howell *et al.,* 2004). However this study revealed that time to treatment failure was 2 months longer with tamoxifen, therefore fulvestrant is inferior as a front line treatment. As a second line treatment the drug still has clinical benefit, and advanced disease patients with progression on aromatase inhibitors (AI; Section 1.2.3) have shown partial response or stable disease for an average of 6 months when treated with fulvestrant (Ingle *et al.,* 2006).

1.2.3. Aromatase Inhibitors

Aromatase is responsible for the synthesis of oestrogens in breast cancer tissue thereby encouraging the growth of local ER^+ breast cancer cells (De Mukhopadhyay *et al.,* 2015). Due to this AIs decrease the responsiveness of the tumour to oestrogen by limiting its availability. This strategy is counter-indicated in the treatment of pre-menopausal women because a large proportion of the hormone is still supplied by the ovaries, although there is clinical data indicating benefit of AIs when combined with treatments to reduce ovarian oestrogen supply (Pagani *et al.,* 2014). The AI anastrozole has been shown to decrease recurrence in ER^+ patients by 4.6% compared to tamoxifen in the neo-adjuvant setting (Cuzick *et al.,* 2010). This success has also been noted for letrozole, another example of an AI, which was shown to be more effective than tamoxifen at increasing disease free survival (Regan *et al.,* 2011).

AIs are also associated with less serious side effects than tamoxifen. For example, tamoxifen is associated with a 4 times greater risk of endometrial cancer than anastrozole (Baum *et al.,* 2002; Cuzick *et al.,* 2010). However ER agonistic properties of tamoxifen provide favourable effects in tissues such as bone, where AIs continue to act as an antagonist leading to side effects. For example, several AIs have been associated with an increase in fracture incidence, although this may only be apparent during the treatment period (Baum *et al.,* 2002; Thurlimann *et al.,* 2005; Coombes *et al.,* 2007; Cuzick *et al.,* 2010). The superiority of AIs at decreasing recurrence and increasing

disease free survival, combined with the favourable side effect profile, has supported the advancement of AIs as the first line treatment for post-menopausal ER^+ breast cancer.

1.2.4. Trastuzumab

Trastuzumab (Herceptin^{TM}) is a human-mouse chimeric monoclonal antibody which prevents HER2 signalling leading to cell cycle arrest and cancer cell death. There are several models to explain the exact mode of action of trastuzumab including: inhibition of extracellular domain function, increased internalisation and degradation of receptor in lysosomes, and recruitment of natural killer immune cells to the tumour (Valabrega *et al.,* 2007).

Studies have shown that when given alongside chemotherapy for $HER2^+$ tumours, 1 year adjuvant trastuzumab can increase 10 year disease free survival by 9% compared to chemotherapy alone (Perez *et al.,* 2014). Extending the treatment period to 2 years has no additional benefit in terms of disease free survival and increased incidence of adverse effects, providing evidence that a treatment period of 1 year is optimal (Goldhirsch *et al.,* 2013).

The most severe adverse effect associated with trastuzumab therapy is cardiac toxicity. It has been shown that 9.8% of patients treated with adjuvant trastuzumab experience decreased cardiac output, which represents a 6.9% increase compared to no adjuvant therapy (Procter *et al.,* 2010). This study also

noted an increase of 0.8% in the incidence of more severe congestive heart failure.

1.2.6. Chemotherapies

Chemotherapeutic agents are often given in combination with targeted therapies to treat tumours with less favourable prognosis. These agents have multiple mechanisms of action but all serve to target rapidly dividing cells. As such cancer cells are particularly sensitive to these drugs, however the same is true for cells in tissues such as the lining of the gut, bone marrow and hair follicles which also have high replication rates. Therefore chemotherapeutic drugs are associated with high toxicity and produce symptoms such as nausea, immunosuppression and alopecia. Chemotherapeutic drugs with multiple distinct mechanisms of action are often used as part of a multi-drug regime in order to maximise the response of the tumour to treatment. Table 1.4 describes some examples of the more commonly used chemotherapeutic agents and their mechanisms of action.

Table 1.4. Examples of chemotherapeutic agents and their mechanisms of action.

Chemotherapeutic	Mechanism of Action
Doxorubicin	Intercalates DNA strands inhibiting DNA transcription
5-Fluorouracil	Inhibits production of the nucleoside thymidine
Cyclophosphamide	Forms DNA crosslinks preventing gene transcription
Docetaxel	Stabilises microtubules by inhibiting cell division
Gemcitabine	Inserted into DNA during cell division and prevents DNA synthesis

1.2.7. Future therapeutic strategies

As discussed in Section 1.1.4 breast cancer can be sub-categorised based on the molecular features of an individual's tumour. However, recent genome wide studies have suggested that there may be at least 10 sub-categories of the disease and only a few genes are commonly mutated with many tumours having rare mutations about which little is known (Curtis *et al.,* 2012). Therefore the molecular features of an individual's tumour are unique and the most benefit could be achieved through personalised therapies which target these molecular drivers. For example, this approach is currently the subject of a clinical trial whereby patients undergo whole genome analysis in order to identify their unique oncogenic abnormalities and this information is then used to determine the most appropriate choice of targeted therapy (NCT02299999). Other clinical trials focus on the ability of drugs to target distinct molecular drivers of the disease. Examples of drugs which are currently in, or recently completed, clinical trials investigating their ability to target a specific oncogenic process are described in Table 1.5.

Table 1.5. Examples of future personalised medicine approaches. Some examples of drugs currently in clinical trials for the treatment of cancer due to their ability to inhibit specific oncogenic processes within an individual's tumour.

Drug	Target	Rationale	Clinical Trials Identifier
Gefitinib	EGFR	HER1, or EGFR, as the name implies belongs to the same receptor tyrosine kinase family as HER2, and is thought	NCT00024154 NCT00052169

		to have a prominent role in the pathogenesis of breast cancer and acquired resistance. Gefitinib (Iressa^{TM}) is a small molecule inhibitor which results in decreased kinase activity of the receptor and reduced signalling. When investigated as a front line treatment patients did not respond to gefitinib, despite receptor inhibition (Baselga *et al.,* 2005). However the drug produces clinical benefit in ER$^+$ patients with acquired tamoxifen resistance and ER$^-$ disease, demonstrating that it has potential as a second line treatment and may be beneficial to ER$^-$ patients (Gutteridge *et al.,* 2010). In both cases this produces a favourable outcome as there are limited options to treat these tumours. Additionally, gefitinib may have promise as part of a combined therapy when used alongside anastrozole and current trials focus on its use in combination with other therapeutics for example trastuzumab, docetaxel or tamoxifen (Cristofanilli *et al.,* 2010).	NCT00080743
AZD5363	Akt	The phosphoinositide 3-kinase (PI3K)/ Akt/ mechanistic target of rapamycin (mTOR) signalling network is commonly up-regulated in cancer and meditates cancer cell survival (Liu *et al.,* 2009). Pre-clinical data indicated that breast cancer cells with mutations in PIK3CA, a downstream activator of Akt, were particularly sensitive to the drug (Davies *et al.,* 2012). This led to a Phase I/ II trial which stratified PIK3CA mutation status.	NCT01625286
Everolimus	mTOR	Activation of the PI3K/ Akt/ mTOR pathway also contributes to chemoresistance and targeting the pathway may prolong the sensitivity of tumours to other therapies. The addition of Everolimus to other breast cancer treatment regimes is the focus of the Breast cancer trials of oral Everolimus (BOLERO) group. This group have found that the drug has clinical benefit in trastuzumab resistant	NCT00876395 NCT01698918

		tumours and on-going trials are evaluating the benefit of the drug in the treatment of ER$^+$ disease (Andre *et al.,* 2014).	
Olaparib	Poly ADP ribose polymerase (PARP)	PARP 1 and PARP 2 enzymes are involved in DNA repair processes and their inhibition by Olaparib results in DNA double strand breaks (Rottenberg *et al.,* 2008). In tumours which have defective DNA repair processes these double strand breaks cannot be repaired and this leads to cell death. Due to this Olaparib has been investigated as a therapy in patients with BRCA mutations where it has shown clinical benefit as a monotherapy or in combination with chemotherapies (Dent *et al.,* 2013; Kaufman *et al.,* 2015).	NCT00679783 NCT00494234 NCT02000622

1.2.8. Drug resistance

Resistance to anti-breast cancer therapies remains an ongoing problem and a further driving force for development of future therapies. The mechanisms of tumour resistance are highly diverse and may involve up-regulation of multiple cell survival pathways and molecular switching, defined as the ability of a tumour to alter its molecular profile and so switch between breast cancer sub-types. For example, it has been demonstrated that 26% of ER$^+$ tumours became HER2$^+$ upon generating resistance to endocrine therapy (Lipton *et al.,* 2005). In order to combat resistance and prevent molecular switching, it may be favourable to simultaneously target multiple pathways. In support of this, trastuzumab has been shown to double progression free survival in patients with metastatic disease treated with anastrozole, compared to anastrozole alone (Kaufman *et al.,* 2009). However, to highlight the problem of resistance it

should be noted that disease progression still occurred within 5 months of treatment in the trastuzumab group.

1.2.9. Drug repurposing

One source of future therapies against breast and other types of cancer may be drugs used in the treatment of other diseases. As these drugs most often already have established toxicity profiles, pharmacophore properties, and identified molecular targets, they are likely to progress to clinical trials much quicker than new drug entities. Due to this, and the fact that many are ex-patent, drug development costs are reduced. Examples of this approach include thalidomide for the treatment of acute myeloid leukaemia (Steins *et al.,* 2002), metformin re-purposed as a breast cancer therapy (Jiralerspong *et al.,* 2009) and rapamycin for leukaemia (Sillaber *et al.,* 2008). Multiple studies have proposed that the alcohol deterrent drug, disulfiram may have anti-cancer activity in breast, prostate, and other tumour types. As disulfiram is ex-patent, it would be cheap to administer for healthcare providers, and may be particularly beneficial in countries where cost is a limiting factor in therapeutic options. This thesis focuses on this drug in breast cancer and merits much more detailed discussion that is provided in Section 1.4.

1.2.10. Clinical history of disulfiram

Disulfiram (Antabuse[TM], tetraethylthiuram disulfide, structure shown in Figure 1.3) was first synthesised in 1881 but received little scientific or commercial

interest until the 1920s when it was used as a vulcanising agent in rubber production (Kragh 2008). In this context it was noted that workers exposed to the compound experienced adverse effects upon ingestion of alcohol. The clinical benefit of the compound was first demonstrated as a treatment for scabies in 1942 and during further investigation researchers also noticed
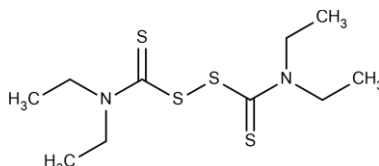
Figure 1.3. Structure of disulfiram.

adverse effects of taking the drug prior to alcohol ingestion (Gordon and Seaton 1942; Jacobsen *et al.,* 1992; Kragh 2008). These observations led to the successful introduction of disulfiram into clinical trials as an alcohol deterrent in 1948 and it was FDA approved for this application in 1951 (Martensen-Larsen, 1948; Chick, 1999).

The first studies demonstrating the anti-cancer potential of disulfiram were described in 1977 and since then it has been proposed to inhibit or stimulate various processes in cancer cells which may provide a mechanism to support its use as a future therapy (Lewison 1977; Cvek 2011). These targets may be exploited to produce favourable outcomes such as altered metal homeostasis, protein turnover, metastasis, angiogenesis, signalling cascades and drug resistance (discussed in Section 1.4 and summarised in Figure 1.4). The ability of disulfiram to bind metal ions, in particular copper, is attributed to many of its anti-cancer properties, however, relatively little has been done to establish

the relationship of this drug with other metals (Sauna *et al.,* 2005; Chen and Dou 2008; Yip *et al.,* 2011; Liu *et al.,* 2013).
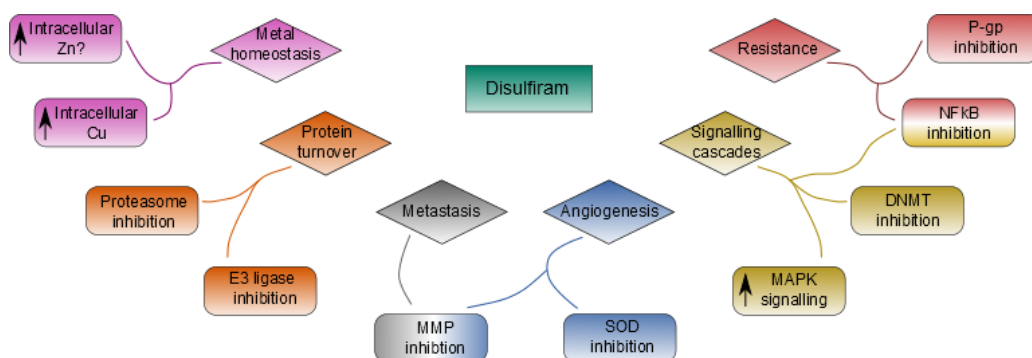
Figure 1.4. Summary of the proposed anti-cancer mechanisms of disulfiram.

1.3. Pharmacokinetic, pharmacodynamic and toxicological properties of disulfiram

Disulfiram is a divalent metal ion chelator with particularly high affinity for copper and zinc (Chung *et al.,* 2000; Brar *et al.,* 2004). Its chemical properties suggest the drug can readily cross biological membranes; small molecular mass of 296.5 and favourable water: lipid solubility with a LogP value of 4.16 (Hann and Keserue 2012). It is still best known as an alcohol deterrent and has been used in this context since the 1950s, during which time it has been established as a relatively safe drug, and is well tolerated in high doses e.g. 800 mg/ day, for prolonged periods (Chick 1999).

Disulfiram is as an irreversible inhibitor of ALDH, preventing effective ethanol metabolism and causing accumulation of acetaldehyde. This substance produces symptoms such as nausea, hypotension and flushing, collectively termed the disulfiram-ethanol reaction and is responsible for the drugs

deterrent properties. The molecular mechanism for this inhibition is through binding cysteine thiol groups in the active site of ALDH, causing ejection of a catalytically essential zinc ion and the irreversible formation of disulfide bonds which permanently deactivate the enzyme, known as the zinc ejection hypothesis (Figure 1.5).
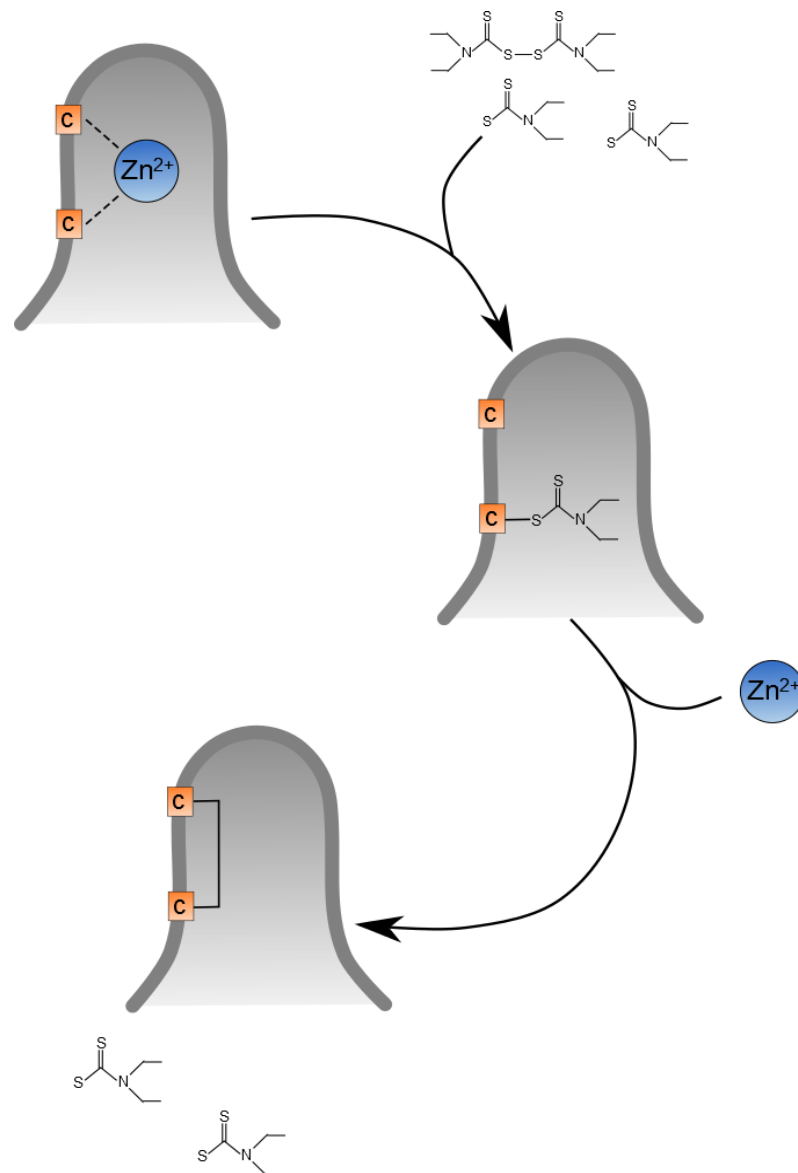
Figure 1.5. Zinc ejection hypothesis of disulfiram. Disulfiram and its metabolites transiently bind cysteine thiol groups in the active site of an enzyme resulting in ejection of a catalytically essential zinc ion and the formation of disulfide bonds.

Disulfiram is considered a "safe drug", with rare and generally mild side effects. A recent meta-analysis revealed that <1% of patients treated with the drug experience adverse events requiring hospitalisation (Skinner *et al.,* 2014). In most cases, side effects are due to severe disulfiram-ethanol reaction, and case studies have documented life threatening cardiac abnormalities due to severe hypotension (Becker and Sugarman 1952; Amuchastegui *et al.,* 2014). However, the risk of cardiac abnormalities is reduced with dose, and is absent upon cessation of ethanol ingestion (Roache *et al.,* 2011). As well as this, there are rare cases of neuropathies resulting in lower limb pain and impaired motor function (Frisoni and Dimonda 1989; Filosto *et al.,* 2008). This may be due to the ability of disulfiram metabolites to accumulate copper into peripheral neuronal cells (Tonkin *et al.,* 2004). In addition severe hepatotoxicity has been associated with disulfiram treatment, although the cause is incompletely understood both the generation of toxic metabolites in this organ and drug-induced hypersensitivity have been implicated (Berlin 1989; Bjornsson *et al.,* 2006). There are also reports that disulfiram may induce or worsen psychosis (Goldstein *et al.,* 1964; Petrakis *et al.,* 2005).

Disulfiram is rapidly and extensively metabolised and its major metabolite, diethyldithiocarbamate (DDC), is generated by reduction of the parent compound across the vulnerable disulphide bond (Figure 1.6A). This process can occur non-enzymatically, however may be enhanced by conjugation to proteins such as albumin or those involved in the glutathione reductase system (Agarwal *et al.,* 1983; Nagendra *et al.,* 1991). The rapid reduction of disulfiram

suggests that under physiological conditions, and in cell culture where disulfiram is added alongside serum, the parent compound has a short half-life. To demonstrate this point, studies have shown that reduction of disulfiram to DDC is complete 4 min after addition of the drug to human blood samples and clinical trials have been unable to detect the parent drug during treatment (Cobby *et al.,* 1977; Johansson 1992; Schweizer *et al.,* 2013). However, *in vivo* DDC is also metabolised rapidly and not found in detectable quantities within4 hr (Stromme and Eldjarn 1966). Further metabolism occurs via glucuronidation, methylation, non-enzymatic digestion, or re-oxidisation into
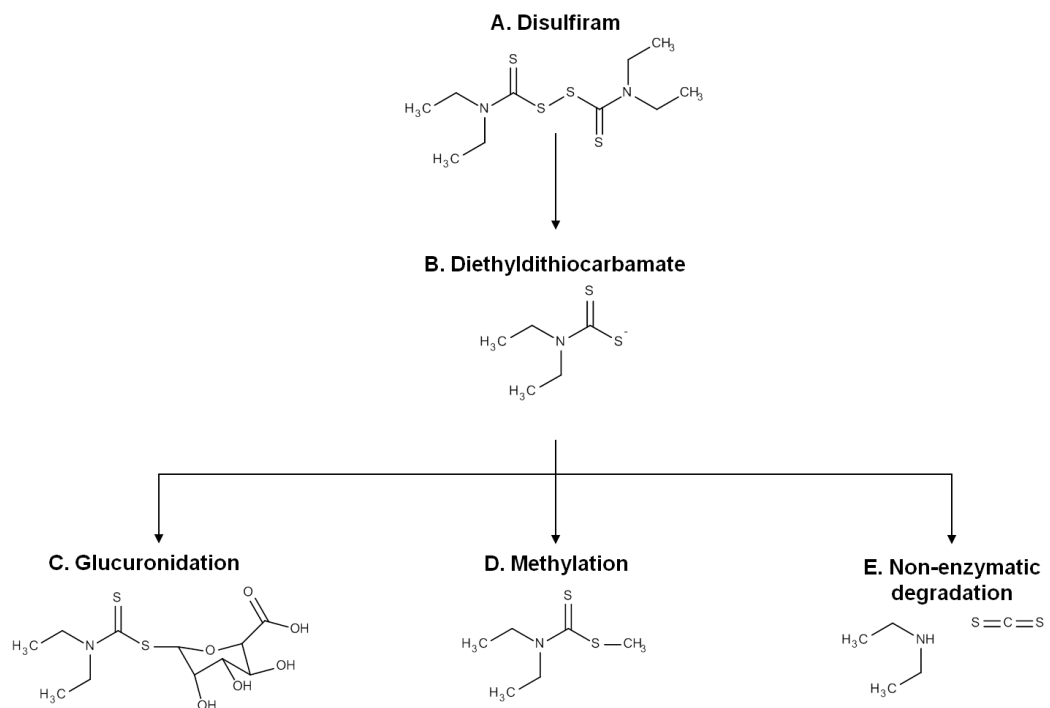
Figure 1.6. Disulfiram's metabolic pathway. Disulfiram is reduced across the vulnerable disulfide bond to form two molecules of diethyldithiocarbamate (B), further metabolism then proceeds via glucuronidation (C), methylation (D) or non-enzymatic degradation (E).

disulfiram (Figure 1.6; Eneanya *et al.,* 1981). Of the disulfiram metabolites, the methylated derivative is thought to be responsible for many of the *in vivo* properties of the parent compound and one clinical study has suggested that the anti-cancer activity of the drug in prostate cancer correlates with S-methyl N,N-diethyldithiocarbamate plasma concentration (Schweizer *et al.,* 2013). Derivatives of the methylated metabolite are thought to be predominately responsible for inhibition of ALDH, and some of the anti-cancer properties of disulfiram may also be attributable to other metabolites (Jin *et al.,* 1994; Loo *et al.,* 2004; Cvek *et al.,* 2008). The metabolic route of disulfiram breakdown is tissue dependent, due to the distribution of the required enzymes, and the parent compound and metabolites are excreted via the renal and biliary routes (Pike *et al.,* 2001).

1.4. Anti-cancer properties of disulfiram

Due to its well established safety profile, disulfiram would make an ideal candidate for repositioning as an anti-cancer therapeutic agent. Research has been conducted to investigate the anti-cancer properties of the drug, which is attributed to its ability to bind cysteine thiol groups and divalent cations, particularly copper (Sauna *et al.,* 2005; Skrott and Cvek 2012). Hence disulfiram is able to interrupt metal dependent processes known to be involved in oncogenic development, and there are multiple mechanisms which may explain its observed anti-cancer properties.

1.4.1. Disulfiram interrupts protein turnover

One of the most widely reported anti-cancer activities of disulfiram is through inhibition of the proteasome. By this mechanism the drug may be able to increase levels of cell cycle regulatory proteins such as cyclin dependent kinase inhibitors and inhibitor of κB (IκB; Hay *et al.,* 1999; Rousseau *et al.,* 1999; Kisselev *et al.,* 2012). Cancer cells have greater sensitivity to proteasome inhibition than non-cancer cells and this has been exploited by development of the proteasome inhibitor bortezomib, currently used in the treatment of multiple myeloma (Drexler *et al.,* 2000; Mateos *et al.,* 2010).

Micromolar concentrations of disulfiram can produce a 75% decrease in proteasome activity and as a consequence inhibit nuclear translocation of transcription factors such as NFκB family members (Lovborg *et al.,* 2006). The NFκB family of transcription factors are responsible for the expression of genes associated with a large variety of biological phenomenon, and in cancer cells are thought to encourage processes such as proliferation, drug resistance, and metastasis (Li *et al.,* 2015). Activation of NFκB is dependent on degradation of its endogenous inhibitor, IκB, by the proteasome and it is partially through stabilisation of IκB upon proteasome inhibition that disulfiram is thought to cause NFκB inhibition; this will be further discussed in Section 1.4.3.

The dependence of metal ions on the proteasomal inhibitory effects of disulfiram has been investigated. Although one study reported that the addition

of copper or zinc had no effect on the drugs proteasome inhibitory activity, others have proposed that inhibition is a result of transporting copper to the proteasome (Chen *et al.,* 2006; Lovborg *et al.,* 2006). The ability of disulfiram to inhibit the proteasome has been reported in myeloma, leukaemic and MDA-MB-231 breast cancer cells and xenographs, and in all cases decreased cancer cell viability was observed upon disulfiram treatment (Rickardson *et al.,* 2007; Lovborg *et al.,* 2006; Chen *et al.,* 2006). Hence proteasome inhibition appears to be independent of cell type and has *in vivo* significance. Additionally, this proteasome inhibitory effect has been demonstrated with DDC and copper co-administration in pancreatic cells and xenographs, suggesting that this mechanism may also contribute to the anti-cancer properties of the metabolite (Han *et al.,* 2013). The hypothesis that disulfiram acts a proteasome inhibitor is the basis of an ongoing clinical trial for the treatment of liver metastases whereby the drug is co-administered with copper (Clinicaltrials.gov; Identifier NCT00742911). As well as copper, other metals have been associated with the ability of disulfiram and its analogues to inhibit the proteasome, such as cadmium and gold (Li *et al.,* 2008; Zhang *et al.,* 2010).

As well as disulfiram itself, studies have investigated the role of its analogues on proteasome inhibition. Here, the most commonly described analogue is pyrollidine dithiocarbamate (PDTC; Figure 1.7A). The structural requirements for proteasome inhibition have been investigated in PDTC analogues via altering the chemical groups attached to the terminal nitrogen (Yu *et al.,* 2007b). This study demonstrated that substitution of the pyrrolidine ring with

larger and more polar groups decreased the ability of the analogues to bind copper and subsequent proteasome inhibition. Some PDTC analogues have been found to inhibit the proteasome without causing ALDH inhibition (Wang *et al.,* 2011), which may prevent off target and potency limiting effects.

As well as inhibiting the proteasome directly, disulfiram has been reported to inhibit an E3 ubiquitin ligase enzyme, termed breast cancer associated gene 2 (BCA2) via disruption of its zinc finger domain (Burger *et al.,* 1998; Burger *et al.,* 2005). Although the exact molecular role of BCA2 in breast cancer has yet to be fully elucidated, studies in our laboratory and others have suggested that it may have a role on EGFR trafficking (Sakane *et al.,* 2007; Wymant 2015). Additional evidence implicating BCA2 in breast cancer is that: (1) its mRNA is enriched in breast cancer cell lines, (2) its transfection into cells increases proliferation, (3) the gene is found in a region of DNA commonly mutated in breast cancer, (4) expression is linked to ER^+ disease and (5) BCA2 mutation
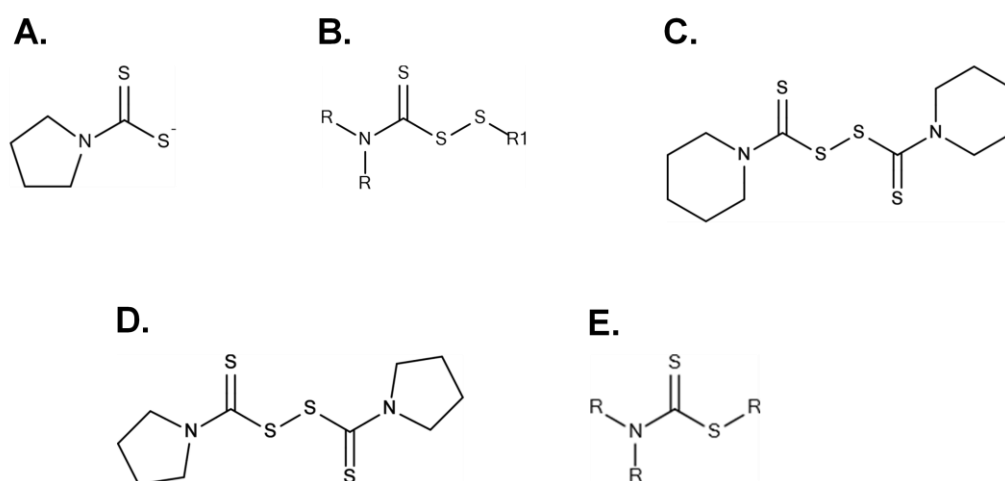
Figure 1.7. Analogues of disulfiram. (A) Pyrollidine dithiocarbamate (PDTC). (B) Base structure of carbamo(diperoxo)thioate analogues. (C) Piperidine analogue of disulfiram. (D) Pyrollidine analogue of disulfiram. (E) Base structure of dithiocarbamate analogues.

results in decreased cell metastasis (Burger *et al.,* 2005; Sakane *et al.,* 2007; Amemiya *et al.,* 2008). Taken together these results suggest that BCA2 may represent a promising therapeutic target in ER$^+$ breast cancer.

The observation that the zinc finger domain of BCA2 was required for activity led to the hypothesis that disulfiram may be a lead drug candidate for BCA2 inhibition (Burger *et al.,* 2005; Brahemi *et al.,* 2010). In a collaborative study between Cardiff University and Barbara Ann Karmanos Cancer Institute, Detroit, several disulfiram analogues were synthesised and their activity investigated in BCA2 positive and negative breast cancer cells (Brahemi *et al.,* 2010). Cell viability studies found that carbamo(dithioperoxo)thioates, piperidine and pyrrolidine analogues were only active in BCA2 positive cells and in ER (BCA2 positive) transfects (Figure 1.7B-D). Interestingly, dithiocarbamate analogues were inactive in all breast cancer cell lines demonstrating that the disulphide bridge was required for activity (Figure 1.7E). Additionally it was observed that analogues which produced growth inhibition also inhibited BCA2 autoubiquitination activity, suggesting a causal link between ubiquitination activity and cell death. Zinc supplementation with disulfiram analogues was shown to inhibit cell death and the authors suggested that these analogues were operating via the zinc ejection hypothesis (Figure 1.5).

1.4.2. Disulfiram inhibits proteins associated with angiogenesis, metastasis and resistance

Angiogenesis, metastasis and resistance are critical events leading to development of more advanced and difficult to treat disease states. Hence restricting these processes, and preventing disease progression, may provide a favourable outcome in breast cancer. Several studies have been conducted to investigate the effects of disulfiram in this regard.

The mechanism of angiogenesis involves hypoxia, followed by release of growth factors and formation of new blood vessels. During this process reactive oxygen species (ROS) are generated which are toxic in high quantities, and require detoxification by enzymes such as superoxide dismutase (SOD; Craige *et al.,* 2015). Disulfiram has been shown to inhibit SOD activity and thereby decrease new vascular growth in mice injected with basic fibroblast growth factor (bFGF) beads (Marikovsky *et al.,* 2002). However, the ability of the drug to inhibit angiogenesis *in vivo* has also been attributed to inhibition of matrix metalloproteinases (MMPs; Shiah *et al.,* 2003). MMP enzymes are responsible for degradation of extracellular matrix (ECM) allowing for migration of endothelial cells towards the tumour, and all MMPs contain a catalytically essential zinc ion. This study noted that addition of zinc abrogated MMP inhibition, suggesting that the drug was able to eject zinc from the enzymes active site.

The migration of cells is not only essential for angiogenesis but also for the progression to metastatic disease which has a significantly worse prognosis. To emphasise the link between angiogenesis and metastasis, disulfiram induced inhibition of MMPs has been associated with both processes in endothelial cells (Shiah *et al.,* 2003). Inhibition of MMP activity has also been noted in the context of breast cancer (Cho *et al.,* 2007). However, it is unclear whether this inhibition occurs at the protein or transcriptional level, as this study noted a decrease in both MMP expression and activity upon disulfiram treatment. As well as this, the drug may alter expression levels of an endogenous MMP inhibitor called reversion-inducing cysteine-rich protein with Kazal motifs (RECK; Murai *et al.,* 2010). In this context, disulfiram was shown to decrease lung metastases following inoculation of fibrosarcoma cells in mice, this may also be relevant to breast cancer as the lung is a common site for breast cancer metastases. These reports demonstrate three potential mechanisms of inhibition of MMP: at the protein level, transcriptional level or up-regulation of endogenous MMP inhibitors.

As mentioned in Section 1.2.8, an ongoing problem in cancer therapy is the eventual development of drug resistance. Although the issue of resistance is complex, one protein family involved are multiple drug resistance (MDR) efflux pumps, responsible for ejection of cytotoxins from the cell. Resistant cancer cells are able to up-regulate MDR family members, including P-glycoprotein (P-gp), and prevent drug access to intracellular targets. For example, chemoresistance of cancer cells to doxorubicin may be a result of

P-gp over-expression and inhibition of this efflux pump has been proposed to re-sensitise resistant cells (Umsumarng *et al.,* 2015). Disulfiram and its metabolites are able to interact with P-gp and other MDR family members at both the ATP and substrate binding sites, and cause irreversible inhibition (Loo *et al.,* 2004; Sauna *et al.,* 2004). However as will be discussed in Section 1.4.3, the drug is also able to activate Jun N-terminal kinase (JNK) signalling, one consequence of which is down-regulation of MDR proteins. This effect has been attributed to the re-sensitisation of doxorubicin resistant leukemic cells upon disulfiram and copper co-administration (Xu *et al.,* 2011).

One potential therapeutic strategy to limit acquired resistance is through co-administration of disulfiram with other chemotherapeutic agents, here disulfiram may inhibit the causes of resistance and increase sensitivity to the chemotherapeutic. To this effect, it has been suggested that encapsulation of disulfiram and doxorubicin within micelles may re-sensitise doxorubicin resistant MCF-7 cells (Duan *et al.,* 2013). In this study, the micelle was manufactured to allow disulfiram release prior to doxorubicin. Encapsulation of both agents increased lysosomal doxorubicin accumulation, ultimately resulting in reduced tumour size *in vivo* and cell death *in vitro*.

It has also been suggested that resistance may be acquired through replication of CSC with resistant properties. Disulfiram in combination with copper has been shown to target cells which express CSC markers, such as ALDH, Sox2 and Nanog, and increase sensitivity of chemotherapy drugs in resistant

MDA-MB-231 cells (Liu *et al.,* 2013). This effect has also been noted in glioblastoma CSC, suggesting that it is a common effect and occurs irrespective of tumour type (Hothi *et al.,* 2012). Interestingly ALDH is a functional marker of breast CSC suggesting that this effect mirrors the alcohol deterrent properties of the drug. To demonstrate this, the ALDH positive population of T47D and MDA-MB-231 cell lines have been shown to decrease upon disulfiram and copper treatment (Yip *et al.,* 2011). This finding is particularly important given the fact that knockdown of ALDH can increase the sensitivity of resistant ovarian cancer cells to docetaxel and cisplatin (Landen *et al.,* 2010). Taken together these observations provide a potential therapeutic strategy for disulfiram in the targeting of CSC, with implications in restoring chemo-sensitivity, and directly relates to its well established ALDH inhibitory activity. Another potential mechanism of resistance is through up-regulation of NFκB signalling, the potential of disulfiram to interfere with this process will be further discussed in Section 1.4.3.

1.4.3. Disulfiram can alter gene transcription and signalling cascades

A common feature of cancer cells is inappropriate induction of signalling cascades and activation of transcription factors leading to cancer cell proliferation. This process is highly complex and disulfiram has been implicated to interfere at various stages and in multiple tumour types.

One of the processes involved in regulating gene transcription is demethylation of histones which inhibits tumour suppressor transcription. One histone

demethylase, JMJD2A, contains a catalytically essential zinc ion and disulfiram has been shown to bind this enzyme and release zinc (Sekirnik *et al.,* 2009). Although the biological significance of this has yet to be determined it is likely that such inhibition will restore expression of tumour suppressors. Additionally, methylation of cytosine bases in promoter regions silences gene transcription and is viewed as an oncogenic phenomenon, particularly noted in prostate cancers (Jones and Baylin 2007). The ability of disulfiram to reduce the methylation status of DNA was first identified in 1979 however has only recently been attributed to its inhibitory effect on DNA methyltransferase 1 (DNMT1), due to its interaction with the proteins cysteine thiol groups (Swenberg *et al.,* 1979; Lin *et al.,* 2011). Although it is likely that through this mechanism disulfiram may restore the expression of multiple tumour suppressors, one which has particular relevance in breast cancer is ER-ß (Sharma *et al.,* 2015). Here both disulfiram and a novel analogue were capable of restoring expression of ERß in prostate cancer cells to levels comparable with non-cancerous cell lines. This affect was able to decrease the viability of prostate cancer cells *in vitro* and in mouse xenographs. The hypothesis that disulfiram can restore expression of tumour suppressors has led to progression of the drug into a Phase II clinical trial, which investigated the ability of disulfiram to inhibit DNMT1 activity in patients with non-metastatic, recurrent prostate cancer (Schweizer *et al.,* 2013). However, only 20-33% of patients showed decreased demethylation activity with daily 250-500 mg oral doses and there was unacceptable toxicity in the high dose cohort. The relevance of DNA methylation in breast cancer is not as well characterised as in prostate, however

increased DNA methylation has been demonstrated in HER2$^+$ breast cancers and decreased expression of ERß is also a feature of breast cancer cells (Fiegl *et al.,* 2006; Omoto and Iwase, 2015). There is also *in vivo* and *in vitro* evidence to suggest that DNMT inhibitors may increase apoptosis in HER2$^+$ (MCF-7) and HER2$^-$ (MDA-MB-231) breast cancer cells (Billam *et al.,* 2010; Chen *et al.,* 2012). Therefore there may be value in further investigation of disulfiram induced DNMT inhibition in certain types of breast cancer.

As previously discussed in Section 1.4.1, the transcription factor NFκB is constitutively over-expressed in many types of cancer including breast and induces the transcription of pro-cancerous genes, including those associated with resistance (Gershtein *et al.,* 2010). As previously discussed, stabilisation of IκB by disulfiram induced proteasome inhibition has been proposed as a mechanism by which the drug inhibits NFκB. As NFκB is associated with chemoresistance, its inhibition would restore sensitivity to drug resistant cancer cells. To this effect studies have demonstrated that the drug alone, and in combination with copper, is able to decrease NFκB DNA binding activity in response to chemotherapeutic agents such as 5-Fluorouracil and gemcitabine in drug resistant colon cancer cell lines (Wang *et al.,* 2003; Guo *et al.,* 2010). Similarly, the inhibitory action of disulfiram and copper on NFκB DNA binding activity has been noted in MCF-7, MDA-MB-231 and T47D breast cancer cells (Yip *et al.,* 2011). The NFκB pathway has also been implicated in survival of breast CSC, and disulfiram induced inhibition may be a contributing factor in breast CSC death (Liu *et al.,* 2010). Taken together this

supports the view that disulfiram targeting of NFκB could provide an effective anti-resistance mechanism with favourable clinical implications.

Cross talk between the NFκB and JNK- and p38-mitogen activated protein kinase (MAPK) pathway is a major obstacle in anti-cancer therapy. Both are activated in response to ROS with competing effects; whilst the MAPK pathway induces cell death, the NFκB pathway mediates survival (McCubrey *et al.,* 2006; Nakano *et al.,* 2006). Therefore, inhibition of NFκB alone may not be sufficient to induce cancer cell death, and a more favourable outcome may be achieved through also inducing the MAPK pathway. The ability of disulfiram to also stimulate MAPK signalling has been demonstrated in breast CSC and doxorubicin resistant leukaemic cells, where it was attributed to CSC death and re-sensitisation effects (Xu *et al.,* 2011; Yip *et al.,* 2011). Both induction of JNK signalling and inhibition of NFκB activity are properties that disulfiram shares with its PDTC analogue (Chung *et al.,* 2000). This dual hit approach of disulfiram provides a powerful potential anti-cancer mechanism, and may restrict cross talk between these two pathways.

1.4.4. Intracellular metal ion homeostasis and redox affects of disulfiram

The widely reported synergistic effect of divalent metal ions on disulfiram toxicity may be a result of altered intracellular metal homeostasis and associated oxidative damage. Oxidative damage may be described as the detrimental effect of highly reactive oxygen species on the chemical composition of proteins, lipids and DNA resulting in their loss of function.

This effect is thought to contribute to the neurotoxicity of disulfiram at high concentrations, whereby DDC is able to increase copper levels and induce oxidative toxicity in neurones (Tonkin *et al.,* 2004). It has also been demonstrated that anti-oxidants, as well as zinc and copper chelators, can abrogate the cytotoxic effects of PDTC in neuronal cells (Chung *et al.,* 2000). This may also contribute to cancer cell death, as copper and zinc are dysregulated in many malignancies and it has been observed that cancer cells are under increased oxidative stress than non-cancer cells (Gupta *et al.,* 1991; Trachootham *et al.,* 2006). Taken together this could provide a therapeutic strategy whereby disulfiram increases oxidative damage though further dysregulation of metal ions. This theory has been applied to copper where it has been shown that co-administration with disulfiram increases ROS production and decreases viability in MCF-7, T47D and MDA-MB-231 cells (Yip *et al.,* 2011). Additionally it has been shown that disulfiram is able to increase copper ions in melanoma cells (Cen *et al.,* 2004). However there is conflicting evidence in the context of this cancer, as it has also been noted that disulfiram and copper were unable to increase fluorescence of a redox sensitive probe and addition of anti-oxidants did not affect toxicity (Brar *et al.,* 2004). Taken together, these studies suggest that the ability of disulfiram to increase oxidative damage is cancer type specific and melanoma cells may be able to tolerate a higher level of copper compared to other tumour types. Not only would oxidative damage contribute to disulfiram cytotoxicity though events such as lipid peroxidation, but also may explain some of the drug's previously reported anti-cancer effects. To demonstrate this, the ability of disulfiram

analogues to inhibit the proteasome has been attributed to ROS production (Zhang *et al.,* 2010).

Many studies investigating the cytotoxic properties of disulfiram and copper focus on the ability of the drug to form a copper complex, capable of inhibiting the proteasome and inducing oxidative damage (Chen *et al.,* 2006; Tardito *et al.,* 2011; Han *et al.,* 2013; Allensworth *et al.,* 2015; Figure 1.8). However,
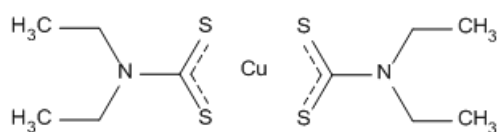
Figure 1.8. Disulfiram-copper complex.

more recently the mechanism explaining disulfiram induced generation of ROS has been suggested to be a result of the reaction between the drug and copper, opposing the idea of this complex being the active form of disulfiram (Lewis *et al.,* 2014). This has led to a new proposal regarding the kinetics of the disulfiram-copper anti-cancer properties which has been hypothesised as a two phase response: rapid cell death caused by a reaction between disulfiram and copper leading to generation of ROS followed by the formation of the disulfiram-copper complex which has intrinsic cytotoxicity (Tawari *et al.,* 2015).

Despite knowledge that disulfiram is also able to bind zinc, relatively little has been done to investigate its role in this paradigm beyond the zinc ejection hypothesis. However, PDTC is able increase intracellular zinc levels and

disulfiram and zinc co-incubation increases oxidative damage (Kim *et al.,* 1999; Pozza *et al.,* 2011). These observations suggest that the relationship between disulfiram and zinc is similar to copper with respect to the ability of these complexes to increase metal dependent toxicity. This may be particularly relevant to the study of disulfiram in the context of breast cancer as zinc is known to be dysregulated in this disease (discussed in Section 1.5). However beyond its synergistic effect, the influence of zinc on the toxicity of disulfiram in breast cancer has yet to be fully elucidated. Interestingly, there is some evidence to suggest that disulfiram-zinc complexes do not inhibit the proteasome but can still induce apoptosis, suggesting that zinc must enhance disulfiram toxicity through separate mechanisms to copper (Li *et al.,* 2008). To support the zinc synergistic effects on disulfiram, a case study has demonstrated remission in a patient with stage IV liver metastasis treated with disulfiram and zinc (Brar *et al.,* 2004).

1.4.5. Disulfiram clinical trials

The extensive literature surrounding the anti-cancer properties of disulfiram in *in vivo* and *in vitro* models have led to its progression into clinical trials. For example it is currently being investigated as a standalone agent for the treatment of prostate cancer (ClinicalTrials.gov identifier: NCT01118741), melanoma (NCT00256230) and with copper co-administration for hepatic metastases (NCT00742911). Clinical trials are also being conducted where the drug is given alongside chemotherapy in non-small cell lung cancer (NCT00312819) and glioblastoma (NCT01907165). Data from two of these

trials have been published, one of which reported that the drug was able to increase survival in patients with advanced lung cancer when used in combination with chemotherapy (Nechushtan *et al.,* 2015). However the other trial noted safety concerns and a lack of efficacy as discussed in Section 1.4.3 (Schweizer *et al.,* 2013). This is consistent with a historical clinical trial in which the addition of disulfiram increased the toxicity of cisplatin chemotherapy in cisplatin sensitive malignancies, but produced no benefit in terms of survival or response rate (Verma *et al.,* 1990). These concerning results may imply that the favourable side effect profile of the drug when used as an alcohol deterrent is not reproduced in its anti-cancer setting. Despite this, a clinical trial investigating the effect of adjuvant DDC in breast cancer noted its good tolerability with mild nausea being the biggest complaint (Dufour *et al.,* 1993). The results of this trial demonstrated that the addition of DDC increased the survival of patients by 26% compared to chemotherapy alone and indicate the potential of the drug as an anti-breast cancer therapeutic.

1.5. Zinc in breast cancer biology

With the sole exception of iron, zinc is the most abundant metal in eukaryotic systems. The approximate concentration of intracellular zinc is estimated to be between 0.1-0.5 mM, although less than 0.001% of this is available in its unbound form (Eide 2006). Dysregulation of zinc is implicated in conditions such as alopecia, immunodeficiency, and impaired childhood development as well as various malignancies including breast (Maret and Sandstead 2006).

Zinc has been implicated in oncogenic processes such as caspase and phosphatase inhibition, which may result in pro-survival events (Kim *et al.,* 2006; Velazquez-Delgado and Hardy 2012). In support of the pro-oncogenic properties of this metal, over-expression of zinc influx transporters (ZIPs) increase breast cancer cell invasiveness and is associated with tamoxifen resistance (Kagara *et al.,* 2007; Taylor *et al.,* 2008). Taken together this would indicate that zinc promotes survival, however at higher concentrations it is also toxic to cancer cells (Bozym *et al.,* 2010). This property may be exploited as the basis for a novel cancer therapy whereby drugs which increase intracellular zinc will target cancer cells, and induce zinc dependent toxicity. The selectivity for this effect is based on the fact that breast cancer cells have higher zinc levels than non-cancer cells and therefore will be less able to tolerate changes in zinc levels (Rizk and Skypeck 1984; Gupta *et al.,* 1991).

Due the complex relationship between intracellular zinc levels and cell viability, intracellular levels of this metal are maintained within tight homeostatic control. Regulation may be achieved through expression of metal binding proteins, such as metallothionein, or sequestration of the ion into intracellular pools including lysosomes (Colvin *et al.,* 2008; Kukic *et al.,* 2014). As an interesting note, the release of zinc from intracellular stores, including the endoplasmic reticulum, in response to extracellular stimuli has been implicated as a signalling event (Yamasaki *et al.,* 2007). Therefore the subcellular location of zinc is a critical cellular feature which determines not only zinc buffering capacity but also signalling processes.

1.6. Hypothesis and aims

The current literature surrounding the anti-cancer properties of disulfiram predominantly focus on its interaction with copper, however little has been done to investigate the role of zinc in this regard. Despite this, there is evidence that breast cancer cells may be predisposed to the toxic effects of this metal due to zinc accumulation in breast cancer cells compared to non-cancerous cells. Therefore this study will investigate the hypothesis that zinc is an important factor when considering the ability of disulfiram to induce breast cancer cell death.

In order to enhance knowledge of the role of zinc in the sensitivity of breast cancer cells to disulfiram, this thesis will address the following aims:

- Characterisation of the cytotoxic effect of disulfiram in cancerous and non-cancerous breast cells.

- Fully investigate the effect of disulfiram on intracellular zinc in breast cancer cells.

- Define mechanisms to describe the potential link between intracellular zinc levels and the anti-breast cancer effect of disulfiram.

References

Agarwal, R. P., McPherson, R. A. and Phillips, M. 1983. Rapid degradation of disulfiram by serumFalbumin. *Research Communications in Chemical Pathology and Pharmacology.* 42(2), p. 293-310.

Al-Hajj, M., Wicha, M. S., Benito-Hernandez, A. and Morrison, S. J. and Clarke, M. F. 2003. Prospective identification of tumorigenic breast cancer cells. *Proceedings of the National Academy of Sciences of the United States of America.* 100(7), p. 3983-3988.

Amemiya, Y., Azmi, P. and Seth, A. 2008. Autoubiquitination of BCA2 RING E3 ligase regulates its own stability and affects cell migration. *Molecular Cancer Research.* 6(9), p. 1385-1396.

Amuchastegui, T., Amuchastegui, M. and Donohue, T. 2014. Disulfiram-alcohol reaction mimicking an acute coronary syndrome. *Connecticut Medicine.* 78(2), p. 81-84.

Anderson, K., Lutz, C., van Delft, F. W., Bateman, C. M., Guo, Y. P., Colman, S. M., Kempski, H., Moorman, A. V., Titley, I., Swansbury, J., Kearney, L., Enver, T. and Greaves, M. 2011. Genetic variegation of clonal architecture and propagating cells in leukaemia. *Nature.* 469(7330), p. 356-361.

Andre, F., O'Regan, R., Ozguroglu, M., Toi, M., Xu, B., Jerusalem, G., Masuda, N., Wilks, S., Arena, F., Isaacs, C., Yap, Y. S., Papai, Z., Lang, I., Armstrong, A., Lerzo, G., White, M., Shen, K., Litton, J., Chen, D., Zhang, Y., Ali, S., Taran, T. and Gianni, L. 2014. Everolimus for women with trastuzumab-resistant, HER2-positive, advanced breast cancer (BOLERO-3): a randomised, double-blind, placebo-controlled phase 3 trial. *Lancet Oncology.* 15(6), p. 580-591.

Baselga, J., Albanell, J., Ruiz, A., Lluch, A., Gascon, P., Guillem, V., Gonzalez, S., Sauleda, S., Marimon, I., Tabernero, J. M., Koehler, M. T. and Rojo, F. 2005. Phase II and tumor pharmacodynamic study of gefitinib in patients with advanced breast cancer. *Journal of Clinical Oncology.* 23(23), p. 5323-5333.

Baum, M., Buzdar, A. U., Cuzick, J., Forbes, J., Houghton, J., Klijn, J. G. M., Sahmoud, T. and Grp, A. T. 2002. Anastrozole alone or in combination with tamoxifen versus tamoxifen alone for adjuvant treatment of postmenopausal

women with early breast cancer: first results of the ATAC randomised trial. *Lancet.* 359(9324), p. 2131-2139.

Becker, M. C. and Sugarman, G. 1952. Death following test drink of alcohol in patients receiving antabuse. *Journal of the American Medical Association.* 149(6), p. 568-571.

Berlin, R. G. 1989. Disulfiram hepatotoxicity: a consideration of its mechanism and clinical spectrum. *Alcohol and alcoholism.* 24(3), p. 241-246.

Billam, M., Sobolewski, M. D. and Davidson, N. E. 2010. Effects of a novel DNA methyltransferase inhibitor zebularine on human breast cancer cells. *Breast Cancer Research and Treatment.* 120(3), p. 581-592.

Biswas, D. K., Singh, S., Shi, Q., Pardee, A. B. and Inglehart, J. D. 2005. Crossroads of estrogen receptor and NF-kappaB signaling. *Science STKE.* 288, ePub 27.

Bozym, R. A., Chimienti, F., Giblin, L. J., Gross, G. W., Korichneva, I., Li, Y., Libert, S., Maret, W., Parviz, M., Frederickson, C. J. and Thompson, R. B. 2010. Free zinc ions outside a narrow concentration range are toxic to a variety of cells *in vitro*. *Experimental Biology and Medicine.* 235(6), p. 741-750.

Brahemi, G., Kona, F. R., Fiasella, A., Buac, D., Soukupova, J., Brancale, A., Burger, A. M. and Westwell, A. D. 2010. Exploring the structural requirements for inhibition of the ubiquitin E3 ligase Breast Cancer Associated Protein 2 (BCA2) as a treatment for breast cancer. *Journal of Medicinal Chemistry.* 53(7), p. 2757-2765.

Brar, S. S., Grigg, C., Wilson, K. S., Holder, W. D., Dreau, D., Austin, C., Foster, M., Ghio, A. J., Whorton, A. R., Stowell, G. W., Whittall, L. B., Whittle, R. R., White, D. P. and Kennedy, T. P. 2004. Disulfiram inhibits activating transcription factor/cyclic AMP-responsive element binding protein and human melanoma growth in a metal-dependent manner *in vitro*, in mice and in a patient with metastatic disease. *Molecular Cancer Therapeutics.* 3(9), p. 1049-1060.

Burger, A., Li, H., Zhang, X. K., Pienkowska, M., Venanzoni, M., Vournakis, J., Papas, T. and Seth, A. 1998. Breast cancer genome anatomy: correlation of morphological changes in breast carcinomas with expression of the novel gene product Di12. *Oncogene.* 16(3), p. 327-333.

Burger, A. M., Gao, Y. G., Amemiya, Y., Kahn, H. J., Kitching, R., Yang, Y. L., Sun, P., Narod, S. A., Hanna, W. M. and Seth, A. K. 2005. A novel RING-type ubiquitin ligase breast cancer-associated gene 2 correlates with outcome in invasive breast cancer. *Cancer Research.* 65(22), p. 10401-10412.

Bjornsson E., Nordlinder, H., and Olsson, R. 2006. Clinical characteristics and prognostic markers in disulfiram-induced liver injury. *Journal of hepatology.* 44(4), p. 791-797.

Cancer Research UK. 2014a. *Breast cancer statistics* [Online]. Available at: http://www.cancerresearchuk.org/cancer-info/cancerstats/types/breast/ [Accessed: 03/11/14].

Cancer Research UK. 2014b. *Worldwide cancer mortality statistics* [Online]. Available at: http://www.cancerresearchuk.org/cancer-info/cancerstats/world/mortality/ [Accessed: 3/11/14].

Cen, D. Z., Brayton, D., Shahandeh, B., Meyskens, F. L. and Farmer, P. J. 2004. Disulfiram facilitates intracellular Cu uptake and induces apoptosis in human melanoma cells. *Journal of Medicinal Chemistry.* 47(27), p. 6914-6920.

Chen, D., Cui, Q. C., Yang, H. and Dou, Q. P. 2006. Disulfiram, a clinically used anti-alcoholism drug and copper-binding agent, induces apoptotic cell death in breast cancer cultures and xenografts via inhibition of the proteasome activity. *Cancer Research.* 66(21), p. 10425-10433.

Chen, D. and Dou, Q. P. 2008. New uses for old copper-binding drugs: converting the pro-angiogenic copper to a specific cancer cell death inducer. *Expert Opinion on Therapeutic Targets.* 12(6), p. 739-748.

Chen, M., Shabashvili, D., Nawab, A., Yang, S. X., Dyer, L. M., Brown, K. D., Hollingshead, M., Hunter, K. W., Kaye, F. J., Hochwald, S. N., Marquez, V. E., Steeg, P. and Zajac-Kaye, M. 2012. DNA Methyltransferase inhibitor, zebularine, delays tumor growth and induces apoptosis in a genetically engineered mouse model of breast cancer. *Molecular Cancer Therapeutics.* 11(2), p. 370-382.

Chen, S. and Parmigiani, G. 2007. Meta-analysis of BRCA1 and BRCA2 penetrance. *Journal of Clinical Oncology.* 25(11), p. 1329-1333.

Chick, J. 1999. Safety issues concerning the use of disulfiram in treating alcohol dependence. *Drug Safety.* 20(5), p. 427-435.

Cho, H. J., Lee, T. S., Park, J. B., Park, K. K., Choe, J. Y., Sin, D. I., Park, Y. Y., Moon, Y. S., Lee, K. G., Yeo, J. H., Han, S. M., Cho, Y. S., Choi, M. R., Park, N. G., Lee, Y. S. and Chang, Y. C. 2007. Disuffiram suppresses invasive ability of osteosarcoma cells via the inhibition of MMP-2 and MMP-9 expression. *Journal of Biochemistry and Molecular Biology.* 40(6), p. 1069-1076.

Chung, K. C., Park, J. H., Kim, C. H., Lee, H. W., Sato, N., Uchiyama, Y. and Ahn, Y. S. 2000. Novel biphasic effect of pyrrolidine dithiocarbamate on neuronal cell viability is mediated by the differential regulation of intracellular zinc and copper ion levels, NF-kappa B, and MAP kinases. *Journal of Neuroscience Research.* 59(1), p. 117-125.

Cobby, J., Mayersohn, M. and Selliah, S. 1977. Rapid reduction of disulfiram in blood and plasma. *Journal of Pharmacology and Experimental Therapeutics.* 202(3), p. 724-731.

Collins, J. J., Anteau, S. E., Swaen, G. M. H., Bodner, K. M. and Bodnar, C. M. 2015. Lymphatic and hematopoietic cancers among benzene-exposed workers. *Journal of Occupational and Environmental Medicine.* 57(2), p. 159-163.

Colvin, R. A., Bush, A. I., Volitakis, I., Fontaine, C. P., Thomas, D., Kikuchi, K. and Holmes, W. R. 2008. Insights into Zn2+ homeostasis in neurons from experimental and modeling studies. *American Journal of Physiology-Cell Physiology.* 294(3), p. 726-742.

Coombes, R. C., Kilburn, L. S., Snowdon, C. F., Paridaens, R., Coleman, R. E., Jones, S. E., Jassem, J., Van de Velde, C. J. H., Delozier, T., Alvarez, I., Del Mastro, L., Ortmann, O., Diedrich, K., Coates, A. S., Bajetta, E., Holmberg, S. B., Dodwell, D., Mickiewicz, E., Andersen, J., Lonning, P. E., Cocconi, G., Forbes, J., Castiglione, M., Stuart, N., Stewart, A., Fallowfield, L. J., Bertelli, G., Hall, E., Bogle, R. G., Carpentieri, M., Colajori, E., Subar, M., Ireland, E. and Bliss, J. M. 2007. Survival and safety of exemestane versus tamoxifen after 2-3 years' tamoxifen treatment (Intergroup Exemestane Study): a randomised controlled trial. *Lancet.* 369(9561), p.559-570.

Craige, S. M., Kant, S. and Keaney, J. F., Jr. 2015. Reactive oxygen species in endothelial function- from disease to adaptation. *Circulation journal.* 79(6), p. 1145-1155.

Cristofanilli, M., Valero, V., Mangalik, A., Royce, M., Rabinowitz, I., Arena, F. P., Kroener, J. F., Curcio, E., Watkins, C., Bacus, S., Cora, E. M., Anderson,

E. and Magill, P. J. 2010. Phase II, randomized trial to compare anastrozole combined with gefitinib or placebo in postmenopausal women with hormone receptor-positive metastatic breast cancer. *Clinical Cancer Research.* 16(6), p. 1904-1914.

Curtis, C., Shah, S. P., Chin, S. F., Turashvili, G., Rueda, O. M., Dunning, M. J., Speed, D., Lynch, A. G., Samarajiwa, S., Yuan, Y., Graef, S., Ha, G., Haffari, G., Bashashati, A., Russell, R., McKinney, S., Langerod, A., Green, A., Provenzano, E., Wishart, G., Pinder, S., Watson, P., Markowetz, F., Murphy, L., Ellis, I., Purushotham, A., Borresen-Dale, A. L., Brenton, J. D., Tavare, S., Caldas, C., Aparicio, S. and Grp, M. 2012. The genomic and transcriptomic architecture of 2,000 breast tumours reveals novel subgroups. *Nature.* 486(7403), p. 346-352.

Cuzick, J., Sestak, I., Baum, M., Buzdar, A., Howell, A., Dowsett, M. and Forbes, J. F. 2010. Effect of anastrozole and tamoxifen as adjuvant treatment for early-stage breast cancer: 10-year analysis of the ATAC trial. *Lancet Oncology.* 11(12), p. 1135-1141.

Cuzick, J., Sestak, I., Cawthorn, S., Hamed, H., Holli, K., Howell, A. and Forbes, J. F. 2015. Tamoxifen for prevention of breast cancer: extended long-term follow-up of the IBIS-I breast cancer prevention trial. *Lancet Oncology.* 16(1), p. 67-75.

Cvek, B. 2011. Targeting malignancies with disulfiram (Antabuse): multidrug resistance, angiogenesis, and proteasome. *Current Cancer Drug Targets.* 11(3), p. 332-337.

Cvek, B., Milacic, V., Taraba, J. and Dou, Q. P. 2008. Ni(II), Cu(II), and Zn(II) diethyldithiocarbamate complexes show various activities against the proteasome in breast cancer cells. *Journal of Medicinal Chemistry.* 51(20), p. 6256-6258.

Davies, B. R., Greenwood, H., Dudley, P., Crafter, C., Yu, D. H., Zhang, J. C., Li, J., Gao, B. R., Ji, Q. S., Maynard, J., Ricketts, S. A., Cross, D., Cosulich, S., Chresta, C. C., Page, K., Yates, J., Lane, C., Watson, R., Luke, R., Ogilvie, D. and Pass, M. 2012. Preclinical pharmacology of AZD5363, an inhibitor of AKT: pharmacodynamics, antitumor activity, and correlation of monotherapy activity with genetic background. *Molecular Cancer Therapeutics.* 11(4), p. 873-887.

Davies, C., Godwin, J., Gray, R., Clarke, M., Darby, S., McGale, P., Wang, Y. C., Peto, R., Pan, H. C., Cutter, D., Taylor, C. and Ingle, J. 2011. Relevance of

breast cancer hormone receptors and other factors to the efficacy of adjuvant tamoxifen: patient-level meta-analysis of randomised trials. *Lancet.* 378(9793), p. 771-784.

de Beca, F. F., Caetano, P., Gerhard, R., Alvarenga, C. A., Gomes, M., Paredes, J. and Schmitt, F. 2013. Cancer stem cells markers CD44, CD24 and ALDH1 in breast cancer special histological types. *Journal of Clinical Pathology.* 66(3), p. 187-191.

De Mukhopadhyay, K., Liu, Z., Bandyopadhyay, A., Kirma, N. B., Tekmal, R. R., Wang, S. and Sun, L. Z. 2015. Aromatase expression increases the survival and malignancy of estrogen receptor positive breast cancer cells. *PLOS One.* 10(4), e0121136.

Dent, R. A., Lindeman, G. J., Clemons, M., Wildiers, H., Chan, A., McCarthy, N. J., Singer, C. F., Lowe, E. S., Watkins, C. L. and Carmichael, J. 2013. Phase I trial of the oral PARP inhibitor olaparib in combination with paclitaxel for first-or second-line treatment of patients with metastatic triple-negative breast cancer. *Breast Cancer Research.* 15(5), R88.

Drexler, H. C. A., Risau, W. and Konerding, M. A. 2000. Inhibition of proteasome function induces programmes cell death in proliferating endothelial cells. *FASEB Journal.* 14(1), p. 65-77.

Duan, X. P., Xiao, J. S., Yin, Q., Zhang, Z. W., Yu, H. J., Mao, S. R. and Li, Y. P. 2013. Smart pH-sensitive and temporal-controlled polymeric micelles for effective combination therapy of doxorubicin and disulfiram. *ACS Nano.* 7(7), p. 5858-5869.

Eide, D. J. 2006. Zinc transporters and the cellular trafficking of zinc. *Biochimica Et Biophysica Acta-Molecular Cell Research.* 1763(7), p. 711-722.

Eneanya, D. I., Bianchine, J. R., Duran, D. O. and Andresen, B. D. 1981. The actions and metabolic-fate of disulfiram. *Annual Review of Pharmacology and Toxicology.* 21, p. 575-596.

Ferlay, J., Soerjomataram, I., Dikshit, R., Eser, S., Mathers, C., Rebelo, M., Parkin, D. M., Forman, D. and Bray, F. 2015. Cancer incidence and mortality worldwide: Sources, methods and major patterns in GLOBOCAN 2012. *International Journal of Cancer.* 136(5), p. E359-386.

Fiegl, H., Millinger, S., Goebel, G., Muller-Holzner, E., Marth, C., Laird, P. W. and Widschwendter, M. 2006. Breast cancer DNA methylation profiles in cancer cells and tumor stroma: Association with HER-2/neu status in primary breast cancer. *Cancer Research.* 66(1), p. 29-33.

Filosto, M., Tentorio, M., Broglio, L., Buzio, S., Lazzarini, C., Pasolini, M. P., Cotelli, M. S., Scarpelli, M., Mancuso, M., Choub, A. and Padovani, A. 2008. Disulfiram neuropathy: Two cases of distal axonopathy. *Clinical Toxicology.* 46(4), p. 314-316.

Fisher, B., Costantino, J. P., Wickerham, D. L., Cecchini, R. S., Cronin, W. M., Robidoux, A., Bevers, T. B., Kavanah, M. T., Atkins, J. N., Margolese, R. G., Runowicz, C. D., James, J. M., Ford, L. G. and Wolmark, N. 2005. Tamoxifen for the prevention of breast cancer: Current status of the National Surgical Adjuvant Breast and Bowel Project P-1 study. *Journal of the National Cancer Institute.* 97(22), p. 1652-1662.

Frasor, J., Danes, J. M., Komm, B., Chang, K. C. N., Lyttle, C. R. and Katzenellenbogen, B. S. 2003. Profiling of estrogen up- and down-regulated gene expression in human breast cancer cells: Insights into gene networks and pathways underlying estrogenic control of proliferation and cell phenotype. *Endocrinology.* 144(10), p. 4562-4574.

Frisoni, G. B. and Dimonda, V. 1989. Disulfiram neuropathy- a review (1971-1988) and report of a case. *Alcohol and Alcoholism.* 24(5), p. 429-437.

Gershtein, E. S., Scherbakov, A. M., Platova, A. M., Tchemeris, G. Y., Letyagin, V. P. and Kushlinskii, N. E. 2010. The expression and DNA-binding activity of NF-kappa B nuclear transcription factor in the tumors of patients with breast cancer. *Bulletin of Experimental Biology and Medicine.* 150(1), p. 71-74.

Goldhirsch, A., Gelber, R. D., Piccart-Gebhart, M. J., de Azambuja, E., Procter, M., Suter, T. M., Jackisch, C., Cameron, D., Weber, H. A., Heinzmann, D., Dal Lago, L., McFadden, E., Dowsett, M., Untch, M., Gianni, L., Bell, R., Koehne, C. H., Vindevoghel, A., Andersson, M., Brunt, A. M., Otero-Reyes, D., Song, S., Smith, I., Leyland-Jones, B. and Baselga, J. 2013. 2 years versus 1 year of adjuvant trastuzumab for HER2-positive breast cancer (HERA): an open-label, randomised controlled trial. *Lancet.* 382(9897), p. 1021-1028.

Goldstein, M., Anagnoste, B., Lauber, E. and McKereghan, M. R. 1964. Inhibition of dopamine-beta-hydroxylase by disulfiram. *Life Sciences.* 3(7), p. 763-767.

Gordon, R. M. and Seaton, D. R. 1942. Treatment of Scabies. *British Medical Journal.* 1(4248), p. 685-687.

Green, K. A. and Carroll, J. S. 2007. Oestrogen-receptor-mediated transcription and the influence of co-factors and chromatin state. *Nature Reviews Cancer.* 7, p. 713-722

Guo, X., Xu, B., Pandey, S., Goessl, E., Brown, J., Armesilla, A. L., Darling, J. L. and Wang, W. 2010. Disulfiram/copper complex inhibiting NF kappa B activity and potentiating cytotoxic effect of gemcitabine on colon and breast cancer cell lines. *Cancer Letters.* 290(1), p. 104-113.

Gupta, S. K., Shukla, V. K., Vaidya, M. P., Roy, S. K. and Gupta, S. 1991. Serum trace-elements and Cu/Zn ratio in breast-cancer patients. *Journal of Surgical Oncology.* 46(3), p. 178-181.

Gutteridge, E., Agrawal, A., Nicholson, R., Cheung, K. L., Robertson, J. and Gee, J. 2010. The effects of gefitinib in tamoxifen-resistant and hormone-insensitive breast cancer: a phase II study. *International Journal of Cancer.* 126(8), p. 1806-1816.

Han, J. B., Liu, L. M., Yue, X. Q., Chang, J. J., Shi, W. D. and Hua, Y. Q. 2013. A binuclear complex constituted by diethyldithiocarbamate and copper(I) functions as a proteasome activity inhibitor in pancreatic cancer cultures and xenografts. *Toxicology and Applied Pharmacology.* 273(3), p. 477-483.

Hanahan, D. and Weinberg, R. A. 2011. Hallmarks of cancer: the next generation. *Cell.* 144(5), p. 646-674.

Hann, M. M. and Keserue, G. M. 2012. Finding the sweet spot: the role of nature and nurture in medicinal chemistry. *Nature Reviews Drug Discovery.* 11(5), p. 355-365.

Hay, R. T., Vuillard, L., Desterro, J. M. P. and Rodriguez, M. S. 1999. Control of NF-kappa B transcriptional activation by signal induced proteolysis of I kappa B alpha. *Philosophical Transactions of the Royal Society of London Series B-Biological Sciences.* 354(1389), p. 1601-1609.

Hillen, F. and Griffioen, A. W. 2007. Tumour vascularization: sprouting angiogenesis and beyond. *Cancer and Metastasis Reviews.* 26(3-4), p. 489-502.

Hope, K. J., Jin, L. Q. and Dick, J. E. 2004. Acute myeloid leukemia originates from a hierarchy of leukemic stem cell classes that differ in self-renewal capacity. *Nature Immunology.* 5(7), p. 738-743.

Hothi, P., Martins, T. J., Chen, L. P., Deleyrolle, L., Yoon, J. G., Reynolds, B. and Foltz, G. 2012. High-throughput chemical screens identify disulfiram as an inhibitor of human glioblastoma stem cells. *Oncotarget.* 3(10), p. 1124-1136.

Howell, A., Robertson, J. E., Abram, P., Lichinitser, M. R., Elledge, R., Bajetta, E., Watanabe, T., Morris, C., Webster, A., Dimery, I. and Osborne, C. K. 2004. Comparison of Fulvestrant versus tamoxifen for the treatment of advanced breast cancer in postmenopausal women previously untreated with endocrine therapy: A multinational, double-blind, randomized trial. *Journal of Clinical Oncology.* 22(9), p. 1605- 1613.

Howlader, N., Noone, A. M., Krapcho, M., Garshell, J., Miller, D., Altekruse, S. F., Kosary, C. L., Yu, M., Ruhl, J., Tatalovich, Z., Mariotto, A., Lewis, D. R., Chen, H. S., Feuer, E. J. and Ka, C. 1975-2012. SEER Cancer Statistics Review. In: Institute, N.C. ed. http://seer.cancer.gov/csr/1975_2012/.

Ingle, J. N., Suman, V. J., Rowland, K. M., Mirchandani, D., Bernath, A. M., Camoriano, J. K., Fishkin, P. A. S., Nikcevich, D. A. and Perez, E. A. 2006. Fulvestrant in women with advanced breast cancer after progression on prior aromatase inhibitor therapy: North central cancer treatment group trial N0032. *Journal of Clinical Oncology.* 24(7), p. 1052-1056.

Inwald, E. C., Klinkhammer-Schalke, M., Hofstaedter, F., Zeman, F., Koller, M., Gerstenhauer, M. and Ortmann, O. 2013. Ki-67 is a prognostic parameter in breast cancer patients: results of a large population-based cohort of a cancer registry. *Breast Cancer Research and Treatment.* 139(2), p. 539-552.

Jackson, S. E. and Chester, J. D. 2015. Personalised cancer medicine. *International Journal of Cancer.* 137(2), p. 262-266.

Jacobsen, E., Gessner, P. K. and Gessner, T. 1992. The road to antabuse. Disulfiram and its metabolite, diethyldithiocarbamate: Pharmacology and status in the treatment of alcoholism, HIV infections, AIDS and heavy metal toxicity. *Journal of Applied Toxicology.* 13(4) p. 347-352.

Jin, L. X., Davis, M. R., Hu, P. and Baillie, T. A. 1994. Identification of novel glutathione conjugates of disulfiram and diethyldithiocarbamate in rat bile by liquid-chromatography tandem mass-spectrometry- evidence for metabolic-activation of disulfiram in-vivo. *Chemical Research in Toxicology.* 7(4), p. 526-533.

Jiralerspong, S., Palla, S. L., Giordano, S. H., Meric-Bernstam, F., Liedtke, C., Barnett, C. M., Hsu, L. M., Hung, M. C., Hortobagyi, G. N. and Gonzalez-Angulo, A. M. 2009. Metformin and pathologic complete responses to neoadjuvant chemotherapy in diabetic patients with breast cancer. *Journal of Clinical Oncology.* 27(20), p. 3297-3302.

Johansson, B. 1992. A review of the pharmacokinetics and pharmacodynamics of disulfiram and its metabolites. *Acta psychiatrica Scandinavica. Supplementum.* 369, p. 15-26.

Jones, P. A. and Baylin, S. B. 2007. The epigenomics of cancer. *Cell.* 128(4), p. 683-692.

Kagara, N., Tanaka, N., Noguchi, S. and Hirano, T. 2007. Zinc and its transporter ZIP10 are involved in invasive behavior of breast cancer cells. *Cancer Science.* 98(5), p. 692-697.

Kanaujiya, J. K., Lochab, S., Kapoor, I., Pal, P., Datta, D., Bhatt, M. L. B., Sanyal, S., Behre, G. and Trivedi, A. K. 2013. Proteomic identification of Profilin1 as a corepressor of estrogen receptor alpha in MCF7 breast cancer cells. *Proteomics.* 13(14), p. 2100-2112.

Kaufman, B., Mackey, J. R., Clemens, M. R., Bapsy, P. P., Vaid, A., Wardley, A., Tjulandin, S., Jahn, M., Lehle, M., Feyereislova, A., Revil, C. and Jones, A. 2009. Trastuzumab plus anastrozole versus anastrozole alone for the treatment of postmenopausal women with Human Epidermal growth factor Receptor 2-positive, hormone receptor-positive metastatic breast cancer: results from the randomized phase III TAnDEM Study. *Journal of Clinical Oncology.* 27(33), p. 5529-5537.

Kaufman, B., Shapira-Frommer, R., Schmutzler, R. K., Audeh, M. W., Friedlander, M., Balmana, J., Mitchell, G., Fried, G., Stemmer, S. M., Hubert, A., Rosengarten, O., Steiner, M., Loman, N., Bowen, K., Fielding, A. and Domchek, S. M. 2015. Olaparib monotherapy in patients with advanced cancer and a germline BRCA1/2 mutation. *Journal of Clinical Oncology.* 33(3), p. 244- 250.

Kim, C. H., Kim, J. H., Xu, J., Hsu, C. Y. and Ahn, Y. S. 1999. Pyrrolidine dithiocarbamate induces bovine cerebral endothelial cell death by increasing the intracellular zinc level. *Journal of Neurochemistry.* 72(4), p. 1586-1592.

Kim, Y. M., Reed, W., Wu, W. D., Bromberg, P. A., Graves, L. M. and Samet, J. M. 2006. Zn2+-induced IL-8 expression involves AP-1, JNK, and ERK activities in human airway epithelial cells. *American Journal of Physiology-Lung Cellular and Molecular Physiology.* 290(5), p. L1028-1035.

Kisselev, A. F., van der Linden, W. A. and Overkleeft, H. S. 2012. Proteasome inhibitors: an expanding army attacking a unique target. *Chemistry & Biology.* 19(1), p. 99-115.

Kragh, H. 2008. From disulfiram to antabuse: the invention of a drug. *Bulletin for the History of Chemistry.* 33(2), p. 82-88.

Kukic, I., Kelleher, S. L. and Kiselyov, K. 2014. Zinc efflux through lysosomal exocytosis prevents zinc-induced toxicity. *Journal of Cell Science.* 127(14), p. 3094-3103.

Landen, C., Goodman, B., Katre, A. A., Steg, A. D., Nick, A. M., Stone, R. L., Miller, L. D., Mejia, P. V., Jennings, N. B., Gershenson, D. M., Bast, R. C., Coleman, R. L., Lopez-Berestein, G. and Sood, A. K. Targeting Aldehyde Dehydrogenase Cancer Stem Cells in Ovarian Cancer. *Therapeutic Discovery.* 9(12), p. 3186-3199.

Lewison, E. F. 1977. Spontaneous regression of breast cancer. *Progress in Clinical and Biological Research.* 12, p. 47-53.

Li, F., Zhang, J. W., Arfuso, F., Chinnathambi, A., Zayed, M. E., Alharbi, S. A., Kumar, A. P., Ahn, K. S. and Sethi, G. 2015. NF-kappa B in cancer therapy. *Archives of Toxicology.* 89(5), p. 711-731.

Li, L., Yang, H., Chen, D., Cui, C. and Dou, Q. P. 2008. Disulfiram promotes the conversion of carcinogenic cadmium to a proteasome inhibitor with pro-apoptotic activity in human cancer cells. *Toxicology and Applied Pharmacology.* 229(2), p. 206-214.

Lin, J., Haffner, M. C., Zhang, Y., Lee, B. H., Brennen, W. N., Britton, J., Kachhap, S. K., Shim, J. S., Liu, J. O., Nelson, W. G., Yegnasubramanian, S. and Carducci, M. A. 2011. Disulfiram is a DNA demethylating agent and inhibits prostate cancer cell growth. *Prostate.* 71(4), p. 333-343.

Lipton, A., Leitzel, K., Ali, S. M., Demers, L., Harvey, H. A., Chaudri-Ross, H. A., Evans, D., Lang, R., Hackl, W., Hamer, P. and Carney, W. 2005. Serum HER-2/neu conversion to positive at the time of disease progression in patients with breast carcinoma on hormone therapy. *Cancer.* 104(2), p. 257-263.

Liu, M., Sakamaki, T., Casimiro, M. C., Willmarth, N. E., Quong, A. A., Ju, X., Ojeifo, J., Jiao, X., Yeow, W. S., Katiyar, S., Shirley, L. A., Joyce, D., Lisanti, M. P., Albanese, C. and Pestell, R. G. 2010. The canonical NF-kappa B pathway governs mammary tumorigenesis in transgenic mice and tumor stem cell expansion. *Cancer Research.* 70(24), p. 10464-10473.

Liu, P., Cheng, H., Roberts, T. M. and Zhao, J. J. 2009. Targeting the phosphoinositide 3-kinase pathway in cancer. *Nature Reviews Drug Discovery.* 8(8), p. 627-644.

Liu, P., Kumar, I. S., Brown, S., Kannappan, V., Tawari, P. E., Tang, J. Z., Jiang, W., Armesilla, A. L., Darling, J. L. and Wang, W. 2013. Disulfiram targets cancer stem-like cells and reverses resistance and cross-resistance in acquired paclitaxel-resistant triple-negative breast cancer cells. *British Journal of Cancer.* 109(7), p. 1876-1885.

Liu, Z. Q., Zhang, X. S. and Zhang, S. H. 2014. Breast tumor subgroups reveal diverse clinical prognostic power. *Scientific Reports.* 4, article number 4002.

Loo, T. W., Bartlett, M. C. and Clarke, D. M. 2004. Disulfiram metabolites permanently inactivate the human multidrug resistance P-glycoprotein. *Molecular Pharmaceutics.* 1(6), p. 426-433.

Lovborg, H., Oberg, F., Rickardson, L., Gullbo, J., Nygren, P. and Larsson, R. 2006. Inhibition of proteasome activity, nuclear factor-KB translocation and cell survival by the antialcoholism drug disulfiram. *International Journal of Cancer.* 118(6), p. 1577-1580.

Maret, W. and Sandstead, H. H. 2006. Zinc requirements and the risks and benefits of zinc supplementation. *Journal of Trace Elements in Medicine and Biology.* 20(1), p. 3-18.

Marikovsky, M., Nevo, N., Vadai, E. and Harris-Cerruti, C. 2002. Cu/Zn superoxide dismutase plays a role in angiogenesis. *International Journal of Cancer.* 97(1), p. 34-41.

Martinkovich, S., Shah, D., Planey, S. L. and Arnott, J. A. 2014. Selective estrogen receptor modulators: tissue specificity and clinical utility. *Clinical Interventions in Aging.* 9, p. 1437-1452.

Martensen-Larsen, O. 1948. Treatment of alcoholism with a sensitizing drug. *Lancet.* 2(6539), p. 1004-1004.

Marotti, J. D., Collins, L. C., Hu, R., and Tamimi, R. M. 2010. Estrogen receptor-β expression in invasive breast cancer in relation to molecular phenotype: results from the Nurses' Health Study. *Modern Pathology.* 23(2), p. 197-204.

Marquez, D. C., Lee, J., Lin, T. and Pietras, R. J. 2001. Epidermal growth factor receptor and tyrosine phosphorylation of estrogen receptor. *Endocrine.* 16(2), p. 73-81.

Mateos, M. V., Richardson, P. G., Schlag, R., Khuageva, N. K., Dimopoulos, M. A., Shpilberg, O., Kropff, M., Spicka, I., Petrucci, M. T., Palumbo, A., Samoilova, O. S., Dmoszynska, A., Abdulkadyrov, K. M., Schots, R., Jiang, B., Esseltine, D. L., Liu, K., Cakana, A., van de Velde, H. and San Miguel, J. F. 2010. Bortezomib plus melphalan and prednisone compared with melphalan and prednisone in previously untreated multiple myeloma: updated follow-up and impact of subsequent therapy in the phase III VISTA trial. *Journal of Clinical Oncology.* 28(13), p. 2259-2266.

McCubrey, J. A., LaHair, M. M. and Franklin, R. A. 2006. Reactive oxygen species-induced activation of the MAP kinase signaling pathways. *Antioxidants & Redox Signaling.* 8(9-10), p. 1775-1789.

Murai, R., Yoshida, Y., Muraguchi, T., Nishimoto, E., Morioka, Y., Kitayama, H., Kondoh, S., Kawazoe, Y., Hiraoka, M., Uesugi, M. and Noda, M. 2010. A novel screen using the Reck tumor suppressor gene promoter detects both conventional and metastasis-suppressing anticancer drugs. *Oncotarget.* 1(4), p. 252-264.

Muthukkaruppan, V. R., Kubai, L. and Auerbach, R. 1982. Tumor-induced neovascularization in the mouse eye. *Journal of the National Cancer Institute.* 69(3), p. 699-708.

Nagendra, S. N., Shetty, K. T., Subhash, M. N. and Guru, S. C. 1991. Role of glutathione-reductase system in disulfiram conversion to diethyldithiocarbamate. *Life Sciences.* 49(1), p. 23-28.

Nakano, H., Nakajima, A., Sakon-Komazawa, S., Piao, J. H., Xue, X. and Okumura, K. 2006. Reactive oxygen species mediate crosstalk between NF-kappa B and JNK. *Cell Death and Differentiation.* 13(5), p. 730-737.

Nechushtan, H., Hamamreh, Y., Nidal, S., Gotfried, M., Baron, A., Shalev, Y. I., Nisman, B., Peretz, T. and Peylan-Ramu, N. 2015. A phase IIb trial assessing the addition of disulfiram to chemotherapy for the treatment of metastatic non-small cell lung cancer. *The Oncologist.* 20(4), p. 366-367.

O'Lone, R., Frith, M. C., Karlsson, E. K., and Hansen, U. 2004. Genomic targets of nuclear estrogen receptors. *Molecular Endocrinology.* 18(8), p. 1859-1875.

Omoto, Y. and Iwase, H. 2015. Clinical significance of estrogen receptor β in breast and prostate cancer from biological aspects. *Cancer Science*. 106(4), p. 337-343.

Pagani, O., Regan, M. M., Walley, B. A., Fleming, G. F., Colleoni, M., Lang, I., Gomez, H. L., Tondini, C., Burstein, H. J., Perez, E. A., Ciruelos, E., Stearns, V., Bonnefoi, H. R., Martino, S., Geyer, C. E., Pinotti, G., Puglisi, F., Crivellari, D., Ruhstaller, T., Winer, E. P., Rabaglio-Poretti, M., Maibach, R., Ruepp, B., Giobbie-Hurder, A., Price, K. N., Bernhard, J., Luo, W. X., Ribi, K., Viale, G., Coates, A. S., Gelber, R. D., Goldhirsch, A. and Francis, P. A. 2014. Adjuvant exemestane with ovarian suppression in premenopausal breast cancer. *New England Journal of Medicine.* 371(2), p. 107-118.

Perez, E. A., Romond, E. H., Suman, V. J., Jeong, J. H., Sledge, G., Geyer, C. E., Jr., Martino, S., Rastogi, P., Gralow, J., Swain, S. M., Winer, E. P., Colon-Otero, G., Davidson, N. E., Mamounas, E., Zujewski, J. A. and Wolmark, N. 2014. Trastuzumab plus adjuvant chemotherapy for Human Epidermal growth factor Receptor 2-positive breast cancer: planned joint analysis of overall survival from NSABP B-31 and NCCTG N9831. *Journal of Clinical Oncology.* 32(33), p. 3744-3752.

Petrakis, I. L., Poling, J., Levinson, C., Nich, C., Carroll, K. and Rounsaville, B. 2005. Naltrexone and disulfiram in patients with alcohol dependence and comorbid psychiatric disorders. *Biological Psychiatry.* 57(10), p. 1128-1137.

Petrucelli, N., Daly, M. B. and Feldman, G. L. 2010. Hereditary breast and ovarian cancer due to mutations in BRCA1 and BRCA2. *Genetics in Medicine.* 12(5), p. 245-259.

Pike, M. G., Mays, D. C., Macomber, D. W. and Lipsky, J. J. 2001. Metabolism of a disulfiram metabolite, S-methyl N,N-diethyldithiocarbamate by flavin monooxygenase in human renal microsomes. *Drug Metabolism and Disposition.* 29(2), p. 127-132.

Pozza, E. D., Donadelli, M., Costanzo, C., Zaniboni, T., Dando, I., Franchini, M., Arpicco, S., Scarpa, A. and Palmieri, M. 2011. Gemcitabine response in pancreatic adenocarcinoma cells is synergistically enhanced by dithiocarbamate derivatives. *Free Radical Biology and Medicine.* 50(8), p. 926-933.

Procter, M., Suter, T. M., de Azambuja, E., Dafni, U., van Dooren, V., Muehlbauer, S., Climent, M. A., Rechberger, E., Liu, W. T. W., Toi, M., Coombes, R. C., Dodwell, D., Pagani, O., Madrid, J., Hall, M., Chen, S. C., Focan, C., Muschol, M., van Veldhuisen, D. J. and Piccart-Gebhart, M. J. 2010. Longer-term assessment of trastuzumab-related cardiac adverse events in the Herceptin Adjuvant (HERA) Trial. *Journal of Clinical Oncology.* 28(21), p. 3422-3428.

Regan, M. M., Neven, P., Giobbie-Hurder, A., Goldhirsch, A., Ejlertsen, B., Mauriac, L., Forbes, J. F., Smith, I., Lang, I., Wardley, A., Rabaglio, M., Price, K. N., Gelber, R. D., Coates, A. S. and Thuerlimann, B. 2011. Assessment of letrozole and tamoxifen alone and in sequence for postmenopausal women with steroid hormone receptor-positive breast cancer: the BIG 1-98 randomised clinical trial at 8.1 years median follow-up. *Lancet Oncology.* 12(12), p. 1101-1108.

Rickardson, L., Wickström M., Larsson, R., and Lövborg, H. 2007. Image-based screening for the identification of novel proteasome inhibitors. *Journal of Biomolecular Screening.* 12(2), p. 203–210

Rimawi, M. F., Shetty, P. B., Weiss, H. L., Schiff, R., Osborne, C. K., Chamness, G. C. and Elledge, R. M. 2010. Epidermal growth factor receptor expression in breast cancer association with biologic phenotype and clinical Outcomes. *Cancer.* 116(5), p. 1234-1242.

Rizk, S. L. and Skypeck, H. H. 1984. Comparison between concentrations of trace-elements in normal and neoplastic human-breast tissue. *Cancer Research.* 44(11), p. 5390-5394.

Roache, J. D., Kahn, R., Newton, T. F., Wallace, C. L., Murff, W. L., De La Garza, R., Rivera, O., Anderson, A., Mojsiak, J. and Elkashef, A. 2011. A double-blind, placebo-controlled assessment of the safety of potential

interactions between intravenous cocaine, ethanol, and oral disulfiram. *Drug and Alcohol Dependence.* 119(1-2), p. 37-45.

Robertson, J. F., Nicholson, R. I., Bundred, N. J., Anderson, E., Rayter, Z., Dowsett, M., Fox, J. N., Gee, J. M. W., Webster, A., Wakeling, A. E., Morris, C. and Dixon, M. 2001. Comparison of the short-term biological effects of 7 alpha- 9-(4,4,5,5,5-pentafluoropentylsulfinyl)-nonyl estra-1,3,5, (10)-triene-3,17 beta-diol (Faslodex) versus tamoxifen in postmenopausal women with primary breast cancer. *Cancer Research.* 61(18), p. 6739-6746.

Rottenberg, S., Jaspers, J. E., Kersbergen, A., van der Burg, E., Nygren, A. O. H., Zander, S. A. L., Derksen, P. W. B., de Bruin, M., Zevenhoven, J., Lau, A., Boulter, R., Cranston, A., O'Connor, M. J., Martin, N. M. B., Borst, P. and Jonkers, J. 2008. High sensitivity of BRCA1-deficient mammary tumors to the PARP inhibitor AZD2281 alone and in combination with platinum drugs. *Proceedings of the National Academy of Sciences of the United States of America.* 105(44), p. 17079-17084.

Rousseau, D., Cannella, D., Boulaire, J., Fitzgerald, P., Fotedar, A. and Fotedar, R. 1999. Growth inhibition by CDK-cyclin and PCNA binding domains of p21 occurs by distinct mechanisms and is regulated by ubiquitin-proteasome pathway. *Oncogene.* 18(21), p. 3290-3302.

Sadler, A. J., Pugazhendhi, D. and Darbre, P. D. 2009. Use of global gene expression patterns in mechanistic studies of oestrogen action in MCF7 human breast cancer cells. *Journal of Steroid Biochemistry and Molecular Biology.* 114(1-2), p. 21-32.

Sakane, A., Hatakeyama, S. and Sasaki, T. 2007. Involvement of Rabring7 in EGF receptor degradation as an E3 ligase. *Biochemical and Biophysical Research Communications.* 357(4), p. 1058-1064.

Sauna, Z. E., Peng, X. H., Nandigama, K., Tekle, S. and Ambudkar, S. V. 2004. The molecular basis of the action of disulfiram as a modulator of the multidrug resistance-linked ATP binding cassette transporters MDR1 (ABCB1) and MRP1 (ABCC1). *Molecular Pharmacology.* 65(3), p. 675-684.

Sauna, Z. E., Shukla, S. and Ambudkar, S. V. 2005. Disulfiram, an old drug with new potential therapeutic uses for human cancers and fungal infections. *Molecular Biosystems.* 1(2), p. 127-134.

Schweizer, M. T., Lin, J., Blackford, A., Bardia, A., King, S., Armstrong, A. J., Rudek, M. A., Yegnasubramanian, S. and Carducci, M. A. 2013. Pharmacodynamic study of disulfiram in men with non-metastatic recurrent prostate cancer. *Prostate Cancer and Prostatic Diseases.* 16(4), p. 357-361.

Sekirnik, R., Rose, N. R., Thalhammer, A., Seden, P. T., Mecinovic, J. and Schofield, C. J. 2009. Inhibition of the histone lysine demethylase JMJD2A by ejection of structural Zn(II). *Chemical Communications.* 14(42), p. 6376-6378.

Sharma, V., Verma, V., Lal, N., Yadav, S. K., Sarkar, S., Mandalapu, D., Porwal, K., Rawat, T., Maikhuri, J. P., Rajender, S., Sharma, V. L. and Gupta, G. Disulfiram and its novel derivative sensitize prostate cancer cells to the growth regulatory mechanisms of the cell by re-expressing the epigenetically repressed tumor suppressor- estrogen receptor β. *Molecular Carcinogenesis.* Epub ahead of print. DOI: 10.1002/mc.22433

Shiah, S. G., Kao, Y. R., Wu, F. Y. H. and Wu, C. W. 2003. Inhibition of invasion and angiogenesis by zinc-chelating agent disulfiram. *Molecular Pharmacology.* 64(5), p. 1076-1084.

Shiau, A. K., Barstad, D., Loria, P. M., Cheng, L., Kushner, P. J., Agard, D. A. and Greene, G. L. 1998. The structural basis of estrogen receptor/coactivator recognition and the antagonism of this interaction by tamoxifen. *Cell.* 95(7), p. 927-937.

Sillaber, C., Mayerhofer, M., Boehm, A., Vales, A., Gruze, A., Aichberger, K. J., Esterbauer, H., Pfeilstoecker, M., Sperr, W. R., Pickl, W. F., Haas, O. A. and Valent, P. 2008. Evaluation of antileukaemic effects of rapamycin in patients with imatinib-resistant chronic myeloid leukaemia. *European Journal of Clinical Investigation.* 38(1), p. 43-52.

Skinner, M. D., Lahmek, P., Pham, H. and Aubin, H. J. 2014. Disulfiram efficacy in the treatment of alcohol dependence: a meta-analysis. *PLOS One.* 9(2), e87366.

Skrott, Z. and Cvek, B. 2012. Diethyldithiocarbamate complex with copper: the mechanism of action in cancer cells. *Mini-Reviews in Medicinal Chemistry.* 12(12), p. 1184-1192.

Sorlie, T., Perou, C. M., Tibshirani, R., Aas, T., Geisler, S., Johnsen, H., Hastie, T., Eisen, M. B., van de Rijn, M., Jeffrey, S. S., Thorsen, T., Quist, H., Matese, J. C., Brown, P. O., Botstein, D., Lonning, P. E. and Borresen-Dale, A.

L. 2001. Gene expression patterns of breast carcinomas distinguish tumor subclasses with clinical implications. *Proceedings of the National Academy of Sciences of the United States of America.* 98(19), p. 10869-10874.

Steins, M. B., Padro, T., Bieker, R., Ruiz, S., Kropff, M., Kienast, J., Kessler, T., Buechner, T., Berdel, W. E. and Mesters, R. M. 2002. Efficacy and safety of thalidomide in patients with acute myeloid leukemia. *Blood.* 99(3), p. 834-839.

Stromme, J. H. and Eldjarn, L. 1966. Distribution and chemical forms of diethyldithiocarbamate and tetraethylthiuram disulphide (disulfiram) in mice in relation to radioprotection. *Biochemical Pharmacology.* 15(3), p. 287-297.

Swenberg, J. A., Cooper, H. K., Bücheler, J. and Kleihues, P. 1979 1,2-Dimethylhydrazine-induced methylation of DNA bases in various rat organs and the effect of pretreatment with disulfiram. *Cancer Research.* 9(2), p.465-467.

Taylor, K. M., Vichova, P., Jordan, N., Hiscox, S., Hendley, R. and Nicholson, R. I. 2008. ZIP7-mediated intracellular zinc transport contributes to aberrant growth factor signaling in antihormone-resistant breast cancer cells. *Endocrinology.* 149(10), p. 4912-4920.

Thurlimann, B., Keshaviah, A., Coates, A. S., Mouridsen, H., Mauriac, L., Forbes, J. F., Paridaens, R., Castiglione-Gertsch, M., Gelber, R. D., Rabaglio, M., Smith, I., Wardly, A., Price, K. N. and Goldhirsch, A. 2005. A comparison of letrozole and tamoxifen in postmenopausal women with early breast cancer. *New England Journal of Medicine.* 353(26), p. 2747-2757.

Tonkin, E. G., Valentine, H. L., Milatovic, D. M. and Valentine, W. M. 2004. N,N-diethyldithiocarbamate produces copper accumulation, lipid peroxidation, and myelin injury in rat peripheral nerve. *Toxicological Sciences.* 81(1), p. 160-171.

Trachootham, D., Zhou, Y., Zhang, H., Demizu, Y., Chen, Z., Pelicano, H., Chiao, P. J., Achanta, G., Arlinghaus, R. B., Liu, J. and Huang, P. 2006. Selective killing of oncogenically transformed cells through a ROS-mediated mechanism by beta-phenylethyl isothiocyanate. *Cancer Cell.* 10(3), p. 241-252.

Tryfonidis, K., Zardavas, D. and Cardoso, F. 2014. Small breast cancers: When and how to treat. *Cancer Treatment Reviews.* 40(10), p. 1129-1136.

Umsumarng, S., Pitchakarn, P., Sastraruji, K., Yodkeeree, S., Ung, A. T., Pyne, S. G. and Limtrakul, P. 2015. Reversal of human multi-drug resistance leukaemic cells by stemofoline derivatives via inhibition of p-glycoprotein function. *Basic & Clinical Pharmacology & Toxicology.* 116(5), p. 390-397.

Valabrega, G., Montemurro, F. and Aglietta, M. 2007. Trastuzumab: mechanism of action, resistance and future perspectives in HER2-overexpressing breast cancer. *Annals of Oncology.* 18(6), p. 977-984.

Velazquez-Delgado, E. M. and Hardy, J. A. 2012. Zinc-mediated allosteric inhibition of caspase-6. *Journal of Biological Chemistry.* 287(43), p. 36000-36011.

Venkitaraman, A. R. 2002. Cancer susceptibility and the functions of BRCA1 and BRCA2. *Cell.* 108(2), p. 171-182.

Verma, S., Stewart D. J., Maroun, J. A. and Nair, R. C. 1990. A randomized phase II study of cisplatin alone versus cisplatin plus disulfiram. *American Journal of Clinical Oncology.* 13(2), p. 119-124.

Vidal, S. J., Rodriguez-Bravo, V., Galsky, M., Cordon-Cardo, C. and Domingo-Domenech, J. 2014. Targeting cancer stem cells to suppress acquired chemotherapy resistance. *Oncogene.* 33(36), p. 4451-4463.

Wang, F., Zhai, S., Liu, X., Li, L., Wu, S., Dou, Q. P. and Yan, B. 2011. A novel dithiocarbamate analogue with potentially decreased ALDH inhibition has copper-dependent proteasome-inhibitory and apoptosis-inducing activity in human breast cancer cells. *Cancer Letters.* 300(1), p. 87-95.

Wang, W. G., McLeod, H. L. and Cassidy, J. 2003. Disulfiram-mediated inhibition of NF-kappa B activity enhances cytotoxicity of 5-fluorouracil in human colorectal cancer cell lines. *International Journal of Cancer.* 104(4), p. 504-511.

Weigelt, B., Peterse, J. L. and van't Veer, L. J. 2005. Breast cancer metastasis: Markers and models. *Nature Reviews Cancer.* 5(8), p. 591-602.

Wymant, J. 2015. The role of BCA2 in receptor tyrosine kinase endocytosis and breast cancer. *Cardiff University.*

Xu, B., Shi, P. C., Fombon, I. S., Zhang, Y. Y., Huang, F., Wang, W. G. and Zhou, S. Y. 2011. Disulfiram/copper complex activated JNK/c-jun pathway and sensitized cytotoxicity of doxorubicin in doxorubicin resistant leukemia HL60 cells. *Blood Cells Molecules and Diseases.* 47(4), p. 264-269.

Yamasaki, S., Sakata-Sogawa, K., Hasegawa, A., Suzuki, T., Kabu, K., Sato, E., Kurosaki, T., Yamashita, S., Tokunaga, M., Nishida, K. and Hirano, T. 2007. Zinc is a novel intracellular second messenger. *Journal of Cell Biology.* 177(4), p. 637-645.

Yao, C. J., Du, W., Chen, H. B., Xiao, S., Huang, L. H. and Chen, F. P. 2015. The Fanconi anemia/BRCA pathway is involved in DNA interstrand cross-link repair of adriamycin-resistant leukemia cells. *Leukemia & Lymphoma.* 56(3), p. 755-762.

Yip, N. C., Fombon, I. S., Liu, P., Brown, S., Kannappan, V., Armesilla, A. L., Xu, B., Cassidy, J., Darling, J. L. and Wang, W. 2011. Disulfiram modulated ROS-MAPK and NF kappa B pathways and targeted breast cancer cells with cancer stem cell-like properties. *British Journal of Cancer.* 104(10), p. 1564-1574.

Yu, F., Yao, H., Zhu, P., Zhang, X., Pan, Q., Gong, C., Huang, Y., Hu, X., Su, F., Lieberman, J. and Song, E. 2007a. Iet-7 regulates self renewal and tumorigenicity of breast cancer cells. *Cell.* 131(6), p. 1109-1123.

Yu, Z., Wang, F., Milacic, V., Li, X., Cui, Q. C., Zhang, B., Yan, B. and Dou, Q. P. 2007b. Evaluation of copper-dependent proteasome-inhibitory and apoptosis-inducing activities of novel pyrrolidine dithiocarbamate analogues. *International Journal of Molecular Medicine.* 20(6), p. 919-925.

Zhang, X., Frezza, M., Milacic, V., Ronconi, L., Fan, Y., Bi, C., Fregona, D. and Dou, Q. P. 2010. Inhibition of tumor proteasome activity by gold-dithiocarbamato complexes via both redox-dependent and -independent processes. *Journal of Cellular Biochemistry.* 109(1), p. 162-172.

2. Materials and Methods

2.1. Chemicals and reagents

2.1.1. Chemicals, reagents and kits

Table 2.1. List of chemicals, reagents and kits used in this study. Where appropriate, information is also included regarding the stock concentration and diluent.

Reagent	Source	Cat. No.	[Stock]	Diluent
3-(4,5-dimethylthiazol-2-yl)-2,5-diphenyltetrazolium bromide (MTT)	Sigma-Aldrich	M5655	5.5 mg/ml	PBS
4-(2-hydroxyethyl)-1-piperazineethanesulfonic acid (HEPES)	Sigma-Aldrich	H3375	-	-
Acetic acid	Sigma-Aldrich	320099	-	-
Acetone	Fisher Scientific	10131560	-	-
Acridine orange (AO)	Life Tech.	A1301	5 mg/ml	dH_2O
Agarose	Bio-Rad	161-3100	-	-
Ammonium chloride	Sigma-Aldrich	A9434	-	-
Bafilomycin	Sigma-Aldrich	B1793	20 µM	DMSO
Bicinchoninic acid (BCA)	Sigma-Aldrich	B9643	-	-
Bovine serum albumin (BSA)	Sigma-Aldrich	A7906	-	-
Bromophenol blue	Sigma-Aldrich	B0126	-	-
CA-074Me	Sigma-Aldrich	C5857	10 mM	DMSO
CellTiter Blue	Promega	G8080	-	
Chloroquine	Sigma-Aldrich	C6628	100 mM	dH_2O
Cholera toxin	Sigma-Aldrich	S8052	-	-
Clarity ECL reagent	Bio-Rad	170-5060	-	-
Copper chloride ($CuCl_2$)	Sigma-Aldrich	203149	20 mM	dH_2O
Copper sulphate	Sigma-Aldrich	C2284	-	-

Dako oil	Dako	S3023	-	-
Dextran-Alexa 647 (10 kDa)	Life Tech.	D-22914	10 mg/ml	PBS
Diethyldithiocarbamate (DDC)	Sigma-Aldrich	228680	10 mM	DMSO
Disulfiram	Sigma-Aldrich	86720	10 mM	DMSO
Dithiothreitol (DTT)	Sigma-Aldrich	DTT-RO	-	-
DMEM/ F12	Life Tech.	11330	-	-
Dimethyl sulfoxide (DMSO)	Fisher Scientific	10080110	-	-
Epidermal growth factor (EGF)	Sigma-Aldrich	E9644	-	-
Ethanol	Fisher Scientific	12468750	-	-
Ethidium bromide	Sigma-Aldrich	E1510	-	-
Ethylenediametetra acetic acid (EDTA)	Sigma-Aldrich	E6758	-	-
Fluozin-3	Life Tech.	F24195	5 mM	DMSO
Foetal bovine serum (FBS)	Life Tech.	16000-044	-	-
Glycerol	Sigma-Aldrich	G5516	-	-
Glycine	Sigma-Aldrich	G8898	-	-
Hoescht 33342	Life Tech.	H3570	-	-
Horse serum	Life Tech.	16050	-	-
Hydrocortisone	Sigma-Aldrich	H0888	-	-
Insulin	Sigma-Aldrich	I 9278	-	-
Isopropanol	Sigma-Aldrich	I9516		
JumpStart™ Taq DNA Polymerase (For use with LookOut® Mycoplasma PCR Detection Kit)	Sigma-Aldrich	D9307	-	-
LookOut® Mycoplasma PCR Detection Kit	Sigma-Aldrich	MP0035-1KT	-	-
LysoSensor Green	Life Tech.	L-7535	-	-
Methanol	Sigma-Aldrich	10365710	-	-

Milk	Marvel		-	-
MitoTracker Red	Life Tech.	M-7512	-	-
N,N,N′,N′-Tetrakis(2-pyridylmethyl)ethylenediamine (TPEN)	Sigma-Aldrich	P4413	10 mM	DMSO
Paraformaldehyde	Sigma-Aldrich	P6148	-	-
Phenol-red free RPMI 1640	Life Tech.	11835-030	-	-
Polyvinylidene fluoride (PVDF) membrane	Fisher Scientific	10344661	-	-
Pre-cast gel: Mini-PROTEAN TGX (12%)	Bio-Rad	4561041	-	-
Propidium iodide (PI)	Life Tech.	P3566	-	-
Protease inhibitor cocktail	Roche Diagnostics	11836153001	-	-
RPMI 1640	Life Tech.	21875	-	-
Sodium chloride	Sigma-Aldrich	S7653	-	-
Sodium dodecyl sulphate (SDS)	Bio-Rad	161-0301	-	-
Sodium pyrithione (NaP)	Sigma-Aldrich	H3261	10 mM	DMSO
Staurosporine	Sigma-Aldrich	S4400	10 mM	DMSO
Sucrose	Sigma-Aldrich	S7903	-	-
Tris-base	Sigma-Aldrich	000000010708976001	-	-
Tris-HCl	Sigma-Aldrich	RES3098T	-	-
Triton X-100	Sigma-Aldrich	X100	-	-
Trypan blue	Fisher Scientific	11538886	-	-
Trypsin/ EDTA	Life Tech.	25300062	-	-
Zinc chloride (ZnCl$_2$)	Sigma-Aldrich	229997	20 mM	dH$_2$O

Disulfiram analogues were designed, synthesised and assessed for purity by Dr. Andrew Westwell. They were dissolved in dimethyl sulfoxide (DMSO) to produce a stock concentration of 10 mM.

2.1.2. Antibodies

Table 2.2. Primary antibody sources and dilutions. List of primary antibodies used for immunofluorescence (IF) or Western blotting (WB) in this thesis. *Dr. Emyr Lloyd-Jones (Cardiff University, School of Biosciences). †HRP conjugated primary antibody. Abbreviations: microtubule associated protein 1 light chain 3 B, LC3B; horse radish peroxidase, HRP.

Antibody	Species	Source	Cat. No.	IF dilution	WB dilution
LC3B	Rabbit	Cell Signaling	2775S	1:400	-
Cathepsin D (H75)	Rabbit	Santa Cruz	sc-10725	1:50-500	1:1000
Cathepsin D (G19)	Goat	Santa Cruz (gifted by ELJ*)	sc-6494	1:200	-
Cathepsin D	Rabbit	Calbiochem (gifted by ELJ*)	219361	1:200	-
Cathepsin B	Goat	Santa Cruz	sc-6493	1:250	1:1000
Clathrin heavy chain	Mouse	BD Biosciences	610449	-	1:1000
Transferrin receptor	Mouse	Life Tech	13-6800	-	1:1000
β-tubulin (HRP)†	Rabbit	Abcam	ab21058	-	1:50,000

Table 2.3. Secondary antibody sources and dilutions. Antibodies were used for either IF or WB experiments with primary antibodies indicated in the "Use with" column. Abbreviation: microtubule associated protein 1 Light Chain 3 B, LC3B; Cathepsin D, CathD; Cathepsin B, CathB.

Antibody	Species	Tag	Source	Cat. No.	Dilution	Use with
For IF:						
Anti-rabbit	Goat	Alexa 647	Life Tech.	A11010	1:400	LC3B, CathD (H75)
Anti-goat	Rabbit	Alexa 647	Life Tech.	A21085	1:400	CathD (G19), CathB
Anti-rabbit	Goat	Alexa 488	Life Tech.	A31556	1:400	CathD (Calbiochem)
For WB:						
Anti-rabbit	Goat	HRP	Thermo Scientific	32460	1:1000	CathD
Anti-goat	Rabbit	HRP	Life Tech.	R21459	1:1000	CathB
Anti-mouse	Goat	HRP	Thermo Scientific	32430	1:1000	Clathrin heavy chain, transferrin receptor

2.2. Cells and cell culture

2.2.1 Cells, media and cell culture conditions

MCF-7, MDA-MB-231, T47D, and BT474 cells were originally obtained from AstraZeneca or directly from ATCC. MCF-10A cells were purchased during the course of this thesis from ATCC. Cells were cultured at 37°C and 5% CO_2 in a humidified incubator and their growth monitored every 2/ 3 days via brightfield microscopy. MCF-7, MDA-MB-231, T47D, and BT474 cells were maintained in RPMI 1640 media containing 300 mg/ ml L-glutamine and phenol red, as obtained from supplier, and additionally supplemented with 10%

heat inactivated FBS (HI-FBS; heat inactivated by 30 min incubation in a 56°C water bath) which was sterile filtered using a 0.22 µm filter. MCF-10A cells were maintained in phenol red and L-glutamine containing DMEM/ F12 additionally supplemented with filter sterilised 5% HI-horse serum, 100 ng/ ml cholera toxin, 10 µg/ ml insulin, 20 ng/ ml EGF, and 500 ng/ ml hydrocortisone (Santner *et al.,* 2001). Herein these are respectively termed cell culture media. All cell lines were grown in the absence of antibiotics.

For microscopy studies, cells were placed in cell imaging media which consisted of phenol red free RPMI 1640 supplemented with 10% HI-FBS and 50 mM HEPES pH 7.4 that was filter sterilised before use.

2.2.2. Routine cell culture

All cell culture solutions were pre-warmed to 37°C in a water bath and cell work was conducted in a sterile cell culture hood which was thoroughly disinfected with 70% ethanol prior to and following use. Once cells had achieved 70% confluency in a T75 cell culture flask they were passaged by washing once with sterile 1.5 ml phosphate buffered saline (PBS) and once briefly with 1 ml 0.05% trypsin/ EDTA. Cells were then incubated for 3 min (MCF-7, MDA-MB-231, T47D, and BT474) or 15 min (MCF-10A) with 1 ml trypsin/ EDTA or until 90% of cells were detached. Cell culture media (6 ml) was added to the resulting suspension which was centrifuged at 900x g for 3 min and the supernatant containing the media and trypsin/ EDTA discarded, hereafter this process is referred to as trypsinisation. The cell containing pellet

was resuspended in 10 ml cell culture media and used in experiments or a proportion added to a new T75 cell culture flask. For MDA-MB-231, cells were split at a ratio of 1/ 5, whereas MCF-7 and MCF-10A cells were split 2/ 5 and T47D and BT474 were split 1/ 2. Cell culture media was then added to the flask so that the final cell culture volume was 10 ml.

Frozen cell stocks were made using cells at the lowest possible passage number (passage 12-16 for MCF-7, MDA-MB-231, T47D, and BT474 and passage 4 for MCF-10A). Prior to freezing, cells were grown in T75 cell culture flasks until 65-70% confluent (log phase growth) before trypsinisation. Cells were then resuspended in 6 ml cell culture media containing 20% HI serum, 5% DMSO and 2 ml of the resulting suspension aliquoted into cryovials. These were then placed in an isopropanol containing Mr. Frosty™ freezing container and placed overnight first at -20°C and then -80°C, before long-term storage in liquid nitrogen. To defrost, cryovials were removed from liquid nitrogen and incubated at 37°C until completely defrosted. Immediately following this, the cells were added to 10 ml pre-warmed cell culture media and the resulting suspension centrifuged at 900x g for 3 min. The cell pellet was then resuspended in 6 ml cell culture media, which was added to a T25 flask. Upon achieving 70% confluency, cells were transferred to a T75 flask and passaged at least once more before use in experiments. Cancer cells (MDA-MB-231, MCF-7, T47D and BT474) were cultured until reaching a maximum passage 28, whilst MCF-10A cells were cultured till passage 11 before new cell aliquots were defrosted.

2.2.3. *Mycoplasma* testing

All cell lines grown in the lab were tested for *Mycoplasma* approximately every 6 months via the commercial polymerase chain reaction (PCR) based "LookOut® *Mycoplasma* PCR Detection Kit" used with "JumpStart™ Taq DNA Polymerase". This assay amplifies a region of DNA highly conserved between *Mycoplasma* and *Acholeplasma* and can therefore detect all common cell culture infectants. For this, 500 µl samples of fresh (<24 hr) cell culture media from cells grown to 90-100% confluency were taken from T75 flasks. Samples were then heated at 95°C for 10 min, centrifuged at 13,000x g for 10 sec and the supernatant retained and stored at 4°C before testing. PCR tubes were supplied pre-loaded with primers, nucleotides, internal control DNA and gel loading buffer, additionally positive control tubes contained DNA from non-infectious *Mycoplasma orale*. A mastermix of 0.5 µl polymerase (stock 2.5 units/ µl) and 22.5 µl rehydration buffer (as provided by supplier) per sample was prepared and added to the pre-loaded PCR tubes. Samples or negative control (autoclaved dH$_2$O) were added to tubes at a volume of 2 µl, so that final volume in the tube was 25 µl, for positive control 25 µl of mastermix only was added to each tube. Samples were then placed in a PCR thermal cycler with a 105°C heated lid and the programme set as follows:

No activation step

1 cycle 94°C for 2 min

40 cycles 94°C for 30 sec

55°C for 30 sec

72°C for 40 sec

Held at 4°C and left over night.

The following day a 1.5% agarose gel was cast by mixing 1.5 g agarose in 100 ml TAE buffer (140 mM Tris-base, 20 mM acetic acid, 1 mM EDTA dissolved in dH_2O). This was gradually heated in a microwave to prevent boiling, until complete dissolution of the agarose and allowed to partially cool. Ethidium bromide (50 µl of 5 µg/ ml stock) was added to the solution and the gel was cast using a 5 mm comb. After the gel had set, the tank was filled with TAE buffer, gel loaded with the 6 µl/ well PCR products and run for 2 hr at 80 V. The gel was then analysed in a BioRad ChemiDoc imaging system.

2.3. Viability studies

2.3.1. Establishing density of cells in solution

To calculate the number of cells per ml solution for use in counting studies (Section 2.3.2) and for plating, cells were trypsinised and resuspended in 10 ml cell culture media. A sample (50 µl) of the cell suspension was mixed in a 1:1 ratio with trypan blue and gradually added to each of two chambers of a haemocytometer. The cells were then visualised using brightfield microscopy, and trypan blue-free cells counted in two of the four grids of each chamber in the haemocytometer, i.e. a total of four grids. The number of cells per ml was determined using the following equation:

Cells per ml= Trypan blue-free cells counted x 2* x 10,000
                                    4†

*to account for 1:1 trypan blue dilution

†number of grids counted

To calculate the volume of cell suspension required for cell plating the following equation was then used:

Volume (ml)= $\underline{\text{Required no. cells per ml x total required volume (ml)}}$
　　　　　　　　　　　　Counted cells per ml

This volume of cell suspension was then added to sufficient cell culture media for the total required volume.

2.3.2. Cell counting to determine cytotoxic effects

Cell counting is an established method to analyse the particular effect of any added reagent and was initially utilised to investigate disulfiram. MCF-7 and MDA-MB-231 cells were plated at a density of 70,000 and 56,000 cells per well respectively in 12 well plates in a final well volume of 2 ml. Cells were allowed to adhere for 24 hr before media was replaced with a 2 ml solution of 1 or 10 µM disulfiram or equivalent volume DMSO in cell culture media. After 24, 48 or 72 hr drug incubation, cells were trypsinised by briefly washing each well first with 500 µl sterile PBS then with 200 µl trypsin/ EDTA. They were then incubated with 150 µl tryspin/ EDTA for 3 min or until 90% detachment was observed and then resuspended in cell culture media to produce a final volume of 2 ml. The total number of cells in this suspension was determined using the methodology and equations described in Section 2.3.1. For each individual experiment duplicate assay points were obtained.

2.3.4. MTT and CellTiter Blue assays

2.3.4.1. Cell plating

To account for different growth rates, cells were seeded in 96 well plates at densities optimised to provide 70% confluency after a total incubation period of 96 hr. These are shown in Table 2.4.

Table 2.4. Table of seeding densities for 96 well plates for each line used in this study.

Cell Line	Number of cells/ well
MCF-7	2500
MDA-MB-231	2000
BT474	12,500
T47D	11,000
MCF-10A	3000

Cells were seeded by preparing a cell suspension of the required density which was then added to wells using a multi-channel pipette. For MTT and cell morphology assays cells were plated in transparent 96 well plates in a volume of 100 μl/ well, whereas for the CellTitre Blue fluorescence assay plating was conducted in black 96 well plates containing 50 μl/ well. For all assays the outermost wells of the plate were kept empty in order to minimise the influence of edge effects. "Blank" wells were also included which were treated identically to treatment wells but in the absence of cells and drugs.

2.3.4.2. Serial dilutions and cell treatments

Stock solutions of drugs were made at the highest possible concentration in order to minimise the effects of diluent on cytotoxicity (stock concentrations summarised in Table 2.1), for many drugs including disulfiram, DDC and disulfiram analogues this was 10 mM. Serial dilutions were typically prepared in a 10 fold dilution series to produce final concentrations ranging between 0.0001 and 100 µM in cell culture media. At 100 µM drug concentration from a 10 mM stock, the volume of drug stock added to the cell culture media was 1% of the total treatment solution, therefore this volume of diluent was added to negative control wells. Serial dilutions were prepared immediately before their addition to treatment wells and added in a volume equivalent to the media already present in the well. Additionally wells were treated with cell culture media in the absence of drug in order to determine the impact of DMSO on viability. Cells were treated in triplicate 24 hr after plating and then incubated for between 4-72 hr as described in results.

2.3.4.3. MTT assay

Exactly 4 hr prior to completion of the incubation time 20 µl MTT (from 5.5 mg/ ml stock in PBS) was added to each well using a multi-channel pipette. The plate was incubated for 4 hr under cell culture conditions before the contents of the wells were removed by inverting the plate. The formazan crystals produced by viable cells were dissolved by adding 200 µl DMSO to each well and the plate incubated at 37°C for 30 min. The absorbance produced by each well was finally measured on a plate reader set at 550 nm.

2.3.4.4. CellTiter Blue assay

In a similar manner to the MTT assay, 20 µl CellTiter Blue reagent, as provided by supplier, was added to each well 4 hr prior to completion of the incubation time. The plate was then maintained under cell culture conditions for the remainder of the experiment and the fluorescence produced by live cells determined using a Fluostar Optima fluorescent plate reader (Excitation filter= 544nm, emission filter= 590nm).

2.3.5. Live cell imaging of cell morphology following disulfiram treatment

The morphology of MCF-7 and MDA-MB-231 cells was evaluated in order to qualitatively assess the toxic effects of disulfiram treatment following 72 hr incubation. For this, MCF-7 and MDA-MB-231 cells were seeded in transparent 96 well plates at a densities described in Table 2.4 at 100 µl/ well. Exactly 24 hr after plating, cells were treated with disulfiram in a 10 fold serial dilution between 1-100 µM, DMSO equivalent to the highest drug concentration (i.e. 1%) or cell culture media, in triplicate. Cells treated with cell culture media in the absence of drug or DMSO served as a comparison to determine the toxic effects of DMSO and ensure that untreated cells retained their characteristic growth rates and morphology as observed under normal cell culture conditions. Wells were incubated with the drug for 72 hr under cell culture conditions before a representative image of their morphology was taken using a Leica wide field DMIRB fluorescence inverted microscope equipped with a 40x objective on its brightfield setting. Media and DMSO treated wells were imaged last to ensure that that any toxic phenotype observed with

disulfiram treatment was not a result of cells being removed from cell culture conditions.

2.3.6. Propidium iodide (PI) uptake in disulfiram treated cells

As a means to measure cytotoxicity, the ability of disulfiram to influence uptake of PI, a dye only permeable to cells with a compromised plasma membrane, was analysed via microscopy. MDA-MB-231 and MCF-7 cells were plated onto 35 mm MatTek imaging dishes at a density of 75,000 and 100,000 cells per dish. After 24 hr incubation, cell culture media was removed and replaced with a 2 ml solution of 1 µM disulfiram or equivalent DMSO in cell culture media. The dish was then incubated under cell culture conditions for an additional 72 hr, after which the treatment solution was replaced with cell culture media containing 500 ng/ ml PI. The dish was then incubated for a further 30 min before it was washed thrice with 1 sterile PBS, and imaging of a representative field conducted in the presence of cell imaging media using a Leica wide field DMIRB fluorescence inverted microscope equipped with a 40x objective. Dishes were prepared immediately prior to imaging which lasted no more than 15 min in order to minimise the time which cells were outside of cell culture conditions.

2.4. Plating and fixation techniques for fluorescence microscopy

2.4.1. Plating cells on coverslips

In order to conduct the mitochondrial fragmentation and immunofluorescence studies described in Sections 2.5.1 and 2.6, cells were first plated onto coverslips. Coverslips were maintained in 70% ethanol, 30% dH_2O to ensure sterility and added to a 12 well plate 30 min before the addition of cells. Coverslips were washed thrice with 1 ml sterile PBS before plating to ensure the complete removal of ethanol immediately prior to cell plating. MCF-7 and MDA-MB-231 cells were then added to the wells at a density of 125,000 and 100,000 cells/ well respectively in 2 ml cell culture media and left overnight to adhere before being processed as described in Sections 2.5.1 and 2.6.

2.4.2. Paraformaldehyde (PFA) fixation

For cathepsin D and B immunofluorescence studies (Section 2.6.2), cells were fixed with PFA. For this fixation technique, wells were washed thrice with 1 ml PBS before the addition of 1 ml 3% PFA dissolved in PBS. Following 15 min incubation at room temperature, they were then subjected to an additional 3x 5 min PBS washes. A 1 ml solution of 50 mM ammonium chloride dissolved in PBS was added to each well and incubated for 10 min at room temperature in order to quench autofluorescence. Wells were finally washed three times with PBS before being further processed for immunofluorescence analysis.

2.4.3. Methanol and acetone fixation

Methanol was used for fixing cells in LC3B immunofluorescence studies (Section 2.6.1), acetone was used in mitochondrial fragmentation studies (Section 2.5.1) and optimisation of cathepsin D immunofluorescence involved both fixatives (Section 2.6.2). For these studies fixation involved removing cells from 37°C incubation and then maintaining them on ice throughout the fixation procedure. Coverslips were first washed three times with 1 ml chilled PBS, and then incubated with 1 ml chilled 100% methanol or 80% acetone, 20% dH$_2$O at -20°C for 10 min. Coverslips were washed again with PBS 3x 5 min before being further processed for analysis.

2.5. Fluorescent probes

2.5.1. Effects of disulfiram on mitochondrial fragmentation

The ability of disulfiram to alter the appearance of the mitochondrial network was determined as a means of more effectively evaluating the drug's cytotoxic effects. MCF-7 or MDA-MB-231 cells were plated onto coverslips (Section 2.4.1) and allowed to adhere overnight. The following day the media was replaced with a 2 ml solution of 1 µM disulfiram or equivalent volume DMSO diluted in cell culture media and incubated under cell culture conditions for between 1-72 hr in duplicate. The media was then removed and replaced with 100 nM of MitoTracker Red reagent diluted in serum free RPMI 1640 and incubated under cell culture conditions for an additional 30 min. Cells were then fixed via acetone (Section 2.4.3) and mounted onto slides using Dako oil.

Slides were allowed to dry for 30 min before being sealed with clear nail varnish and a representative field imaged a Leica SP5 confocal inverted microscope equipped with a 40x objective and 633 nm laser.

2.5.2. Live cell imaging of intracellular zinc

The zinc dye, Fluozin-3, was used to visualise changes in intracellular zinc levels in live cells upon disulfiram treatment. MCF-7 or MCF-10A cells were plated onto 35 mm MatTek imaging dishes at densities of 250,000 and 300,000 cells/ dish and left to adhere overnight. The following day, media was replaced with 1 ml cell culture media containing 5 µM Fluozin-3 and incubated under cell culture conditions for 30 min. The dish was then washed three times with PBS, 1 ml cell imaging media added and placed on a confocal microscopy stage pre-heated to 37°C. Representative regions of cells were captured using a 488 nm laser before and subsequent to the drop wise addition of 1 ml cell imaging media containing 10 µM disulfiram, sodium pyrithione (NaP; positive control) or diluent control. The same field was then imaged as indicated in the results over a period of 30 min.

2.5.3. Flow cytometry to quantify disulfiram effects on Fluozin-3 fluorescence

A flow cytometry assay was developed to quantify changes in Fluozin-3 fluorescence upon disulfiram treatment under various experimental conditions. For this MCF-7, MDA-MB-231 and MCF-10A cells were plated into 12 well

plates at densities of 125,000, 100,000 and 150,000 cells/ well respectively and returned to cell culture conditions overnight. Under normal experimental conditions, the following day media was replaced by 1 ml cell culture media containing 5 μM Fluozin-3 and incubated for 30 min. However, where indicated in results cells were instead incubated with serum free media +/- 20 μM $ZnCl_2$ or $CuCl_2$ containing 5 μM Fluozin-3. In these studies this variation in media constituents was maintained throughout the experimental procedure. Wells were then washed three times with 1 ml PBS and treated for 10 min with media containing 1-100 μM disulfiram, 100 μM DDC, 100 μM FS03EB, 10 μM NaP or DMSO equivalent to the highest drug concentration. Cells were detached as described in Section 2.3.2, resuspended in 500 μl PBS per well, added to a pre-cooled eppendorf and maintained on ice for all subsequent steps. Detached cells were pelleted by centrifugation at 200x g, $4^{o}C$ for 5 min, the supernatant discarded, and washed with 500 μl pre-cooled PBS. They were centrifuged again before being resuspended in cell imaging media or serum free imaging media +/- 20 μM $ZnCl_2$ or $CuCl_2$. Flow cytometry was conducted using a BD Biosciences FACSVerse system using a 488 nm laser. For each assay point, 10,000 events were analysed and the geometric mean of samples recorded.

2.5.4. Comparative localisation of intracellular zinc with endocytic probes in disulfiram treated cells

As the endocytic fluorescent probe dextran-Alexa 647, specifically pre-labels the fluid phase endocytic pathway and lysosomes of cells, it therefore could be

used to investigate whether disulfiram localised zinc to endocytic organelles (Al-Taei *et al.,* 2006; Sayers *et al.,* 2014). MCF-7 cells were plated onto 35 mm MatTek dishes as described in Section 2.5.2 and returned to cell culture conditions overnight. To label the entire fluid phase endocytic network, the following day media was replaced with 500 µl cell imaging media containing 250 µg/ ml dextran-Alexa 647 for 4 hr. To specifically label lysosomes, cells were incubated with dextran-Alexa 647 for 2 hr followed by three 1 ml PBS washes and 4 hr chase incubation with 500 µl cell imaging media. During the final stages of this incubation, the media was supplemented with 5 µM Fluozin-3 for 30 min, washed with PBS, and treated with 10 µM disulfiram for 10 min. Cells were then washed three times with 1 ml PBS, which was replaced with cell imaging media and representative images taken on a 37$^{\text{o}}$C pre-heated stage via live cell confocal microscopy using 633 and 488 nm lasers.

Pearson's coefficient is a commonly used statistic that describes the extent of co-localisation between two differently coloured images where 1.0 is perfect co-localisation, 0 reflects random distribution and -1.0 is a perfect inverse co-localisation. Pearson's coefficient is calculated by analysis of each pixel's intensity within two corresponding differently coloured channels, in this case red and green channels, to determine if there is a relationship between them. For this, ImageJ was used in combination with the JaCOP plug-in to quantify the extent of co-localisation between dextran-Alexa 647 and Fluozin-3. JaCOP was downloaded via the following link:

and saved in the "Plugins" folder of the ImageJ software. For analysis, confocal images from both fluorescent channels were opened in ImageJ individually. The JaCOP plug-in was opened in a new window by following the path: Plugins>JaCOP. Pearson's co-efficient was selected under "Analysis to perform" and the "Analyze" button produced the Pearson's coefficient value.

2.5.5. Effect of bafilomycin on disulfiram induced zinc uptake

Bafilomycin was used as an inhibitor of the endosomal H^+-ATPase pump to determine whether the sequestration of endo-lysosomal zinc in response to disulfiram required the pH gradient that exists between these compartments and the cytosol. For this MCF-7 cells were plated onto 35 mm MatTek dishes as described in Section 2.3.6 and the following day the media replaced with 2 ml cell culture media containing 80 nM bafilomycin or DMSO and returned to cell culture conditions for 2 hr. During the final stages of the incubation, cells were additionally treated with 5 μM Fluozin-3 for 30 min, washed three times with 1 ml PBS and treated for 10 min with 10 μM disulfiram or DMSO in cell culture media. Cells were then washed thrice with PBS and imaged in the presence of 2 ml cell imaging media via confocal microscopy using a 40x objective and a 488 nm laser on a stage pre-heated to 37°C. In order to ensure that this incubation period and concentration of bafilomycin could effectively decrease lysosomal pH, a bafilomycin control dish was prepared whereby cells were treated with 80 nM of the drug or DMSO for 2 hr as above and loaded

with 1 μM LysoSensor Green for the final 30 min of the incubation. LysoSensor Green is a fluorescent probe which localises to lysosomes and its fluorescent output is inversely proportional to lysosomal pH. Cells were then washed three times with PBS and imaged in cell imaging media via confocal microscopy.

2.5.6. Optimisation of acridine orange (AO) as an indicator of lysosomal membrane permeabilisation (LMP)

AO, a dye which becomes sequestered only in lysosomal compartments with intact membranes, was investigated for its potential to visualise LMP. For these studies, MCF-7 cells were plated onto 35 mm MatTek dishes as described in Section 2.3.6. After 24 hr under cell culture conditions, media was removed and replaced with 1 ml of 1.25, 2.5 or 5 μg/ ml AO in cell culture media. Cells were then incubated for 15 min under cell culture conditions before being washed three times with 1 ml PBS and addition of 1 ml cell imaging media. The dish was placed on a pre-heated 37°C microscope stage of a confocal microscope and a representative field imaged using a 488 nm laser and 40x objective (Pre-treatment). A "mock" treatment was added to the dish which consisted of 1 ml cell imaging media in the absence of drug and images of the same field taken between 2-10 min after treatment.

2.6. Immunofluorescence microscopy

2.6.1. Effect of disulfiram on localisation of LC3B as an indicator of autophagy

Immunofluorescence analysis was used to visualise changes in the localisation of LC3B, a protein which accumulates on autophagic membranes, upon disulfiram treatment. For this MCF-7 cells were plated onto coverslips as described in Section 2.4.1, and incubated overnight to allow adherence. The following day, cells were treated with disulfiram at a concentration of 10 μM for 6 hr, 1 μM for 24 hr, or an equivalent volume of DMSO in duplicate and maintained in cell culture conditions. Chloroquine (100 μM, 6 hr), an agent that causes LC3B accumulation via stabilisation of autophagosomal membranes, served as a positive control (Geng *et al.,* 2010). Coverslips were fixed with methanol, as described in Section 2.4.3 and then removed from 12 well plates and placed cell side down on 150 μl of blocking solution (5% FBS in PBS) for 1 hr at room temperature. They were then incubated overnight at 4°C in a new 12 well plate which was placed in a humidified chamber and contained a 1:400 dilution of LC3B primary antibody (Table 2.2) in 300 μl antibody dilution buffer (1% BSA in PBS) per well. The following day cells were washed with PBS 3x 5 min and coverslips placed cell side down on 150 μl of antibody dilution buffer containing Alexa 647 conjugated goat anti-rabbit secondary antibody diluted 1:400 (Table 2.3) and 1 μg/ ml Hoescht 33342 to label the nucleus. As secondary only controls, antibody dilution buffer only in the absence of primary antibodies was used. Coverslips were incubated with the antibody and dye for 2 hr at room temperature before being placed back in

the 12 well plate and washed with PBS 3x 5 min. Finally, coverslips were dipped in PBS then dH$_2$O and mounted onto slides. Imaging of representative fields was conducted via epi-fluorescence microscopy on a Leica wide field DMIRB fluorescence inverted microscope or confocal microscopy on a Leica SP5 confocal inverted microscope equipped with a 40x objective as indicated in results.

2.6.2. Optimisation of immunofluorescence methods for the detection of cathepsin B and D

The fact that disulfiram was shown to cause accumulation of zinc in endo-lysosomal compartments led to the investigation of whether these structures were damaged in response to the drug. For this, the ability of disulfiram to alter the localisation of lysosomal peptidases cathepsin B and D was determined via immunofluorescence. MCF-7 cells were plated onto coverslips (Section 2.4.1) and incubated overnight. Where indicated in results, cells were treated for 1 hr with 100 μM disulfiram or equivalent DMSO diluted in cell culture media and then fixed using PFA (Section 2.4.2), acetone or methanol (Section 2.4.3). Following washing in PBS the coverslips were placed on 150 μl of blocking solution (in the case of PFA fixation blocking solution was additionally supplemented with 0.3% Triton X-100 as a permeabilising agent) for 1 hr at room temperature. Coverslips were then returned to the 12 well plate and 300 μl of a 1:50-1:250 final dilution (as indicated in results) of primary antibody diluted in antibody dilution buffer (with 0.3% Triton X-100 for PFA fixed cells) added per well. Plates were then placed in a humidified chamber

and incubated overnight at 4°C. The following day coverslips were washed 3x 5 min with 1 ml PBS and placed on 150 µl of Alexa fluorophore conjugated secondary antibodies, as indicated in Table 2.3 and results in Chapter 6, diluted 1:400 in antibody dilution buffer and incubated at room temperature for 2 hr. Coverslips were finally washed in PBS 3x 5 min, dipped once in PBS, once in dH$_2$O and mounted onto slides. Imaging of a representative field was then conducted via confocal microscopy with a 40x objective using 633 nm or 488 nm lasers.

2.7. Lysate collection for Western blotting

The ability of antibodies to detect cathepsin D and B lysosomal proteases via Western blotting was investigated using untreated MCF-7 lysates. To collect the lysates MCF-7 cells were plated into 6 well plates at a density of 250,000 cells per well and left to adhere overnight. Plates were maintained on ice throughout the lysate collection procedure. They were first washed twice with ice-cold PBS (1 ml) and then 100 µl lysis buffer (150 mM sodium chloride, 50 mM Tris-base, 1% NP-40, pH 8 and protease inhibitor cocktail) added per well. Cells were incubated with the lysis buffer for 5 min whilst subjected to continual shaking and then removed from the wells by cell scraping. The resulting lysate suspension was transferred to a pre-cooled eppendorf, centrifuged at 13,000x g, 4°C for 10 min and the supernatant collected into a sterile pre-chilled eppendorf. Western blotting (Section 2.9) was then used for the detection of cathepsins D and B.

2.8. Subcellular fractionation to generate membrane and cytosolic fractions of cells

Subcellular fractionation was used to separate intracellular compartments and investigate localisation of cathepsin D and B within membrane and cytosolic fractions upon disulfiram treatment. For these studies MCF-7 cells were grown in 2x 10 cm cell culture dishes in a volume of 10 ml until 70-80% confluent, (Figure 2.1). Dishes were treated with 100 μM disulfiram or equivalent DMSO in 5 ml cell culture media for 1 hr, then the dishes were transferred onto ice, washed three times with 2 ml ice-cold HES buffer (20 mM HEPES, 1 mM EDTA, 250 mM sucrose, protease inhibitor cocktail, pH 7.4) and finally overlaid with 1 ml HES buffer. The cells were detached from plates via scraping, the resulting cell suspension added to a pre-chilled eppendorf and centrifuged at 200x g, 4^oC for 5 min to isolate a cell pellet. The supernatant was discarded and cell pellets from dishes under the same experimental conditions (for example, pellets from two dishes treated with 100 μM disulfiram) combined in 500 μl HES buffer and added to a single eppendorf. Cells were then passed through a 21 gauge needle approximately 40 times until plasma membranes, but not nuclear envelopes, were lysed. This process was monitored via microscopy using trypan blue staining that will not label intact cells but clearly labels released nuclei. This suspension was centrifuged at 4000x g, 4^oC for 2 min, and the resulting post nuclear fraction (PNF) collected
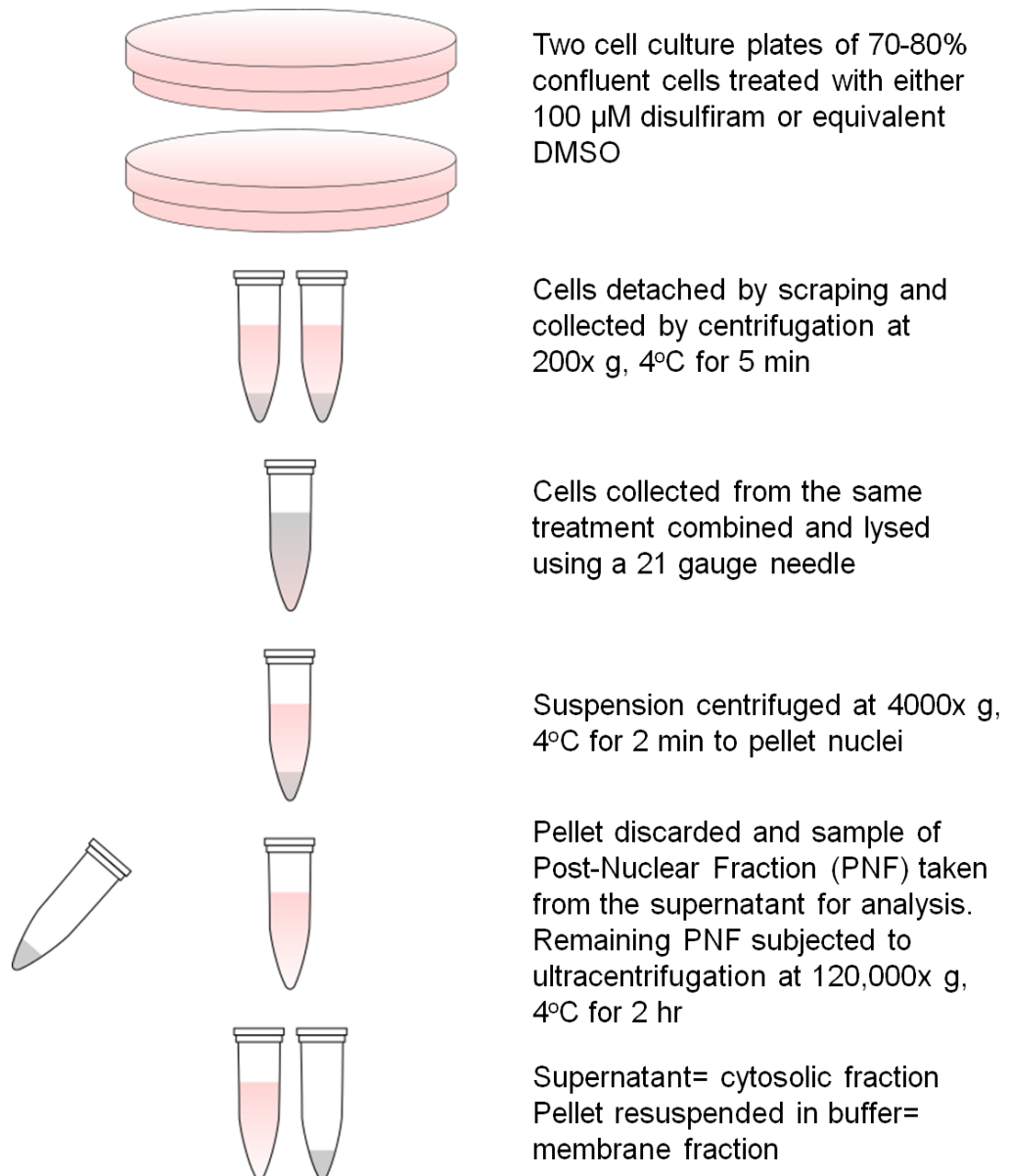
Figure 2.1. Schematic of the subcellular fractionation procedure.

as a supernatant. A 50 µl sample of PNF was retained and the remaining volume transferred to a clean pre-chilled tube and subjected to ultra-centrifugation at 120,000x g, 4°C for 2 hr. The cytosolic fraction was collected from the supernatant and the pellet (membrane fraction) was resuspended in 60 µl HES buffer. Cathepsin B and D was then detected via Western blotting, as described in Section 2.9.

2.9. Protein quantification and Western blotting

2.9.1. Protein quantification: Bicinchoninic Acid (BCA) assay

Once samples had been prepared (Sections 2.7 and 2.8), their protein concentration was determined via the BCA assay. BSA was used for preparation of protein calibration curves at concentrations of 0-1 mg/ ml. BSA was prepared in lysis or HES buffer for samples collected from cell lysates or subcellular fractionation respectively. Sample concentrations were expected to exceed the linear BSA range and were further diluted 1:2 with lysate or HES buffer. A solution of 49 parts BCA to 1 part copper sulphate was prepared and 200 µl added to each well of a 96 well plate which was maintained on ice. BSA protein standards (in triplicate) and diluted samples (in duplicate) were added to the wells in a volume of 10 µl per well. The plate was then incubated at 37°C for 30 min and absorbance measured using an automated plate reader at 562 nm. The concentration of samples was determined by extrapolating from a calibration curve generated in Microsoft Excel using BSA standards. Samples were then diluted in buffer so that they were all at the same concentration for electrophoresis.

2.9.2. SDS-PAGE electrophoresis, and Western blotting

Samples were mixed in a 3:1 ratio with loading buffer (2% SDS, 10% glycerol, 0.02% bromophenol blue, 62.5 mM Tris-HCl, 400 mM dithiothreitol (DTT)), and heated to 95°C for 5 min. They were then centrifuged at 13,000x g for 1 min to pellet debris and either stored at -20°C or used immediately. A 12% pre-

cast gel (Mini-PROTEAN TGX, Bio-Rad) was added to the electrophoresis tank which was filled with running buffer (385 mM glycine, 250 mM Tris-base, 0.5% SDS dissolved in dH_2O). Wells were washed in running buffer, 25 µl of the samples added to six lanes and 5-10 µl of molecular weight marker added to two lanes of the gel. The proteins were separated for 1 hr 25 min at 100 V and then the gels were then removed from the electrophoresis tanks and washed for 5 min with transfer buffer (250 mM glycine, 20 mM Tris-base pH 8, 20% methanol and 80% dH_2O) in preparation for protein transfer.

2.9.3. Protein transfer and immunodetection

PVDF membranes were pre-soaked for 1 min in methanol and 10 min in transfer buffer. Additionally the blotting paper and sponges was soaked for 10 min in transfer buffer. The transfer sandwich was prepared with sponges, blotting paper, gel and PVDF membrane and added to the transfer tank which contained pre-chilled transfer buffer and an ice block. Transfer was conducted at 100 V for 1 hr during which the buffer was continually stirred with a magnetic stirrer. The membrane was removed from the transfer sandwich, washed once with dH_2O, incubated at room temperature for 5 min with Ponceau S solution and washed again with dH_2O. The Ponceau S stained membrane was used to check protein loading and transfer efficiency. The membrane was washed again with dH_2O and blocked for 1 hr in 5% milk diluted in PBST (0.025% Tween in PBS). It was then cut into strips at appropriate molecular weight for the proteins of interest and incubated overnight at 4^oC with 2% milk diluted in PBST containing primary antibodies

(cathepsin D, cathepsin B, transferrin receptor, and clathrin heavy chain) at concentrations indicated in Table 2.2. For subcellular fractionation samples ß-tubulin and transferrin receptor was detected as loading controls for cytosolic and membrane proteins respectively and in order to normalise band intensities between disulfiram and DMSO treatment for each fraction. The membrane was then washed in PBST 3x 5 min and incubated with HRP conjugated secondary antibodies diluted in 2% milk for 1 hr as indicated in Table 2.3. The exception to this procedure was when using the HRP conjugated ß-tubulin primary antibody which was diluted in 5% milk and incubated with the membrane for 1 hr at room temperature directly after blocking. The membrane was subjected to 3x 5 min PBST washes and developed by 5 min incubation at room temperature with Clarity ECL substrate. The membrane was then imaged using a Bio-Rad ChemiDoc.

2.9.4. Densitometry

Images were assessed for saturation using Bio-Rad's Image Lab software which labels saturated pixels red. Non-saturated TIFF images were chosen for densitometry analysis, and were opened in ImageJ and converted to greyscale by Image>Type>8-bit. The "Rectangular Selections" tool was used to highlight the first band and the path Analyze>Gels>Select First Lane used to label the band as lane "1". The rectangular selection was then dragged to the second lane and Analyze>Gels>Select Next Lane used to label lane "2". This process was repeated until all lanes had been labelled and then Analyze>Gels>Plot Lanes used to show the profile plot of each selection with the height of the peak

indicating band intensity. The "Straight Line Tool" was used to mark the base of each peak in order to distinguish between band intensity and background noise. Using the "Wand Tool", each peak was selected and the peak area displayed in a pop up window. Peak areas were copied into Microsoft Excel. Results are expressed as a percentage of the DMSO band intensity for each fraction.

2.10. Statistical testing

Unless otherwise stated in figure legends, the data presented represent analysis from three independent experiments. Significance of differences between two datasets were determined, as appropriate, using students two tailed T-test in Microsoft Excel and displayed as $*p<0.05$ or $**0.001$. For comparisons of three or more datasets, significance was determined by one-way analysis of variance (ANOVA) combined with Dunnett's test using GraphPad Prism software. Data is presented as the mean, or for flow cytometry data geometric mean, and error bars represent standard error of the mean.

References

Al-Taei, S., Penning, N. A., Simpson, J. C., Futaki, S., Takeuchi, T., Nakase, I. and Jones, A. T. 2006. Intracellular traffic and fate of protein transduction domains HIV-1 TAT peptide and octaarginine. Implications for their utilization as drug delivery vectors. *Bioconjugate Chemistry.* 17(1), p. 90-100.

Geng, Y., Kohli, L., Klocke, B. J. and Roth, K. A. 2010. Chloroquine-induced autophagic vacuole accumulation and cell death in glioma cells is p53 independent. *Neuro-Oncology.* 12(5), p. 473-481.

Santner, S. J., Dawson, P. J., Tait, L., Soule, H. D., Eliason, J., Mohamed, A. N., Wolman, S. R., Heppner, G. H. and Miller, F. R. 2001. Malignant MCF10CA1 cell lines derived from premalignant human breast epithelial MCF10AT cells. *Breast Cancer Research and Treatment.* 65(2), p. 101-110.

Sayers, E. J., Cleal, K., Eissa, N. G., Watson, P. and Jones, A. T. 2014. Distal phenylalanine modification for enhancing cellular delivery of fluorophores, proteins and quantum dots by cell penetrating peptides. *Journal of Controlled Release.* 195, p. 55-62.

3. Cytotoxic effects of disulfiram in breast cancer cells

3.1. Introduction

Disulfiram induced cytotoxicity has been reported in a variety of cancer cell lines including myeloma, prostate, melanoma, glioblastoma, colorectal, osteosarcoma and breast, indicating that the drug may have potential in the treatment of a wide range of cancer types (Wang *et al.,* 2003; Brar *et al.,* 2004; Chen *et al.,* 2006; Lovborg *et al.,* 2006; Cho *et al.,* 2007; Lin *et al.,* 2011; Hothi *et al.,* 2012). However, a biphasic response to the drug has been observed whereby despite sensitivity at lower concentrations viability is partially restored at ~10 μM which may have implications in its therapeutic use (Wickstrom *et al.,* 2007; Guo *et al.,* 2010; Yip *et al.,* 2011). Despite its frequency within the literature and the possible clinical limitation, this effect remains largely uncharacterised and its molecular causes are unresolved. It has, however, been noted for the disulfiram analogue PDTC that extracellular signal regulated kinase (ERK) dephosphorylation and JNK phosphorylation in response to the drug also occurs biphasically (Chung *et al.,* 2000). The ability of disulfiram to induce cell death has been largely attributed to occur via apoptosis as determined by cleavage of the caspase target protein poly ADP ribose polymerase (PARP) and increased Annexin V staining, a measurement of the apoptotic redistribution of phosphatidylserine onto the outer leaflet of the plasma membrane (Cen *et al.,* 2004; Chen *et al.,* 2006). However little has been done to determine the role of other cell death modalities in the anti-cancer response to the drug, although one study in fibrosarcoma and cervical cancer

cells has observed paraptosis, defined as the vacuolisation of the endoplasmic reticulum, in response to disulfiram (Tardito *et al.,* 2011).

One of the most widely studied potential anti-cancer applications of disulfiram is as a future breast cancer therapy; particularly as a supplement to other treatments. Here the drug's cytotoxicity has most frequently been investigated in MDA-MB-231, MCF-7 and T47D cell lines (Yip *et al.,* 2011). However there is conflicting evidence regarding the sensitivity of MDA-MB-231 cells to the drug, as it has been shown that IC_{50} values range from <0.5 μM to >10 μM (Brahemi *et al.,* 2010; Yip *et al.,* 2011; Liu *et al.,* 2013). One study has suggested that these cells lack disulfiram sensitivity due to low expression of BCA2, an E3 ubiquitin ligase thought to be associated with ER^+ breast cancer development and a proposed target of the drug (Brahemi *et al.,* 2010). However other potential anti-breast cancer mechanisms exist and it has been observed that disulfiram is also able to inhibit the proteasome, NFκB signalling and act as a copper ionophore which may also contribute towards its toxic effects (Chen *et al.,* 2006; Yip *et al.,* 2011; Allensworth *et al.,* 2015). Interestingly breast cancer cells also differ in their biphasic response which has only been observed in MDA-MB-231 and MCF-7 but not T47D cells (Yip *et al.,* 2011). Additionally, there is some evidence to suggest that disulfiram is selectively toxic to breast cancer cells, as MCF-10A breast epithelial cells retain normal morphology in conditions which produce apoptosis in the metastatic form of this cell line (Chen *et al.,* 2006).

Many assays exist to measure viability effects, commonly they rely on end-points such as morphological features, metabolic enzyme activity, membrane permeability, cell cycle arrest and detection of proteins involved in specific cell death pathways, for example caspases. An ideal viability assay would be highly reproducible, easy to implement and interpret and high through-put.

Aims and Objectives

The primary objective of this chapter is to compare commonly used viability assays and assess which is the most suitable for the study of disulfiram cytotoxic effects. A secondary objective is to provide further characterisation of disulfiram cytotoxicity in a range of breast cancer cell lines. The aims of this chapter are therefore:

- To compare and optimise different cytotoxicity assays to measure the response of breast cancer cells to disulfiram.
- To investigate the cytotoxicity profile of the drug in these cells.
- To provide insight into the method of cell death in response to disulfiram.

3.2. Results

3.2.1. Effect of disulfiram on cell number and morphology

Studies were initially conducted to investigate the suitability of various viability assays in determining the sensitivity of MCF-7 (ER$^+$) and MDA-MB-231 (ER$^-$) cells to disulfiram. These cell lines were chosen due to reported differences in BCA2 expression and the inhibitory effects of disulfiram on this protein; more importantly they also differ in their expression of ER which could be used to identify potential future treatment populations (Brahemi *et al.,* 2010). Initial experiments focussed on the effects of the drug on physical properties of cells, namely cell number and morphology. For counting experiments, cells were treated with 1 or 10 µM disulfiram or diluent control for 24-72 hr before detachment and cell counting on a haemocytometer. In MCF-7 cells 1 µM disulfiram significantly decreased cell number at 24 hr, however no statistical significance was achieved at longer time points, possibly due to high variability between repeat experiments (Figure 3.1A). When MCF-7 cells were treated with 10 µM disulfiram no significant data were obtained at any time point, although a 40% decrease in cell count was noted at 72 hr (Figure 3.1B). In comparison, the drug was unable to decrease the number of MDA-MB-231 cells at any concentration or time point, suggesting that this cell line is unresponsive to disulfiram viability effects (Figure 3.1C-D).
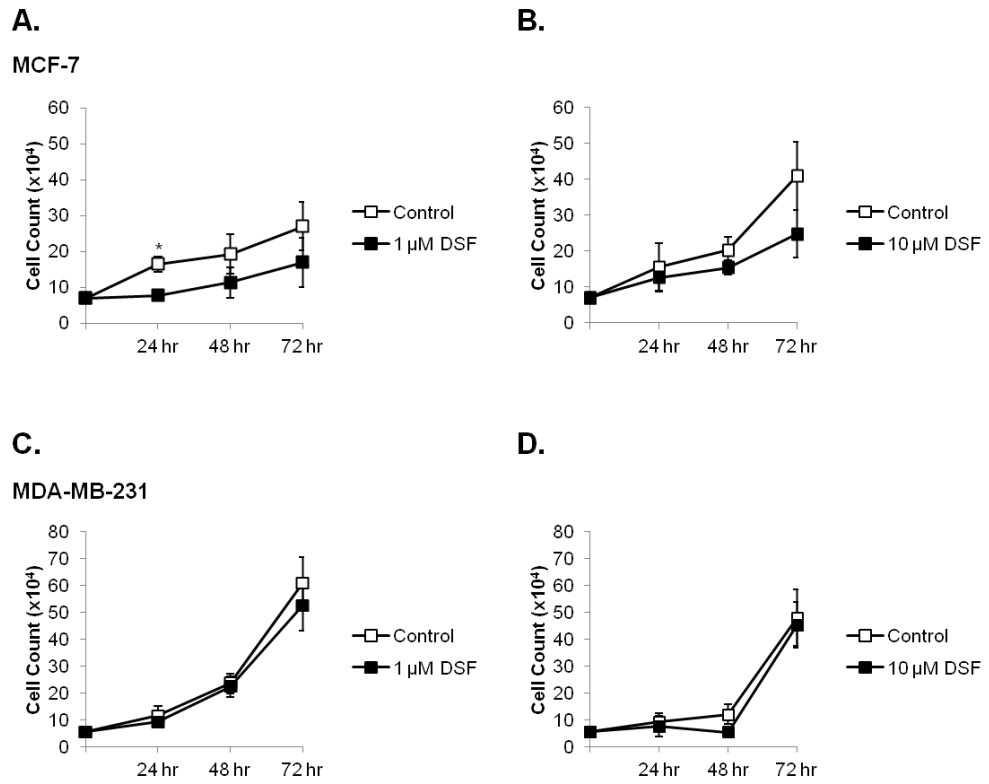
Figure 3.1. The effects of disulfiram on cell number. MCF-7 (A, B) and MDA-MB-231 (C, D) were treated with 1 (A, C) or 10 µM (B, D) disulfiram (DSF) or diluent control (DMSO) for the indicated time points. Cells were then detached and counted using a haemocytometer. T-tests were conducted between equivalent time points to compare disulfiram and control data. *p<0.05. Error bars show standard error.

To investigate the effects of disulfiram on cell morphology, cells were treated with 1-100 µM disulfiram and imaged via brightfield microscopy after 72 hr. In MCF-7 cells a biphasic response to the drug was observed whereby at 10 µM morphology was comparable with diluent control, however at 1 and 100 µM there was clear morphological damage indicating loss of viability (Figure 3.2A). In MDA-MB-231 cells, 1 µM disulfiram did not produce a toxic phenotype, however some cells exhibited signs of damage at 10 µM and at 100 µM very few viable cells remained (Figure 3.2B).
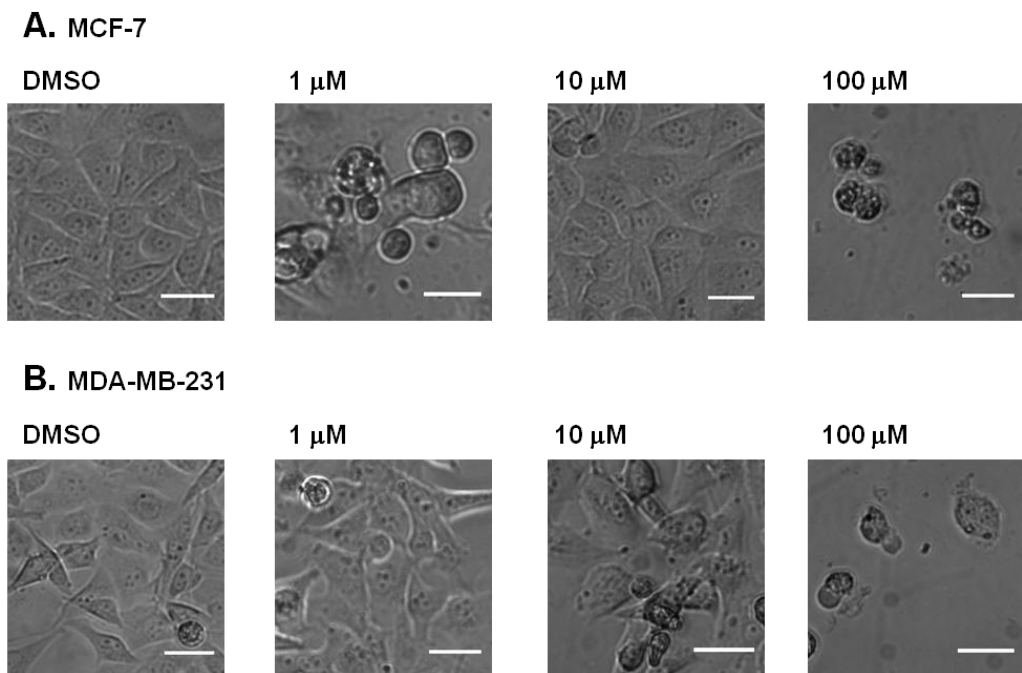

Figure 3.2. Representative images of the effects of disulfiram on cell morphology. MCF-7 (A) and MDA-MB-231 (B) cells were treated with the indicated concentration of disulfiram or diluent control (DMSO) for 72 hr before imaging via brightfield microscopy. Scale bars show 10 µm.

3.2.2. Disulfiram increases uptake of Propidium Iodide (PI) in MCF-7 but not MDA-MB-231 cells

To determine whether membrane permeability was an appropriate measurement for the cytotoxic effects of disulfiram, PI a dye which is only permeable to cells with a compromised plasma membrane, was investigated. This dye is often used to measure necrosis in short incubations and as a complementary necrosis probe in apoptosis assays that also measure the flipping of phosphatidylserine. For these studies cells were treated with 1 μM disulfiram for 72 hr before being stained with PI and live cells imaged 30 min later via epi-fluorescence microscopy. Accurate quantification of this technique using microscopy was not possible as the confluency of cells varied between fields of view and it was difficult to distinguish between individual cells in brightfield images. Despite this, the number of PI positive MCF-7 cells appeared to increase upon disulfiram treatment compared to diluent control (Figure 3.3A). In comparison and consistent with data from cell counting studies, MDA-MB-231 cells did not respond to the drug and the proportion of PI positive cells appeared similar between disulfiram and DMSO treatment (Figure 3.3B).
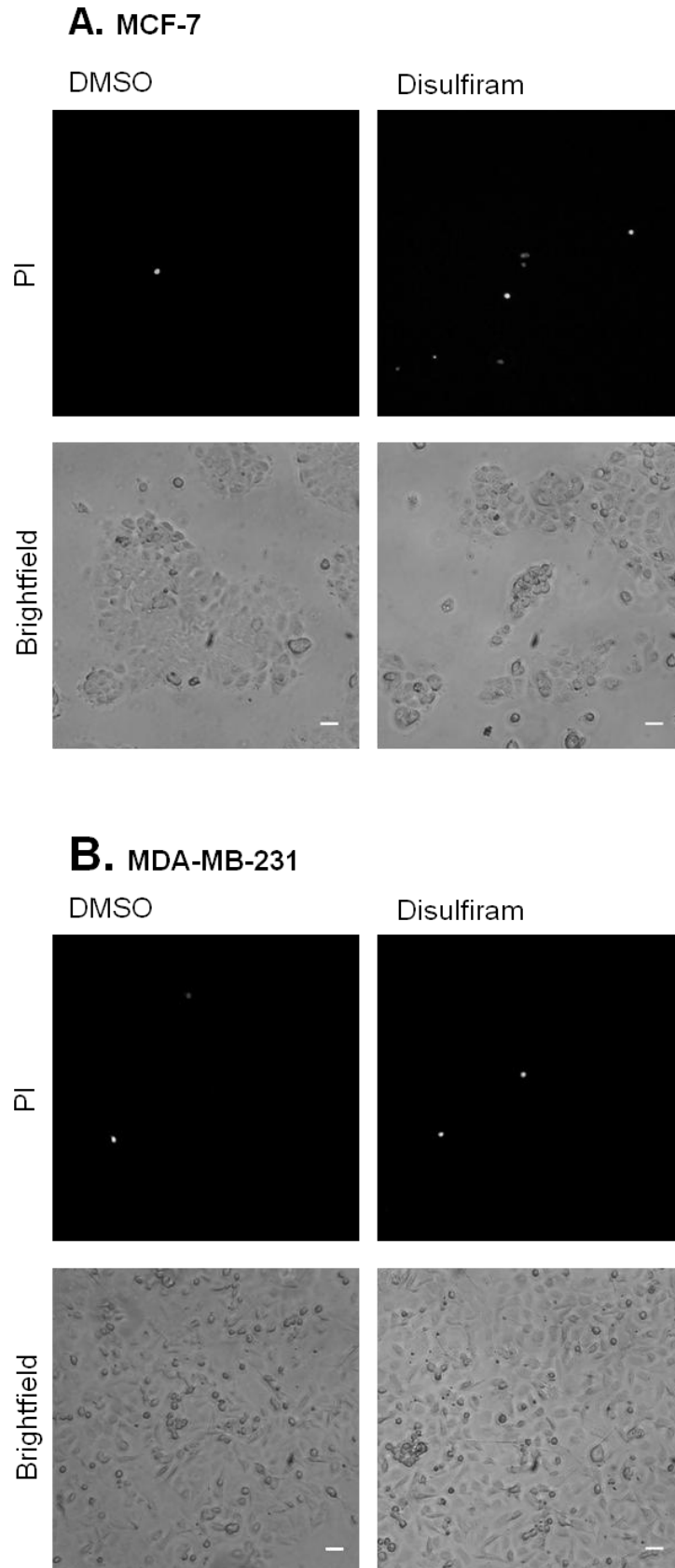
A. MCF-7

B. MDA-MB-231

Figure 3.3. Disulfiram increases propidium iodide uptake in MCF-7 but not MDA-MB-231 cells. MCF-7 (A) or MDA-MB-231 (B) cells were treated with 1 μM disulfiram or diluent control (DMSO) for 72 hr prior to staining with propidium iodide (PI). Live cells were then imaged via epi-fluorescence microscopy. Scale bars show 10 μm.

100

3.2.3. Disulfiram produces a biphasic toxicity profile in MCF-7 cells

Viability of disulfiram treated cells was then determined using assays which measure the activity of reductase enzymes. These enzymes alter the spectral properties of the redox sensitive dyes MTT and CellTiter Blue, therefore the detection of colorimetric or fluorescent products is higher in live cells. Initial experiments were conducted with serial dilutions of disulfiram for 72 hr prior to the addition of MTT or CellTiter Blue reagent. Reduction of MTT was then measured by dissolution of the resulting crystals in DMSO and analysis using a colorimetric plate reader. The CellTiter Blue assay provided a much simpler protocol whereby fluorescence was measured via an automated plate reader directly following incubation with the reagent, without the need for crystal dissolution. In both assays MCF-7 cells were highly sensitive to the drug with IC_{50} values of ~0.3 µM (Figure 3.4A-B). In support of earlier findings these cells also exhibited a biphasic peak where at 10 µM viability was partially restored, however this effect was more exaggerated in the CellTiter Blue assay. Despite data from the MTT assay indicating the sensitivity of MDA-MB-231
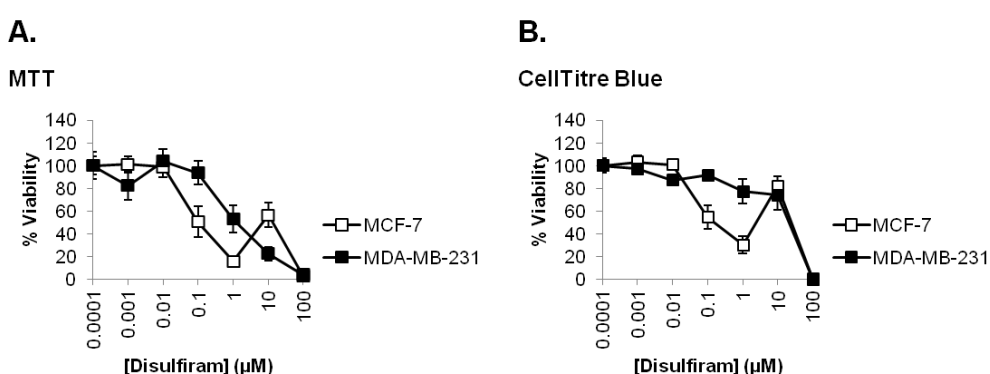

Figure 3.4. Disulfiram produces biphasic toxicity in MCF-7. MCF-7 or MDA-MB-231 cells were treated with a serial dilution of disulfiram and viability analysed after 72 hr via MTT (A) or CellTiter Blue (B) assay. Error bars show standard error.

cells at 1 and 10 μM, limited cytotoxic effects were observed at these concentrations when the CellTiter Blue assay was employed. Due to the consistency between these and earlier findings and the ease of implementation, the CellTiter Blue assay was used in further studies.

3.2.4. DMSO decreases cell viability at 1% and staurosporine produces a dose-response effect

To provide negative and positive controls for the CellTiter Blue assay, cells were treated with serial dilutions of either DMSO or staurosporine, a drug commonly used as a potent apoptosis inducer (Hasegawa *et al.,* 2012), for 72 hr and viability measured. Both cell lines were sensitive to the effects of DMSO at 1%, equivalent to 100 μM disulfiram, where viability was reduced to 67% and 80% for MCF-7 and MDA-MB-231 cells respectively (Figure 3.5A). However, no viability effects were noted below this concentration for either cell line. This data implies that some of the toxicity observed at 100 μM disulfiram in earlier studies may be attributable to the diluent. Despite the observed toxicity of DMSO at 1%, subsequent studies continued to extend the
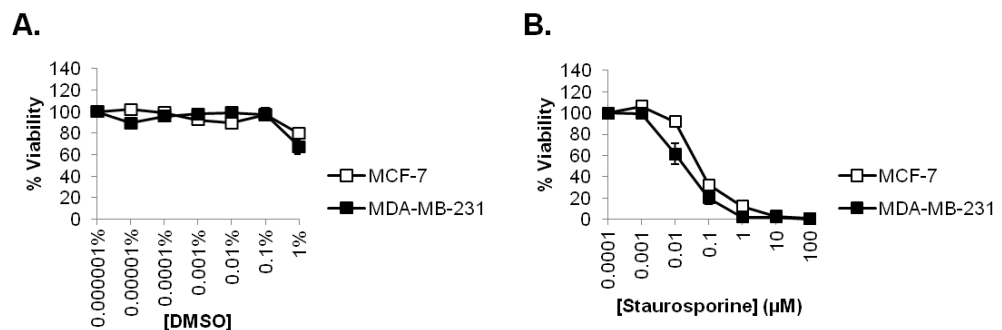

Figure 3.5. The cytotoxic profile of DMSO and staurosporine. Cells were treated with serial dilutions of DMSO (A) or staurosporine (B) for 72 hr and viability analysed via CellTiter Blue assay. 1% DMSO is equivalent to 100 μM disulfiram. Error bars show standard error.

concentration of the drug from 0.0001-100 µM for typical viability assays in order to demonstrate the limits of the biphasic peak observed at 10 µM (Figure 3.4). Both cell lines exhibited similar sensitivity to staurosporine which potently decreased cell viability with IC_{50} for both cell lines <0.1 µM (Figure 3.5B). Importantly, no biphasic peak was observed in MCF-7 cells demonstrating that this effect noted in previous studies is disulfiram dependent and not a result of this assay.

3.2.5. The cytotoxic effect of disulfiram is dependent on cell line, time and concentration

Viability studies using the CellTiter Blue assay were conducted in order to further characterise the cytotoxic effect of disulfiram on breast cancer cells. Viability was assessed in an extended panel of breast cancer cell lines chosen to model clinically relevant disease sub-types, these included ER^+/ $HER2^-$ (T47D), ER^+/ $HER2^+$ (BT474) and the non-cancerous breast epithelial MCF-10A line. Similarly to MCF-7, toxicity was observed in the ER^+ BT474 cell line (IC_{50} 0.3 µM) and produced a biphasic profile (Figure 3.6A). However not all ER^+ cells responded equally to the drug (T47D IC_{50} >10 µM) indicating that the presence of ER is not a pre-requisite for sensitivity. Equally, disulfiram was unable to produce cytotoxicity in the MCF-10A cell line (<10 µM) demonstrating that the drug is selectively toxic to cancer cells.
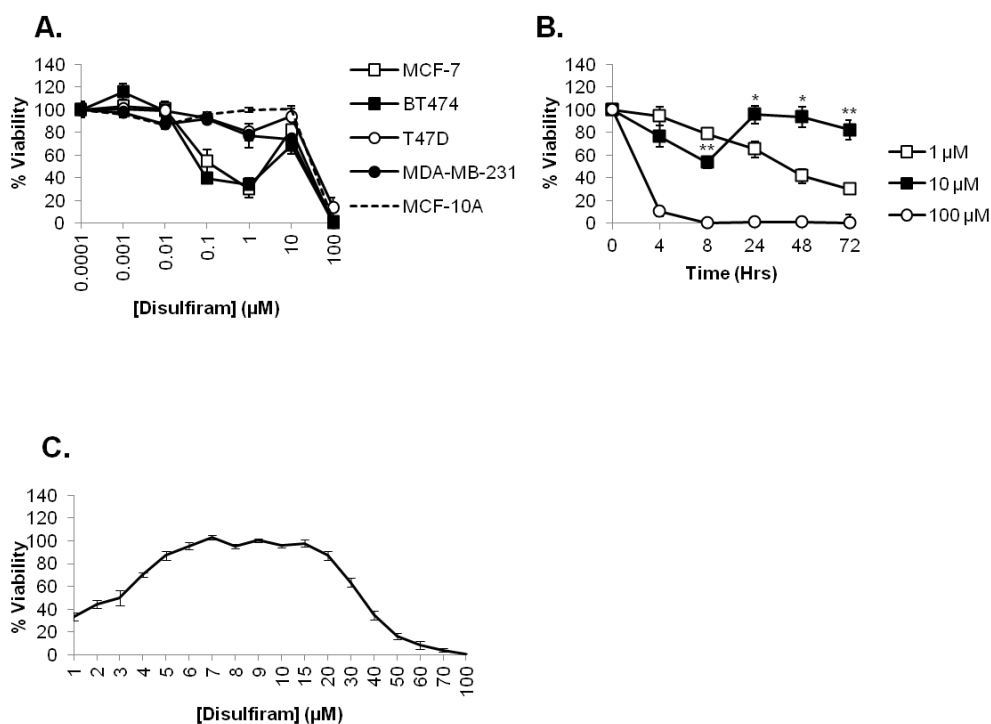
A.

B.

C.

Figure 3.6. The cytotoxic profile of disulfiram in breast cancer cells. (A) Cells were treated with a serial dilution of disulfiram and viability analysed after 72 hr using the CellTiter blue assay. (B) MCF-7 cells were treated for 8-72 hr with disulfiram prior to analysing viability. T-tests were conducted between equivalent time points to compare 1 and 10 µM data. *$p<0.05$ **$p<0.001$. (C) MCF-7 cells were treated for 72 hr with disulfiram at concentrations between 1-100 µM prior to analysing viability. Error bars show standard error.

It was then investigated whether this biphasic response was affected by incubation times. MCF-7 cells were treated with 1, 10 and 100 µM disulfiram over a range of time points and cell viability was then determined. Despite an initial cytotoxic phase at <8 hr, cell viability at 10 µM was restored at greater than 24 hr (Figure 3.6B). For other concentrations disulfiram produced a time dependent decrease in viability; at 1 µM viability steadily decreased between 4 and 72 hr whereas at 100 µM there was a rapid loss of viability to <10% within 4 hr. This data demonstrates that the 10 µM disulfiram response is due to recovery from initial effects and not inactivity of this drug at this concentration. When the biphasic peak in MCF-7 cells was investigated at

concentrations between 1 and 100 µM at a single 72 hr time point, viability was restored to >80% between 5-20 µM concentrations of the drug (Figure 3.6C).

3.2.6. Disulfiram causes fragmentation of the mitochondrial network

The morphology of mitochondria treated with disulfiram was analysed in order to determine whether there were any cytotoxic changes in this organelle. As mitochondria and apoptosis are intrinsically linked the data may also provide information on the mechanism of action of this drug. MCF-7 and MDA-MB-231 cells were treated with 1 µM disulfiram for 1-72 hr before being stained with the mitochondrial probe MitoTracker Red and live cells imaged via confocal microscopy. High resolution images of DMSO treated MCF-7 cells show the mitochondria as a network of interconnected structures (Figure 3.7A). Upon incubation with disulfiram however mitochondria appear punctate at time points as early as 1 hr, indicating rapid mitochondrial fragmentation. In comparison fragmentation of MDA-MB-231 cell mitochondria is more subtle and only apparent after 24 hr (Figure 3.7B). The organisation of mitochondria within these two cell lines is very different and is a more obvious phenotypic change than the effects of disulfiram. In addition, data interpretation was made more difficult as within a single population of cells the morphology of the mitochondria within both cell lines was highly variable.
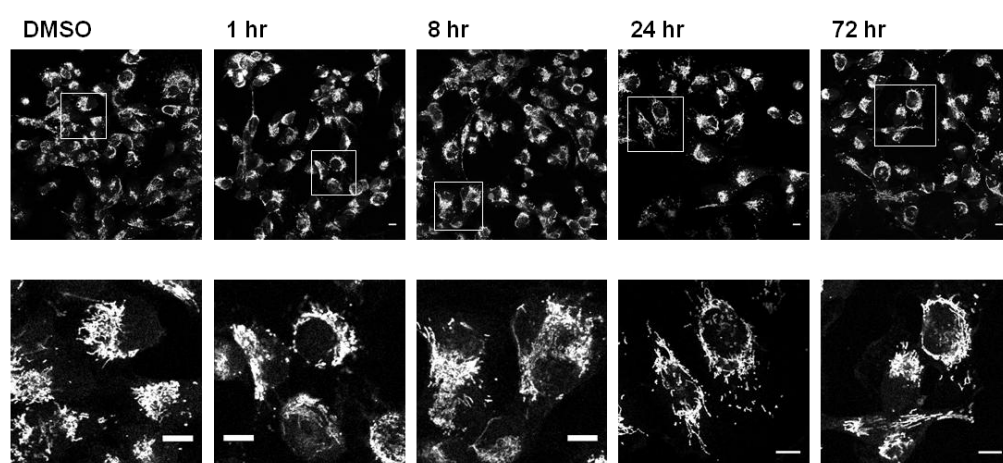
A. MCF-7
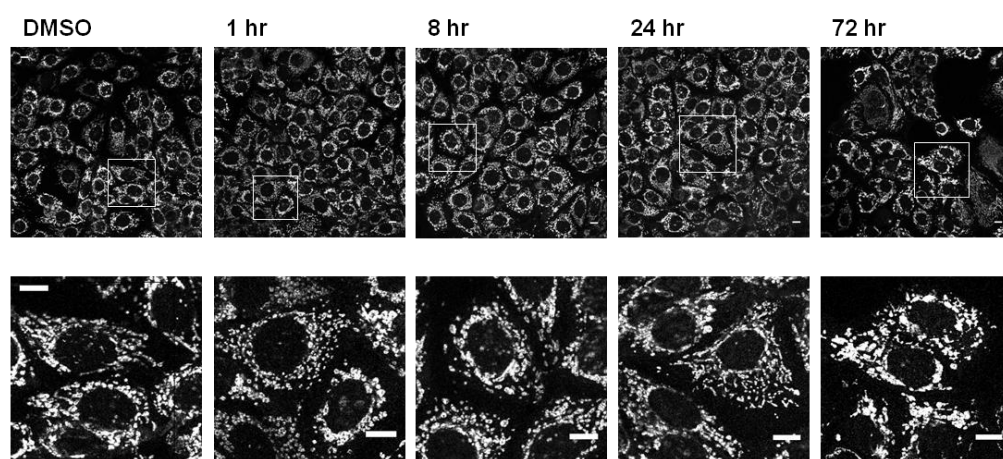
B. MDA-MB-231

Figure 3.7. Disulfiram causes changes in mitochondrial structure. MCF-7 (A) and MDA-MB-231 (B) cells were treated with 1 µM disulfiram or equivalent DMSO for the indicated time points, stained using MitoTracker Red and fixed with acetone. Images were obtained via confocal microscopy and show a single z-projection through centre of the cells. Scale bars show 10 µm.

3.2.7. Disulfiram does not induce autophagy

In order to determine whether disulfiram promotes autophagy, MCF-7 cells were treated with 1 or 10 µM disulfiram for 6 or 24 hr respectively and analysed via immunofluorescence with antibodies recognising LC3B, a marker of autophagic membranes. For these experiments 6 hr treatment with 100 µM

chloroquine, an agent which causes accumulated LC3B via stabilisation of autophagosomal membranes, was used as a positive control (Geng *et al.,* 2010). Chloroquine treatment produced large LC3B containing structures representing autophagosomes, however this phenotype was absent in cells treated with disulfiram at both 10 µM for 6 hr (Figure 3.8A) and 1 µM for 24 hr (Figure 3.8B).
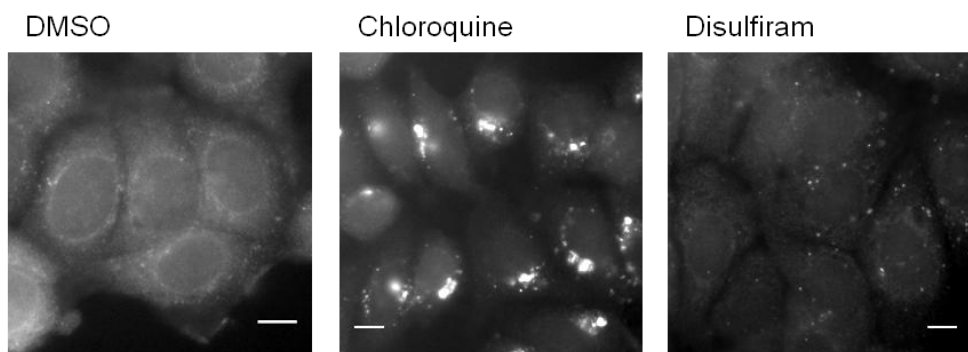
Figure 3.8. Disulfiram does not alter the localisation of autophagic membranes. MCF-7 cells were treated with 10 µM disulfiram for 6 hr (A), 1 µM for 24 hr (B), chloroquine (100 µM, 6 hr) or diluent control (DMSO). Immunofluorescence analyses were then conducted using antibodies recognising LC3B and in (A) nuclei were labelled with Hoescht 33342. Imaging was conducted via confocal microscopy in (A) where images show a single z-projection or epi-fluorescence microscopy in (B). Scale bars show 10 µm.

3.3. Discussion

Previous studies have investigated the ability of disulfiram to induce cytotoxicity using a variety of techniques including analysis of DNA content to indicate apoptosis, PARP fragmentation and MTT assays (Chen *et al.,* 2006; Yip *et al.,* 2011). The primary aim of this chapter was to determine which assay is the most suitable for studying the cytotoxicity of disulfiram in breast cancer cells. Initial studies focussed on the number of cells that remained attached to the plastic surface after disulfiram treatment and the morphology of those that were still adherent. Of these, cell counting studies (in MCF-7 and MDA-MB-231 cells) were unable to produce statistical significance between disulfiram and diluent control treated cells in all but one condition (1 µM, 24 hr) despite an obvious trend indicating the toxic effect of the drug at this concentration at other time points. The lack of significant data is likely to be due to poor reproducibility between repeat experiments as indicated by the large standard error bars. Cell morphology studies very clearly demonstrated that MCF-7 cells exhibit a biphasic toxicity response, whereby at 10 µM viability is restored. Images demonstrating viability effects of disulfiram in MDA-MB-231 cells reveal that there is no effect at 1 µM although partial sensitivity occurs at 10 µM and there is extensive cell death at 100 µM. It should be noted that this effect in not solely attributed to the drug and that the diluent at 1% concentration had some inherent cytotoxicity. Previous reports conflict regarding the sensitivity of the MDA-MB-231 cell line to disulfiram. In one study, the morphology of cells treated with 15 µM for 24 hr do not display a toxic phenotype (Chen *et al.,* 2006). Consistent with this, other

studies have also noted that disulfiram IC_{50} values in MDA-MB-231 cells, as determined by the MTT assay are >10 μM (Brahemi *et al.,* 2010). Others have demonstrated IC_{50} values for disulfiram treated MDA-MB-231 cells of between 0.5-1.5 μM indicating much higher sensitivity than previously suggested (Yip *et al.,* 2011; Liu *et al.,* 2013). Additionally when these cells are used in xenograph models disulfiram inhibits tumour growth suggesting that the apparent lack of sensitivity is an *in vitro* artefact, possibly due to low copper concentrations in cell culture conditions and the requirement of this metal in disulfiram toxicity (Chen *et al.,* 2006).

Many viability assays are dependent on the metabolic activity of reductase enzymes in altering the spectral properties of a dye. What is therefore measured is the metabolic rate of a cell at a particular point in time rather than whether the cell is alive or dead. These assays have the advantage of being conducted in 96 well plates meaning that it is possible to investigate multiple conditions at the same time. This study compared two of these dyes that form part of the MTT and CellTiter Blue assays. Data from these studies produced conflicting results regarding the sensitivity of MDA-MB-231 cells, and it is possible that this is a result of differences in reduction of MTT and CellTiter Blue reagent within these cells. There was, however, correlation between the results of the CellTiter blue assay and morphology studies for this cell line and the data from MCF-7 cells reinforced the biphasic viability peak observed in the morphology studies. The CellTiter Blue assay was simple to perform and produced a fluorescent product which resulted in low standard error and a high

signal to noise ratio. In comparison the MTT assay involved multiple steps and a colorimetric product producing higher standard error. Due to this, and the good correlation of the results with earlier findings, the CellTiter Blue assay was chosen for all further studies. Further studies were not conducting using PI based methods as quantification using this technique was difficult.

To further investigate the viability effects of disulfiram in breast cancer cells, cytotoxicity studies were carried out in an extended panel of breast cancer cell lines including BT474, T47D and non-cancerous breast epithelial MCF-10A. Of these only BT474 cells showed sensitivity to the drug at concentrations <100 μM, and produced a biphasic viability profile similar to that obtained with MCF-7 cells which occurred between 5-20 μM. Interestingly, both these disulfiram responsive cell lines are ER^+ raising the possibility that the drug is only toxic to this breast cancer sub-type, although data with the T47D cell line indicates that not all ER^+ tumours may respond to the drug. The selectivity of disulfiram for ER^+ breast cancer cells, including T47D, has been previously been noted and attributed to the fact that these cells are also $BCA2^+$ (Brahemi *et al.,* 2010). Interestingly, this study also demonstrated that transfection of ER into MDA-MB-231 cells increased disulfiram sensitivity. As well as this, others have reported on the disulfiram sensitivity of T47D cells, however in this paper the cells were seeded at a lower density of 5000 cells per well compared to the 11,000 used in this thesis which may explain this apparent difference (Yip *et al.,* 2011). Importantly, MCF-10A cells did not respond to the drug at concentrations <100 μM demonstrating selectivity towards breast

cancer versus non-cancerous breast epithelial cells which may indicate a favourable adverse effect profile in its clinical application.

To further characterise the biphasic toxicity profile of the drug, experiments were conducted to investigate its time dependency at concentrations within this biphasic range. These studies demonstrated that this response is due to recovery of initially affected cells and is therefore highly time dependent. Importantly this may explain why it is frequently reported in the literature at time points greater than 24 hr (Wickstrom *et al.,* 2007; Yip *et al.,* 2011; Rae *et al.,* 2013), however, to our knowledge, no studies have investigated the sensitivity of cells to disulfiram at shorter (<8 hr) time points. Although the clinical significance of this effect remains to be determined there is *in vivo* evidence that disulfiram doses of 25 µg/ mouse/ day are more effective at decreasing tumour weight in glioma xenographs than 120 µg/ mouse/ day (Marikovsky *et al.,* 2002). No studies have provided a mechanism to describe the underlying cause of this biphasic effect, which has never been reported to increase viability beyond 100% indicating that this represents loss of cytotoxic effects rather than a growth promoting action at this concentration. A curious feature of this biphasic effect was that it was noted in all cell lines which demonstrated significant sensitivity to disulfiram in this study, indicating that this is a universal feature under the conditions used here. Several possibilities exist which could explain the biphasic nature of disulfiram, although none have been investigated thoroughly or provide a full explanation. It may be the case that the hydrophobic nature of disulfiram prevents its complete dissolution in

aqueous solutions, and the drug forms an inactive precipitate at 10 µM. However, this explanation does not explain the fact that at time points <24 hrs MCF-7 cells demonstrated significant sensitivity of the drug in this study or that cytotoxicity is restored at concentrations >10 µM. A complicating factor in disulfiram viability studies is the drug's extensive metabolism and this feature may also provide an explanation for this biphasic phenomenon. It may be the case that an inactive disulfiram metabolite competes with the cytotoxic form of the drug, possibly by chelating copper or zinc ions within the cell which enhance the drugs cytotoxicity (Cen *et al.,* 2004; Yip *et al.,* 2011). Finally it has been proposed that this biphasic effect, also noted for the disulfiram analogue PDTC, may occur due to the activation of either ERK or JNK at certain concentrations and therefore may be a result of concentration dependent activation of signalling cascades (Chung *et al.,* 2000).

Apoptosis has been proposed to be the main route of disulfiram induced cell death as the drug has been demonstrated to promote cleavage of caspase substrates, indicating activation of these pro-apoptotic enzymes, and the generation of Annexin V positive cells (Cen *et al.,* 2004; Yip *et al.,* 2011). This protein (as a fluorescent conjugate) has binds phosphatidylserine that is flipped from the inner to the outer leaflet of the plasma membrane during apoptosis. The mitochondria are critical for apoptotic cell death whereby translocation of Bcl family members, including Bax and Bak, to the mitochondrial outer membrane, triggers release of cytochrome c from the inter membrane space of the organelle to the cell cytosol (Lalier *et al.,* 2007). As well as this Bax/ Bak

mitochondrial translocation promote mitochondrial fission events and the resulting fragmentation of the mitochondrial network is a morphological feature of apoptosis (Sheridan *et al.,* 2008; Young *et al.,* 2010). For example treatment of cardiac cells with the anti-cancer agent doxorubicin caused visible mitochondrial fragmentation as revealed using mitochondrial dyes and confocal microscopy (Catanzaro *et al.,* 2015). Extensive disulfiram induced mitochondrial fragmentation was noted in MCF-7 as early as 1 hr following treatment with 1 μM drug, indicating that this process occurs before reduction in metabolic activity as measured by the CellTiter Blue assay. This finding supports the hypothesis that cell death due to disulfiram occurs as a result of mitochondria induced apoptosis. Additionally when autophagy was investigated as an alternative cell death mechanism it was found that this process did not occur, providing further support for apoptosis being the cause of disulfiram induced cell death.

References

Allensworth, J. L., Evans, M. K., Bertucci, F., Aldrich, A. J., Festa, R. A., Finetti, P., Ueno, N. T., Safi, R., McDonnell, D. P., Thiele, D. J., Van Laere, S. and Devi, G. R. 2015. Disulfiram (DSF) acts as a copper ionophore to induce copper-dependent oxidative stress and mediate anti-tumor efficacy in inflammatory breast cancer. *Molecular oncology.* 9(6), p. 1155-1168.

Brahemi, G., Kona, F. R., Fiasella, A., Buac, D., Soukupova, J., Brancale, A., Burger, A. M. and Westwell, A. D. 2010. Exploring the structural requirements for inhibition of the ubiquitin E3 ligase Breast Cancer Associated Protein 2 (BCA2) as a treatment for breast cancer. *Journal of Medicinal Chemistry.* 53(7), p. 2757-2765.

Brar, S. S., Grigg, C., Wilson, K. S., Holder, W. D., Dreau, D., Austin, C., Foster, M., Ghio, A. J., Whorton, A. R., Stowell, G. W., Whittall, L. B., Whittle, R. R., White, D. P. and Kennedy, T. P. 2004. Disulfiram inhibits activating transcription factor/cyclic AMP-responsive element binding protein and human melanoma growth in a metal-dependent manner *in vitro*, in mice and in a patient with metastatic disease. *Molecular Cancer Therapeutics.* 3(9), p. 1049-1060.

Catanzaro, M., Kobayashi, S., Gerdes, M. and Liang, Q. 2015. Mitochondrial fragmentation and mitophagy contribute to doxorubicin-induced cardiomyocyte death. *The FASEB Journal.* 29(1), Supplement 1036.12.

Cen, D. Z., Brayton, D., Shahandeh, B., Meyskens, F. L. and Farmer, P. J. 2004. Disulfiram facilitates intracellular Cu uptake and induces apoptosis in human melanoma cells. *Journal of Medicinal Chemistry.* 47(27), p. 6914-6920.

Chen, D., Cui, Q. C., Yang, H. and Dou, Q. P. 2006. Disulfiram, a clinically used anti-alcoholism drug and copper-binding agent, induces apoptotic cell death in breast cancer cultures and xenografts via inhibition of the proteasome activity. *Cancer Research.* 66(21), p. 10425-10433.

Cho, H. J., Lee, T. S., Park, J. B., Park, K. K., Choe, J. Y., Sin, D. I., Park, Y. Y., Moon, Y.S., Lee, K. G., Yeo, J. H., Han, S. M., Cho, Y. S., Choi, M. R., Park, N. G., Lee, Y. S. and Chang, Y. C. 2007. Disulfiram suppresses invasive ability of osteosarcoma cells via the inhibition of MMP-2 and MMP-9 expression. *Journal of Biochemistry and Molecular Biology.* 40(6), p. 1069-1076.

Chung, K. C., Park, J. H., Kim, C. H., Lee, H. W., Sato, N., Uchiyama, Y. and Ahn, Y. S. 2000. Novel biphasic effect of pyrrolidine dithiocarbamate on neuronal cell viability is mediated by the differential regulation of intracellular zinc and copper ion levels, NF-kappa B, and MAP kinases. *Journal of Neuroscience Research.* 59(1), p. 117-125.

Geng, Y., Kohli, L., Klocke, B. J. and Roth, K. A. 2010. Chloroquine-induced autophagic vacuole accumulation and cell death in glioma cells is p53 independent. *Neuro-Oncology.* 12(5), p. 473-481.

Guo, X., Xu, B., Pandey, S., Goessl, E., Brown, J., Armesilla, A. L., Darling, J. L. and Wang, W. 2010. Disulfiram/copper complex inhibiting NF kappa B activity and potentiating cytotoxic effect of gemcitabine on colon and breast cancer cell lines. *Cancer Letters.* 290(1), p. 104-113.

Hasegawa, Y., Shimizu, T., Takahashi, N. and Okada, Y. (2012). The apoptotic volume decrease is an upstream event of MAP Kinase activation during staurosporine-induced apoptosis in HeLa cells. *International Journal of Molecular Sciences.* 13(7), p. 9363-9379.

Hothi, P., Martins, T. J., Chen, L. P., Deleyrolle, L., Yoon, J. G., Reynolds, B. and Foltz, G. 2012. High-throughput chemical screens identify disulfiram as an inhibitor of human glioblastoma stem cells. *Oncotarget.* 3(10), p. 1124-1136.

Lalier, L., Cartron, P. F., Juin, P., Nedelkina, S., Manon, S., Bechinger, B. and Vallette, F. M. 2007. Bax activation and mitochondrial insertion during apoptosis. *Apoptosis.* 12(5), p. 887-896.

Lin, J., Haffner, M. C., Zhang, Y., Lee, B. H., Brennen, W. N., Britton, J., Kachhap, S. K., Shim, J. S., Liu, J. O., Nelson, W. G., Yegnasubramanian, S. and Carducci, M. A. 2011. Disulfiram is a DNA demethylating agent and inhibits prostate cancer cell growth. *Prostate.* 71(4), p. 333-343.

Liu, P., Kumar, I. S., Brown, S., Kannappan, V., Tawari, P. E., Tang, J. Z., Jiang, W., Armesilla, A. L., Darling, J. L. and Wang, W. 2013. Disulfiram targets cancer stem-like cells and reverses resistance and cross-resistance in acquired paclitaxel-resistant triple-negative breast cancer cells. *British Journal of Cancer.* 109(7), p. 1876-1885.

Lovborg, H., Oberg, F., Rickardson, L., Gullbo, J., Nygren, P. and Larsson, R. 2006. Inhibition of proteasome activity, nuclear factor-KB translocation and

cell survival by the antialcoholism drug disulfiram. *International Journal of Cancer.* 118(6), p. 1577-1580.

Marikovsky, M., Nevo, N., Vadai, E. and Harris-Cerruti, C. 2002. Cu/Zn superoxide dismutase plays a role in angiogenesis. *International Journal of Cancer.* 97(1), p. 34-41.

Rae, C., Tesson, M., Babich, J. W., Boyd, M., Sorensen, A. and Mairs, R. J. 2013. The role of copper in disulfiram-induced toxicity and radiosensitization of cancer cells. *Journal of Nuclear Medicine.* 54(6), p. 953-960.

Sheridan, C., Delivani, P., Cullen, S. P. and Martin, S. J. 2008. Bax- or Bak-induced mitochondrial fission can be uncoupled from cytochrome c release. *Molecular Cell.* 31(4), p. 570-585.

Tardito, S., Bassanetti, I., Bignardi, C., Elviri, L., Tegoni, M., Mucchino, C., Bussolati, O., Franchi-Gazzola, R. and Marchio, L. 2011. Copper binding agents acting as copper ionophores lead to caspase inhibition and paraptotic cell death in human cancer cells. *Journal of the American Chemical Society.* 133(16), p. 6235-6242.

Wang, W. G., McLeod, H. L. and Cassidy, J. 2003. Disulfiram-mediated inhibition of NF-kappa B activity enhances cytotoxicity of 5-fluorouracil in human colorectal cancer cell lines. *International Journal of Cancer.* 104(4), p. 504-511.

Wickstrom, M., Danielsson, K., Rickardson, L., Gullbo, J., Nygren, P., Isaksson, A., Larsson, R. and Lovborg, H. 2007. Pharmacological profiling of disulfiram using human tumor cell lines and human tumor cells from patients. *Biochemical Pharmacology.* 73(1), p. 25-33.

Yip, N. C., Fombon, I. S., Liu, P., Brown, S., Kannappan, V., Armesilla, A. L., Xu, B., Cassidy, J., Darling, J. L. and Wang, W. 2011. Disulfiram modulated ROS-MAPK and NF kappa B pathways and targeted breast cancer cells with cancer stem cell-like properties. *British Journal of Cancer.* 104(10), p. 1564-1574.

Young, K. W., Pinon, L. G. P., Bampton, E. T. W. and Nicotera, P. 2010. Different pathways lead to mitochondrial fragmentation during apoptotic and excitotoxic cell death in primary neurons. *Journal of Biochemical and Molecular Toxicology.* 24(5), p. 335-341.

4. Investigation into the zinc ionophore effect of disulfiram and its relation to viability in breast cancer cells

4.1. Introduction

Much of the current literature surrounding the anti-cancer properties of disulfiram focuses on its interaction with copper. It is well established that the drug forms a copper complex which is capable of inhibiting the proteasome, and is also an ionophore of this metal resulting in increased oxidative damage to cancer cells (Chen *et al.,* 2006; Tardito *et al.,* 2011; Han *et al.,* 2013; Allensworth *et al.,* 2015). Despite knowledge that the drug is also able to bind zinc, little has been done to characterise the effect of this metal in the anti-cancer activities of the drug. However, the proteasomal inhibitory action of a complex involving the drug's major metabolite, DDC, and zinc has been demonstrated in breast cancer cells (Cvek *et al.,* 2008). The metabolite has also been shown to increase intracellular zinc levels in bovine endothelial cells, and through this mechanism inhibit NFκB activation (Kim *et al.,* 2000). Additionally, the ability of the disulfiram analogue PDTC to induce pancreatic cancer cell death may be reversed by addition of zinc chelators raising the possibility that these anti-cancer properties are dependent on its demonstrated zinc ionophore action (Donadelli *et al.,* 2009). As well as this, there is evidence to support the possibility that disulfiram may also have ionophore effects as it has been shown to elevate ROS levels in pancreatic cancer cells when co-incubated with zinc (Pozza *et al.,* 2011). However others have noted that the

117

drug decreases intracellular zinc levels in hepatic cells and attributed this to its zinc chelation activity (Hao and Maret 2006).

To demonstrate the importance of zinc in biological systems, it has been estimated that 10% of the human proteome contains zinc binding proteins and 40% of these are transcription factors (Andreini *et al.,* 2006). Due to the important role of this metal in cellular processes, total intracellular zinc levels are between 0.1 and 0.5 mM, however the majority of this is in its protein bound form and <0.001% is available as free zinc (Eide 2006). The low availability of free zinc is likely due to the acute toxicity of this metal, whereby addition of as little as 1 µM free zinc ions to cell media can induce cell death (Bozym *et al.,* 2010). Therefore intracellular zinc levels are maintained within a narrow range and zinc homeostasis mechanisms are critical to cell survival. Zinc binding proteins, including the metallothionein protein family, are thought to be predominantly responsible for this buffering effect under steady state conditions (Colvin *et al.,* 2010). In support of this, expression of metallothioneins is regulated by zinc availability and their up-regulation protects cells from metal induced oxidative damage (Andrews 2000; Qu *et al.,* 2013). In zinc challenged cells these buffering processes are supported by the action of zinc transporter proteins which shuttle the metal into certain subcellular compartments to combat raises in free intracellular zinc levels, this is known as the "muffler model" (Colvin *et al.,* 2010). Zinc transport to organelles requires the involvement of zinc transporter protein families including zinc transporters (ZnTs) which facilitate removal of the metal ion

from the cytosol and zinc influx transporters (ZIPs) responsible for zinc movement in the opposite direction. The subcellular location of transporters such as ZnT1, ZnT7 and ZnT2 have identified their role in delivering zinc to the endoplasmic reticulum, Golgi apparatus and secretory vesicles and endo-lysosomes respectively (Kirschke and Huang 2003; Lazarczyk *et al.,* 2008; Lopez and Kelleher 2009). In particular the endo-lysosomal accumulation of zinc has been noted in response to the zinc ionophore clioquinol and high oxidative stress, indicating that this may be a detoxification mechanism (Hwang *et al.,* 2008; Yu *et al.,* 2009). Additionally, the over-expression of ZnT2 has been shown to protect breast cancer cells from the cytotoxic effects of the metal ion by sequestering it in vesicles (Lopez *et al.,* 2011).

It has been widely reported that in breast cancer tissues, zinc levels are higher in cancer cells compared to the surrounding stoma (Rizk and Skypeck 1984; Riesop *et al.,* 2015). In support of this, serum zinc levels are lower in breast cancer patients presumably as a result of zinc transport from the serum to the tumour (Gupta *et al.,* 1991; Pavithra *et al.,* 2015). Although to the best of our knowledge no comparative studies have quantified zinc levels in cancerous versus non-cancerous cells, semi-quantitative analysis in *in vitro* breast cancer cell models has revealed that zinc levels may be 2.5-5 fold greater than in non-cancerous cell lines (Lopez *et al.,* 2011; Chandler *et al.,* 2016). This effect has also been observed in histology samples from breast cancer patients which report 72-320% higher zinc levels in breast cancer tissue compared to non-cancerous breast from the same patient (Margalioth *et al.,* 1983; Geraki *et al.,*

2002). The ability of breast tumours to accumulate zinc is most likely due to increased expression of ZIP influx transporters, which in *in vitro* cell models also increase drug resistance and metastatic activity (Taylor *et al.,* 2008; Hogstrand *et al.,* 2013). Therefore not only is zinc accumulation a feature of breast tumours but also provides an indication of disease aggression, which has been demonstrated in patients where there is a correlation between tumour zinc levels and histological grade (Riesop *et al.,* 2015). In this study histology samples were taken from nine tumours and zinc levels assessed in cancer and stroma cells. Not only did the results reveal that cancer cells contain higher zinc levels than stroma cells but also when the zinc levels were compared with histological grading, tumours with the highest grading (Grade 3) also contained cells with the most zinc.

Despite these observations, the molecular mechanisms surrounding the role of zinc in the pathogenesis of breast cancer remains unclear, however there is mounting evidence to implicate the ion in signalling processes. For example its release from endoplasmic reticulum stores in response to calcium influx and MAPK activation results in inhibition of phosphatases in mast cells, which has led to the suggestion that here it acts as a secondary messenger (Yamasaki *et al.,* 2007). In breast cancer cells, addition of zinc to cell culture media has been shown to activate EGFR signalling which may be related to the metal's phosphatase inhibitory activity (Taylor *et al.,* 2008). In this context release of zinc from intracellular stores maybe regulated via phosphorylation of ZIP7, demonstrating an additional regulatory mechanism which breast cancer cells

may utilise to raise intracellular zinc levels and facilitate signalling effects of the metal (Taylor *et al.,* 2012).

The literature surrounding zinc sequestration in breast cancer tissue implies that levels inside these cells may be closer to the toxic threshold than non-cancer cells. This would therefore make them more sensitive to the toxic effects of zinc ionophores.

Aims and Objectives

This chapter investigates the potential zinc ionophore activity of disulfiram and how this may relate to the cytotoxic effects of the drug in breast cancer cells. The aims are therefore:

- To develop methods to measure the effects of disulfiram on intracellular zinc levels of breast cancer cells.
- To determine whether disulfiram produces different effects on the intracellular zinc levels of cancer and non-cancerous breast epithelial cells.
- To investigate whether extracellular metal ion availability affects the cytotoxicity profile of disulfiram.

4.2. Results

4.2.1. Disulfiram specifically increases intracellular zinc levels in breast cancer cells

Initial experiments were conducted in order to visualise the effects of disulfiram on intracellular zinc levels in breast cancer cells. For this the intracellular zinc probe Fluozin-3 was employed which, according to the manufacturer, has a zinc affinity of 5 nM. Due to the fact that the affinity constant for many zinc binding proteins may be in the femtomolar range, this dye is thought to detect the labile zinc pool (Kochanczyk *et al.,* 2015). Cells were pre-loaded with dye for 30 min and live cell confocal analysis conducted before and after the addition of the drug. In MCF-7 cells before the addition of disulfiram, weak zinc labelling was observed in punctate compartments and the addition of the drug rapidly (<10 min) increased intracellular zinc to levels comparable to those observed using the well established zinc ionophore sodium pyrithione (NaP; Figure 4.1). A proportion of NaP treated cells were also noted for displaying diffuse cytosolic Fluozin-3 labelling whereas zinc in disulfiram treated cells was only observed in punctate structures. Surprisingly, zinc levels remained unaffected by either disulfiram or NaP treatment in the non-cancerous MCF-10A cell line.

In order to further investigate the disulfiram effects seen by microscopy, a flow cytometry assay was developed for the specific purpose of quantitative comparison of intracellular zinc levels in disulfiram and NaP treated cells. The
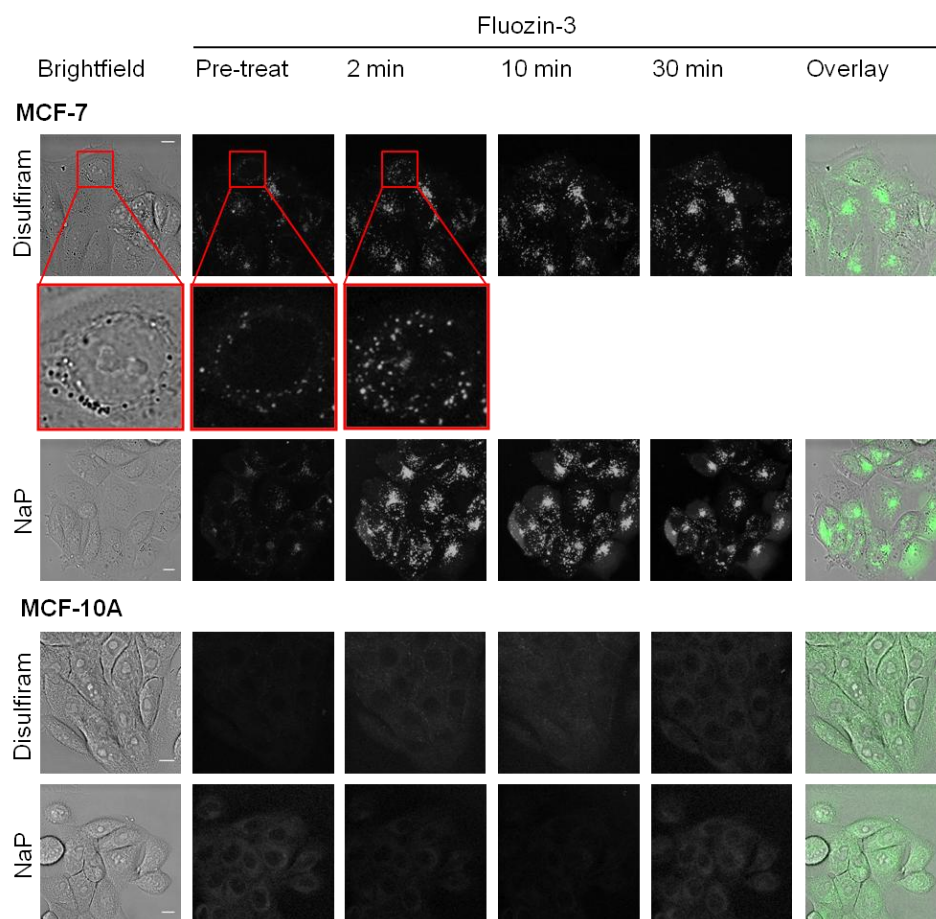
Figure 4.1. Disulfiram selectively increases intracellular zinc levels in punctate structures of breast cancer cells. Cells were pre-loaded with Fluozin-3 for 30 min and imaged before (Pre-treat) and subsequent to the addition of 10 µM disulfiram or sodium pyrithione (NaP) in cell imaging media. Images are multiple z-projections from a series of 10 equally spaced, single projections and are representative from three independent experiments. Scale bars show 10 µm.

data supported the microscopy findings as 100 µM disulfiram was shown to significantly increase intracellular zinc levels in both MCF-7 and MDA-MB-231 cell lines (Figure 4.2A), while zinc levels in MCF-10A cells remained unaffected by the same treatment. To rule out the possibility that the increase in fluorescence observed in disulfiram treated MCF-7 and MDA-MB-231 cells was due to higher autofluorescence of dead cells,
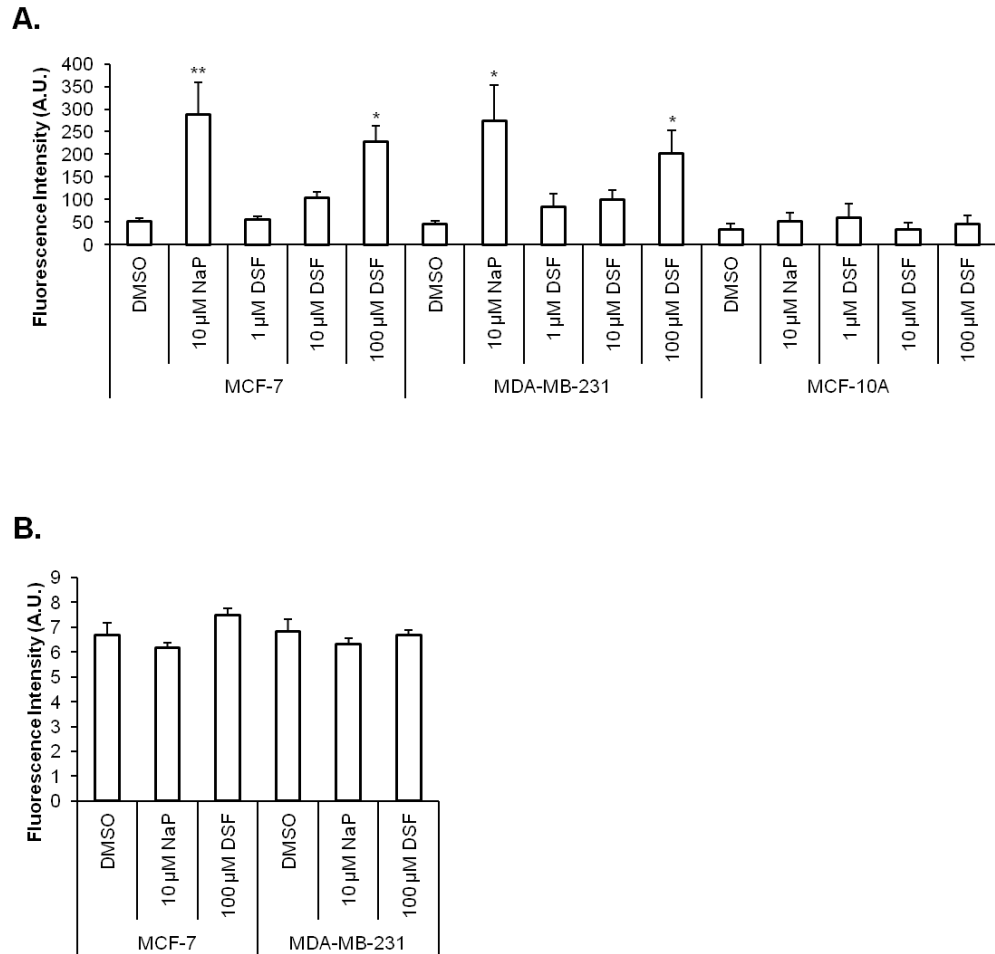
A.

B.

Figure 4.2. Disulfiram increases fluorescence of intracellular Fluozin-3. Cells were pre-loaded with Fluozin-3 (A) or diluent control (B) and treated with disulfiram (DSF), DMSO or Sodium Pyrithione (NaP) for 10 min in complete media. Fluozin-3 fluorescence was then determined via flow cytometry. Error bars show standard error. Statistical testing was conducted using ANOVA and Dunnett's test to compare DMSO and treatment groups. *p<0.05, **p<0.001.

experiments were conducted using the same method as described above but in the absence of Fluozin-3 (Figure 4.2B). Statistical tests (ANOVA) revealed that there was not a significant difference between DMSO and either NaP or disulfiram for both cell lines, demonstrating that the results in Figure 4.2A are a result of increased Fluozin-3 fluorescence and not autofluorescence.

To further investigate the source of increased Fluozin-3 fluorescence, and minimise the effects of extracellular zinc in serum, the flow cytometry experiments were conducted in serum free media to lower zinc and copper concentration in the system. Under these conditions, neither NaP nor disulfiram evoked a statistically significant increase in intracellular zinc in MCF-7 cells (Figure 4.3A). Supplementation of serum free media with 20 μM zinc was sufficient to completely restore, and in fact exaggerate, the zinc ionophore ability of both disulfiram and NaP, demonstrating that this ionophore activity is dependent on extracellular zinc levels. This effect, with respect to the selectivity of the dye for zinc versus copper, which could possibly also provide Fluozin-3 fluorescence, was tested by conducting the experiments in serum free media supplemented with copper. Here copper was unable to significantly restore the fluorescence of Fluozin-3 in disulfiram or NaP treated cells (Figure
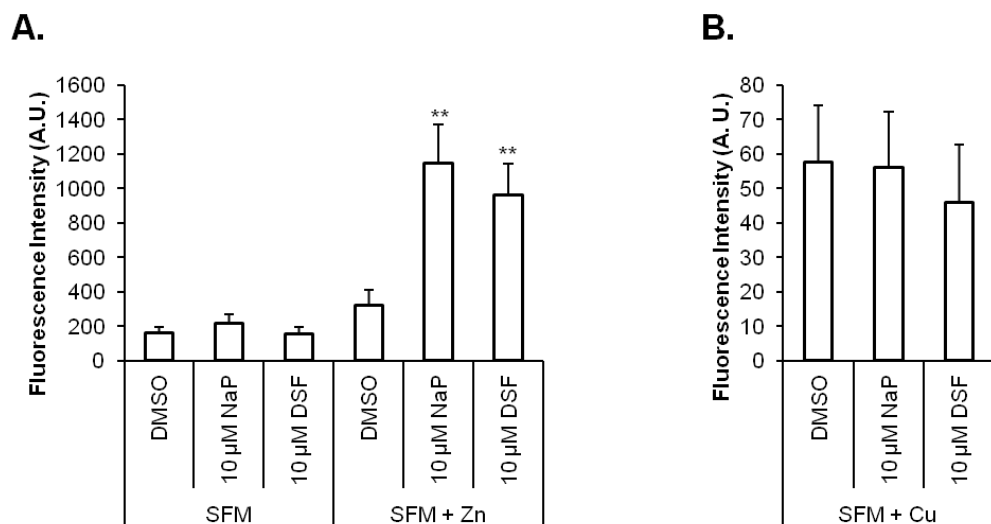

Figure 4.3. Disulfiram delivers extracellular zinc into cells rather than releasing intracellular stores. MCF-7 cells were pre-loaded with Fluozin-3 and treated with disulfiram, DMSO or Sodium Pyrithione (NaP) for 10 min in Serum Free Media (SFM) +/- 20 μM zinc (Zn; A) or copper (Cu; B). Fluozin-3 fluorescence was then determined via flow cytometry. Error bars show standard error. T-tests were conducted between SFM and SFM + Zn/Cu for each treatment. *$p<0.05$, **$p<0.001$.

4.3B), demonstrating that the increased fluorescence of Fluozin-3 observed in Figures 4.1-4.3 were specifically due to the effects of zinc.

4.2.2. Disulfiram sequesters intracellular zinc in endo-lysosomal compartments

The observation that disulfiram sequestered zinc in punctate structures led to investigation of the subcellular nature of these compartments. In order to determine whether they were components of the endocytic network, fluorescent dextran was utilised as a fluid-phase endocytic probe for confocal microscopy co-localisation studies. By conducting a 2 hr endocytic pulse with dextran-Alexa 647 followed by cell washing and a further 4 hr chase, the probe can be trafficked and confined to lysosomes (Al-Taei *et al.,* 2006). Dextran pulse-chase experiments were performed and cells were co-stained with Fluozin-3 and finally treated with disulfiram; the degree of co-localisation between dextran-Alexa 647 and Fluozin-3 was then analysed using live cell confocal microscopy and the ImageJ software plug-in JaCOP to determine the Pearson's coefficient (full description in Materials and Methods Section 2.5.4). Figure 4.4A demonstrates that a significant portion of dextran labelled lysosomes were also labelled with Fluozin-3 and very few dextran only structures were observed (Pearson's coefficient= 0.49 ± 0.06 for three independent experiments). When the entire fluid phase network was labelled with dextran as a single 4 hr endocytic pulse (Figure 4.4B), a higher degree of co-localisation was observed between the two probes (Pearson's coefficient= 0.67 ± 0.04)

suggesting that disulfiram was also driving zinc into earlier compartments of the endocytic network.
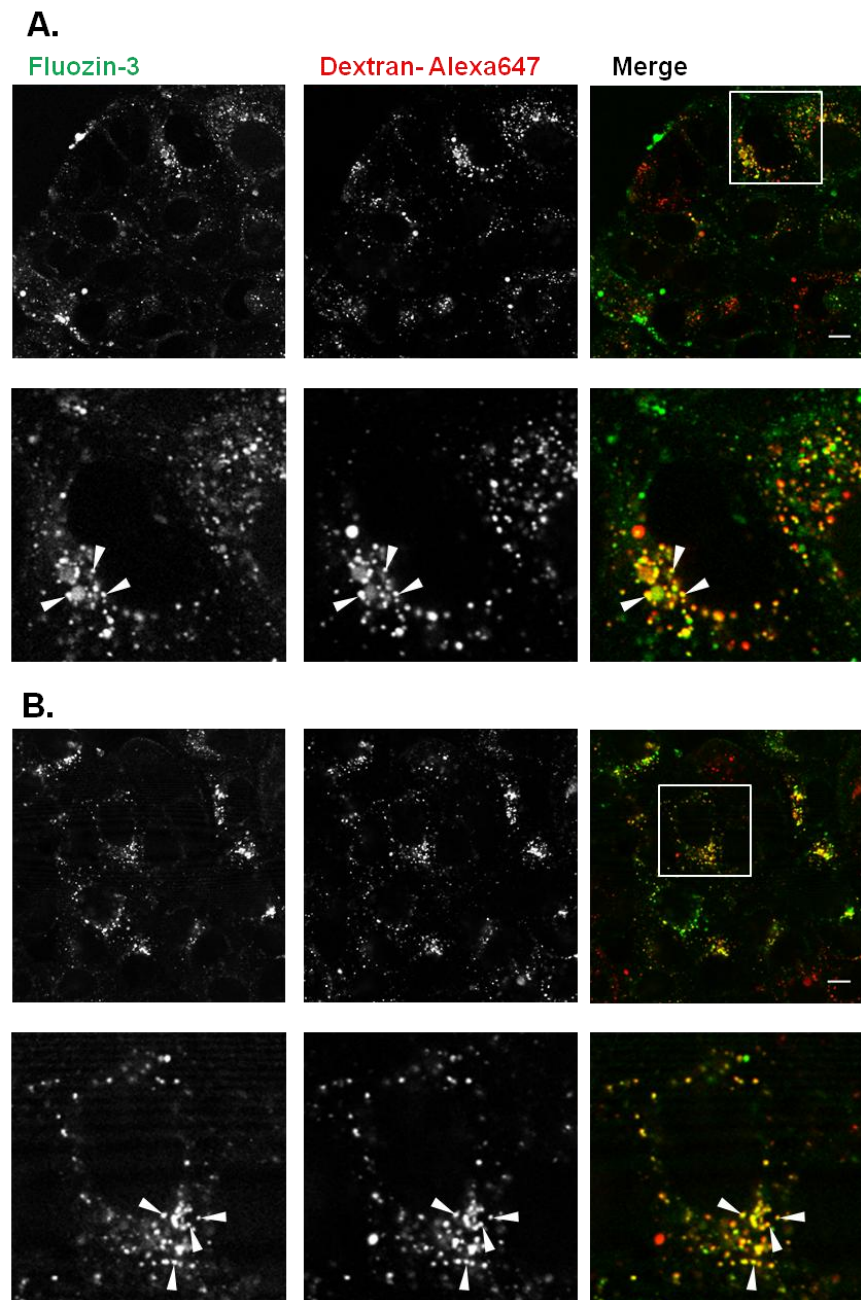

Figure 4.4. Disulfiram increases intracellular zinc in endo-lysosomal compartments of breast cancer cells. Dextran-Alexa 647 was used to highlight late endo-lysosomal compartments (A) or the entire fluid phase endocytic network (B) in MCF-7 cells, as described in Materials and Methods Section 2.5.4. Cells were then incubated with Fluozin-3, treated with 10 μM disulfiram for 10 min and co-localisation between Fluozin-3 and dextran-Alexa 647 analysed via confocal microscopy. Images show single z-projections through the cells and lower panel in (A) and (B) show a zoomed image of an identified cell in upper panel. Images shown are representative from three independent experiments. Co-localisation is marked by arrow heads. Scale bars show 10 μm.

4.2.3. The zinc ionophore effect of disulfiram occurs does not require acidic lysosomal pH

To investigate whether the lysosomal zinc accumulation induced by disulfiram required the pH gradient between lysosomal and cytosolic compartments, experiments were conducted using the H^+-ATPase inhibitor bafilomycin which inhibits acidification of lysosomes (Yoshimori *et al.,* 1991). In initial experiments MCF-7 cells were treated with bafilomycin or diluent control for 2 hr and then stained with LysoSensor to ensure that this protocol would increase lysosomal pH. LysoSensor is a pH sensitive dye which accumulates in lysosomes, and its fluorescence negatively correlates with the acidity of this organelle i.e. the lower the pH the greater the fluorescence. Data in Figure 4.5A shows that LysoSensor in control cells labelled predominantly punctate compartments indicating distinctive endo-lysosomal staining. However, bafilomycin treatment resulted in almost complete loss of punctate structures and instead produced faint cytosolic and plasma membrane staining indicating raised lysosomal pH. Cells were then treated with bafilomycin as described above and in the final stages of the incubation stained with Fluozin-3 and treated with disulfiram or diluent control. In this experiment bafilomycin did not decrease Fluozin-3 fluorescence in endo-lysosomal compartments, and in fact seemed to increase Fluozin-3 fluorescence (Figure 4.5B). These images are comparable with both those in Figure 4.1 and 4.5C where cells were treated following the same protocol as for Figure 4.5B with the exception that DMSO was used as a control instead of bafilomycin. This demonstrates that the ability

of disulfiram to increase endo-lysosomal zinc levels occurs independently of lysosomal pH.
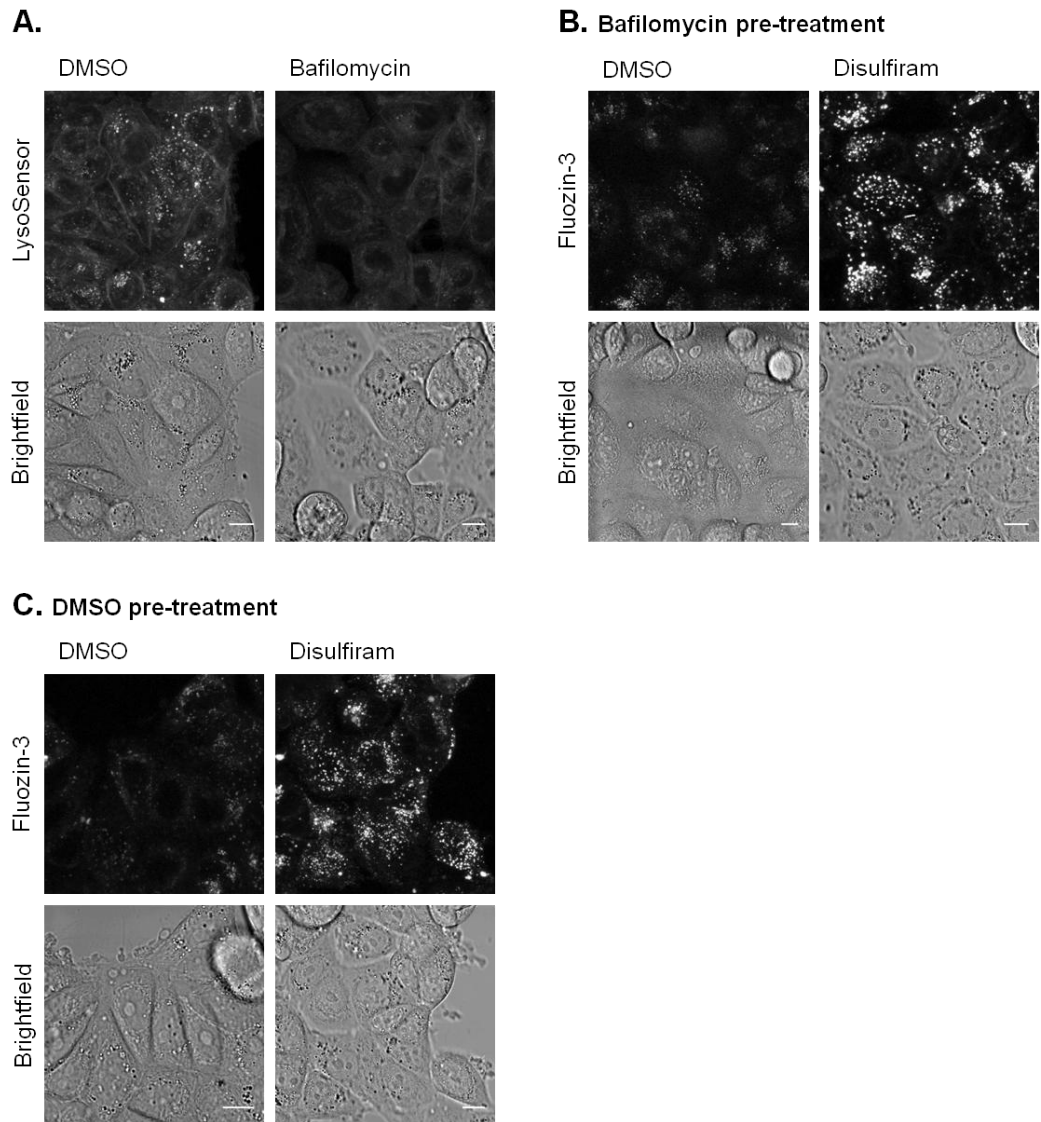

Figure 4.5. The zinc ionophore activity of disulfiram is independent of lysosomal pH. (A) MCF-7 cells were treated with 80 nM bafilomycin or DMSO for 2 hr before staining with LysoSensor. (B, C) Cells were pre-treated with bafilomycin (B) or DMSO (C) for a total of 2 hr and in the final stages of the incubation stained with Fluozin-3 and treated with disulfiram or DMSO. Images are multiple z-projections from a series of 10 equally spaced, single projections and are representative from three independent experiments. Scale bars show 10 μm.

4.2.4. Supplementation with zinc or copper increases disulfiram potency

The interaction between disulfiram and zinc observed in the previous results raised the possibility that enrichment of complete media with zinc or copper could affect the cytotoxicity of the drug in cancerous and non-cancerous breast cells. As control experiments, it was initially determined whether supplementing cell media with increasing concentrations of zinc or copper in the absence of disulfiram had any effect on cell viability. These studies demonstrated that ≤ 20 µM zinc or copper was without effect but toxicity was observed at higher concentrations of both metals (Figure 4.6A-B). Interestingly in MCF-7 and MCF-10A cells 200 µM copper produced a greater effect on cell viability than the same concentration of zinc, indicating a favourable effect on the tolerability of non-cancerous cells to this metal compared to copper. When a non-toxic dose of zinc or copper (20 µM) was given in combination with disulfiram, cytotoxicity was significantly enhanced in all cell lines (Figure 4.7A-C). In the case of MCF-7 cells, the disulfiram biphasic response was completely abolished by both zinc and copper supplementation, however
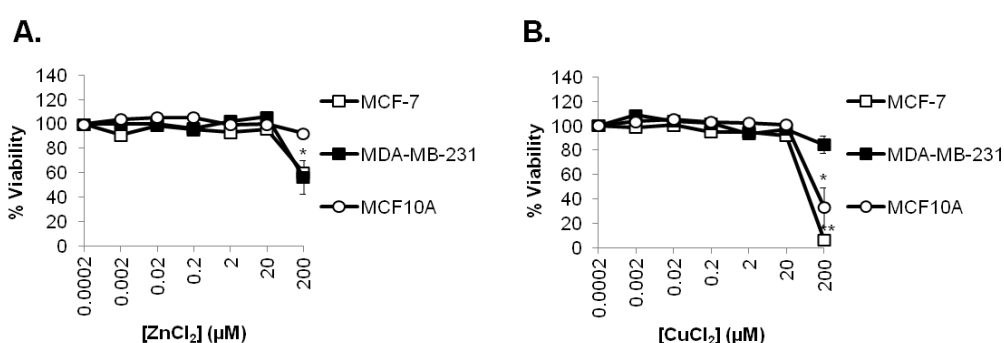

Figure 4.6. Zinc and copper do not effect MCF-7, MDA-MB-231 and MCF-10A cell viability <20 µM. Cells were treated with a serial dilution of zinc (A) or copper (B) for 72 hr in the presence of complete growth media before cell viability analysis was performed. Error bars show standard error.
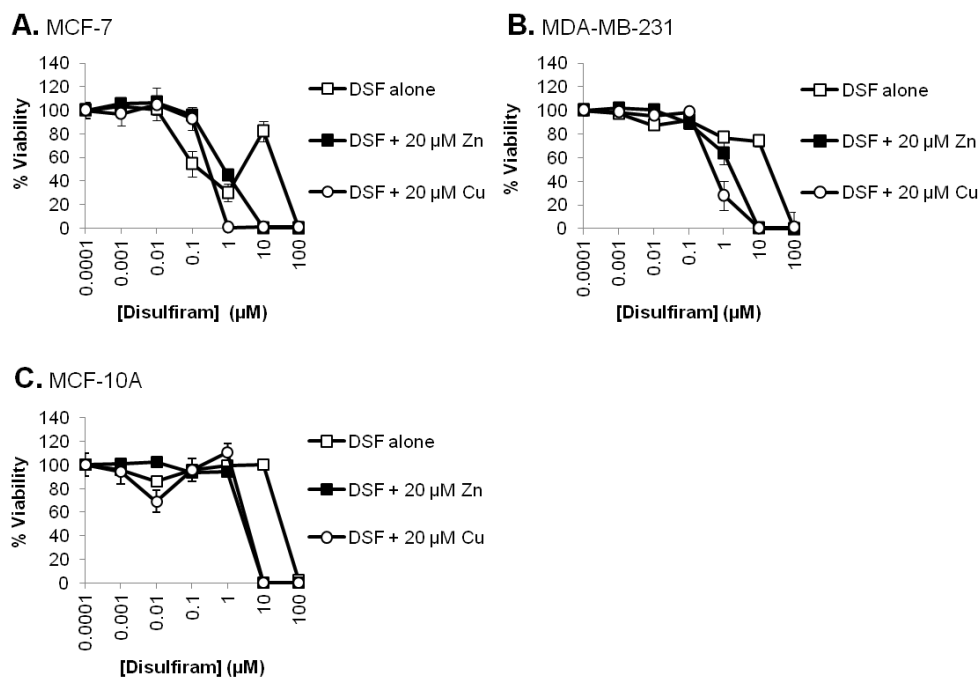
Figure 4.7. Zinc and copper enhance the cytotoxicity of disulfiram enhance the cytotoxicity of disulfiram. MCF-7 (A), MDA-MB-231 (B) and MCF-10A (C) cells were treated with disulfiram +/- 20 µM zinc or copper in complete media for 72 hr prior to performing viability analysis. Error bars show standard error.

cytotoxicity of disulfiram at lower concentrations was reduced by addition of either metal supplement. The minimum concentration of copper and zinc supplement required to influence cell recovery (biphasic peak) in MCF-7 cells was then determined and data in Figure 4.8A and B shows that 2.0 µM zinc and 0.125 µM copper significantly reduced the ability of the cells to recover from disulfiram effects. At higher concentrations both metals completely reversed the biphasic response.

Further experiments were conducted to determine whether decreasing zinc availability in media affected disulfiram cytotoxicity in MCF-7 cells. For this, the cell permeable zinc chelator TPEN was employed alone or in combination
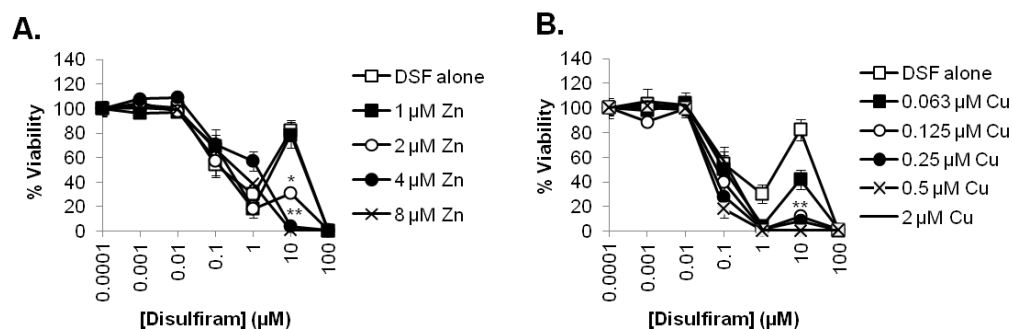
Figure 4.8. A minimum of 2 µM zinc and 0.125 µM copper is required to significantly affect the 10 µM biphasic peak of disulfiram. Viability of MCF-7 cells treated with disulfiram +/- zinc (A) or copper (B) in complete media was analysed after 72 hr. Error bars show standard error. Statistical testing was conducted using ANOVA and Dunnett's test to compare DMSO and treatment groups. *$p<0.05$, **$p<0.001$.

with disulfiram (Figure 4.9). No viability effects were observed at concentrations below 1 µM for cells treated with TPEN alone, however at higher concentrations cell viability was decreased to <5%. The addition of 1 µM TPEN to disulfiram serial dilution had no effect of the cytotoxicity of disulfiram at 1-100 µM. However, at lower disulfiram concentration (0.1 µM) TPEN was able to reverse the cytotoxicity of the drug.
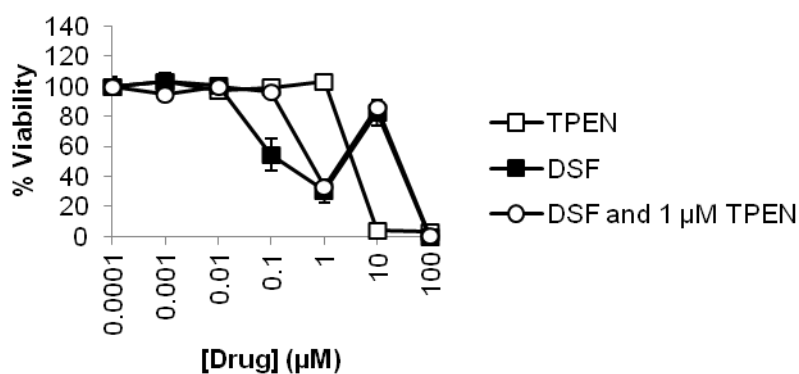

Figure 4.9. The addition of the cell permeable zinc chelator TPEN does not affect disulfiram viability. MCF-7 cells were treated with disulfiram, TPEN alone or disulfiram + 1 µM TPEN for 72 hr before cell viability analysis. Error bars show standard error.

132

4.2.5. Sodium pyrithione does not produce a biphasic viability peak

The observations that disulfiram was able to increase intracellular zinc levels and the biphasic viability peak was sensitive to the addition of zinc, led to investigation into whether the biphasic peak was a feature of other zinc ionophores. Viability studies were therefore performed using NaP in normal cell culture conditions in MCF-7 and MDA-MB-231 cells. Results in Figure 4.10 demonstrate that NaP potently decreased cell viability in both cell lines with IC_{50} <1 µM. Importantly however a biphasic response to NaP was not observed in either cell line, demonstrating that the recovery peak observed in earlier studies with disulfiram is not a universal feature of zinc ionophores.
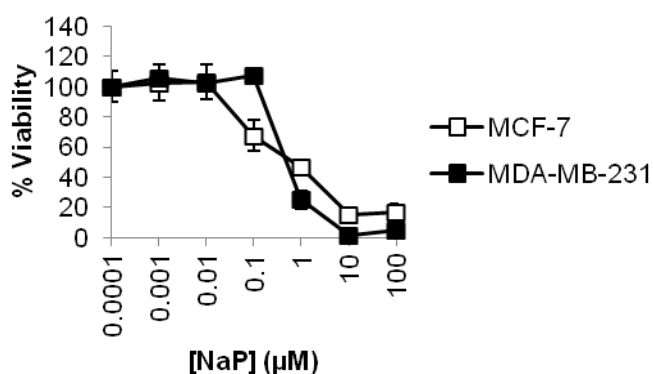

Figure 4.10. Sodium pyrithione does not produce a biphasic cell viability peak. MCF-7 and MDA-MB-231 cells were treated with sodium pyrithione (NaP) for 72 hr before cell viability analysis. Error bars show standard error.

4.3. Discussion

Much of the literature surrounding the anti-cancer properties of disulfiram focuses on its interaction with copper, particularly as a disulfiram-copper complex (Chen *et al.,* 2006; Liu *et al.,* 2012). In contrast, the effect of zinc on the drugs toxicity is under-reported, despite knowledge that this metal is dysregulated in breast cancer cells (Rizk and Skypeck 1984; Riesop *et al.,* 2015). The aim of this work was to determine the role of intra and extracellular zinc in the anti-breast cancer properties of disulfiram. The data shown in this chapter represents the first real time visual observations of intracellular zinc in disulfiram treated cells. Additionally the findings demonstrate that under normal conditions (complete media) disulfiram selectively increases intracellular zinc in breast cancer cells. This property may have numerous cellular effects with some leading to toxicity, for example studies have shown that supplementing media with zinc to increase intracellular levels, presumably through zinc channels, induces oxidative toxicity and inhibits NFκB signalling (Uzzo *et al.,* 2006; Bozym *et al.,* 2010). It has previously been proposed that acetaldehyde produced as a result of disulfiram induced ALDH inhibition releases zinc from proteins (Hao and Maret 2006), raising the possibility that the source of this metal which accumulates inside drug treated cells may be from intracellular sources. However, the studies in this chapter show that the ability of the drug to increase intracellular zinc is dependent on the availability of extracellular levels of this metal, supporting the hypothesis that the drug is acting as a zinc ionophore. This finding could have far reaching clinical consequences as a recent study has demonstrated that zinc concentration in

breast cancer tissue is higher than in non-cancerous tissue and zinc accumulation correlates with histological grade (Riesop *et al.,* 2015). This therefore implies that breast cancer cells may be more sensitive to the toxic effects of zinc than the surrounding stroma and additionally that through its zinc ionophore capability disulfiram may have particular benefit in more aggressive disease types. This is further supported by the observation in this chapter that the non-cancerous MCF-10A cell line was resistant to the zinc ionophore effects of disulfiram, although it is possible that there was an effect which was beyond the sensitivity limit of the microscopy and flow cytometry assays. The reason for this selectivity is unclear, it may be the case that these cells contain a greater zinc buffering capacity then cancerous cells and upon experiencing the zinc ionophore effect of disulfiram this metal is removed from the cell. To support this hypothesis it has been demonstrated that protein levels of ZnT efflux transporters are increased in MCF-10A compared to T47D cells, indicating that this cell line is more capable of removing zinc from the cell than cancerous cell lines (Chandler *et al.,* 2016).

The observation that disulfiram was able to increase endo-lysosomal zinc levels is previously unreported, and may have important implications in its selective anti-breast cancer effect. When under conditions of zinc overload, the cell may utilise certain compartments as a cytoprotective mechanism (Colvin *et al.,* 2008). The distribution of excess zinc to lysosomes has recently been reported, however high lysosomal zinc sequestration was also able to induce apoptosis when lysosomal release mechanisms were compromised (Kukic *et*

al., 2014). In addition, and particularly relevant to the studies of this chapter, this paper also noted that bafilomycin increased zinc levels in endo-lysosomal compartments. The authors hypothesised that this was due to bafilomycin inhibiting the ability of lysosomes to fuse with the plasma membrane and release their contents. This mechanism may also explain the increased zinc levels observed in the bafilomycin treated cells of this chapter. Increased lysosomal storage of zinc has been observed in cancer cells treated with clioquinol, another zinc ionophore (Yu *et al.*, 2009). The link between lysosomal zinc accumulation and cell death has also been demonstrated in neuronal cells, where zinc accumulation in this organelle was implicated in permeabilisation of its membrane causing release of hydrolytic enzymes (Hwang *et al.*, 2008). The potential for disulfiram in producing a similar effect is the subject of Chapter 6. The fact that in untreated breast cancer cells zinc was still observed in endo-lysosomal compartments may provide further evidence to support the hypothesis that breast cancer cells have an intrinsic zinc burden which may be exploited by the zinc ionophore action of disulfiram.

It has previously been reported that the addition of copper (Brar *et al.*, 2004; Wang *et al.*, 2011; Yip *et al.*, 2011; Liu *et al.*, 2012), zinc (Brar *et al.*, 2004) and other metal ions such as cadmium (Li *et al.*, 2008) to the extracellular media increases the potency of disulfiram across a range of cancer cell types. The incubation of copper to remove the biphasic phase has previously been reported (Yip *et al.*, 2011) but here it is demonstrated that zinc supplement has the same effect. Critically the ability of either metal ion to remove the biphasic

peak implies that the toxicity of disulfiram at 10 µM is limited by the availability of copper and zinc in the media. When considering the ability of disulfiram to increase intracellular zinc and copper levels, it is likely that an increase in extracellular copper and zinc allows disulfiram to transport more of these metal ions into the cell, which accounts for the increased toxicity at this concentration. The low concentrations of either copper and zinc required to increase disulfiram potency, suggest that increasing the availability of either metal ion could be achievable *in vivo* with oral supplements to enhance the cytotoxic effects of the drug. However, data with the MCF-10A cell line imply that such supplementation may adversely alter the selectivity of the drug for breast cancer cells and could cause non-specific toxicity. The fact that MDA-MB-231 cells in this chapter were sensitive to the zinc ionophore effect but remained insensitive to the cytotoxic effect of disulfiram suggest that this resistance must occur via a different mechanism to MCF-10A cells which were resistant to both cytotoxicity and ionophore effects. It may be the case that these cells may tolerate higher levels of zinc than MCF-10A, perhaps by increased expression of detoxification enzymes such as SOD (Papa *et al.,* 2014).

Surprisingly the addition of a non-toxic concentration of the zinc chelator TPEN did not affect the disulfiram response in MCF-7 cells, as would be expected if toxicity of the drug was dependent on zinc ion availability. However, the use of TPEN in this study was limited by its toxicity at higher concentrations in these cells and may have been insufficient to produce a

meaningful decrease in the availability of zinc ions. To demonstrate this, several studies have used a 10 fold higher concentration of TPEN to reduce zinc levels and affect the ability of the metal to inhibit cancer cell migration and induce cytotoxicity in response to PDTC (Kagara *et al.,* 2007; Donadelli *et al.,* 2009). Further optimisation studies to clarify whether the concentration of TPEN used in this study was able to affect intracellular zinc levels would determine whether this was the cause of the chelators inability to inhibit disulfiram induced cell death. This would additionally demonstrate the contribution of disulfiram's zinc ionophore effects to cytotoxicity in comparison to other cytotoxic mechanisms which have previously been described.

References

Al-Taei, S., Penning, N. A., Simpson, J. C., Futaki, S., Takeuchi, T., Nakase, I. and Jones, A. T. 2006. Intracellular traffic and fate of protein transduction domains HIV-1 TAT peptide and octaarginine. Implications for their utilization as drug delivery vectors. *Bioconjugate Chemistry.* 17(1), p. 90-100.

Allensworth, J. L., Evans, M. K., Bertucci, F., Aldrich, A. J., Festa, R. A., Finetti, P., Ueno, N. T., Safi, R., McDonnell, D. P., Thiele, D. J., Van Laere, S. and Devi, G. R. 2015. Disulfiram (DSF) acts as a copper ionophore to induce copper-dependent oxidative stress and mediate anti-tumor efficacy in inflammatory breast cancer. *Molecular oncology.* 9(6), p. 1155-1168.

Andreini, C., Banci, L., Bertini, I. and Rosato, A. 2006. Counting the zinc-proteins encoded in the human genome. *Journal of Proteome Research.* 5(1), p. 196-201.

Andrews, G. K. 2000. Regulation of metallothionein gene expression by oxidative stress and metal ions. *Biochemical Pharmacology.* 59(1), p. 95-104.

Bozym, R. A., Chimienti, F., Giblin, L. J., Gross, G. W., Korichneva, I., Li, Y., Libert, S., Maret, W., Parviz, M., Frederickson, C. J. and Thompson, R. B. 2010. Free zinc ions outside a narrow concentration range are toxic to a variety of cells *in vitro*. *Experimental Biology and Medicine.* 235(6), p. 741-750.

Brar, S. S., Grigg, C., Wilson, K. S., Holder, W. D., Dreau, D., Austin, C., Foster, M., Ghio, A. J., Whorton, A. R., Stowell, G. W., Whittall, L. B., Whittle, R. R., White, D. P. and Kennedy, T. P. 2004. Disulfiram inhibits activating transcription factor/cyclic AMP-responsive element binding protein and human melanoma growth in a metal-dependent manner *in vitro*, in mice and in a patient with metastatic disease. *Molecular Cancer Therapeutics.* 3(9), p. 1049-1060.

Chandler, P., Kochupurakkal, B. S., Alam, S., Richardson, A. L., Soybel, D. I., and Kelleher, S. H. 2016. Subtype-specific accumulation of intracellular zinc pools is associated with the malignant phenotype in breast cancer. *Molecular Cancer.* 15(2).

Chen, D., Cui, Q. C., Yang, H. and Dou, Q. P. 2006. Disulfiram, a clinically used anti-alcoholism drug and copper-binding agent, induces apoptotic cell

death in breast cancer cultures and xenografts via inhibition of the proteasome activity. *Cancer Research.* 66(21), p. 10425-10433.

Colvin, R. A., Bush, A. I., Volitakis, I., Fontaine, C. P., Thomas, D., Kikuchi, K. and Holmes, W. R. 2008. Insights into Zn2+ homeostasis in neurons from experimental and modeling studies. *American Journal of Physiology-Cell Physiology.* 294(3), p. 726-742.

Colvin, R. A., Holmes, W. R., Fontaine, C. P. and Maret, W. 2010. Cytosolic zinc buffering and muffling: Their role in intracellular zinc homeostasis. *Metallomics.* 2(5), p. 306-317.

Cvek, B., Milacic, V., Taraba, J. and Dou, Q. P. 2008. Ni(II), Cu(II), and Zn(II) Diethyldithiocarbamate complexes show various activities against the proteasome in breast cancer cells. *Journal of Medicinal Chemistry.* 51(20), p. 6256-6258.

Donadelli, M., Pozza, E. D., Scupoli, M. T., Costanzo, C., Scarpa, A. and Palmieri, M. 2009. Intracellular zinc increase inhibits p53(-/-) pancreatic adenocarcinoma cell growth by ROS/AIF-mediated apoptosis. *Biochimica Et Biophysica Acta-Molecular Cell Research.* 1793(2), p. 273-280.

Eide, D. J. 2006. Zinc transporters and the cellular trafficking of zinc. *Biochimica Et Biophysica Acta-Molecular Cell Research.* 1763(7), p. 711-722.

Geraki, K., Farquharson, M. J. and Bradley, D. A. 2004. X-ray fluorescence and energy dispersive X-ray diffraction for the quantification of elemental concentrations in breast tissue. *Physics in Medicine and Biology.* 49(1), p. 99-110.

Gupta, S. K., Shukla, V. K., Vaidya, M. P., Roy, S. K. and Gupta, S. 1991. Serum trace-elements and Cu/Zn ratio in breast-cancer patients. *Journal of Surgical Oncology.* 46(3), p. 178-181.

Han, J. B., Liu, L. M., Yue, X. Q., Chang, J. J., Shi, W. D. and Hua, Y. Q. 2013. A binuclear complex constituted by diethyldithiocarbamate and copper(I) functions as a proteasome activity inhibitor in pancreatic cancer cultures and xenografts. *Toxicology and Applied Pharmacology.* 273(3), p. 477-483.

Hao, Q. and Maret, W. 2006. Aldehydes release zinc from proteins. A pathway from oxidative stress/lipid peroxidation to cellular functions of zinc. *FEBS Journal.* 273(18), p. 4300-4310.

Hogstrand, C., Kille, P., Ackland, M. L., Hiscox, S. and Taylor, K. M. 2013. A mechanism for epithelial-mesenchymal transition and anoikis resistance in breast cancer triggered by zinc channel ZIP6 and STAT3 (signal transducer and activator of transcription 3). *Biochemical Journal.* 455(2), p. 229-237.

Hwang, J. J., Lee, S. J., Kim, T. Y., Cho, J. H. and Koh, J. Y. 2008. Zinc and 4-hydroxy-2-nonenal mediate lysosomal membrane permeabilization induced by H2O2 in cultured hippocampal neurons. *Journal of Neuroscience.* 28(12), p. 3114-3122.

Kagara, N., Tanaka, N., Noguchi, S. and Hirano, T. 2007. Zinc and its transporter ZIP10 are involved in invasive behavior of breast cancer cells. *Cancer Science.* 98(5), p. 692-697.

Kim, C. H., Kim, J. H., Moon, S. J., Hsu, C. Y., Seo, J. T. and Ahn, Y. S. 2000. Biphasic effects of dithiocarbamates on the activity of nuclear factor-kappa B. *European Journal of Pharmacology.* 392(3), p. 133-136.

Kirschke, C. P. and Huang, L. P. 2003. ZnT7, a novel mammalian zinc transporter, accumulates zinc in the Golgi apparatus. *Journal of Biological Chemistry.* 278(6), p. 4096-4102.

Kochanczyk, T., Drozd, A. and Krezel, A. 2015. Relationship between the architecture of zinc coordination and zinc binding affinity in proteins - insights into zinc regulation. *Metallomics.* 7(2), p. 244-257.

Kukic, I., Kelleher, S. L. and Kiselyov, K. 2014. Zinc efflux through lysosomal exocytosis prevents zinc-induced toxicity. *Journal of Cell Science*. 127(14), p. 3094-3103.

Lazarczyk, M., Pons, C., Mendoza, J. A., Cassonnet, P., Jacob, Y. and Favre, M. 2008. Regulation of cellular zinc balance as a potential mechanism of EVER-mediated protection against pathogenesis by cutaneous oncogenic human papillomaviruses. *Journal of Experimental Medicine.* 205(1), p. 35-42.

Li, L., Yang, H., Chen, D., Cui, C. and Dou, Q. P. 2008. Disulfiram promotes the conversion of carcinogenic cadmium to a proteasome inhibitor with pro-

apoptotic activity in human cancer cells. *Toxicology and Applied Pharmacology.* 229(2), p. 206-214.

Liu, P., Brown, S., Goktug, T., Channathodiyil, P., Kannappan, V., Hugnot, J. P., Guichet, P. O., Bian, X., Armesilla, A. L., Darling, J. L. and Wang, W. 2012. Cytotoxic effect of disulfiram/copper on human glioblastoma cell lines and ALDH-positive cancer-stem-like cells. *British Journal of Cancer.* 107(9), p. 1488-1497.

Lopez, V., Foolad, F. and Kelleher, S. L. 2011. ZnT2-overexpression represses the cytotoxic effects of zinc hyper-accumulation in malignant metallothionein-null T47D breast tumor cells. *Cancer Letters.* 304(1), p. 41-51.

Lopez, V. and Kelleher, S. L. 2009. Zinc transporter-2 (ZnT2) variants are localized to distinct subcellular compartments and functionally transport zinc. *Biochemical Journal.* 422, p. 43-52.

Margalioth, E. J., Schenker, J. G. and Chevion, M. 1983. Copper and zinc levels in normal and malignant tissues. *Cancer.* 52, p. 868–872

Papa, L., Hahn, M., Marsh E. L., Evans, B. S., and Germain, D. SOD2 to SOD1 switch in breast cancer. *Journal of Biological Chemistry.* 289(9), p. 5412-5416.

Pavithra, V., Sathisha, T. G., Kasturi, K., Mallika, D. S., Amos, S. J. and Ragunatha, S. 2015. Serum levels of metal ions in female patients with breast cancer. *Journal of Clinical and Diagnostic Research.* 9(1), p. 25-27.

Pozza, E. D., Donadelli, M., Costanzo, C., Zaniboni, T., Dando, I., Franchini, M., Arpicco, S., Scarpa, A. and Palmieri, M. 2011. Gemcitabine response in pancreatic adenocarcinoma cells is synergistically enhanced by dithiocarbamate derivatives. *Free Radical Biology and Medicine.* 50(8), p. 926-933.

Qu, W., Pi, J. B. and Waalkes, M. P. 2013. Metallothionein blocks oxidative DNA damage *in vitro*. *Archives of Toxicology.* 87(2), p. 311-321.

Riesop, D., Hirner, A. V., Rusch, P. and Bankfalvi, A. 2015. Zinc distribution within breast cancer tissue: A possible marker for histological grading? *Journal of Cancer Research and Clinical Oncology.* 141(7), p. 1321-1331.

Rizk, S. L. and Skypeck, H. H. 1984. Comparison between concentrations of trace-elements in normal and neoplastic human-breast tissue. *Cancer Research.* 44(11), p. 5390-5394.

Tardito, S., Bassanetti, I., Bignardi, C., Elviri, L., Tegoni, M., Mucchino, C., Bussolati, O., Franchi-Gazzola, R. and Marchio, L. 2011. Copper binding agents acting as copper ionophores lead to caspase inhibition and paraptotic cell death in human cancer cells. *Journal of the American Chemical Society.* 133(16), p. 6235-6242.

Taylor, K. M., Hiscox, S., Nicholson, R. I., Hogstrand, C. and Kille, P. 2012. Protein kinase CK2 triggers cytosolic zinc signaling pathways by phosphorylation of zinc channel ZIP7. *Science Signaling.* 5(210), ra 11.

Taylor, K. M., Vichova, P., Jordan, N., Hiscox, S., Hendley, R. and Nicholson, R. I. 2008. ZIP7-mediated intracellular zinc transport contributes to aberrant growth factor signaling in antihormone-resistant breast cancer cells. *Endocrinology.* 149(10), p. 4912-4920.

Uzzo, R. G., Crispen, P. L., Golovine, K., Makhov, P., Horwitz, E. M. and Kolenko, V. M. 2006. Diverse effects of zinc on NF-kappa B and AP-1 transcription factors: implications for prostate cancer progression. *Carcinogenesis.* 27(10), p. 1980-1990.

Wang, F., Zhai, S., Liu, X., Li, L., Wu, S., Dou, Q. P. and Yan, B. 2011. A novel dithiocarbamate analogue with potentially decreased ALDH inhibition has copper-dependent proteasome-inhibitory and apoptosis-inducing activity in human breast cancer cells. *Cancer Letters.* 300(1), p. 87-95.

Yamasaki, S., Sakata-Sogawa, K., Hasegawa, A., Suzuki, T., Kabu, K., Sato, E., Kurosaki, T., Yamashita, S., Tokunaga, M., Nishida, K. and Hirano, T. 2007. Zinc is a novel intracellular second messenger. *Journal of Cell Biology.* 177(4), p. 637-645.

Yip, N. C., Fombon, I. S., Liu, P., Brown, S., Kannappan, V., Armesilla, A. L., Xu, B., Cassidy, J., Darling, J. L. and Wang, W. 2011. Disulfiram modulated ROS-MAPK and NF kappa B pathways and targeted breast cancer cells with cancer stem cell-like properties. *British Journal of Cancer.* 104(10), p. 1564-1574.

Yoshimori, T., Yamamoto, A., Moriyama, Y., Futai, M. and Tashiro, Y. 1991. Bafilomycin-A1, a specific inhibitor of vacuolar-type H+-ATPase, inhibits

acidification and protein-degradation in lysosomes of cultured-cells. *Journal of Biological Chemistry.* 266(26), p. 17707-17712.

Yu, H., Zhou, Y., Lind, S. E. and Ding, W. Q. 2009. Clioquinol targets zinc to lysosomes in human cancer cells. *Biochemical Journal.* 417(1), p. 133-139.

5. Investigation into the structure-activity relationship of disulfiram analogues in breast cancer cells

5.1. Introduction

The fact that disulfiram is rapidly and extensively metabolised may imply its metabolic breakdown products are responsible for the drug's biological effects. Initial metabolism proceeds via cleavage of the weak disulfide bond to form two molecules of DDC (Figure 5.1). Although this process is thought to occur
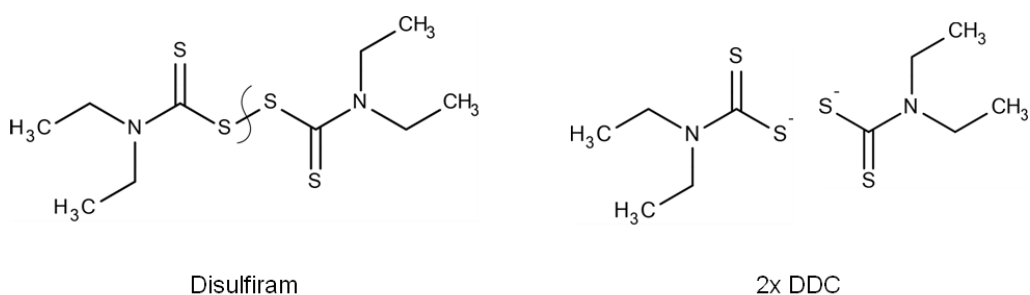

Disulfiram   2x DDC

Figure 5.1. Reduction of disulfiram across the vulnerable disulfide bond to produce two molecules of DDC.

non-enzymatically, binding of the parent drug to serum albumin has been shown to enhance DDC formation (Agarwal *et al.,* 1983). Additionally in a cell free system, reduction of disulfiram is dependent on glutathione reductase enzyme activity (Nagendra *et al.,* 1991). These processes mean that within 4 min of disulfiram administration to blood it is completely reduced to DDC, and the parent drug is undetectable in clinical trials which instead must rely on detection of metabolites to address its pharmacokinetic properties (Cobby *et al.,* 1977; Johansson 1992; Schweizer *et al.,* 2013). Following reduction to DDC, further metabolism proceeds via enzymatic routes leading to methylated or glucuronidated DDC derivatives or non-enzymatic routes producing

diethylamine and carbon disulfide (Eneanya *et al.,* 1981). The issues surrounding the instability of disulfiram imply that DDC, and other metabolites, could be responsible for the drug's biological activity. In support of this, a disulfiram clinical trial has revealed that the ability of the drug to demethylate promoter DNA in prostate cancer cells, leading to re-expression of tumour suppressor genes, correlates with the ability of individuals to form the methylated DDC derivative, S-methyl N,N-diethyldithiocarbamate (Schweizer *et al.,* 2013). However, this extensive metabolic pathway may limit the efficacy of the drug and improving its stability by encapsulation within liposomes has been shown to decrease tumour size in breast cancer mouse models when administered with copper more effectively than non-encapsulated disulfiram-copper treatment (Liu *et al.,* 2014).

How the chemical features of disulfiram relate to its biological activity is incompletely understood, however some compounds with similar chemical structures also share its ability to alter biological processes, for example proteasome function and apoptosis. Of particular interest is PDTC which retains one thioester moiety of disulfiram but replaces the terminal ethyl groups with a nitrogen containing five membered ring known as pyrollidine (full structure compared to that of disulfiram and DDC in Figure 5.2). This compound is cytotoxic to pancreatic adenocarcinoma cells, an effect which can be enhanced by zinc co-incubation, and can also increase levels of
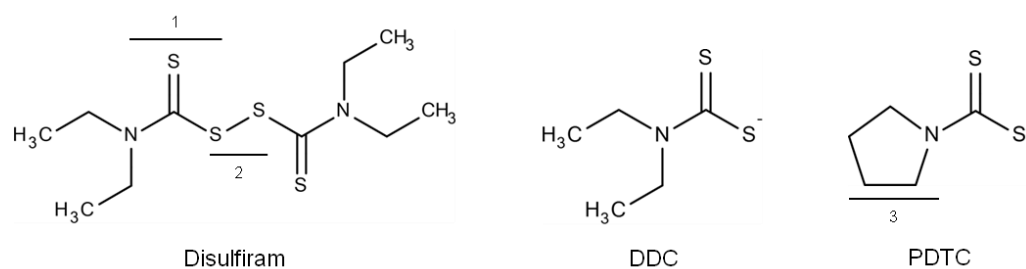
Figure 5.2. Comparison of the chemical structures of disulfiram, DDC and PDTC. (1) Indicates the N(C=S)S thioester moiety. (2) Disulfide bond. (3) Pyrollidine group.

ROS. Interestingly these properties are also observed, but to a greater extent, when these cells are treated with disulfiram (Pozza *et al.,* 2011). Structure-activity relationship studies have revealed that the chemical groups attached to the nitrogen are critical for the ability of PDTC analogues to induce breast cancer cell death and inhibit the proteasome (Yu *et al.,* 2007; Wang *et al.,* 2011). Specifically, analogues with the capacity to induce cytotoxicity in MDA-MB-231 cells at <10 µM contain a phenyl ring with a single or double carbon link and a single or double carbon chain attached to the nitrogen (Wang *et al.,* 2011). One compound, chosen as docking studies revealed that it was unlikely to inhibit ALDH, was shown to inhibit the proteasome and induce apoptosis when combined with copper. This therefore indicates that the anti-cancer activities of compounds structurally related to disulfiram may be separated from their ability to inhibit ALDH, an effect which potentially decreases *in vivo* efficacy. Other studies have focussed on combining dithiocarbamate analogues with thalidomide and shown that these are more potent at inducing cell death and inhibiting growth and migration of endothelial cells compared to thalidomide alone (El-Aarag *et al.,* 2014).

In contrast to the knowledge of structural features which enhance the PDTC anti-cancer effect, little has been done to investigate the structure-activity relationship of disulfiram. The work in this chapter is an extension of a previous report produced by collaboration between Cardiff University and the Barbara Ann Karmanos Institute, Detroit, where four series of novel disulfiram analogues were investigated for their ability to produce cytotoxicity in ER$^+$ breast cancer cells (Brahemi *et al.,* 2010). This work highlighted the importance of the central N(C=S)S-S bond in the ability of disulfiram analogues to induce viability effects in breast cancer cells and hypothesised that two classes of compounds were selectively toxic to ER$^+$ and not ER$^-$ breast cancer cell lines. These were: "disulfiram analogues" (referred to in this chapter as thiuram disulfide analogues) defined by a central structure of two thioester moieties joined by a disulfide bond with two R groups attached to each nitrogen, and "carbamo(dithioperoxo)thioates" which contained a core structure of a single thioester joined by a disulfide bond to an R1 group with two additional R groups attached to the nitrogen atom (core structures of both series compared in Figure 5.3). In this chapter the term "disulfiram analogues" is reserved for collectively describing all thiuram disulfide and carbamo(dithioperoxo)thioate analogues.
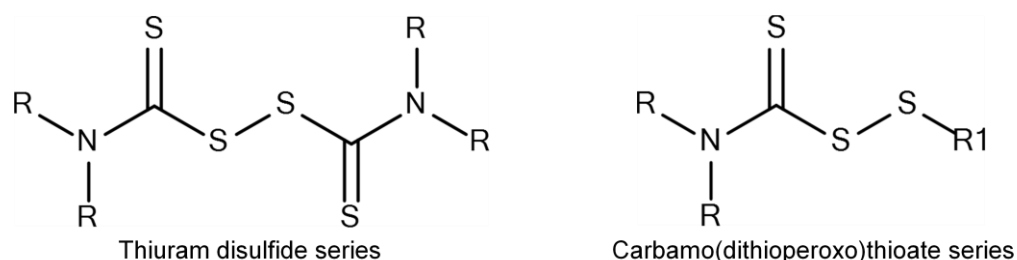

Figure 5.3. Core structures of the thiuram disulfide and carbamo(dithioperoxo)thioate series of disulfiram analogues used in this study.

Aims and Objectives

The primary objective of this chapter is to further investigate the structure-activity relationship of disulfiram analogues with respect to their ability to induce cell death. In addition the zinc ionophore activity of DDC and its effect on cell viability will be compared with the parent drug. With these objectives in mind, the aims of this chapter are:

- To compare the viability effects produced by thiuram disulfide and carbamo(dithioperoxo)thioate analogues in MCF-7, MDA-MB-231 and MCF-10A cells.

- To further investigate how modifying the R group of disulfiram analogues alters their cytotoxicity profile.

- To determine the relationship between DDC and disulfiram analogue cytotoxicity and possible zinc ionophore action.

5.2. Results

5.2.1. MCF-7 and MDA-MB-231 viability effects in the thiuram disulfide series are dependent on R group size

Disulfiram analogues were synthesised by Dr. Andrew Westwell (Cardiff University, School of Pharmacy and Pharmaceutical Sciences) and co-workers (Francesca Solfa and Matteo Morelli), and their ability to induce cytotoxicity was determined in breast cell lines chosen to model three disease states: ER^+ breast cancer (MCF-7), ER^- breast cancer (MDA-MB-231) and non-tumourigenic breast epithelium (MCF-10A). Viability studies in these cells were conducted using the CellTiter Blue assay following 72 hr incubation with the analogue; structure and viability plots for each analogue are shown in Figure 5.4-5.9. Table 5.1 represents a summary of this data, with additional information regarding molecular weight. The extent of cytotoxicity in MCF-7 and MDA-MB-231 cells varied between analogues with IC_{50} values for both cell lines between 0.1 and 60 μM. In contrast, no analogue produced IC_{50} values <10 μM in the MCF-10A cell line demonstrating that these cells were highly resistant to the effects of compounds which share the thioester moiety and disulfide bond characteristic of disulfiram.

Analogues were designed in order to determine which structural features were necessary for cytotoxic effects in MCF-7 and MDA-MB-231 cells. Two series of compounds were synthesised which differed in their core moiety; the thiuram disulfide series retained the two thioester groups joined by a disulfide bridge, characteristic of the parent drug, alternatively the

150

Table 5.1. Summary of the chemical properties and viability effects of disulfiram and analogues. Formula and molecular weight (Mw) information was obtained from reproducing the structure in "MarvinView 6.2.0" software and using Tools>Elemental Analysis. IC_{50} values are an estimation based on interpolation at 50% from viability curves shown in Figures 5.4-5.9. Disulfiram (DSF) is included as a comparison. *indicates a biphasic viability profile, defined as a statistical significance between viability effects at 1 and 10 μM where 1 μM produces a >45% cytotoxicity. Light grey indicates thiuram disulfide series; dark grey indicates carbamo(dithioperoxo)thioate series. Analogues are ranked by molecular weight.

Analogue	Formula	Mw	IC_{50} MCF-7 (μM)	IC_{50} MDA-MB-231 (μM)	IC_{50} MCF-10A (μM)
FS07PY	$C_7H_{13}NOS_3$	223.4	0.5	60	60
FS06DE	$C_7H_{15}NOS_3$	225.4	0.6*	0.8*	60
MM005	$C_{11}H_{21}NS_3$	263.5	0.9	50	70
KT06	$C_{11}H_{23}NS_3$	265.5	0.7*	30	60
MM002	$C_{12}H_{23}NS_3$	277.5	0.6*	50	50
MM003	$C_{11}H_{21}NOS_3$	279.5	1	10	NA
ANF-D12	$C_{10}H_{16}N_2S_4$	292.5	0.4	0.7	50
MM004	$C_{12}H_{24}N_2S_3$	292.6	0.9	50	80
DSF	$C_{10}H_{20}N_2S_4$	296.5	0.3*	40	60
ANF-D24	$C_{12}H_{20}N_2S_4$	320.6	0.1*	40	65
FS01BM	$C_{18}H_{20}N_2S_4$	392.6	1*	60	90
FS02MP	$C_{20}H_{24}N_2S_4$	420.7	40	60	NA
FS03EB	$C_{20}H_{24}N_2S_4$	420.7	50	60	NA

carbamo(dithioperoxo)thioate series contained a single thioester and disulfide bond (Figure 5.3). By comparing the cytotoxicity profiles of analogues which contained these core structures it was possible to assess the importance of the symmetry of the thioester moieties around the disulfide bond. Additionally, the R1 and R groups of each core structure allowed further chemical modification

which provided insight into how the chemical structures at each terminus altered analogue cytotoxicity.

The thiuram disulfide series contained five structural analogues: ANF-D12, ANF-D24, FS01BM, FS02MP, and FS03EB. Of these, ANF-D24 was the most structurally comparable with disulfiram as the R groups were substituted with piperidine moieties (six membered ring containing five carbons and one nitrogen atom) and therefore similar in size to the two ethyl groups found on the parent molecule (Figure 5.4A). This analogue produced a viability profile almost identical to that of the parent drug; cytotoxicity in MCF-7 cells was biphasic and produced an IC_{50} of 0.1 μM (compared to 0.3 μM for disulfiram), whereas MDA-MB-231 cells were resistant to viability effects with an IC_{50} of 40 μM (Figure 5.4B). Interestingly when these piperidine groups were substituted for the smaller pyrollidine structures, as in the case of ANF-D12, a markedly different cytotoxic profile was observed (Figure 5.4C-D). Here, MCF-7 cells did not exhibit the characteristic biphasic cytotoxicity profile of disulfiram and instead there was almost complete loss of viable cells at 10 μM. In comparison, a slight biphasic peak was observed for MDA-MB-231 cells where viability was restored to 32% at 10 μM despite 1 μM reducing viability to 20%, however statistical testing revealed that the difference between viability at 1 and 10 μM was not significant. From comparison of these structurally similar analogues it is apparent that the size of groups attached to the terminal nitrogen are of critical importance for both the biphasic profile
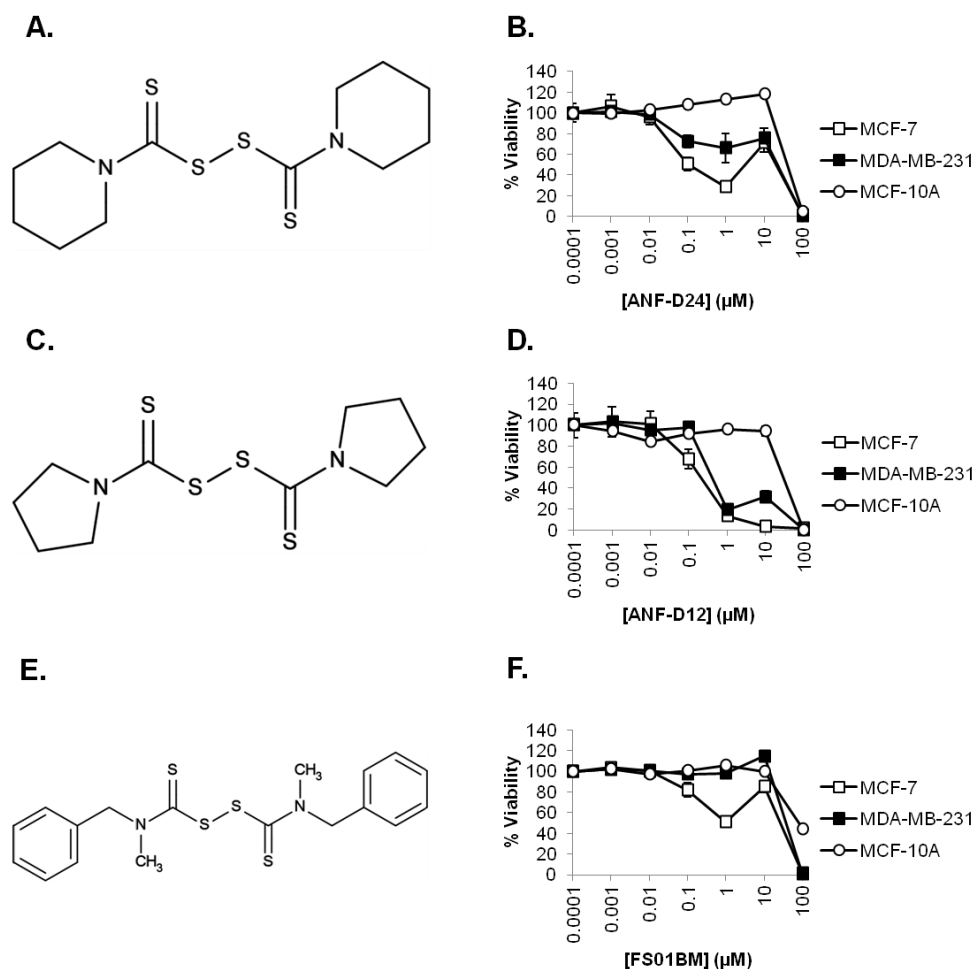
Figure 5.4. Structure and viability data for ANF-D24, ANF-D12 and FS01BM. (A, C, E) Chemical structure of thiuram disulfide analogues. (B, D, F) MCF-7, MDA-MB-231 and MCF-10A cells were incubated with analogue in serial dilution for 72 hr prior to viability analysis via the CellTiter Blue assay. Error bars show standard error.

seen in MCF-7 cells and the sensitivity of MDA-MB-231 cells. To further demonstrate this when the R groups were replaced with even larger moieties, as in the case of FS01BM which contained methyl and benzyl groups, the viability profile of MCF-7 cells was biphasic although sensitivity at 1 μM was reduced compared ANF-D12 and ANF-D24, and no viability effects were observed with MDA-MB-231 cells <10 μM (Figure 5.4E-F).

The final two analogues of this series differ from FS01BM by a single carbonyl at each of the two R groups; FS02MP contains methyl and phenethyl groups whereas FS03EB contains ethyl and benzyl groups (Figure 5.5A, C). In both cases IC_{50} values were >10 µM for both MCF-7 and MDA-MB-231 cells, demonstrating that the addition of a single carbonyl is sufficient to completely remove the sensitivity of MCF-7 cells to the effects of these analogues and indicating that size is a critical feature for cytotoxicity within this analogue series. The importance of analogue size in the thiuram disulfide series is further demonstrated when analogues are ranked by the percentage of viable cells remaining after 1 µM treatment:

ANF-D12<ANF-D24< FS01BM<FS02MP and FS03EB (Figure 5.4-5.5), this sequence exactly correlates with molecular weight (Table 5.1).
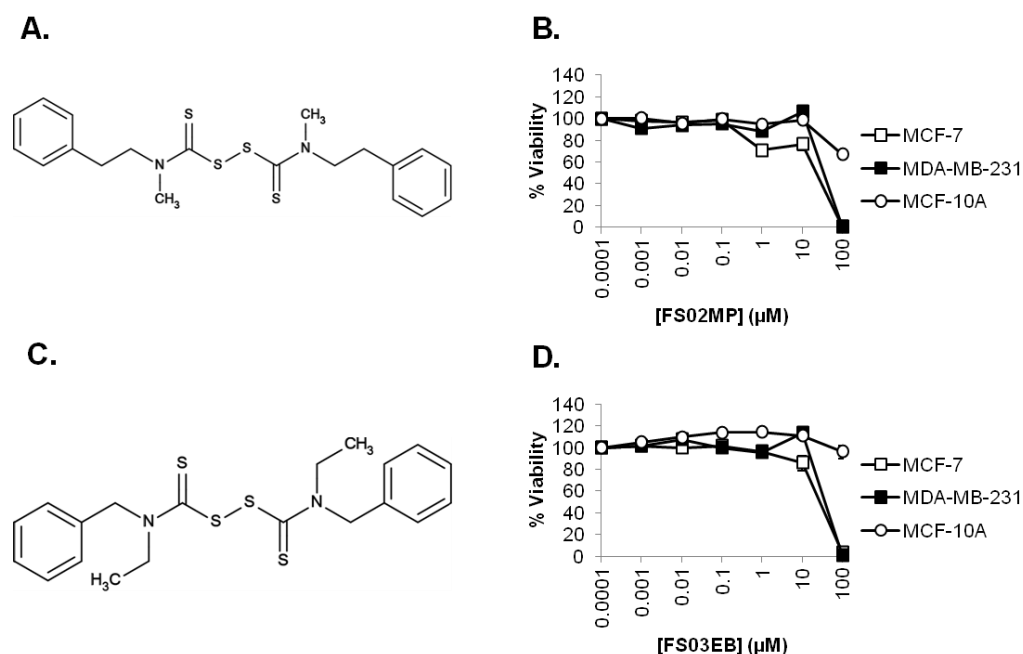

Figure 5.5. Structure and viability data for FS02MP and FS03EB. (A, C) Chemical structure of thiuram disulfide analogues. (B, D) MCF-7, MDA-MB-231 and MCF-10A cells were incubated with analogue in serial dilution for 72 hr prior to viability analysis via the CellTiter Blue assay. Error bars show standard error.

5.2.2. The chemical properties of moieties bound to the nitrogen (R), rather than those bound to the disulfide bond (R1), govern the response to MCF-7 and MDA-MB-231 cells to carbamo(dithioperoxo)thioate analogues

Seven analogues (FS06DE, FS07PY, KT06, MM002, MM003, MM004 and MM005) belonged to the carbamo(dithioperoxo)thioate structural series, defined by a single thioester moiety attached to the disulfide bond (Figure 5.3). Viability profiles from five of these analogues formed part of a publication which also described their synthesis (Cilibrase *et al.,* 2015). Similarly to the thiuram disulfide series, viability results within this dataset provided mixed results in terms of the response of MDA-MB-231 cells and although MCF-7 viability effects were noted for all analogues within this series their ability to induce biphasic effects differed. This indicates that removal of the second thioester group does not produce an overall effect on the cytotoxicity profile of disulfiram analogues in terms of the MCF-7 biphasic peak and MDA-MB-231 cell sensitivity. In further support of this, one analogue within this series, MM002, provided a biphasic MCF-7 viability profile and did not produce viability effects in MDA-MB-231 cells, in a similar manner to disulfiram despite lacking this second thioester group (Table 5.1).

The fact that the core structure of the carbamo(dithioperoxo)thioate series was asymmetrical meant that it was possible to investigate the effect of altering the chemical groups on either terminus of the N(C=S)S-S bond. Initially analogues were compared which were identical with respect to the chemical moieties

attached to the disulfide bond (R1) but where groups bonded to the nitrogen (R) were altered. For example, FS06DE and FS07PY both contained a 2-hydroxyethyl group at R1, whereas R was consisted of two ethyl groups for FS06DE and pyrollidine for FS07PY (Figure 5.6A, C). Both analogues produced markedly different viability profiles; biphasic cytotoxicity was observed for both MCF-7 and MDA-MB-231 cells treated with FS06DE and for FS07PY only MCF-7 cells responded to the analogue at concentrations <10 μM and no biphasic effect was observed. The fact that these profiles differ so dramatically despite having identical R1 groups suggests viability effects are a result of the chemical group attached to the nitrogen. The influence of the chemical moieties at R were further assessed by an extended panel of five
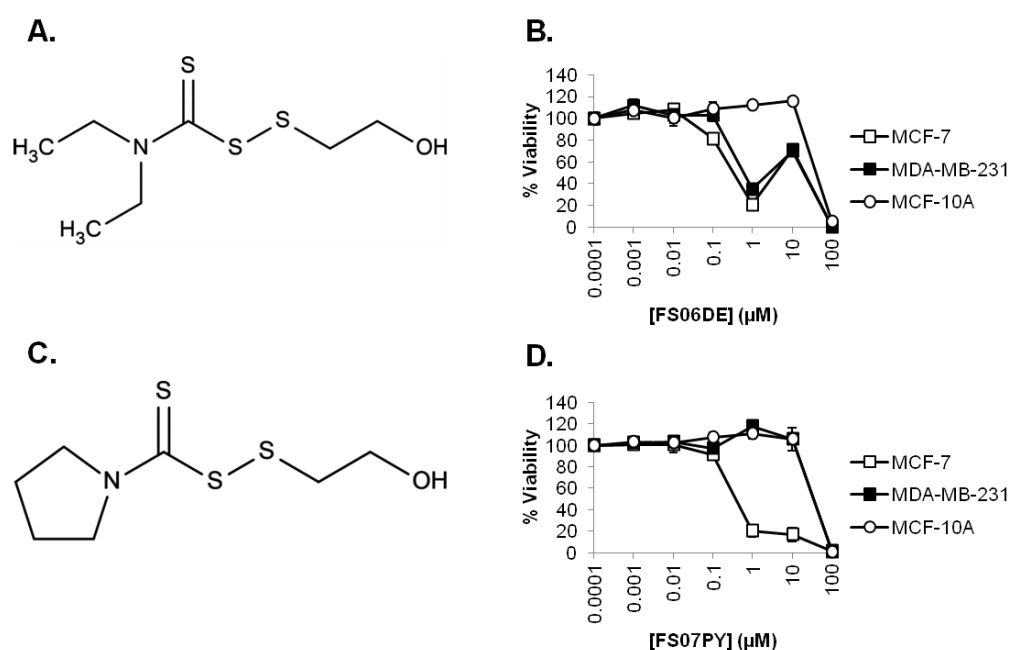

Figure 5.6. Structure and viability data for FS06DE and FS07PY. (A, C) Chemical structure of carbamo(dithioperoxo)thioate analogues. (B, D) MCF-7, MDA-MB-231 and MCF-10A cells were incubated with analogue in serial dilution for 72 hr prior to viability analysis via the CellTiter Blue assay. Error bars show standard error.

analogues (MM002, MM003, MM004 and MM005, KT06) which all contained

identical hexane moieties R1 but varied with respect to the chemical group at

R. Three of these analogues contained a six membered ring (MM002, MM003

and MM004) and exhibited distinct differences in both their selectivity for

MCF-7 cells versus MDA-MB-231 cells and ability to produce a biphasic

profile: MM002 contained a piperidine moiety and produced biphasic viability

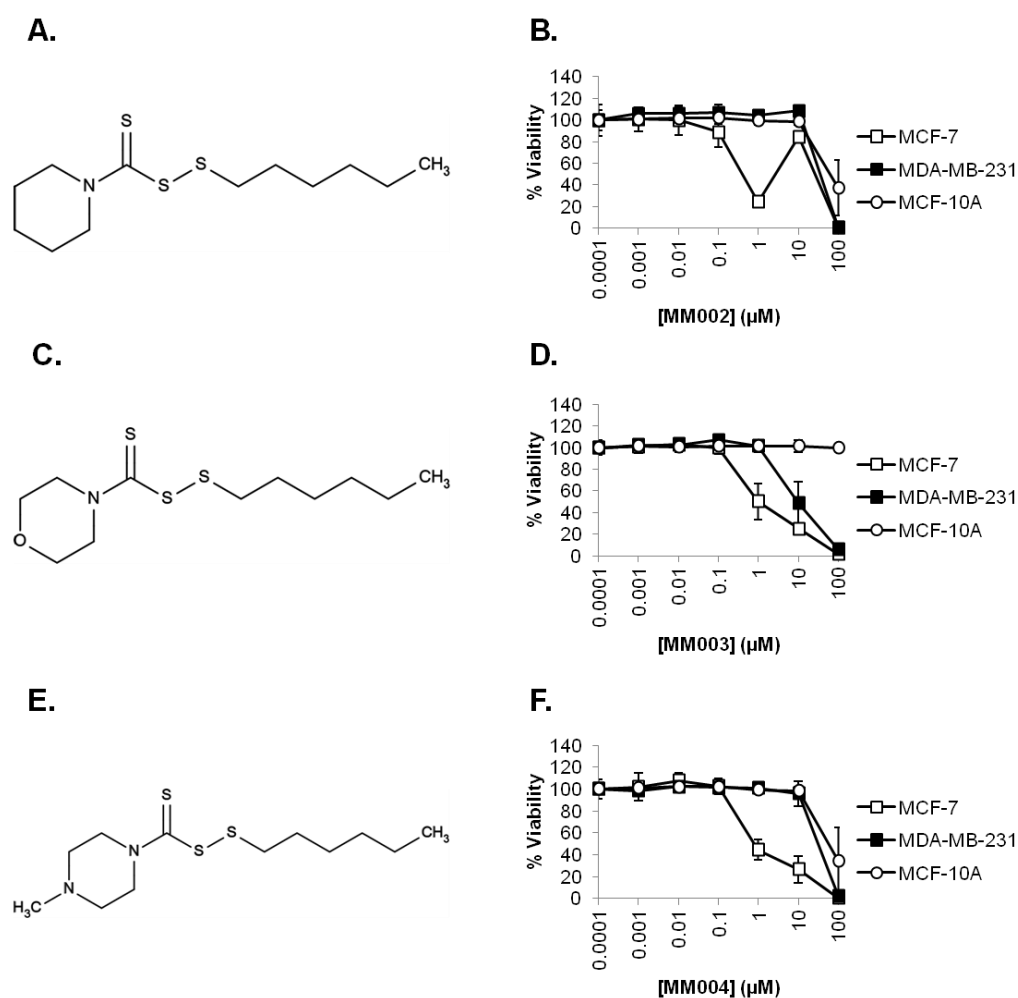effects in MCF-7 with no effect in MDA-MB-231 cells <100 μM (Figure 5.7A,

Figure 5.7. Structure and viability data for MM002, MM003 and MM004. (A, C, E) Chemical structure of carbamo(dithioperoxo)thioate analogues. (B, D) MCF-7, MDA-MB-231 and MCF-10A cells were incubated with analogue in serial dilution for 72 hr prior to viability analysis via the CellTiter Blue assay. Error bars show standard error.

B); MM003 contained a morpholine ring and produced viability effects in both cell lines at <10 µM and no biphasic effect was observed (Figure 5.7C, D); MM004 contained a N-methylpiperazine moiety and was selectively toxic to MCF-7 cells however did not produce a biphasic response (Figure 5.7E, F). These results demonstrate that the substitution of a carbon atom in the chemical moiety at R to an electronegative atom, such as oxygen or nitrogen, is able to remove the biphasic effect observed in MCF-7 cells. The fact that MM003 and MM004 differ in their ability to produce viability effects in MDA-MB-231 cells at 10 µM indicates that the addition of oxygen, but not nitrogen, to the R group is able to produce cytotoxicity in this cell line. To further address the hypothesis that the chemical groups bound to the nitrogen (R) were critical for the cytotoxic properties of carbamo(dithioperoxo)thioate analogues, viability profiles were compared between analogues which were identical R but differed with respect to the chemical moiety bound at R1. The ability of MM005 and FS07PY, which both contained pyrollidine moieties at R but hexanyl or 2-hydroxyethyl respectively at R1, to induce viability effects was analysed (Figure 5.8). Neither analogue was able to produce cytotoxicity in MDA-MB-231 cells at concentrations under <100 µM, and both were cytotoxic to MCF-7 cells (IC_{50} <1 µM) without producing a biphasic effect. Interestingly, the viability profile of MCF-7 cells in response to MM005 and FS07PY is also similar to ANF-D12 and all contain pyrollidine moieties, providing further evidence to support the hypothesis of Section 5.2.1 that the MCF-7 biphasic effect can be ablated by the addition of smaller chemical groups bound to the nitrogen (compare Figure 5.8B, D and 5.4D).
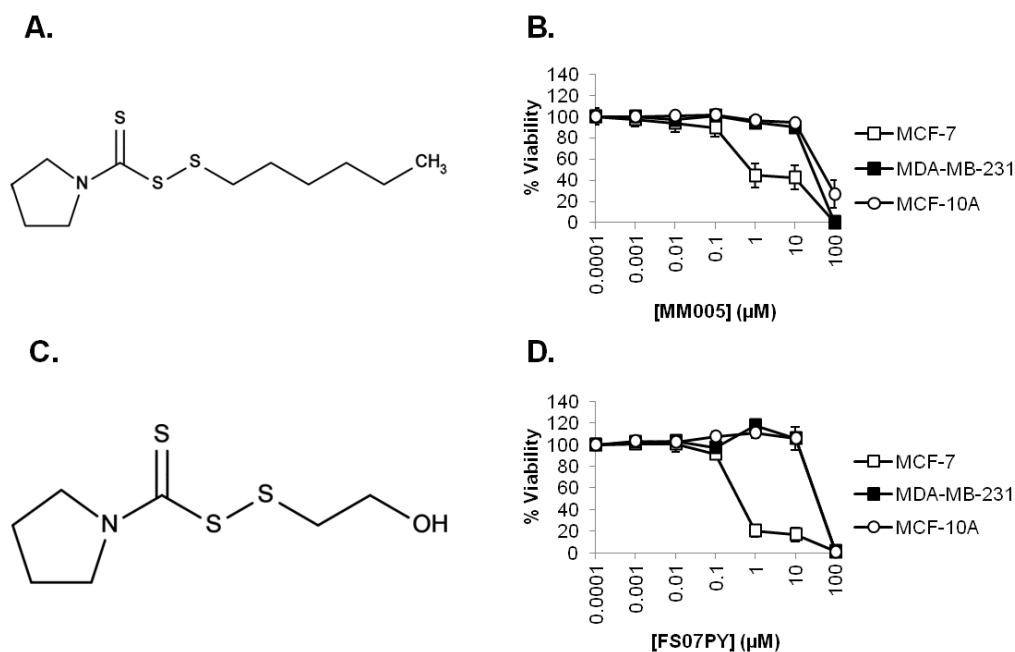
Figure 5.8. Structure and viability data for MM005 and FS07PY. (A, C) Chemical structure of carbamo(dithioperoxo)thioate analogues. (B, D) MCF-7, MDA-MB-231 and MCF-10A cells were incubated with analogue in serial dilution for 72 hr prior to viability analysis via the CellTiter Blue assay. Error bars show standard error.

The critical importance of chemical groups at R was additionally investigated by comparison of carbamo(dithioperoxo)thioate analogues KT06 and FS06DE which both were identical at R (two ethyl groups) but KT06 contained a hexane chain and FS06DE contained 2-hydroxyethyl at R1 (Figure 5.9A, C). Both analogues demonstrate a trend towards biphasic cytotoxicity in MCF-7 and MDA-MB-231 cells, although statistical significance was not achieved to indicate a difference in MDA-MB-231 cells treated with 1 or 10 μM KT06.
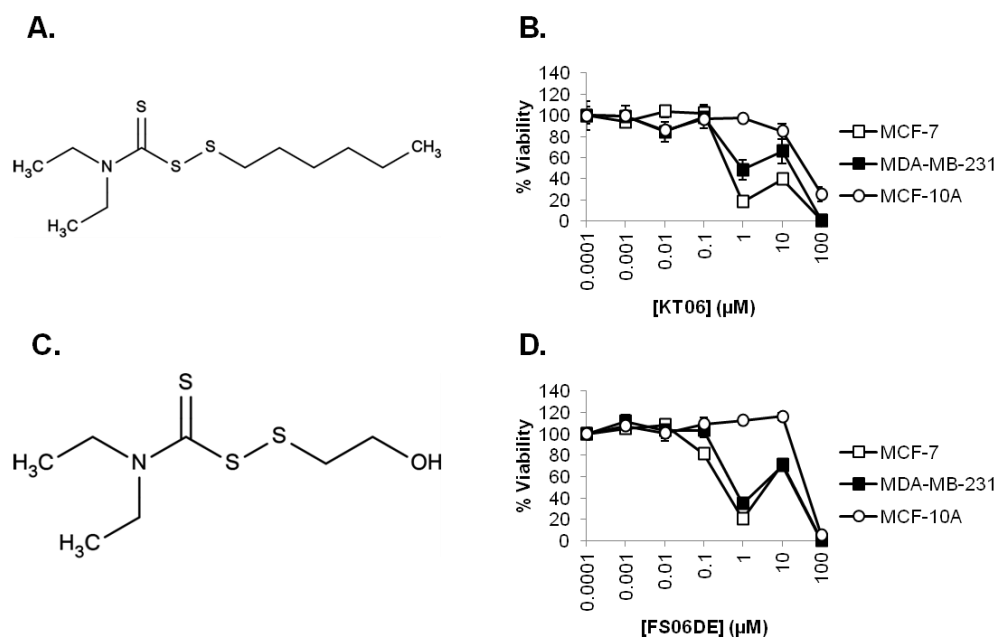
Figure 5.9. Structure and viability data for KT06 and FS06DE. (A, C) Chemical structure of carbamo(dithioperoxo)thioate analogues. (B, D) MCF-7, MDA-MB-231 and MCF-10A cells were incubated with analogue in serial dilution for 72 hr prior to viability analysis via the CellTiter Blue assay. Error bars show standard error.

5.2.3. Cytotoxicity of DDC and FS03EB correlates with zinc ionophore activity

Using compounds structurally related to disulfiram, it was next investigated how the cytotoxic response of MCF-7 cells related to zinc ionophore activity. In biological solutions disulfiram thought to be rapidly converted to DDC raising the possibility that metabolites are responsible for much of the drug's biological functions (Agarwal *et al.,* 1983). The cytotoxic and zinc ionophore properties of DDC were initially compared to those of disulfiram in MCF-7 cells. DDC displayed a sharp increase in toxicity at concentrations higher than 0.1 μM with evidence of recovery being observed at 100 μM, rather than at 10 μM as in the case of the parent drug (Figure 5.10A). Supplementation with
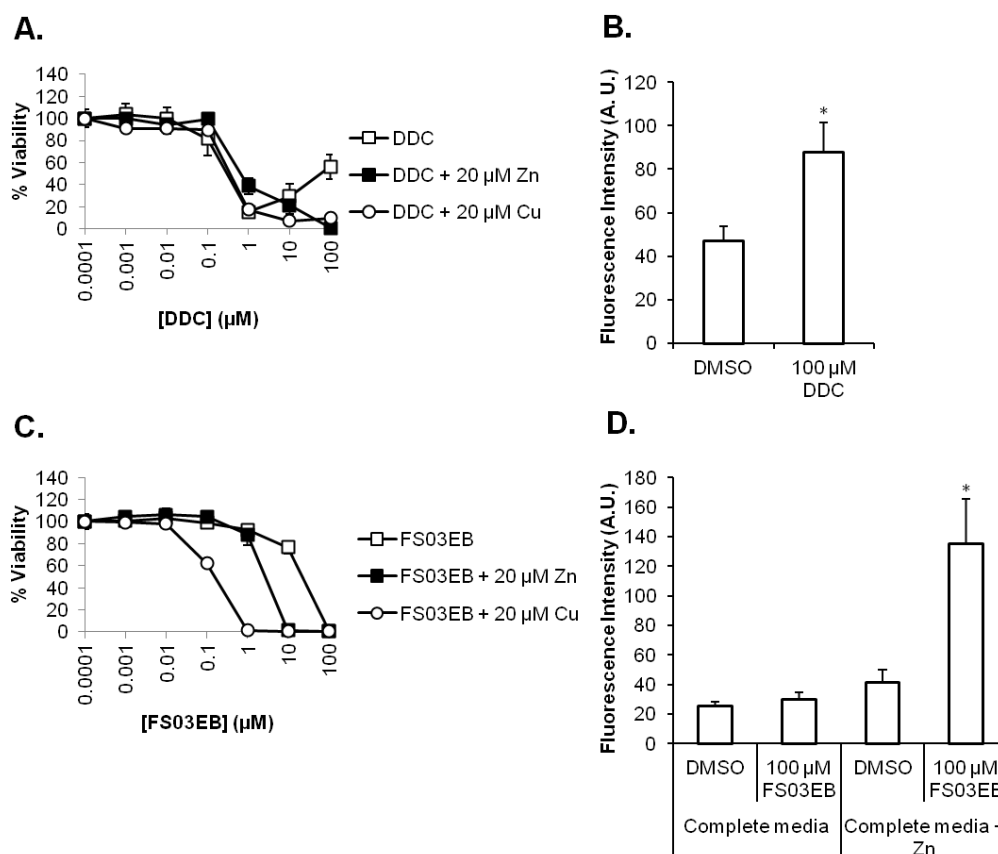
160

Figure 5.10. Toxicity of DDC and FS03EB correlates with zinc ionophore activity. (A, C) MCF-7 cells were treated with DDC (A) or FS03EB (C) +/- 20 μM copper or zinc in complete media for 72 hr prior to performing viability analysis. (B, D) MCF-7 cells were pre-loaded with Fluozin-3, treated with DDC (B) or FS03EB +/- 20 μM zinc (D) for 10 min prior to measuring Fluozin-3 fluorescence via flow cytometry. Error bars show standard error. *p<0.05

copper and zinc completely ablated the DDC biphasic effects and significantly enhanced its toxicity. The metabolite was also able to increase intracellular zinc levels (Figure 10B) but was a less potent zinc ionophore compared with disulfiram (Figure 4.2A).

To address the issue of whether cytotoxicity may relate to the capacity of disulfiram and DDC to deliver zinc, studies were conducted to investigate the relationship between metal ions and the FS03EB analogue, chosen as it was

161

non-toxic under normal cell culture conditions at concentrations <100 µM. Viability studies revealed that co-incubation of this compound (>1 µM) with 20 µM zinc or copper was able to significantly enhance toxicity leading to complete loss of viability at 1 µM and 10 µM for copper and zinc respectively. The ability of FS03EB to increase fluorescence of Fluozin-3 was then assessed using flow cytometry under normal cell culture (complete media) and high zinc (complete media + 20 µM zinc) conditions. In complete media, and contrary to the effects observed with disulfiram and DDC, data in Figure 5.10D show that the analogue was unable to significantly increase intracellular zinc levels in complete media. However, when the zinc ionophore activity of 100 µM FS03EB was investigated in conditions which induced toxicity at <10 µM (complete media + 20 µM zinc), it resulted in a >3 fold increase in Fluozin-3 fluorescence. The fact that FS03EB cytotoxicity at concentrations <10 µM in MCF-7 cells is entirely dependent on the availability of metal ions within the media and only occurs under conditions which also produce a detectable increase in intracellular zinc levels, indicates that the zinc ionophore activity of the analogue is a requirement for these cytotoxic effects.

162

5.3. Discussion

This chapter aimed to provide insight into how the chemical features of disulfiram analogues relate to its biological activity, particularly its ability to induce viability effects in breast cancer cells. Little prior research has been done to determine the structure-activity relationship of the drug, aside from a previous collaboration between Cardiff University and Barbara Ann Karmanos Institute, Detroit (Brahemi *et al.,* 2010). This paper describes the effect of four classes of disulfiram analogues on the viability of breast cancer and epithelial cell lines. Two of these, benzisothiazolones and dithiocarbamates, lacked the disulfide bond and all analogues within these series' (a total of 36) were inactive at <10 µM in breast cancer cell lines. In addition a further analogue, 4,4-dithiomorpholine, lacking the thioester bond, was also unable to induce breast cancer cell cytotoxicity. Taken together these results demonstrated the requirement of both the disulfide bond and thioester in the biological activity of disulfiram. Due to this, further analysis was conducted using a panel of three thiuram disulfide and ten carbamo(dithioperoxo)thioate analogues which contained these structural features and demonstrated that these analogue series' could produce IC_{50} values of <1 µM in ER^+ breast cancer cells. This chapter is an extension of the previous collaboration focussing on a larger panel of thiuram disulfide and carbamo(dithioperoxo)thioate analogues and their activities in MCF-7, MDA-MB-231 and MCF-10A cells.

This work represents the first time size has been described as a factor which determines the sensitivity of breast cancer cells to disulfiram analogues. This is

demonstrated by the observation that analogues containing a piperidine moiety in the R group were capable of inducing biphasic viability effects which could be removed by substitution with the slightly smaller pyrollidine. This result is particularly interesting in view of the literature surrounding a compound structurally related to disulfiram, PDTC, which also contains a pyrollidine group. Unlike the pyrollidine containing analogues of this chapter, biphasic viability has been observed with PDTC in neuronal cells and attributed to the ability of the compound to activate ERK or JNK at different concentrations (Chung *et al.,* 2000). The fact that the biphasic effect was not observed for the pyrollidine containing analogues in this study may indicate that PDTC operates via a different mechanism of action compared to disulfiram analogues or that neuronal and MCF-7 cells respond differently to these compounds. Other studies investigating the structure-activity relationship of PDTC-copper complexes have found that substitution of the piperidine moiety for pyrollidine had no effect on breast cancer cell viability, although the effect of PDTC analogues in the absence of copper was not investigated (Yu *et al.,* 2007). Interestingly and in accordance with the findings of this chapter, when the pyrollidine moiety of PDTC was replaced with larger R groups cytotoxic effects were dramatically reduced. The relationship between the structure of disulfiram analogues and how this relates to their ability to bind and transport zinc across the plasma membrane of cells is not known and could be the subject of further experimentation. The observation that cytotoxicity of PDTC has previously been demonstrated to be enhanced by zinc supplementation

indicates that the pyrollidine containing analogues of this chapter may also retain the drug's zinc ionophore effect (Pozza *et al.,* 2011).

The fact that the core structure of the carbamo(dithioperoxo)thioate series was asymmetrical meant that it was possible to assess the impact of altering groups on either side of the disulfide bond on the viability profile of analogues. From these studies it is apparent that the chemical groups bound directly to the nitrogen atom (R) have a greater impact on the biphasic effect in MCF-7 cells and MDA-MB-231 cell sensitivity compared to the chemical groups bound to the disulfide bond (R1). Studies investigating the structure-activity relationship of PDTC analogues have previously focussed on altering the chemical groups bound to the nitrogen atom and found that chemical modification at this position could alter the ability of analogues to inhibit the proteasome and induce viability effects (Yu *et al.,* 2007; Wang *et al.,* 2011). These studies did not compare the effect of modifying the chemical groups at other positions, however imply that the biological activity of both PDTC and disulfiram are dependent of the chemical groups bound to the nitrogen atom. This finding could have implications not only in identifying other compounds with disulfiram-like activity in breast cancer cells but also may be used to aid characterisation of the drug's biological effects.

In vivo disulfiram is rapidly and extensively metabolised in a systemic manner; the first degradation product is DDC and this metabolite is thought to be a major contributor in the clinical effects of the drug (Nagendra *et al.,* 1991).

DDC has been shown to have toxicity against breast cancer cells *in vitro* and increases intracellular copper in other model systems (Tonkin *et al.,* 2004; Cvek *et al.,* 2008). Additionally, a clinical trial has shown that adjuvant DDC is able to increase survival in patients at high risk of metastatic breast cancer (Dufour *et al.,* 1993). In this chapter DDC, albeit to a lesser extent than disulfiram, was also able to increase intracellular zinc levels and this may be a mechanism behind its increased cytotoxicity in the presence of high extracellular levels of these metal ions.

The fact that not all disulfiram analogues produced viability effects allowed further investigation into how cytotoxicity relates to zinc ionophore effects. These studies utilised FS03EB as it did not produce viability effects in MCF-7 cells <100 µM under physiological conditions and compared its ability to induce cell death and alter intracellular zinc levels in either physiological or zinc enriched conditions. Contrary to effects observed with disulfiram and DDC, FS03EB under physiological conditions was unable to significantly increase intracellular zinc levels. Therefore, the lack of toxicity in cells treated with this analogue alone could be due to reduced zinc ionophore activity. However in zinc enriched conditions both cytotoxicity at 10 µM and zinc ionophore activity at 100 µM of the analogue were dramatically increased. This data provides a potential link between zinc ionophore activity and cytotoxicity, such that the observed toxicity profiles for disulfiram, DDC and FS03EB relate to their capacity to deliver intracellular zinc. An important limitation of this experiment is the fact that 100 µM FS03EB produced

cytotoxicity in both physiological and zinc enriched conditions, however this concentration only produced an ionophore effect in the rich enriched scenario. This therefore indicates that at 100 µM other mechanisms must contribute to FS03EB cytotoxicity independent of its zinc ionophore properties. The use of a lower concentration of FS03EB would provide a stronger link between cytotoxicity and zinc ionophore action, to demonstrate this 10 µM FS03EB was only cytotoxic in the zinc enriched scenario and not under physiological conditions. A further study could be to determine the ionophore properties of this concentration of FS03EB in conditions of high (zinc enriched) and low (full serum media) MCF-7 cell sensitivity, this would provide strong evidence that the analogue is only cytotoxic in conditions which also provide zinc ionophore action.

References

Agarwal, R. P., McPherson, R. A. and Phillips, M. 1983. Rapid degradation of disulfiram by serumFalbumin. *Research Communications in Chemical Pathology and Pharmacology.* 42(2), p. 293-310.

Brahemi, G., Kona, F. R., Fiasella, A., Buac, D., Soukupova, J., Brancale, A., Burger, A. M. and Westwell, A. D. 2010. Exploring the structural requirements for inhibition of the ubiquitin E3 ligase Breast Cancer Associated Protein 2 (BCA2) as a treatment for breast cancer. *Journal of Medicinal Chemistry.* 53(7), p. 2757-2765.

Chung, K. C., Park, J. H., Kim, C. H., Lee, H. W., Sato, N., Uchiyama, Y. and Ahn, Y. S. 2000. Novel biphasic effect of pyrrolidine dithiocarbamate on neuronal cell viability is mediated by the differential regulation of intracellular zinc and copper ion levels, NF-kappa B, and MAP kinases. *Journal of Neuroscience Research.* 59(1), p. 117-125.

Cilibrasi, V., Tsang, K., Morelli, M., Solfa, F., Wiggins, H. L., Jones, A. T. and Westwell, A. D. 2015. Synthesis of substituted carbamo(dithioperoxo)thioates as potential BCA2-inhibitory anticancer agents. *Tetrahedron Letters.* 56(20), p. 2583-2585.

Cobby, J., Mayersohn, M. and Selliah, S. 1977. Rapid reduction of disulfiram in blood and plasma. *Journal of Pharmacology and Experimental Therapeutics.* 202(3), p. 724-731.

Cvek, B., Milacic, V., Taraba, J. and Dou, Q. P. 2008. Ni(II), Cu(II), and Zn(II) Diethyldithiocarbamate complexes show various activities against the proteasome in breast cancer cells. *Journal of Medicinal Chemistry.* 51(20), p. 6256-6258.

Dufour, P., Lang, J. M., Giron, C., Duclos, B., Haehnel, P., Jaeck, D., Jung, J. M. and Oberling, F. 1993. Sodium ditiocarb as adjuvant immunotherapy for high-risk breast-cancer- a randomized study. *Biotherapy.* 6(1), p. 9-12.

El-Aarag, B. Y. A., Kasai, T., Zahran, M. A. H., Zakhary, N. I., Shigehiro, T., Sekhar, S. C., Agwa, H. S., Mizutani, A., Murakami, H., Kakuta, H. and Seno, M. 2014. *In vitro* anti-proliferative and anti-angiogenic activities of thalidomide dithiocarbamate analogs. *International Immunopharmacology.* 21(2), p. 283-292.

Eneanya, D. I., Bianchine, J. R., Duran, D. O. and Andresen, B. D. 1981. The actions and metabolic-fate of disulfiram. *Annual Review of Pharmacology and Toxicology.* 21, p. 575-596.

Johansson, B. 1992. A review of the pharmacokinetics and pharmacodynamics of disulfiram and its metabolites. *Acta psychiatrica Scandinavica. Supplementum.* 369, p. 15-26.

Liu, P., Wang, Z., Brown, S., Kannappan, V., Tawari, P. E., Jiang, W., Irache, J. M., Tang, J. Z., Britland, S., Armesilla, A. L., Darling, J. L., Tang, X. and Wang, W. 2014. Liposome encapsulated disulfiram inhibits NF kappa B pathway and targets breast cancer stem cells *in vitro* and *in vivo*. *Oncotarget.* 5(17), p. 7471-7485.

Nagendra, S. N., Shetty, K. T., Subhash, M. N. and Guru, S. C. 1991. Role of glutathione-reductase system in disulfiram conversion to diethyldithiocarbamate. *Life Sciences.* 49(1), p. 23-28.

Pozza, E. D., Donadelli, M., Costanzo, C., Zaniboni, T., Dando, I., Franchini, M., Arpicco, S., Scarpa, A. and Palmieri, M. 2011. Gemcitabine response in pancreatic adenocarcinoma cells is synergistically enhanced by dithiocarbamate derivatives. *Free Radical Biology and Medicine.* 50(8), p. 926-933.

Schweizer, M. T., Lin, J., Blackford, A., Bardia, A., King, S., Armstrong, A. J., Rudek, M. A., Yegnasubramanian, S. and Carducci, M. A. 2013. Pharmacodynamic study of disulfiram in men with non-metastatic recurrent prostate cancer. *Prostate Cancer and Prostatic Diseases.* 16(4), p. 357-361.

Tonkin, E. G., Valentine, H. L., Milatovic, D. M. and Valentine, W. M. 2004. N,N-diethyldithiocarbamate produces copper accumulation, lipid peroxidation, and myelin injury in rat peripheral nerve. *Toxicological Sciences.* 81(1), p. 160-171.

Wang, F., Zhai, S., Liu, X., Li, L., Wu, S., Dou, Q. P. and Yan, B. 2011. A novel dithiocarbamate analogue with potentially decreased ALDH inhibition has copper-dependent proteasome-inhibitory and apoptosis-inducing activity in human breast cancer cells. *Cancer Letters.* 300(1), p. 87-95.

Yu, Z., Wang, F., Milacic, V., Li, X., Cui, Q. C., Zhang, B., Yan, B. and Dou, Q. P. 2007. Evaluation of copper-dependent proteasome-inhibitory and apoptosis-inducing activities of novel pyrrolidine dithiocarbamate analogues. *International Journal of Molecular Medicine.* 20(6), p. 919-925.

6. Investigation into the ability of disulfiram to induce lysosomal membrane permeabilisation

6.1. Introduction

The observation that disulfiram was able to increase zinc levels specifically in endo-lysosomal compartments (Chapter 4) raised the possibility that the drug may induce damage to these structures. The phenomenon of lysosomal membrane permeabilisation (LMP) has previously been noted to occur in response to clioquinol, another zinc ionophore, upon sequestration of the metal in lysosomes, and as both drugs produce similar zinc loading effects in this organelle it may be the case that LMP also occurs in disulfiram treated cells (Yu *et al.,* 2009). LMP involves the release of lysosomal proteases to the cell cytosol, of which the cathepsin family are considered the major contributors to cell death (Mrschtik and Ryan 2015). Cathepsins are categorised into three sub-families based on the amino acid found within their active site, namely serine (cathepsin A and G), cysteine (B, C, F, H, K, L, O, S, V, W and X), and aspartate (D and E) cathepsins. In particular cathepsins B, D and L are thought to be critical inducers of LMP and their chemical or genetic inhibition is able to partially protect cells from LMP inducers such as etoposide and acetate (Oberle *et al.,* 2010; Marques *et al.,* 2013). The subcellular location of mature cathepsins in the lysosome is a result of complex sorting and trafficking events which shuttle the immature protein from the endoplasmic reticulum and Golgi network via vesicles to the lysosome (Braulke and Bonifacino 2009). Once in the lysosome the immature protease undergoes cleavage of N-terminal residues to produce the mature cathepsin (Laurent-Matha *et al.,* 2006).

One of the mechanisms by which LMP induces cell death is as an upstream mediator of apoptosis, in this context it has been demonstrated that pro-apoptotic Bcl-2 family members are cathepsin substrates leading to their activation and LMP precedes cytochrome c release (Johansson *et al.,* 2003; Droga-Mazovec *et al.,* 2008). However it has also been proposed that LMP acts as a mediator of the apoptotic response, and has been shown to occur downstream of caspase activation in response to apoptosis inducers (Huai *et al.,* 2013). Interestingly, over-expression of mutant cathepsin D is equally as effective as wild-type at inducing apoptosis, as measured by cytochrome c release and caspase activation, indicating that LMP may not be dependent on the protease activity of this protein (Beaujouin *et al.,* 2006).

Over-expression of cathepsins is frequently noted in breast cancer where cathepsin D and B levels correlate with increased lymph node involvement and decreased disease free survival (Westley and May 1987; Thomssen *et al.,* 1995; Lah *et al.,* 2000; Nouh *et al.,* 2011). Their mechanism within this context may be explained by the fact that inhibition of cathepsin B decreases degradation of ECM and attenuates bone metastases by breast cancer cells (Victor *et al.,* 2011; Withana *et al.,* 2012). In this model cathepsin B translocates to the invasive edge of the tumour where it is secreted into the tumour micro-environment resulting in ECM degradation, allowing more favourable conditions for tumour cell metastasis (Aggarwal and Sloane 2014). Similar data exists implicating cathepsin D in metastatic processes; here it has

been shown to activate ECM degradation enzymes in conditions which simulate the breast tumour micro-environment (Maynadier *et al.,* 2013).

The over-expression of these highly proteolytic enzymes in tumours may be a characteristic which could be clinically exploited. The fact that lysosome associated membrane proteins 1 and 2 (LAMP 1 and 2) required for lysosomal stability are down-regulated by cathepsins, imply that cancer cells may be more sensitive to LMP than non-cancer cells due to a less stable lysosomal membrane (Fehrenbacher *et al.,* 2008). This may be particularly relevant for tumours which harbour apoptosis-limiting p53 mutation, due to the fact that LMP induced cell death has been shown to occur in p53-null cell lines (Erdal *et al.,* 2005). Agents which increase ROS levels within cells have been shown to induce cell death via this mechanism, indicating that the lysosome may be particularly sensitive to oxidative damage (Kagedal *et al.,* 2001a). Equally LMP has been demonstrated to be a consequence of lysosome sequestered zinc in conditions of zinc overload (Hwang *et al.,* 2008; Kukic *et al.,* 2014). Taken together these observations suggest that drugs which increase ROS levels, such as zinc ionophores, are potential LMP inducers and cancer cells may be more sensitive to this effect than non-cancer cells. Perhaps surprisingly, the accumulation of lysosomal zinc and subsequent cell death via LMP is a feature of non-cancerous breast epithelial cells during mammary gland involution, the process responsible for the reduction of mammary gland size after weaning (Hennigar *et al.,* 2015). This therefore implicates the sequestering of lysosomal

zinc and subsequent LMP as an endogenous means of regulating cell number within breast tissue during normal (non-cancerous) development.

Particularly relevant to the study of disulfiram, proteasome inhibitors have previously been demonstrated to cause lysosomal release of cathepsin D by an unknown mechanism (Berndtsson *et al.,* 2009). Here, disulfiram-copper co-incubation was shown to increase cytosolic staining of cathepsin D and its knockdown was able to partially protect cells from disulfiram-copper induced cell death. However, the involvement of disulfiram alone has not been investigated. The hypothesis that the drug can alter the functioning of lysosomes is supported by immunofluorescence studies conducted by PhD student Jen Wymant in the laboratory which demonstrated that the drug influences the spatial organisation of LAMP 2 but not the early endosomal marker, early endosome antigen 1 (EEA1; Wymant 2015). Here, disulfiram was observed to have no effect on the localisation of early endocytic structures (Figure 6.1A), however caused late endosomes and lysosomes to be redistributed from typical perinuclear clusters observed in control cells to more diffuse scattering throughout the cytoplasm (Figure 6.1B). This provides evidence that the drug is capable of altering the biological processes of these organelles as the intracellular localisation of endo-lysosomal components is integral to their cellular function. For example, starvation and altered intracellular pH have been shown to redistribute lysosomes between perinuclear and peripheral regions of the cell (Korolchuk *et al.,* 2011; Malek *et al.,* 2012).

A. EEA 1

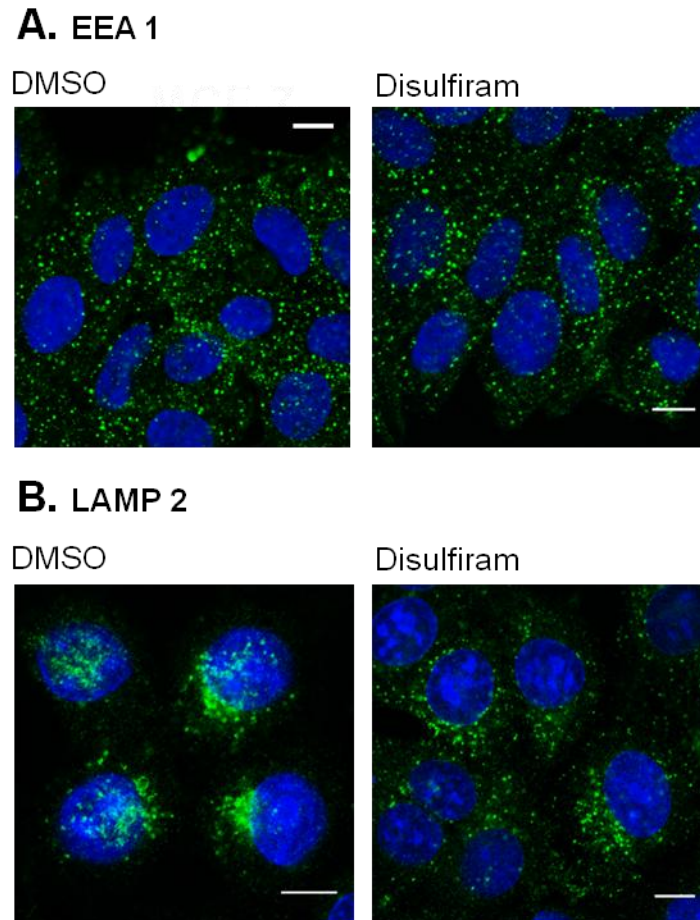DMSO   Disulfiram

B. LAMP 2

DMSO   Disulfiram

Figure 6.1. Disulfiram causes mislocalisation of lysosomes, however does not alter localisation of early endosomes. Experiment conducted by Jen Wymant and figure taken from Wiggins *et al.,* 2015. MCF-7 cells were treated with 1 µM disulfiram for 3 hr and then analysed via immunofluorescence microscopy using antibodies recognising EEA 1 (A), or LAMP 2 (B). Blue nuclei are labelled with Hoechst 33342. Images show a single projection through the centre of cells and are representative from three independent experiments. Scale bars show 10 µm.

Subcellular fractionation

Subcellular fractionation describes the process of separating intracellular organelles from the nucleus and cytosol and may be used to monitor the intracellular location of cathepsins (Oberle *et al.,* 2010; Amritraj *et al.,* 2013). In order to gain access to these subcellular structures it is first necessary to

disrupt the plasma membrane whilst leaving the organelles intact, typically by gentle homogenisation or repeated freeze thaw cycles in isotonic buffers. For basic subcellular fractionation, this homogenate is centrifuged first to remove the nuclei and cellular debris, retaining the post nuclear fraction from the supernatant and then further separated by high speed ($>100,000 \times$ g) ultra-centrifugation to produce the membrane fraction (containing organelles) and cytosol. More complex methods may be used to isolate specific organelles by virtue of their buoyancy within a density gradient of viscose material. This method, however, involves high technical precision and is labour intensive.

The basic subcellular fractionation method is commonly used to monitor the release of cathepsin proteases from membrane bound fractions into the cytosol of cells in response to apoptotic stimuli (Oberle *et al.,* 2010; Amritraj *et al.,* 2013). However, no study has previously investigated the effects of disulfiram in this regard.

Aims and Objectives

It is the hypothesis of this chapter that disulfiram is able to induce LMP as a consequence of its ability to increase lysosomal zinc levels. The aims of this chapter are:

- To compare and optimise different methods to measure LMP, including subcellular fractionation.
- To investigate the ability of disulfiram to cause release of cathepsins from the lysosome to the cytosol.

- To determine whether LMP precedes apoptosis in disulfiram treated cells.

- To characterise the role of LMP in the disulfiram cytotoxic response.

6.2. Results

6.2.1. Analysis of the use of acridine orange (AO) as a marker of LMP in live cells

One commonly employed method to measure LMP is by monitoring the fluorescence of AO, a membrane permeable dye that accumulates in acidic endo-lysosomal compartments (Erdal *et al.,* 2005). When localised in these structures AO produces orange/ red fluorescence when excited with 488 nm photons (Kagedal *et al.,* 2001b; Boya and Kroemer 2008; Oberle *et al.,* 2010). However, the dye is also capable of binding nucleic acids upon which it omits green fluorescence. Initially it was determined how AO localised in MCF-7 cells. For this cells were pre-loaded with AO at 1.25, 2.5 and 5 μg/ ml and live cells imaged before (Pre-treat) or after a "mock" treatment whereby an eqi-volume of imaging media, in the absence of drug, was added to the dish. Subsequent images were then taken between 2-10 min after treatment (Figure 6.2). Pre-treatment images show ubiquitous red staining in punctate compartments within cells at all AO concentrations, although this phenotype is more obvious at the highest concentration. However, after the addition of "mock" treatment these endo-lysosomal structures rapidly photobleached and there was substantial loss of fluorescence within these compartments at time points as early as 2 min, particularly at concentrations <5 μg/ ml. By 5 min there was almost complete loss of vesicular AO staining at all concentrations of the dye. In comparison, green nucleic acid staining was more photostable and little bleaching occurred at any dye concentration up to 10 min post-treatment.
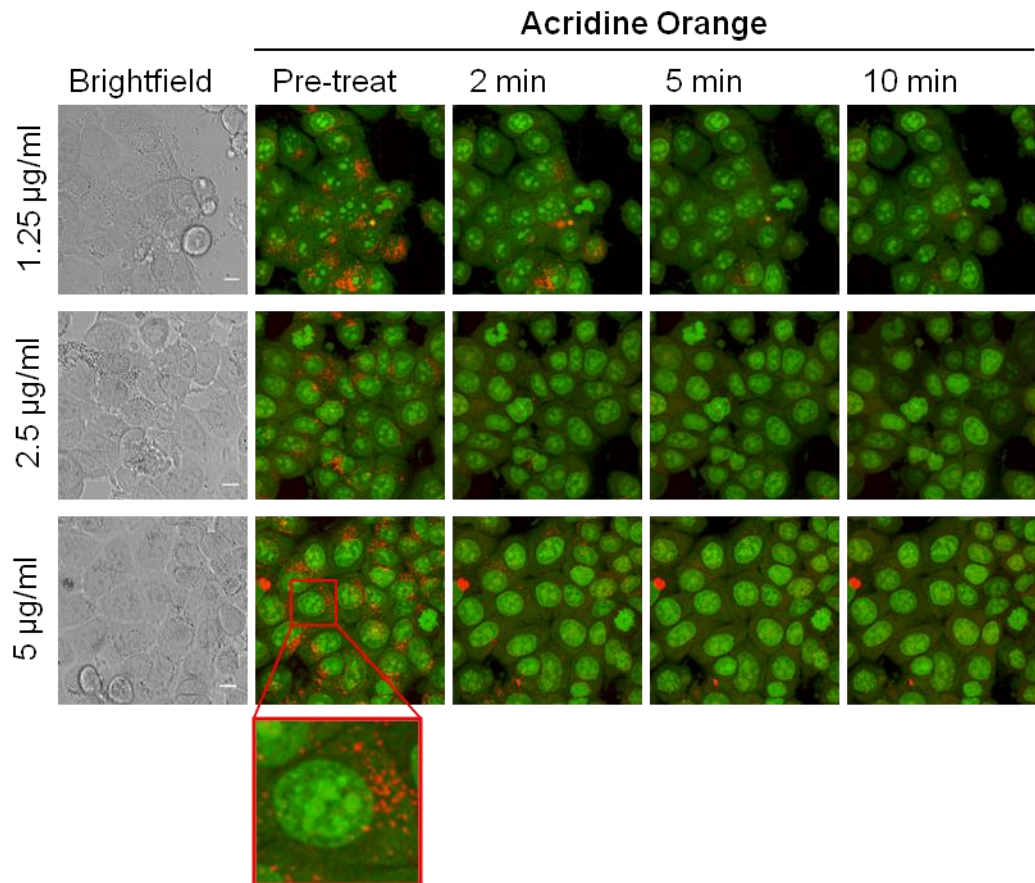
Figure 6.2. Extensive photobleaching of acridine orange occurs rapidly after the addition of "mock" treatment. MCF-7 cells were pre-loaded with AO at a concentration of 1.25, 2.5 or 5 μg/ ml for 15 min and imaged before (Pre-treat) and subsequent to the addition of cell imaging media representing a "mock" treatment. Images are multiple z-projections from a series of 10 equally spaced, single projections. Red represents AO localised in endo-lysosomal structures and green represents AO bound to nucleic acids. Scale bars show 10 μm.

6.2.2. Optimisation of cathepsin D and B antibodies for immunofluorescence and Western blot

The rapid photobleaching of AO prevented its use as an indicator of LMP, and instead immunofluorescence techniques were enlisted in an attempt to image localisation of cathepsin D and B using fluorescence microscopy. As, in their mature form, these proteins are usually localised to the lysosome and translocate to the cytosol upon LMP, their subcellular location may be used to

indicate lysosomal membrane damage and leakage (Erdal *et al.,* 2005; Berndtsson *et al.,* 2009). Initial studies were carried out to optimise an immunofluorescence protocol in MCF-7 cells based on the use of commercial antibodies. For this cells were plated, 24 hr later fixed with PFA and probed with antibodies purchased from Santa Cruz (hereafter referred to as H75 antibody in reference to its product code, full details of all antibodies used in this chapter are given in Material and Methods, Table 2.2) at either 1:50 or 1:250 dilution. Images in Figure 6.3A demonstrate that very little punctate staining was observed and instead the antibody produced predominantly cytosolic staining, with evidence of nucleolus accumulation. Due to the limitations of imaging vesicular cathepsin D using the H75 antibody alternate cathepsin D antibodies were obtained as a gift from Dr. Emyr Lloyd-Jones (School of Biosciences, Cardiff University), these are referred to as G19 and Calbiochem antibodies. Similarly to the images produced by H75, cells probed with the G19 antibody demonstrated a cytosolic staining pattern but notably there was no nucleolus labelling (Figure 6.2B). When the Calbiochem antibody was used occasional punctate staining was observed however the majority of cells displayed faint a non-specific cytosolic staining pattern.

Experiments were then conducted comparing acetone and methanol as alternative fixation methods to PFA, using the H75 antibody. Both acetone and methanol provided much lower cytosolic staining compared to PFA but again there was no evidence of the location of this protein in vesicles; in the case of methanol fixation, fluorescence was almost completely absent (Figure 6.3C).
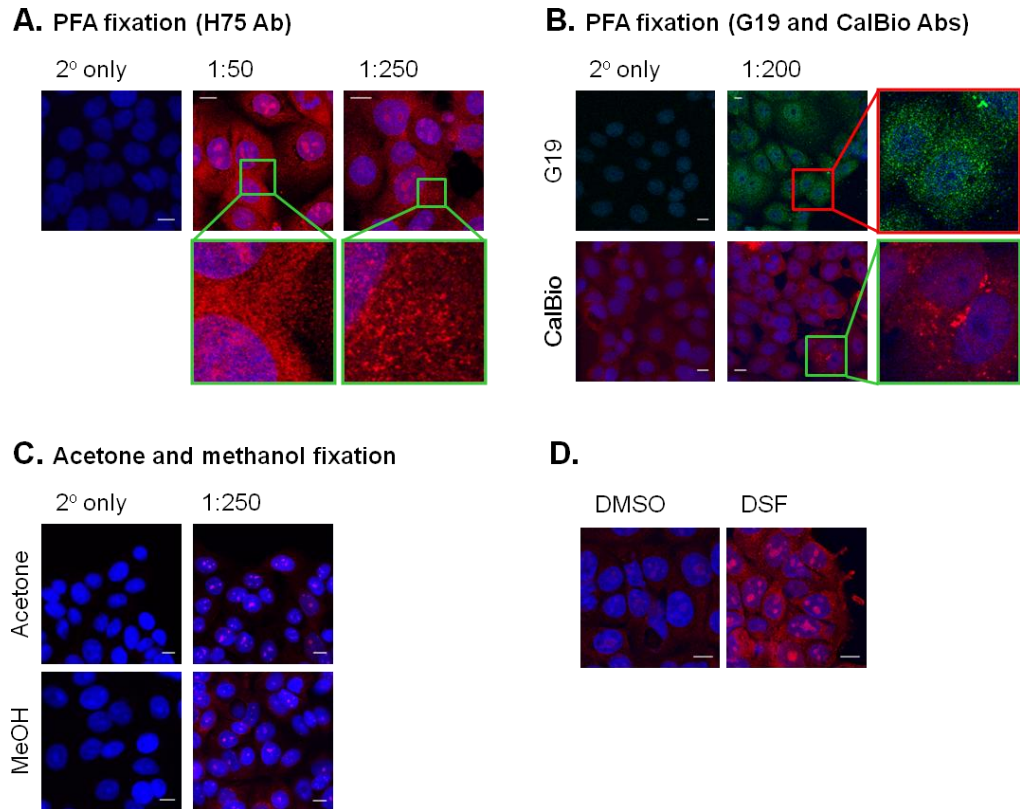
Figure 6.3. Immunofluorescence analysis using cathepsin D antibodies. MCF-7 cells were fixed via PFA (A, B, D), acetone or methanol (C) and subjected to immunofluorescence analysis conducted with the indicated dilutions of H75, G19 or CalBiochem (CalBio) primary antibodies recognising cathepsin D or secondary antibody only controls (2° only). In (D) cells were treated with either 100 µM disulfiram or equivalent DMSO for 1 hr prior to being fixed via PFA and immunofluorescence analysis conducted with the H75 cathepsin D antibody at a dilution of 1:50. Nuclei were labelled with Hoescht 33342 and all studies represent an n=1. Images show a single z-projection through the centre of cells and scale bars represent 10 µm.

Similarly to images in Figure 6.3A, a high level of nucleolus staining was also observed with both fixatives. Immunofluorescence studies have previously demonstrated the release of cathepsin D into the cytosol by increased immunoreactivity of antibodies; here it was noted that cells undergoing LMP and subjected to immunofluorescence analysis using anti-cathepsin D primary antibodies produced a higher level of fluorescence compared to control (Hwang *et al.,* 2010). Therefore it was next determined whether disulfiram altered the immunoreactivity of antibodies. For this, MCF-7 cells were treated

for 1 hr with 100 µM disulfiram or diluent, fixed with PFA and labelled with the H75 cathepsin D primary antibody. Images in Figure 6.3D show that, although there was no difference in staining patterns, disulfiram produced a marked increase in both cytosolic and nucleolus labelling compared to diluent. This therefore indicates that upon addition of the drug there is greater availability of the cathepsin D.

Due to the failure of cathepsin D antibodies to visualise vesicular protein, it was instead investigated whether a cathepsin B antibody produced better results. For these experiments only one cathepsin B primary antibody was used and three secondary antibodies were compared in order to optimise the immunofluorescence protocol. Here, PFA fixed MCF-7 cells were probed with a cathepsin B antibody and secondary antibodies conjugated with Alexa 488 or 647 raised in rabbit or donkey (Figure 6.4). All secondary antibodies produced limited evidence of punctate fluorescence, and staining patterns were comparable in secondary only control cells indicating that the fluorescence produced with the primary antibody was non-specific.
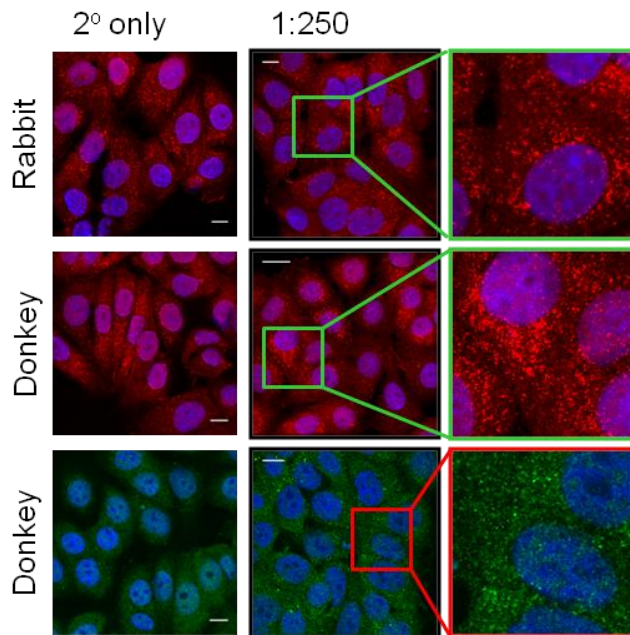
Figure 6.4. Immunofluorescence analysis using a cathepsin B primary antibody. MCF-7 cells were PFA fixed and labelled with a primary antibody recognising cathepsin B at 1:250 dilution or secondary antibody only control. Secondary antibodies were generated in rabbit conjugated with Alexa 647 or donkey conjugated with Alexa 647 or 488 as indicated. Studies represent n=2 and nuclei are labelled with Hoescht 33342. Images show a single z-projection through the centre of cells and scale bars represent 10 μm.

These unsuccessful attempts to visualise cathepsin localisation within the lysosome using immunofluorescence meant that alternative techniques were necessary to measure LMP and subcellular fractionation was selected as this has previously been used to demonstrate release of these enzymes into the cytosol (Oberle *et al.,* 2010). Methods were initially optimised to detect cathepsin D and B via Western blotting of MCF-7 cell lysates. For this, lysates were collected from untreated cells and the amount of protein quantified via the BCA assay. The same amount of protein was then added to each well of an SDS-PAGE gel and Western blotting conducted using cathepsin D and B primary antibodies; clathrin heavy chain and transferrin receptor were used as loading controls as they were of an appropriate molecular weight and the

antibodies were well characterised by the laboratory (for full methods see

Materials and Methods Section 2.7 and 2.9). A single strong band was detected

for both proteins at approximately 48 and 35 kDa for cathepsin D and B

respectively (Figure 6.5). The observed molecular weight of cathepsin D (~52

KDa) corresponds to the immature form of the protein, which undergoes

cleavage of N-terminal residues to form the mature protease (Laurent-Matha *et al.,* 2006). Whereas the molecular weight observed for cathepsin B relates to
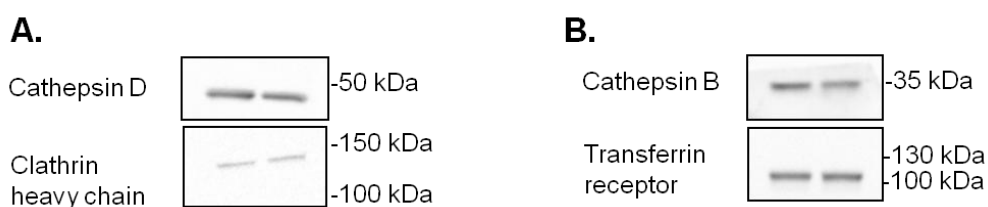
the mature form of the protein.

A.

Cathepsin D   -50 kDa

Clathrin
heavy chain   -150 kDa
     -100 kDa

B.

Cathepsin B   -35 kDa

Transferrin
receptor   -130 kDa
     -100 kDa

Figure 6.5. Detection of Cathepsin D and B in untreated MCF-7 whole cell lysates. Lysates were collected from untreated MCF-7 cells and protein levels of cathepsin D (A) and B (B) analysed via Western blotting in duplicate. For cathepsin D the H75 antibody was used. Clathrin heavy chain and transferrin receptor are shown as molecular weight appropriate loading controls using antibodies well characterised in the laboratory.

6.2.3. Disulfiram causes translocation of cathepsin D and B from membrane to cytosolic compartments

The fact that cathepsin antibodies were capable of detecting these proteins via

Western blotting meant that this technique could be used in combination with

subcellular fractionation in order to separate intracellular compartments. For

these studies MCF-7 cells were treated with 100 μM disulfiram or diluent for

1 hr before detachment and ultra-centrifugation to produce post-nuclear (PNF),

cytosolic (CYT) and membrane (MEM) fractions (detailed in Materials and

Methods Section 2.8). The level of cathepsin D and B in each fraction was then

compared via Western blotting. Blots were also probed for transferrin receptor and ß tubulin as markers of the membrane and cytosolic fractions respectively. Data in Figure 6.6A shows that there is almost no overlap of transferrin receptor and ß tubulin between membrane and cytosolic compartments indicating that subcellular fractionation had effectively segregated these fractions. In cells treated with DMSO cathepsin D and B were almost entirely found in the PNF and membrane fraction indicative of their sequestration within membrane bound structures.
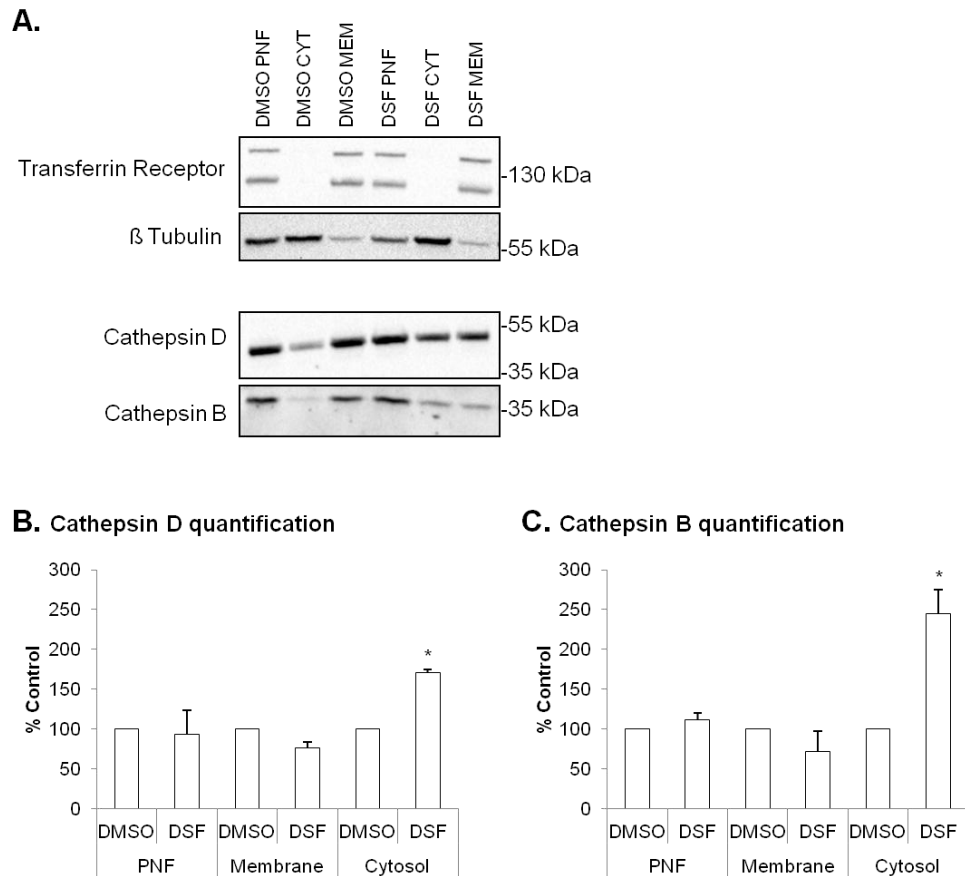

Figure 6.6. Disulfiram increases levels of cathepsin D and B in cytosolic compartments. (A) MCF-7 cells were treated with either 100 μM disulfiram or diluent for 1 hr prior to the collection of PNF, CYT or MEM subcellular fractions as described in Materials and Methods Section 2.8. Fractions were then blotted for transferrin receptor, ß tubulin, cathepsin D or B. (B, C) Western blots were quantified via densitometry and changes in levels of cathepsin D (B) or B (C) expressed as a percentage compared to DMSO control for each fraction. Error bars represent standard error, n=2 *p<0.05.

However disulfiram treatment resulted in simultaneous reduction in the amount of cathepsin D and B found in membrane fractions and increased levels of these proteins in the cytosolic compartments. When these results were quantified via densitometry, disulfiram produced a statistically significant increase in cytosolic levels of cathepsin D and cathepsin B producing a 1.71 and 2.45 fold increase compared to diluent (Figure 6.6B, C). Despite this, statistical significance to indicate decreased levels in membrane compartments upon drug treatment was not achieved for either cathepsin. These results therefore demonstrate that disulfiram is able to increase cytosolic levels of cathepsin D and B, and indicate that the drug is capable of inducing LMP.

In order to determine whether the disulfiram induced increase in cytosolic levels of cathepsin D and B occur before the morphological features of cell death, cells were treated under the same conditions as described for subcellular fractionation (100 μM disulfiram or diluent, 1 hr) and imaged via brightfield microscopy. In these studies, MCF-7 cells retain normal morphology and images of cells treated with disulfiram are comparable to DMSO treatment (Figure 6.7). In comparison cells treated with staurosporine, a protein kinase inhibitor known to induce apoptosis, demonstrate morphological changes consistent with apoptosis and extensive cell blebbing is observed (Hasegawa *et al.,* 2012). These results indicate that the release of cathepsins into the cytosol occurs prior to cell morphological effects.
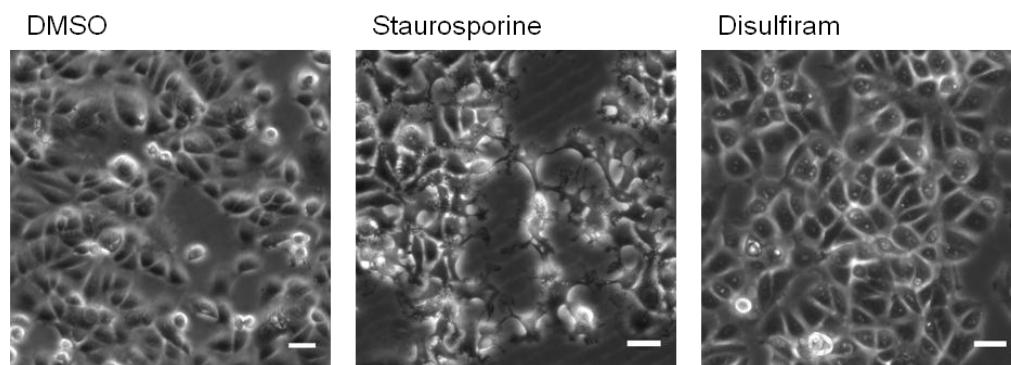
| DMSO | Staurosporine | Disulfiram |

Figure 6.7. Lysosomal membrane permeabilisation precedes disulfiram induced cytotoxic changes in morphology. Brightfield imaging was conducted in MCF-7 cells treated for 1 hr with 100 µM disulfiram, equivalent DMSO or positive control (1 µM staurosporine, 30 min). Scale bars show 10 µm.

6.2.4. The cathepsin B inhibitor, CA-074Me does not protect cells from disulfiram induced death

The release of cathepsin B from lysosomes to the cytosol has previously been shown to promote apoptosis (Guicciardi *et al.,* 2000). In order to determine whether the activity of cathepsin B was required for disulfiram induced cell death in MCF-7 cells, the inhibitor CA-074Me was employed. CA-074Me is a cell permeable cathepsin B inhibitor, although it has also been proposed to inhibit other cysteine proteases (Montaser *et al.,* 2002). Studies were initially conducted to determine the maximum concentration of the inhibitor which could be used without effecting MCF-7 cell viability (Figure 6.8). Almost no viable cells remained after 100 µM CA-074Me treatment however 10 µM was without effect, therefore further studies were conducted in cells treated with serial dilution of disulfiram in combination with 10 µM CA-074Me. The addition of the inhibitor to disulfiram produced little effect on the viability profile of the drug, although at 10 µM disulfiram the magnitude of the biphasic

peak was reduced. This data therefore suggests that CA-074Me is unable to protect cells from disulfiram induced cell death. Time constraints inhibited further analysis regarding the localisation of cathepsin B and D in these cells in the presence of disulfiram.
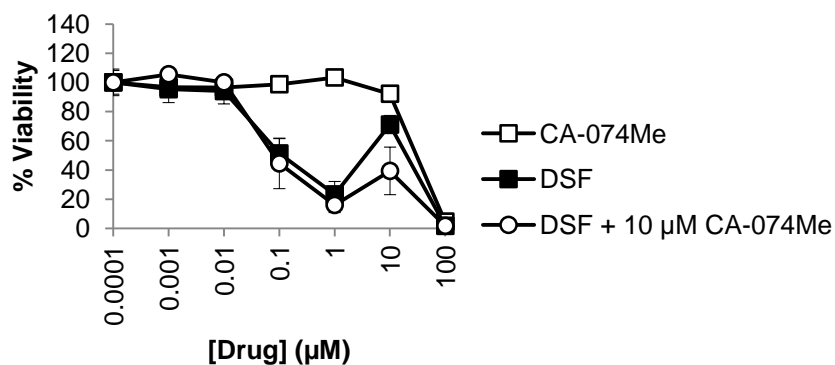

Figure 6.8. The cathepsin B inhibitor, CA-074Me does not protect cells from disulfiram cytotoxicity. Viability of MCF-7 cells treated with CA-074Me alone or disulfiram +/-10 µM CA-074Me was analysed after 72 hr treatment. Error bars show standard error.

6.3. Discussion

The fact that the zinc ionophore activity of disulfiram, described in Chapter 4, significantly raised levels of this metal in endo-lysosomal compartments led to investigation of whether this had any effect on their integrity. In order to examine the toxic consequences of disulfiram induced endo-lysosomal zinc sequestration, LMP was investigated as a potential cell death mechanism. Determination of LMP via imaging techniques i.e. the lysosomal dissipation of AO and changes in intracellular localisation of cathepsin D and B proteases proved problematic due to the rapid photobleaching of AO and poor labelling by cathepsin antibodies. Other studies have successfully employed AO as an indicator of LMP in live cells (Erdal *et al.,* 2005), however these studies focussed on a single time point and it remains to be determined whether this would sufficiently improve the dye's photostability for use in this work. Previous immunofluorescence studies using cathepsin D and B antibodies provide mixed results in terms of their localisation, however diffuse cytosolic staining with limited evidence of punctate structures is frequently observed in the literature, similar to the cathepsin D studies of this chapter (Hwang *et al.,* 2010; Lipton 2013). This makes data interpretation very difficult. Despite this, immunofluorescence has been used to determine LMP, measured by an observed increase in the immunoreactivity of cathepsin D and B antibodies upon drug treatment, indicating increased availability of these proteases within the cytosol (Hwang *et al.,* 2010). In this study, similar results were obtained for disulfiram treated cells whereby the drug increased fluorescence in cells probed with cathepsin D antibodies, however the fact that the antibodies did not

recognise the proteases inside endo-lysosomal structures led to ambiguity as to whether this truly represented cathepsin D translocation. In addition to the imaging techniques used in this chapter, fluorogenic cathepsin B and L substrates exist which may be used to measure the activity of these enzymes within cells (Creasy *et al.,* 2007). This method utilises the protease activity of cysteine cathepsins to cleave a non-fluorescent substrate into a fluorescent product which can then be measured via flow cytometry or fluorescence microscopy. Using this technique studies have previously demonstrated cathepsin B activity in lysosomes of untreated cells which then becomes cytosolic upon treatment with the LMP inducer Docetaxel (Mediavilla-Varela *et al.,* 2009). Whether such a method may provide a more powerful means of visually determining the translocation of cathepsin proteases between the lysosome and cytosol in disulfiram treated breast cancer cells remains to be determined.

As a more definite method of measuring LMP, subcellular fractionation studies were developed to compare levels of cathepsin D and B in membrane and cytosolic fractions of disulfiram or diluent treated cells. The data from this method represents the first time that the release of lysosomal cathepsin D and B into the cytosol has been observed following disulfiram treatment, although disulfiram-copper co-incubation has previously been shown to have this effect on cathepsin D (Berndtsson *et al.,* 2009). This process was shown to occur prior to morphological changes associated with cell death, indicating that disulfiram induced LMP occurs upstream of apoptosis. The sequestration of

zinc into breast epithelial cell lysosomes and subsequent LMP has previously been demonstrated to occur as an endogenous means of regulating the number of cells within non-cancerous breast tissue following weaning (Hennigar *et al.,* 2015). This, when viewed in the context of the data in this chapter, implies that by increasing lysosomal zinc levels disulfiram may be promoting endogenous cell death processes which normally occur in non-cancerous tissue. As the release of lysosomal cathepsins has previously been shown to occur in response to oxidative damage and accumulation of metal ions within this organelle, this data suggests that the disulfiram induced sequestration of zinc in lysosomes promotes oxidative damage to these structures ultimately leading to their rupture (Kagedal *et al.,* 2001a; Hwang *et al.,* 2008; Kukic *et al.,* 2014). Not only does this provide a novel mechanism which may contribute to disulfiram's observed cytotoxicity, it may also implicate the drug as an agent to enhance endosomal escape of therapeutic agents and therefore aid drug delivery. In this context, the delivery of endocytic cargo to the lysosome prevents the access of therapeutic drugs to their intracellular targets (Shete *et al.,* 2014). By promoting lysosomal rupture, disulfiram may be able to increase the intracellular delivery and therefore efficacy of anti-cancer drugs. Chloroquine has this effect and is often used as endosomolytic agent in drug delivery research (El-Sayed *et al.,* 2009). This may provide an alternate mechanism to describe the ability of disulfiram to act in synergy with cancer drugs such as 5-Fluorouracil, gemcitabine and paclitaxel (Wang *et al.,* 2003; Guo *et al.,* 2010; Liu *et al.,* 2013).

The fact that CA-074Me, an inhibitor of cathepsin B protease activity, was unable to rescue cells from disulfiram suggests that cathepsin B activity is not essential for the drug's cytotoxicity. However, as multiple cathepsins including B, D, and L are released during LMP it is possible that there is redundancy within this cell death response or other cathepsins are required for this effect (Oberle *et al.,* 2010). To fully examine this possibility, multiple chemical inhibitors targeting several cathepsins or silencing their expression of these proteins with siRNA may provide a more conclusive approach to study their role in the disulfiram cytotoxic response.

References

Aggarwal, N. and Sloane, B. F. 2014. Cathepsin B: Multiple roles in cancer. *Proteomics Clinical Applications.* 8(5-6), p. 427-437.

Amritraj, A., Wang, Y., Revett, T. J., Vergote, D., Westaway, D. and Kar, S. 2013. Role of Cathepsin D in U18666A-induced neuronal cell death potential implication in niemann-pick type c disease pathogenesis. *Journal of Biological Chemistry.* 288(5), p. 3136-3152.

Beaujouin, M., Baghdiguian, S., Glondu-Lassis, M., Berchem, G. and Liaudet-Coopman, E. 2006. Overexpression of both catalytically active and -inactive cathepsin D by cancer cells enhances apoptosis-dependent chemo-sensitivity. *Oncogene.* 25(13), p. 1967-1973.

Berndtsson, M., Beaujouin, M., Rickardson, L., Havelka, A. M., Larsson, R., Westman, J., Liaudet-Coopman, E. and Linder, S. 2009. Induction of the lysosomal apoptosis pathway by inhibitors of the ubiquitin-proteasome system. *International Journal of Cancer.* 124(6), p. 1463-1469.

Boya, P. and Kroemer, G. 2008. Lysosomal membrane permeabilization in cell death. *Oncogene.* 27(50), p. 6434-6451.

Braulke, T. and Bonifacino, J. S. 2009. Sorting of lysosomal proteins. *Biochimica Et Biophysica Acta-Molecular Cell Research.* 1793(4), p. 605-614.

Creasy, B. M., Hartmann, C. B., White, F. K. H. and McCoy, K. L. 2007. New assay using fluorogenic substrates and immunofluorescence staining to measure cysteine cathepsin activity in live cell subpopulations. *Cytometry Part A.* 71(2), p. 114-123.

Droga-Mazovec, G., Bojic, L., Petelin, A., Ivanova, S., Romih, R., Repnik, U., Salvesen, G. S., Stoka, V., Turk, V. and Turk, B. 2008. Cysteine cathepsins trigger caspase-dependent cell death through cleavage of Bid and antiapoptotic Bcl-2 homologues. *Journal of Biological Chemistry.* 283(27), p. 19140-19150.

El-Sayed, A., Futaki, S. and Harashima, H. 2009. Delivery of Macromolecules Using Arginine-Rich Cell-Penetrating Peptides: Ways to Overcome Endosomal Entrapment. *AAPS Journal.* 11(1), p. 13-22.

Erdal, H., Berndtsson, M., Castro, J., Brunk, U., Shoshan, M. C. and Linder, S. 2005. Induction of lysosomal membrane permeabilization by compounds that activate p53-independent apoptosis. *Proceedings of the National Academy of Sciences of the United States of America.* 102(1), p. 192-197.

Fehrenbacher, N., Bastholm, L., Kirkegaard-Sorensen, T., Rafn, B., Bottzauw, T., Nielsen, C., Weber, E., Shirasawa, S., Kallunki, T. and Jaattela, M. 2008. Sensitization to the lysosomal cell death pathway by oncogene-induced down-regulation of lysosome-associated membrane proteins 1 and 2. *Cancer Research.* 68(16), p. 6623-6633.

Guicciardi, M. E., Deussing, J., Miyoshi, H., Bronk, S. F., Svingen, P. A., Peters, C., Kaufmann, S. H. and Gores, G. J. 2000. Cathepsin B contributes to TNF-alpha-mediated hepatocyte apoptosis by promoting mitochondrial release of cytochrome c. *Journal of Clinical Investigation.* 106(9), p. 1127-1137.

Guo, X., Xu, B., Pandey, S., Goessl, E., Brown, J., Armesilla, A. L., Darling, J. L. and Wang, W. 2010. Disulfiram/copper complex inhibiting NF kappa B activity and potentiating cytotoxic effect of gemcitabine on colon and breast cancer cell lines. *Cancer Letters.* 290(1), p. 104-113.

Hasegawa, Y., Shimizu, T., Takahashi, N. and Okada, Y. 2012. The apoptotic volume decrease is an upstream event of MAP Kinase activation during staurosporine-induced apoptosis in HeLa cells. *International Journal of Molecular Sciences.* 13(7), p. 9363-9379.

Hennigar, S. R., Seo, Y. A., Sharma, S., Soybel, D. I. and Kelleher, S. L. 2015. ZnT2 is a critical mediator of lysosomal-mediated cell death during early mammary gland involution. *Scientific Reports.* 5, article number 8033.

Huai, J., Voegtle, F. N., Joeckel, L., Li, Y., Kiefer, T., Ricci, J. E. and Borner, C. 2013. TNF alpha-induced lysosomal membrane permeability is downstream of MOMP and triggered by caspase-mediated NDUFS1 cleavage and ROS formation. *Journal of Cell Science.* 126(17), p. 4015-4025.

Hwang, J. J., Kim, H. N., Kim, J., Cho, D. H., Kim, M. J., Kim, Y. S., Kim, Y., Park, S. J. and Koh, J. Y. 2010. Zinc(II) ion mediates tamoxifen-induced

autophagy and cell death in MCF-7 breast cancer cell line. *Biometals.* 23(6), p. 997-1013.

Hwang, J. J., Lee, S. J., Kim, T. Y., Cho, J. H. and Koh, J. Y. 2008. Zinc and 4-hydroxy-2-nonenal mediate lysosomal membrane permeabilization induced by H2O2 in cultured hippocampal neurons. *Journal of Neuroscience.* 28(12), p. 3114-3122.

Johansson, A. C., Steen, H., Ollinger, K. and Roberg, K. 2003. Cathepsin D mediates cytochrome c release and caspase activation in human fibroblast apoptosis induced by staurosporine. *Cell Death and Differentiation.* 10(11), p. 1253-1259.

Kagedal, K., Johansson, U. and Ollinger, K. 2001a. The lysosomal protease cathepsin D mediates apoptosis induced by oxidative stress. *FASEB Journal* 15(7), p. 1592-1594.

Kagedal, K., Zhao, M., Svensson, I. and Brunk, U. T. 2001b. Sphingosine-induced apoptosis is dependent on lysosomal proteases. *Biochemical Journal.* 359(2), p. 335-343.

Korolchuk, V. I., Saiki, S., Lichtenberg, M., Siddiqi, F. H., Roberts, E. A., Imarisio, S., Jahreiss, L., Sarkar, S., Futter, M., Menzies, F. M., O'Kane, C. J., Deretic, V. and Rubinsztein, D. C. 2011. Lysosomal positioning coordinates cellular nutrient responses. *Nature Cell Biology.* 13(4), p. 453-460.

Kukic, I., Kelleher, S. L. and Kiselyov, K. 2014. Zinc efflux through lysosomal exocytosis prevents zinc-induced toxicity. *Journal of Cell Science*. 127(14), p. 3094-3103.

Lah, T. T., Kalman, E., Najjar, D., Gorodetsky, E., Brennan, P., Somers, R. and Daskal, I. 2000. Cells producing cathepsins D, B, and L in human breast carcinoma and their association with prognosis. *Human Pathology.* 31(2), p. 149-160.

Laurent-Matha, V., Derocq, D., Prebois, C., Katunuma, N. and Liaudet-Coopman, E. 2006. Processing of human cathepsin D is independent of its catalytic function and auto-activation: Involvement of cathepsins L and B. *Journal of Biochemistry.* 139(3), p. 363-371.

Lipton, P. 2013. Lysosomal membrane permeabilization as a key player in brain ischemic cell death: a "lysosomocentric" hypothesis for ischemic brain damage. *Translational Stroke Research.* 4(6), p. 672-684.

Liu, P., Kumar, I. S., Brown, S., Kannappan, V., Tawari, P. E., Tang, J. Z., Jiang, W., Armesilla, A. L., Darling, J. L. and Wang, W. 2013. Disulfiram targets cancer stem-like cells and reverses resistance and cross-resistance in acquired paclitaxel-resistant triple-negative breast cancer cells. *British Journal of Cancer.* 109(7), p. 1876-1885.

Malek, M., Guillaumot, P., Huber, A. L., Lebeau, J., Petrilli, V., Kfoury, A., Mikaelian, I., Renno, T. and Manie, S. N. 2012. LAMTOR1 depletion induces p53-dependent apoptosis via aberrant lysosomal activation. *Cell Death & Disease.* 3, e300.

Marques, C., Oliveira, C. S. F., Alves, S., Chaves, S. R., Coutinho, O. P., Corte-Real, M. and Preto, A. 2013. Acetate-induced apoptosis in colorectal carcinoma cells involves lysosomal membrane permeabilization and cathepsin D release. *Cell Death & Disease.* 4, e507.

Maynadier, M., Farnoud, R., Lamy, P.-J., Laurent-Matha, V., Garcia, M. and Rochefort, H. 2013. Cathepsin D stimulates the activities of secreted plasminogen activators in the breast cancer acidic environment. *International Journal of Oncology.* 43(5), p. 1683-1690.

Mediavilla-Varela, M., Pacheco, F. J., Almaguel, F., Perez, J., Sahakian, E., Daniels, T. R., Leoh, L. S., Padilla, A., Wall, N. R., Lilly, M. B., De Leon, M. and Casiano, C. A. 2009. Docetaxel-induced prostate cancer cell death involves concomitant activation of caspase and lysosomal pathways and is attenuated by LEDGF/p75. *Molecular Cancer.* 8: 68.

Montaser, M., Lalmanach, G. and Mach, L. 2002. CA-074, but not its methyl ester CA-074Me, is a selective inhibitor of cathepsin B within living cells. *Biological Chemistry.* 383(7-8), p. 1305-1308.

Mrschtik, M. and Ryan, K. M. 2015. Lysosomal proteins in cell death and autophagy. *FEBS Journal.* 282(10), p. 1858-1870.

Nouh, M. A., Mohamed, M. M., El-Shinawi, M., Shaalan, M. A., Cavallo-Medved, D., Khaled, H. M. and Sloane, B. F. 2011. Cathepsin b: a potential prognostic marker for inflammatory breast cancer. *Journal of Translational Medicine.* 9:1.

Oberle, C., Huai, J., Reinheckel, T., Tacke, M., Rassner, M., Ekert, P. G., Buellesbach, J. and Borner, C. 2010. Lysosomal membrane permeabilization and cathepsin release is a Bax/Bak-dependent, amplifying event of apoptosis in fibroblasts and monocytes. *Cell Death and Differentiation.* 17(7), p. 1167-1178.

Shete, H. K., Prabhu, R. H. and Patravale, V. B. 2014. Endosomal escape: a bottleneck in intracellular delivery. *Journal of Nanoscience and Nanotechnology.* 14(1), p. 460-474.

Thomssen, C., Schmitt, M., Goretzki, L., Oppelt, P., Pache, L., Dettmar, P., Janicke, F. and Graeff, H. 1995. Prognostic value of the cysteine proteases cathespins B and cathepsin L in human breast cancer. *Clinical Cancer Research.* 1(7), p. 741-746.

Victor, B. C., Anbalagan, A., Mohamed, M. M., Sloane, B. F. and Cavallo-Medved, D. 2011. Inhibition of cathepsin B activity attenuates extracellular matrix degradation and inflammatory breast cancer invasion. *Breast Cancer Research.* 13: R115.

Wang, W. G., McLeod, H. L. and Cassidy, J. 2003. Disulfiram-mediated inhibition of NF-kappa B activity enhances cytotoxicity of 5-fluorouracil in human colorectal cancer cell lines. *International Journal of Cancer.* 104(4), p. 504-511.

Westley, B. R. and May, F. E. B. 1987. Estrogen regulates cathepsin-d messenger-rna levels in estrogen responsive human-breast cancer-cells. *Nucleic Acids Research.* 15(9), p. 3773-3786.

Wiggins, H., Wymant, J., Solfa, F., Hiscox, S., Taylor, K., Westwell, A. and Jones, A. 2015. Disulfiram-induced cytotoxicity and endo-lysosomal sequestration of zinc in breast cancer cells. *Biochemical Pharmacology.* 93(3), p. 332-342.

Withana, N. P., Blum, G., Sameni, M., Slaney, C., Anbalagan, A., Olive, M. B., Bidwell, B. N., Edgington, L., Wang, L., Moin, K., Sloane, B. F., Anderson, R. L., Bogyo, M. S. and Parker, B. S. 2012. Cathepsin B inhibition limits bone metastasis in breast cancer. *Cancer Research.* 72(5), p. 1199-1209.

Wymant, J. 2015. The role of BCA2 in receptor tyrosine kinase endocytosis and breast cancer. *Cardiff University.*

Yu, H., Zhou, Y., Lind, S. E. and Ding, W. Q. 2009. Clioquinol targets zinc to lysosomes in human cancer cells. *Biochemical Journal.* 417(1), p. 133-139.

7. General discussion

The fact that the clinically approved anti-alcoholism drug disulfiram is well tolerated in patients, ex-patent and cheap to administer, make it an ideal candidate for repurposing as an anti-cancer agent. Considering the drug has relatively few adverse effects, when given in the absence of alcohol, it is perhaps surprising that it has been reported to interfere with so many biological processes by virtue of its capacity to bind thiol groups and divalent cations (Sauna *et al.,* 2005; Skinner *et al.,* 2014). Much of the current literature surrounding the potential therapeutic benefits of disulfiram as an anti-cancer agent focuses on its interaction with copper, in particular as a copper complex, which can inhibit the proteasome and NFκB activity (Chen *et al.,* 2006; Guo *et al.,* 2010; Liu *et al.,* 2012; Duan *et al.,* 2014). Despite evidence that zinc co-incubation can increase the oxidative damage produced by disulfiram and knowledge that the drug is also a zinc chelator, little has been done establish the role of zinc in the anti-breast cancer properties of the drug (Pozza *et al.,* 2011). The interaction between zinc and disulfiram is particularly relevant to the study of anti-breast cancer therapeutics due to the fact that accumulation of the metal within breast cancer cells positively correlates with metastasis, resistance and histological grading (Taylor *et al.,* 2008; Hogstrand *et al.,* 2013; Riesop *et al.,* 2015). With this in mind the goal of this study was to provide the first time that the relationship between disulfiram and zinc in breast cancer cells had been investigated in detail.

Previous studies have investigated the anti-breast cancer effect of disulfiram and attributed cell death due to inhibition of the proteasome, BCA2, NFκB and ALDH activity (Chen *et al.,* 2006; Brahemi *et al.,* 2010; Guo *et al.,* 2010; Liu *et al.,* 2013). The data from Chapter 3 provides further evidence to support this anti-breast cancer potential, and expands upon knowledge of the cytotoxic profile of the drug in breast cancer cell lines. One of the key findings from this chapter was that of the breast cancer cell lines examined only ER$^+$ MCF-7 and BT474 breast cancer cells responded to disulfiram at <100 μM, indicating that the drug may have therapeutic potential in this breast cancer sub-type. In further support of this it has been demonstrated that transfection of ER into ER$^-$ MDA-MB-231 cells increases their disulfiram sensitivity (Brahemi *et al.,* 2010). The fact that in this work T47D cells were resistant to disulfiram cytotoxicity suggests that not all ER$^+$ tumours may respond to be drug, although previous studies have demonstrated sensitivity of these cells when plated at a lower density to that used in this thesis (Yip *et al.,* 2011). It has previously been suggested that the E3 ubiquitin ligase BCA2 is a disulfiram target and as some studies have indicated its over-expression in ER$^+$ breast tumours this may explain, or at least contribute, to the selective toxicity towards these cell lines (Burger *et al.,* 2005; Brahemi *et al.,* 2010). How expression levels of this protein relate to its oncogenic properties are unknown, however studies from our laboratory have suggested that it has a role in EGFR trafficking (Wymant 2015). This thesis from PhD student Jen Wymant also revealed relatively high expression of BCA2 in MDA-MB-231 and T47D cells, neither of which responded to disulfiram in the studies of Chapter 3; this

indicates that the sensitivity of breast cancer cells is not exclusively determined by expression of BCA2, but instead other mechanisms must also play a role. Additionally, the fact that other studies have previous demonstrated that MDA-MB-231 cells are sensitive to disulfiram cytotoxic effects further questions this apparent BCA2/ disulfiram selectivity (Yip *et al.,* 2011; Liu *et al.,* 2013).

The cell lines which responded to disulfiram produced an intriguing biphasic cytotoxicity profile, whereby viability was partially restored at ~10 μM despite being reduced to >50% at 1 μM. This effect has been previously reported in a variety of cell lines including MCF-7 and MDA-MB-231 (Wickstrom *et al.,* 2007; Guo *et al.,* 2010; Yip *et al.,* 2011). Surprisingly, this had not received further attention. This disulfiram recovery could limit its potential therapeutic application and it may be the case that this translates into the clinic, especially considering *in vivo* studies have demonstrated that doses of 25 μg/ mouse/ day produce a greater anti-cancer effect in glioma xenographs than 120 μg/ mouse/ day (Marikovsky *et al.,* 2002). The results in Chapter 3 provide greater insight regarding the concentration range (5-20 μM) and time dependency of this peak; in particular that it represents recovery of cells from initial cytotoxic events which occur within 8 hr rather than complete inactivity of the drug at this concentration. This thesis highlights strategies that could reverse this efficacy limiting phenomenon, either by co-incubation with copper or zinc (Chapter 4) or through the use of disulfiram analogues (Chapter 5) which do not display the biphasic effect. Other studies have previously shown

that copper co-incubation can reduce the impact of biphasic peak but to our knowledge this is the first time that zinc has also been shown to have this effect (Yip *et al.,* 2011; Rae *et al.,* 2013). The fact that such low concentrations of these metal supplements produced dramatic differences in the biphasic response (peak height) may imply that this could be achievable in physiological conditions with dietary supplements. However it should be noted that copper/ zinc co-incubation increased the potency of disulfiram, not only in breast cancer cells, but also in the non-cancerous MCF-10A cell line. This finding raises the possibility that this combination may produce toxic effects in non-cancerous tissue, made particularly important given that a recent clinical trial involving disulfiram noted toxicity concerns (Schweizer *et al.,* 2013). Despite this, the studies of Chapter 4 investigating the toxicity of both metals (in the absence of disulfiram) in MCF-10A cells found that 200 µM copper produced a threefold greater decrease in cell viability compared to this concentration of zinc. This may indicate that in a clinical setting zinc supplementation could produce fewer side effects than copper whist still increasing disulfiram efficacy.

Experiments were then performed to determine whether disulfiram could alter intracellular zinc levels and how this may contribute to its cytotoxic effects. The theory that disulfiram could act as a zinc ionophore in breast cancer cells was supported by evidence that co-incubation with zinc enhances levels of ROS in pancreatic cancer cells and that the disulfiram analogue PDTC and metabolite DDC had this ionophore activity in pancreatic cancer and bovine

endothelial cells respectively (Kim *et al.,* 2000; Donadelli *et al.,* 2009; Pozza *et al.,* 2011). The fact that zinc can be toxic to cells and its intracellular levels are tightly regulated implies that a zinc ionophore may increase levels of this metal beyond the toxic threshold (Bozym *et al.,* 2010). The development of the flow cytometry assay to measure fluorescence of the zinc dye Fluozin-3 (Chapter 4) allowed us to quantitatively compare zinc levels under various conditions; it would have been quite difficult to perform this analysis using confocal microscopy. The flow cytometry work supported the fluorescence microscopy data, and unequivocally demonstrated that disulfiram could potently and rapidly increase zinc levels in MCF-7 and MDA-MB-231 cells but not non-cancerous MCF-10A breast epithelial cells. When considering this ionophore action together with the previously reported observation that ER^+ breast tumours contain 80% higher zinc levels than ER^-, it may be the case that ER^+ tumours are closer to the toxic threshold for zinc and therefore more sensitive to zinc ionophores (Farquharson *et al.,* 2009). Despite this, the results in Chapter 4 did not reveal a difference in basal zinc levels between these cell lines, although this may be beyond the sensitivity limit of the assay. The relationship between the zinc ionophore activity of disulfiram and its ability to induce cytotoxicity was further assessed by the use a non-toxic analogue (FS03EB) in Chapter 5. Here it was shown that under physiological conditions FS03EB was unable to increase intracellular zinc levels. However, in zinc enriched conditions both cytotoxicity and zinc ionophore activity of the analogue were dramatically increased indicating these two factors were intrinsically linked. Similarly the fact that zinc (and copper) supplementation

could enhance the disulfiram cytotoxic effect indicates that toxicity is limited by extracellular metal availability. The relationship between the zinc ionophore activity of disulfiram and cytotoxicity is further demonstrated by the fact that MCF-10A cells are resistant to both cytotoxic effects and zinc ionophore activity of the drug. However, it is also apparent that ionophore independent mechanisms contribute to disulfiram cytotoxicity, as 1 µM disulfiram did not show a measurable increase in intracellular zinc levels in MCF-7 cells (Chapter 4), however produced >50% decrease in cell viability (Chapter 3). The fact that the drug is able to raise intracellular zinc levels within breast cancer cells may have important clinical applications. It has previously been shown that breast cancer cells harbour higher zinc levels than non-cancerous cells and that zinc levels correlate with histological grade (Riesop *et al.,* 2015). This therefore indicates that increasing zinc levels further in these tissues will provide not only a selective mechanism of action to target cancer cells but also that the drug may have an enhanced effect in more aggressive disease types.

Not only did the use of analogues in Chapter 5 provide structures which avoid the biphasic effects observed with disulfiram, they also allowed for investigation into which of the drug's chemical features are responsible for its effect on breast cancer cell viability. The results in this chapter indicated that the chemical groups bound to the nitrogen had a greater effect on breast cancer cell viability than those bound to the disulfide bond and that R group size was also an important consideration in MDA-MB-231 cell sensitivity and MCF-7 biphasic effects. This is the first time these observations have been described

and may allow for identification of other disulfiram-like compounds which may also possess anti-cancer properties and operate through similar mechanisms. Importantly none of the analogues studies in this chapter exhibited cytotoxicity in MCF-10A cells at concentrations <100 μM; demonstrating that non-cancerous cells are highly resistant to the effects of compounds which share the core structure of disulfiram. This chapter also investigated the cytotoxic and zinc ionophore effects of the drug's major metabolite DDC. As *in vivo* disulfiram is rapidly metabolised and undetectable within 4 min of addition to blood, metabolites are thought to contribute to the drug's biological properties (Cobby *et al.,* 1977; Nagendra *et al.,* 1991). The idea that metabolites are important for disulfiram effects is further supported by a clinical trial in which its efficacy correlated with the ability of individuals to form the methylated DDC derivative, S-methyl N,N-diethyldithiocarbamate (Schweizer *et al.,* 2013). In Chapter 5 DDC produced a similar cytotoxic profile (metal dependant biphasic peak) and zinc ionophore effects as the parent drug, providing further evidence that this metabolite may be the active form of the drug in cell culture systems.

Chapter 4 represents the first real time visual observation of intracellular zinc in cells treated with disulfiram, and a major finding from this study was that the drug raises zinc levels specifically in endo-lysosomal compartments. It has previously been noted that increased lysosomal zinc is required for inducing autophagy in tamoxifen treated MCF-7 cells (Hwang *et al.,* 2010). Despite increasing lysosomal zinc levels, the results in Chapter 3 reveal that disulfiram

did not induce autophagy and also represent the first time autophagy has been investigated in response to this drug. The increase in endo-lysosomal zinc levels could, however, affect processes regulated by these organelles in different ways. In support of this was data from PhD student Jen Wymant indicating that disulfiram causes mislocalisation of these organelles, whether this mislocalisation is a consequence of the increased zinc burden remains to be determined (Wiggins *et al.,* 2015; Wymant 2015).

The sequestering of zinc into certain sub-cellular compartments has been proposed as a mechanism to limit the toxic effects of this metal and has been noted to occur upon treatment with another zinc ionophore, clioquinol (Colvin *et al.,* 2008; Yu *et al.,* 2009). However, studies have also demonstrated that lysosomal zinc sequestration damages lysosomal membrane integrity and increases porosity, leading to release of hydrolytic enzymes and eventual apoptosis; indicating that there is a limit to this cytoprotective effect (Hwang *et al.,* 2008). The ability of disulfiram (in the absence of copper) to induce lysosomal membrane permeabilisation (LMP) has never before been investigated and was the subject of Chapter 6. In this chapter several assays were developed to determine whether LMP occurs in disulfiram treated cells, and of these, subcellular fractionation to specifically determine the subcellular location of cathepsins D and B produced the most fruitful results. The mature forms of these hydrolytic proteases are enriched in lysosomes, however upon LMP they are released to the cytosol (Oberle *et al.,* 2010; Amritraj *et al.,* 2013). Using subcellular fractionation, the results in Chapter 6 reveal that

disulfiram was able to cause release of cathepsin B and D from membrane bound compartments into the cytosol. Although a disulfiram-copper co-incubation has previously been shown to have this effect, this chapter represents the first time disulfiram alone has been shown to induce LMP (Berndtsson *et al.,* 2009). As the release of cathepsins into the cytosol has been observed to initiate an apoptotic response, this could provide a new mechanism to describe disulfiram induced cell death (Johansson *et al.,* 2003; Huai *et al.,* 2013). In this model the drug increases lysosomal zinc, causing permeabilisation of the lysosomal membrane and the release of cathepsins in the cytosol that then promotes apoptosis (Figure 7.1). This model is further supported by the fact that LMP occurs before the morphological features of cell death and provides evidence that LMP precedes apoptosis under these conditions.
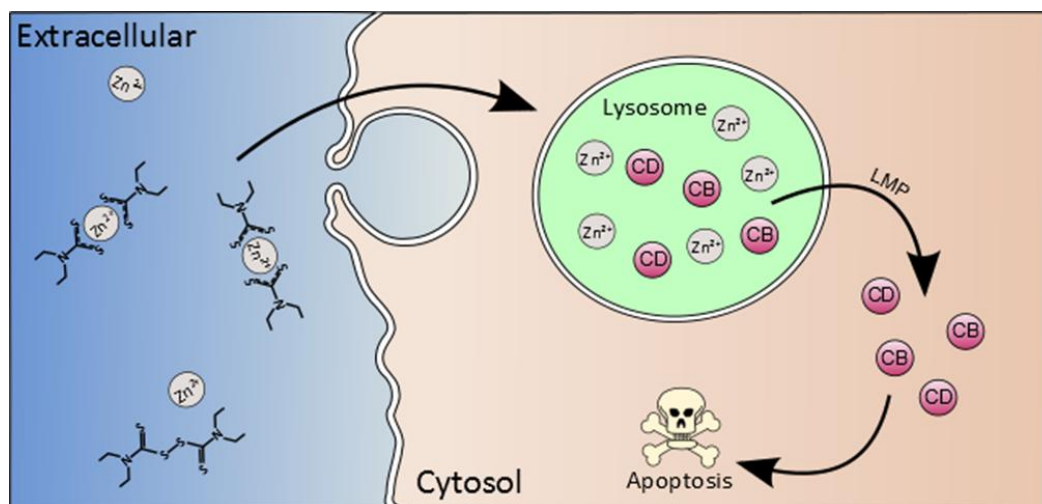

Figure 7.1. Model of disulfiram induced lysosomal membrane permeabilisation following endo-lysosomal zinc sequestration. Disulfiram binds extracellular zinc and transports it into cancer cell lysosomes, leading to permeabilisation of the organelle's membrane and release of cathepsin D (CD) and B (CB) into the cytosol, promoting apoptosis.

7.1. Further studies emanating from this work

One possible limitation of this work is that it has been conducted in two dimensional cell culture models which limit its physiological relevance. In addition, results from the cytotoxicity studies of this thesis may be dependent on the number of cells plated and their confluency, which may explain the apparent discrepancy between the results in this thesis regarding the insensitivity of MDA-MB-231 and T47D cells to disulfiram and the work of others (Yip *et al.,* 2011). This previous study also used three dimensional "mammosphere" cell culture systems to demonstrate the sensitivity of MDA-MB-231 and T47D cells to disulfiram-copper co-incubation, although disulfiram alone had little effect. One possible extension of this thesis could be to examine multiple cell lines using this mammosphere approach in order to further address the issue of ER^+ sensitivity and compare the effects of zinc and copper on mammosphere formation.

Another consideration is the fact that in cancer cells Fluozin-3 was exclusively observed in endo-lysosomes. Although disulfiram raised zinc levels within these subcellular compartments, it may be the case that the dye accumulated within these organelles was unable to enter other structures. Fluozin-3 is the most widely used zinc dye; however there has been very recent developments in the detection of free zinc by using fluorescence resonance energy transfer (FRET) sensors which make use of targeting sequences to measure zinc levels in specific organelles. The FRET method was successfully employed to quantify zinc concentration in subcellular regions such as the

cytosol, mitochondria, endoplasmic reticulum and vesicles (Hessels *et al.,* 2015). One future study could be to measure zinc concentration using these FRET sensors in other organelles following disulfiram treatment.

Although this thesis has highlighted the fact that disulfiram is able to induce LMP, it remains to be determined whether this occurs as a result of its zinc ionophore activity. Further work to address this could be conducted to determine whether disulfiram induced LMP is exaggerated with greater zinc availability (zinc co-incubation) and inhibited when zinc levels are reduced, either by conducting the experiments in serum free media or through the use of established zinc chelators.

7.2. Conclusions

This thesis aimed to investigate the role of both intra and extracellular zinc in the anti-breast cancer properties of disulfiram. The fact that the drug was observed to increase endo-lysosomal zinc levels and that supplementation with low concentrations of this metal could enhance the disulfiram anti-breast cancer effect, indicates that zinc should be an important consideration in its future therapeutic application. Although further work is required, data in this thesis supports a new model which may partially explain the drugs cytotoxicity; disulfiram induced sequestration of zinc in endo-lysosomes leads to rupture of these compartments and release of hydrolytic enzymes to the cytosol. This model may be particularly relevant in conditions where the cell is

already under increased zinc load and more susceptible to zinc induced damage, for example ER^+ or high histological grade breast tumours.

References

Amritraj, A., Wang, Y., Revett, T. J., Vergote, D., Westaway, D. and Kar, S. 2013. Role of Cathepsin D in U18666A-induced neuronal cell death potential implication in niemann-pick type c disease pathogenesis. *Journal of Biological Chemistry.* 288(5), p. 3136-3152.

Berndtsson, M., Beaujouin, M., Rickardson, L., Havelka, A. M., Larsson, R., Westman, J., Liaudet-Coopman, E. and Linder, S. 2009. Induction of the lysosomal apoptosis pathway by inhibitors of the ubiquitin-proteasome system. *International Journal of Cancer.* 124(6), p. 1463-1469.

Bozym, R. A., Chimienti, F., Giblin, L. J., Gross, G. W., Korichneva, I., Li, Y., Libert, S., Maret, W., Parviz, M., Frederickson, C. J. and Thompson, R. B. 2010. Free zinc ions outside a narrow concentration range are toxic to a variety of cells *in vitro. Experimental Biology and Medicine.* 235(6), p. 741-750.

Brahemi, G., Kona, F. R., Fiasella, A., Buac, D., Soukupova, J., Brancale, A., Burger, A. M. and Westwell, A. D. 2010. Exploring the structural requirements for inhibition of the ubiquitin E3 ligase Breast Cancer Associated Protein 2 (BCA2) as a treatment for breast cancer. *Journal of Medicinal Chemistry.* 53(7), p. 2757-2765.

Burger, A. M., Gao, Y. G., Amemiya, Y., Kahn, H. J., Kitching, R., Yang, Y. L., Sun, P., Narod, S. A., Hanna, W. M. and Seth, A. K. 2005. A novel RING-type ubiquitin ligase breast cancer-associated gene 2 correlates with outcome in invasive breast cancer. *Cancer Research.* 65(22), p. 10401-10412.

Chen, D., Cui, Q. C., Yang, H. and Dou, Q. P. 2006. Disulfiram, a clinically used anti-alcoholism drug and copper-binding agent, induces apoptotic cell death in breast cancer cultures and xenografts via inhibition of the proteasome activity. *Cancer Research.* 66(21), p. 10425-10433.

Cobby, J., Mayersohn, M. and Selliah, S. 1977. Rapid reduction of disulfiram in blood and plasma. *Journal of Pharmacology and Experimental Therapeutics.* 202(3), p. 724-731.

Colvin, R. A., Bush, A. I., Volitakis, I., Fontaine, C. P., Thomas, D., Kikuchi, K. and Holmes, W. R. 2008. Insights into Zn2+ homeostasis in neurons from

experimental and modeling studies. *American Journal of Physiology-Cell Physiology.* 294(3), p. 726-742.

Donadelli, M., Pozza, E. D., Scupoli, M. T., Costanzo, C., Scarpa, A. and Palmieri, M. 2009. Intracellular zinc increase inhibits p53(-/-) pancreatic adenocarcinoma cell growth by ROS/AIF-mediated apoptosis. *Biochimica Et Biophysica Acta-Molecular Cell Research.* 1793(2), p. 273-280.

Duan, L., Shen, H., Zhao, G., Yang, R., Cai, X., Zhang, L., Jin, C. and Huang, Y. 2014. Inhibitory effect of Disulfiram/copper complex on non-small cell lung cancer cells. *Biochemical and Biophysical Research Communications.* 446(4), p. 1010-1016.

Farquharson, M. J., Al-Ebraheem, A., Geraki, K., Leek, R. and Harris, A. L. 2009. Zinc presence in invasive ductal carcinoma of the breast and its correlation with oestrogen receptor status. *Physics in Medicine and Biology.* 54(13), p. 4213-4223.

Guo, X., Xu, B., Pandey, S., Goessl, E., Brown, J., Armesilla, A. L., Darling, J. L. and Wang, W. 2010. Disulfiram/copper complex inhibiting NF kappa B activity and potentiating cytotoxic effect of gemcitabine on colon and breast cancer cell lines. *Cancer Letters.* 290(1), p. 104-113.

Hessels, A. M., Chabosseau, P., Bakker, M. H., Engelen, W., Rutter, G. A., Taylor, K. M., and Merkx, M. 2015. eZinCh-2: A Versatile, Genetically Encoded FRET Sensor for Cytosolic and Intraorganelle Zn2+ Imaging. *ACS Chemical Biology.* 10(9), p. 2126-2134.

Hogstrand, C., Kille, P., Ackland, M. L., Hiscox, S. and Taylor, K. M. 2013. A mechanism for epithelial-mesenchymal transition and anoikis resistance in breast cancer triggered by zinc channel ZIP6 and STAT3 (signal transducer and activator of transcription 3). *Biochemical Journa.l* 455, p. 229-237.

Huai, J., Voegtle, F. N., Joeckel, L., Li, Y., Kiefer, T., Ricci, J. E. and Borner, C. 2013. TNF alpha-induced lysosomal membrane permeability is downstream of MOMP and triggered by caspase-mediated NDUFS1 cleavage and ROS formation. *Journal of Cell Science.* 126(17), p. 4015-4025.

Hwang, J. J., Kim, H. N., Kim, J., Cho, D. H., Kim, M. J., Kim, Y. S., Kim, Y., Park, S. J. and Koh, J. Y. 2010. Zinc(II) ion mediates tamoxifen-induced

autophagy and cell death in MCF-7 breast cancer cell line. *Biometals.* 23(6), p. 997-1013.

Hwang, J. J., Lee, S. J., Kim, T. Y., Cho, J. H. and Koh, J. Y. 2008. Zinc and 4-hydroxy-2-nonenal mediate lysosomal membrane permeabilization induced by H2O2 in cultured hippocampal neurons. *Journal of Neuroscience.* 28(12), p. 3114-3122.

Johansson, A. C., Steen, H., Ollinger, K. and Roberg, K. 2003. Cathepsin D mediates cytochrome c release and caspase activation in human fibroblast apoptosis induced by staurosporine. *Cell Death and Differentiation.* 10(11), p. 1253-1259.

Kim, C. H., Kim, J. H., Moon, S. J., Hsu, C. Y., Seo, J. T. and Ahn, Y. S. 2000. Biphasic effects of dithiocarbamates on the activity of nuclear factor-kappa B. *European Journal of Pharmacology.* 392(3), p. 133-136.

Liu, P., Brown, S., Goktug, T., Channathodiyil, P., Kannappan, V., Hugnot, J. P., Guichet, P. O., Bian, X., Armesilla, A. L., Darling, J. L. and Wang, W. 2012. Cytotoxic effect of disulfiram/copper on human glioblastoma cell lines and ALDH-positive cancer-stem-like cells. *British Journal of Cancer.* 107(9), p. 1488-1497.

Liu, P., Kumar, I. S., Brown, S., Kannappan, V., Tawari, P. E., Tang, J. Z., Jiang, W., Armesilla, A. L., Darling, J. L. and Wang, W. 2013. Disulfiram targets cancer stem-like cells and reverses resistance and cross-resistance in acquired paclitaxel-resistant triple-negative breast cancer cells. *British Journal of Cancer.* 109(7), p. 1876-1885.

Marikovsky, M., Nevo, N., Vadai, E. and Harris-Cerruti, C. 2002. Cu/Zn superoxide dismutase plays a role in angiogenesis. *International Journal of Cancer.* 97(1), p. 34-41.

Nagendra, S. N., Shetty, K. T., Subhash, M. N. and Guru, S. C. 1991. Role of glutathione-reductase system in disulfiram conversion to diethyldithiocarbamate. *Life Sciences.* 49(1), p. 23-28.

Oberle, C., Huai, J., Reinheckel, T., Tacke, M., Rassner, M., Ekert, P. G., Buellesbach, J. and Borner, C. 2010. Lysosomal membrane permeabilization and cathepsin release is a Bax/Bak-dependent, amplifying event of apoptosis in fibroblasts and monocytes. *Cell Death and Differentiation.* 17(7), p. 1167-1178.

Pozza, E. D., Donadelli, M., Costanzo, C., Zaniboni, T., Dando, I., Franchini, M., Arpicco, S., Scarpa, A. and Palmieri, M. 2011. Gemcitabine response in pancreatic adenocarcinoma cells is synergistically enhanced by dithiocarbamate derivatives. *Free Radical Biology and Medicine.* 50(8), p. 926-933.

Rae, C., Tesson, M., Babich, J. W., Boyd, M., Sorensen, A. and Mairs, R. J. 2013. The role of copper in disulfiram-induced toxicity and radiosensitization of cancer cells. *Journal of Nuclear Medicine.* 54(6), p. 953-960.

Riesop, D., Hirner, A. V., Rusch, P. and Bankfalvi, A. 2015. Zinc distribution within breast cancer tissue: A possible marker for histological grading? *Journal of cancer research and clinical oncology.* 141(7), p. 1321-1331.

Sauna, Z. E., Shukla, S. and Ambudkar, S. V. 2005. Disulfiram, an old drug with new potential therapeutic uses for human cancers and fungal infections. *Molecular Biosystems.* 1(2), p. 127-134.

Schweizer, M. T., Lin, J., Blackford, A., Bardia, A., King, S., Armstrong, A. J., Rudek, M. A., Yegnasubramanian, S. and Carducci, M. A. 2013. Pharmacodynamic study of disulfiram in men with non-metastatic recurrent prostate cancer. *Prostate Cancer and Prostatic Diseases.* 16(4), p. 357-361.

Skinner, M. D., Lahmek, P., Pham, H. and Aubin, H. J. 2014. Disulfiram efficacy in the treatment of alcohol dependence: a meta-analysis. *Plos One.* 9(2), e87366.

Taylor, K. M., Vichova, P., Jordan, N., Hiscox, S., Hendley, R. and Nicholson, R. I. 2008. ZIP7-mediated intracellular zinc transport contributes to aberrant growth factor signaling in antihormone-resistant breast cancer cells. *Endocrinology.* 149(10), p. 4912-4920.

Wickstrom, M., Danielsson, K., Rickardson, L., Gullbo, J., Nygren, P., Isaksson, A., Larsson, R. and Lovborg, H. 2007. Pharmacological profiling of disulfiram using human tumor cell lines and human tumor cells from patients. *Biochemical Pharmacology.* 73(1), p. 25-33.

Wiggins, H., Wymant, J., Solfa, F., Hiscox, S., Taylor, K., Westwell, A. and Jones, A. 2015. Disulfiram-induced cytotoxicity and endo-lysosomal sequestration of zinc in breast cancer cells. *Biochemical Pharmacology.* 93(3), p. 332-342.

Wymant, J. 2015. The role of BCA2 in receptor tyrosine kinase endocytosis and breast cancer. *Cardiff University.*

Yip, N. C., Fombon, I. S., Liu, P., Brown, S., Kannappan, V., Armesilla, A. L., Xu, B., Cassidy, J., Darling, J. L. and Wang, W. 2011. Disulfiram modulated ROS-MAPK and NF kappa B pathways and targeted breast cancer cells with cancer stem cell-like properties. *British Journal of Cancer.* 104(10), p. 1564-1574.

Yu, H., Zhou, Y., Lind, S. E. and Ding, W. Q. 2009. Clioquinol targets zinc to lysosomes in human cancer cells. *Biochemical Journal.* 417(1), p. 133-139.

Appendix

Disulfiram-induced cytotoxicity and endo-lysosomal sequestration of zinc in breast cancer cells

Helen L. Wiggins, Jennifer M. Wymant, Francesca Solfa, Stephen E. Hiscox,
Kathryn M. Taylor, Andrew D. Westwell, Arwyn T. Jones *

Cardiff School of Pharmacy and Pharmaceutical Sciences, Cardiff University, Redwood Building, Cardiff, Wales CF10 3NB, UK

ABSTRACT

Disulfiram, a clinically used alcohol-deterrent has gained prominence as a potential anti-cancer agent due to its impact on copper-dependent processes. Few studies have investigated zinc effects on disulfiram action, despite it having high affinity for this metal. Here we studied the cytotoxic effects of disulfiram in breast cancer cells, and its relationship with both intra and extracellular zinc. MCF-7 and BT474 cancer cell lines gave a striking time-dependent biphasic cytotoxic response between 0.01 and 10 μM disulfiram. Co-incubation of disulfiram with low-level zinc removed this effect, suggesting that availability of extracellular zinc significantly influences disulfiram efficacy. Live-cell confocal microscopy using fluorescent endocytic probes and the zinc dye Fluozin-3 revealed that disulfiram selectively and rapidly increased zinc levels in endo-lysosomes. Disulfiram also caused spatial disorganization of late endosomes and lysosomes, suggesting they are novel targets for this drug. This relationship between disulfiram toxicity and ionophore activity was consolidated via synthesis of a new disulfiram analog and overall we demonstrate a novel mechanism of disulfiram-cytotoxicity with significant clinical implications for future use as a cancer therapeutic.

© 2015 The Authors. Published by Elsevier Inc. This is an open access article under the CC BY license (http://creativecommons.org/licenses/by/4.0/).

1. Introduction

Many current cancer therapies are limited by the severity and frequency of adverse side effects and there is high demand for non-toxic alternatives. One source of new therapies may be through repurposing of clinically approved drugs, where safety in patients has already been demonstrated. Disulfiram has a long medical history as an alcohol deterrent, however more recently has demonstrated anti-cancer effects in a range of solid and hematological malignancies [1]. The biological activity of disulfiram is attributed to its ability to bind divalent cations and consequently disrupt metal dependent processes, particularly those involving copper and zinc [2,3]. Observations that both these metal ions are involved in oncogenic development have led to increased interest in the anti-cancer potential of this drug [4]. As part of a copper complex, disulfiram has been reported to induce apoptosis in both cultured breast cancer cells and xenografts through proteasomal inhibition [5–7]. These complexes have also been shown to stabilize the NFκB inhibitor protein, IκB, thus

re-sensitizing gemcitabine resistant tumors with enhanced NFκB signaling [8]. In a case study of a patient with stage IV ocular melanoma with liver metastases, combination therapy involving disulfiram and zinc gluconate was able to induce remission with almost no side effects [9]. These observations have led to its introduction to clinical trials, including one involving patients with hepatic malignancies treated with disulfiram and copper gluconate (NCT00742911, University of Utah). Additionally, disulfiram treatment has been reported to remove essential copper and zinc ions from enzymes that regulate extracellular matrix degradation and oxygen metabolism resulting in suppression of cancer invasion and angiogenesis in vitro and in vivo [2,3].

Much of the current literature surrounding disulfiram focuses on its capacity to bind copper ions, via two metal binding regions in its structure (Fig. 1A). Relatively little has been done to determine the role of zinc in its anti-cancer properties despite the fact that it also has high affinity for this metal [3]. Studies have highlighted the role of zinc in the etiology of breast cancer where high expression of zinc transporter proteins such as ZIP7 and ZIP10, in breast cancer cell models increases intracellular zinc levels and is associated with endocrine therapy resistance and increased invasiveness [10,11]. Additionally, zinc has been reported to increase pro-survival signaling [12] and inhibit caspases [13] in
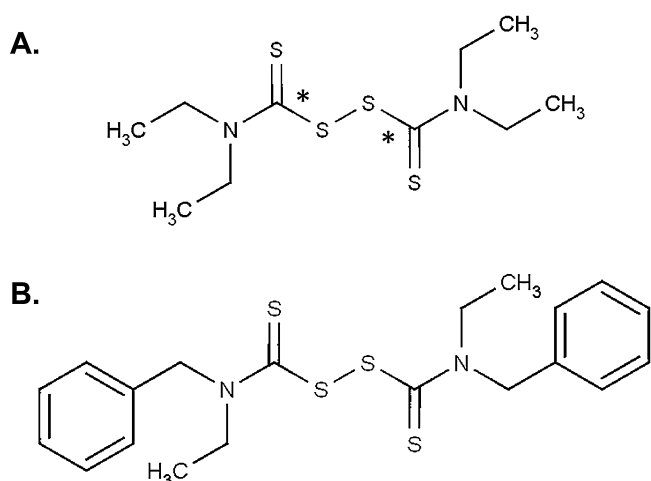
Fig. 1. Structure of disulfiram and the disulfiram analog FS03EB. (A) *Indicates metal binding regions within the structure. (B) ^{1}H NMR (500 MHz, CDCl$_3$) d 1.30 (3H, bs, CH$_3$), 1.47 (3H, s, CH$_3$), 4.05 (4H, bs, C$\underline{H_2}$CH$_3$), 5.26 (2H, s, CH$_2$Ph), 5.41 (2H, s, CH$_2$Ph), 7.39 (10H, m, ArH); ^{13}C NMR (125 MHz, CDCl$_3$) d 11.12 (CH$_3$), 13.20 (CH$_3$), 47.18 (CH$_2$), 52.04 (CH$_2$), 55.80 (CH$_2$), 59.54 (CH$_2$), 127.48 (ArCH), 127.72 (ArCH), 128.20 (ArCH), 128.49 (ArCH), 128.79 (ArCH), 128.99 (ArCH), 134.57 (ArC), 135.24 (ArC), 198.82 (C=S), 195.33 (C=S); MS (EI$^+$) *m/z* 420.08 (M$^+$); HR-MS (ESI$^+$) *m/z* [M+H]$^+$ calculated 421.0895, found 421.0896.

vitro. Taken together these reports suggest that high zinc levels promote cancer cell survival. Paradoxically, high intracellular zinc is also associated with oxidative toxicity, implying that the cell maintains tight homeostatic control of this metal and that drugs which dysregulate this fine balance may induce toxicity [14]. As the concentration of zinc is higher in cancerous compared to non-cancerous breast tissue [15] it is possible that drugs which alter intracellular zinc levels would be selectively toxic to cancer cells.

In this study we investigate the role of both intra and extracellular zinc in the anti-cancer activity of disulfiram. We demonstrate the effect of zinc and copper on the cytotoxicity of the drug across a panel of cancerous and non-cancerous breast cell lines. We describe a novel mechanism of action for disulfiram, via its ability to rapidly increase intracellular zinc levels in endo-lysosomal compartments and alter the subcellular localization specifically of late lysosomal structures. Both these effects potentially impact on lysosome function. Interestingly, zinc levels in a non-cancerous breast cell line remain unaltered by disulfiram treatment and taken in the context of the literature surrounding zinc dysregulation in breast cancer, our results demonstrate a selective effect of disulfiram that may have significant clinical implications for its future clinical use.

2. Materials and methods

2.1. Chemicals and reagents

Disulfiram, diethyldithiocarbamate (DDC), sodium pyrithione, DMSO, Na-HEPES, NH$_4$Cl, Triton X-100, BSA, ZnCl$_2$, CuCl$_2$, cholera toxin, insulin, epidermal growth factor, and hydrocortisone were obtained from Sigma–Aldrich (Dorset, UK). Disulfiram, DDC, and sodium pyrithione were dissolved in DMSO to produce a stock concentration of 10 mM and stored at −20 °C. CellTiter blue viability reagent was purchased from Promega (Southampton, UK). Anti-EEA1 (#6104490), anti-LAMP2 (#H4B4), and anti-LC3B (#2775) antibodies were obtained from BD Bioscience (Oxford, UK), Developmental Studies Hybridoma Bank (Iowa, USA) and Cell Signaling Technology (MA, USA) respectively. RPMI, FBS, DMEM/F12, horse serum, Fluozin-3, Hoechst 33342, dextran-Alexa 647 (10 kDa), Alexa-488 (A-11001) and Alexa-546 (A-11010)

conjugated anti-mouse and anti-rabbit antibodies were from Life Technologies (Paisley, UK).

2.2. Synthesis of disulfiram analog

FS03EB (bis(N-benzylethylthiocarbamoyl)disulphide; Fig. 1B) was synthesized according to the method of Liang et al. [16]. Briefly, N-benzylethylamine and carbon disulphide (2:1 molar ratio) were mixed together in the presence of carbon tetrabromide (one equivalent) in dimethylformamide as solvent at room temperature. Following purification by column chromatography, the identity and purity of the product was confirmed using NMR spectroscopy and mass spectrometry [17]. FS03EB was then dissolved in DMSO to produce a stock concentration of 10 mM.

2.3. Cell culture

MDA-MB-231, MCF-7, T47D, and BT474 were maintained in RPMI 1640 supplemented with 10% FBS. MCF-10A cells were maintained in DMEM/F12 supplemented with 5% horse serum, 100 ng/ml cholera toxin, 10 μg/ml insulin, 20 ng/ml epidermal growth factor, and 500 ng/ml hydrocortisone [18]. Herein these are respectively termed complete media. All cell lines were obtained from ATCC and routinely tested for mycoplasma infection.

2.4. Viability assays

To account for different growth rates, cells were seeded in black 96-well plates at densities that provided 70% confluency after 72 h. After a minimum of 24 h, cells were treated with disulfiram, disulfiram metabolite DDC, FS03EB or DMSO ± copper or zinc supplements for the indicated time points. Viability studies were conducted using the CellTiter Blue assay according to manufacturer's protocol. All viability studies were conducted in complete media.

2.5. Live cell imaging of intracellular zinc

Microscopy analysis was conducted on a Leica SP5 confocal inverted microscope equipped with a 488 nm laser and 40× objective using Leica LAS AF software. For this, cells were preloaded with 5 μM Fluozin-3 diluted in cell imaging media (phenol red free RPMI media supplemented with 10% FBS and 50 mM Na-HEPES pH 7.4) for 30 min, before being washed thrice with PBS which was then replaced with 1 ml cell imaging media. In live cells representative region of interest was captured before and subsequent to addition of a 1 ml solution of 10 μM disulfiram, sodium pyrithione (positive control) or diluent control. Images are displayed as a multiple projection of 10 z-planes through the cells.

2.6. Flow cytometry

Cells were preloaded with Fluozin-3 for 30 min as above and treated with disulfiram, DDC, FS03EB, sodium pyrithione or diluent control in cell imaging media or serum free imaging media (phenol red free RPMI supplemented with 50 mM Na-HEPES pH 7.4) ±20 μM zinc or copper for 10 min. Following trypsinization, cells were resuspended in PBS, and centrifuged three times at 150 × g. Cells were then resuspended in media, and 10,000 events were analyzed via flow cytometry using a BD Biosciences FACSVerse system equipped with a 488 nm laser.

2.7. Comparative localization of intracellular zinc with endocytic probes in disulfiram treated cells

To label the entire fluid-phase endocytic network, MCF-7 cells were incubated for 4 h with 2.5 mg/ml dextran-Alexa 647 diluted

in cell imaging media. To specifically label lysosomes, cells were incubated with dextran-Alexa 647 for 2 h followed by a 4 h chase [19]. During the final stages of this incubation, cells were incubated with Fluozin-3 for 30 min, washed with PBS, and treated with 10 μM disulfiram for 10 min. Cells were then washed three times with PBS, and analyzed via live cell confocal microscopy.

2.8. Localization of endocytic organelles and induction of autophagy in disulfiram treated cells

MCF-7 cells were treated with 1 μM disulfiram or equivalent diluent control for 3 h (for endosomes and lysosomes) or 24 h (for autophagosomes) before being washed in PBS, fixed and permeabilised by either -20 °C methanol for 10 min (for LAMP2 and LC3B labeling) or with 3% PFA for 15 min, 50 mM NH$_4$Cl for 10 min and 0.2% Triton X-100 for 5 min (for EEA1 labeling). After fixation the cells were washed three times in PBS, incubated for 1 h in blocking buffer (2% FBS, 2% BSA in PBS) then incubated for 1 h with primary antibody diluted 1:200 (LAMP2 and EEA1) or 1:400 (LC3B) in blocking buffer. The cells were then washed three times in PBS before being incubated for 1 h with secondary antibodies and Hoechst 33342 (1 μg/ml). Following a further three washes with PBS they were mounted in oil. Imaging was conducted via confocal microscopy for LAMP2 and EEA1. For LC3B imaging was conducted on a Leica DMIRB inverted epi-fluorescent microscope, equipped with a 40× objective.

2.9. Statistical testing

For all studies three independent experiments were conducted in triplicate (for viability studies) or duplicate (for flow cytometry studies) and significance of data determined, as appropriate, using students two tailed *T*-test in Microsoft Excel and displayed as $^*p < 0.05$ or $^{**}0.001$. Data is presented as the mean and standard error of the mean. Co-localization via microscopy was determined using JaCOP plugin of ImageJ and the Pearsons coefficient was used as a measure of the ratio of pixels which were labeled with dextran-Alexa 647 and Fluozin-3 where 1.0 is complete co-localization [20]. Pearson's coefficient is expressed as ±standard error of the mean.

3. Results

3.1. Disulfiram produces a biphasic cytotoxic response in some breast cancer cell lines

Initial cell viability experiments were conducted to investigate the sensitivity of a panel of breast cancer cell lines to disulfiram. These were chosen to model clinically relevant disease sub types, including estrogen receptor positive (ER$^+$), human epidermal growth factor receptor 2 (HER2) negative (MCF-7 and T47D), ER$^+$/HER2$^+$ (BT474) and ER$^-$/HER2$^-$ (MDA-MB-231) and the non-cancerous breast epithelial MCF-10A line. Disulfiram over 72 h was only toxic to ER$^+$ cells (MCF-7 and BT474, IC$_{50}$ 0.3 μM vs. MDA-MB-231 IC$_{50}$ and MCF-10A IC$_{50}$ > 10 μM; Fig. 2A), however not all
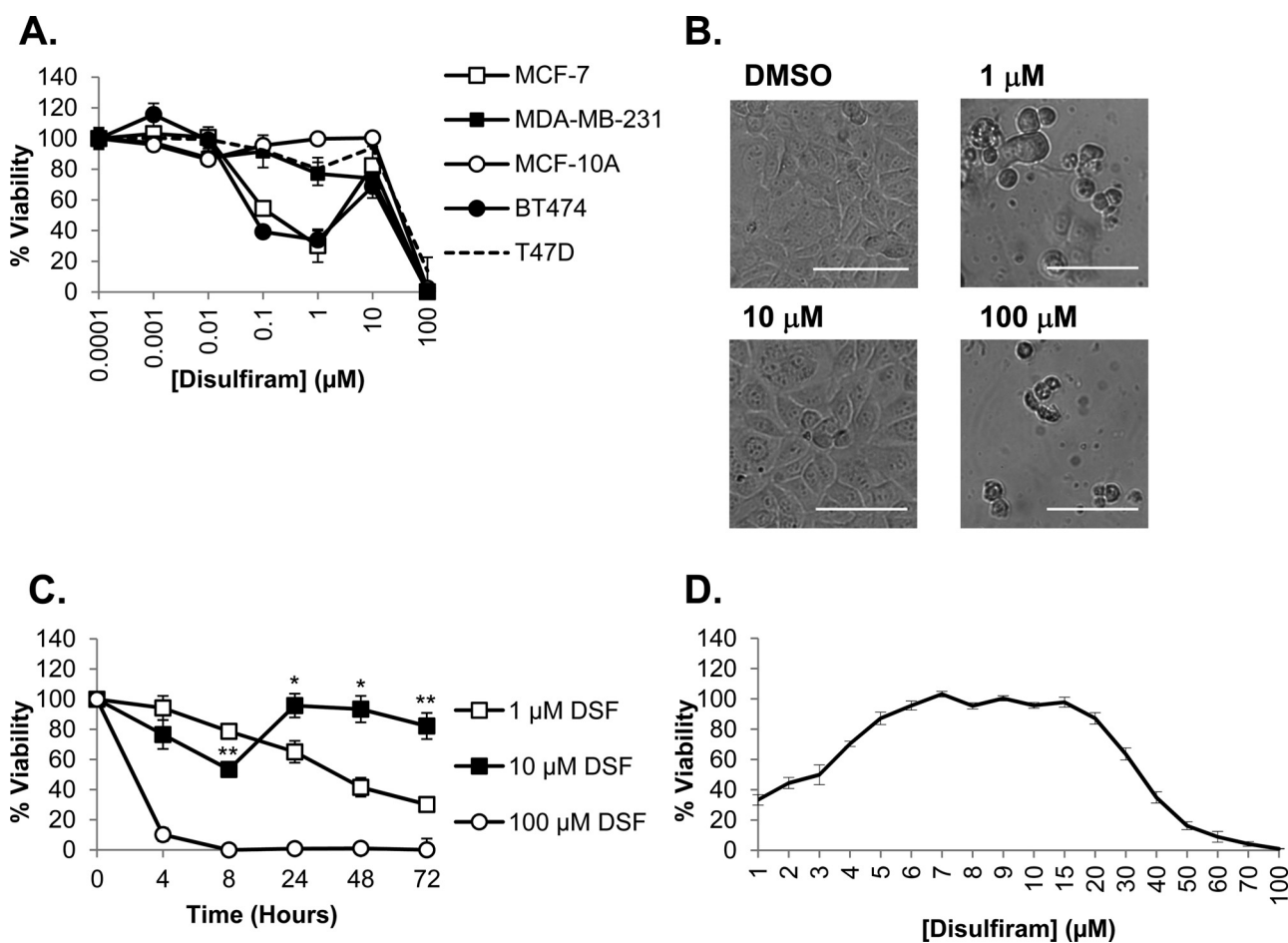

Fig. 2. The cytotoxic profile of disulfiram in breast cancer cell models. (A) Cells were treated with a serial dilution of disulfiram in complete media and viability analyzed after 72 h. (B) MCF-7 cells were imaged using brightfield microscopy following 72 h disulfiram (DSF) treatment. Scale bar shows 100 μm. (C) MCF-7 cells were treated for 8–72 h with disulfiram prior to analyzing viability. *T*-tests were conducted between equivalent time points to compare 1 and 10 μM data, $^*p < 0.05$, $^{**}p < 0.001$. (D) MCF-7 cells were treated for 72 h with disulfiram at concentrations between 1 and 100 μM prior to analyzing viability. Error bars show standard error.

ER^{+} cells responded equally to the drug (T47D $IC_{50} > 10 \mu M$) demonstrating that the presence of ER is not a prerequisite for sensitivity. In disulfiram responsive cells (MCF-7 and BT474) cytotoxicity was biphasic, producing a recovery peak at 10 μM with almost complete restoration of viability. The biphasic effect in MCF-7 cells was confirmed by microscopy showing clear morphological damage at 1 μM that is consistent with loss of cell viability. These effects were absent at 10 μM where morphology was comparable to diluent controls; increasing the disulfiram concentration to 100 μM then restored the toxic 1 μM phenotype (Fig. 2B).

To further investigate this biphasic response we determined whether it was affected by disulfiram concentration at different incubation times. MCF-7 cells were treated with 1, 10 and 100 μM disulfiram over a range of time points and cell viability was then determined. Despite an initial cytotoxic phase at <8 h, cell viability at 10 μM was restored at greater than 24 h (Fig. 2C). For other concentrations disulfiram produced a time dependent decrease in viability; at 1 μM viability steadily decreased between 4 and 72 h whereas at 100 μM there was a rapid loss of viability to <10% within 4 h. This data demonstrates that the 10 μM disulfiram response is due to recovery from initial effects that are not manifest as cell death but rather a reduction in metabolic rate as determined by this assay. When the biphasic peak in MCF-7 cells was investigated at concentrations between 1 and 100 μM at a single 72 h time point, viability was restored to >80% between 5 and 20 μM concentrations of the drug (Fig. 2D).

3.2. Disulfiram specifically increases intracellular zinc levels in breast cancer cells

To investigate the relationship between disulfiram and intracellular zinc levels we employed live cell confocal microscopy using the zinc probe Fluozin-3. In complete media, disulfiram rapidly (<10 min) increased intracellular zinc levels in MCF-7 cells, specifically to label punctate compartments, to levels comparable to those obtained using the well established zinc ionophore sodium pyrithione (Fig. 3). A significant proportion of sodium pyrithione treated cells were also noted for displaying diffuse cytosolic Fluozin-3 labeling whereas zinc in disulfiram treated cells was only observed in punctate structures. Surprisingly, zinc levels remained unaffected by either disulfiram or sodium pyrithione treatment in the non-cancerous MCF-10A cell line.

In order to further investigate the disulfiram effects seen by microscopy, a flow cytometry assay was developed to enable quantitative comparison of intracellular zinc levels in disulfiram and sodium pyrithione treated cells. The data supported the microscopy findings as 10–100 μM disulfiram significantly increased intracellular zinc levels in both MCF-7 and MDA-MB-231 cell lines (Fig. 4A), while zinc levels in MCF-10A cells remained
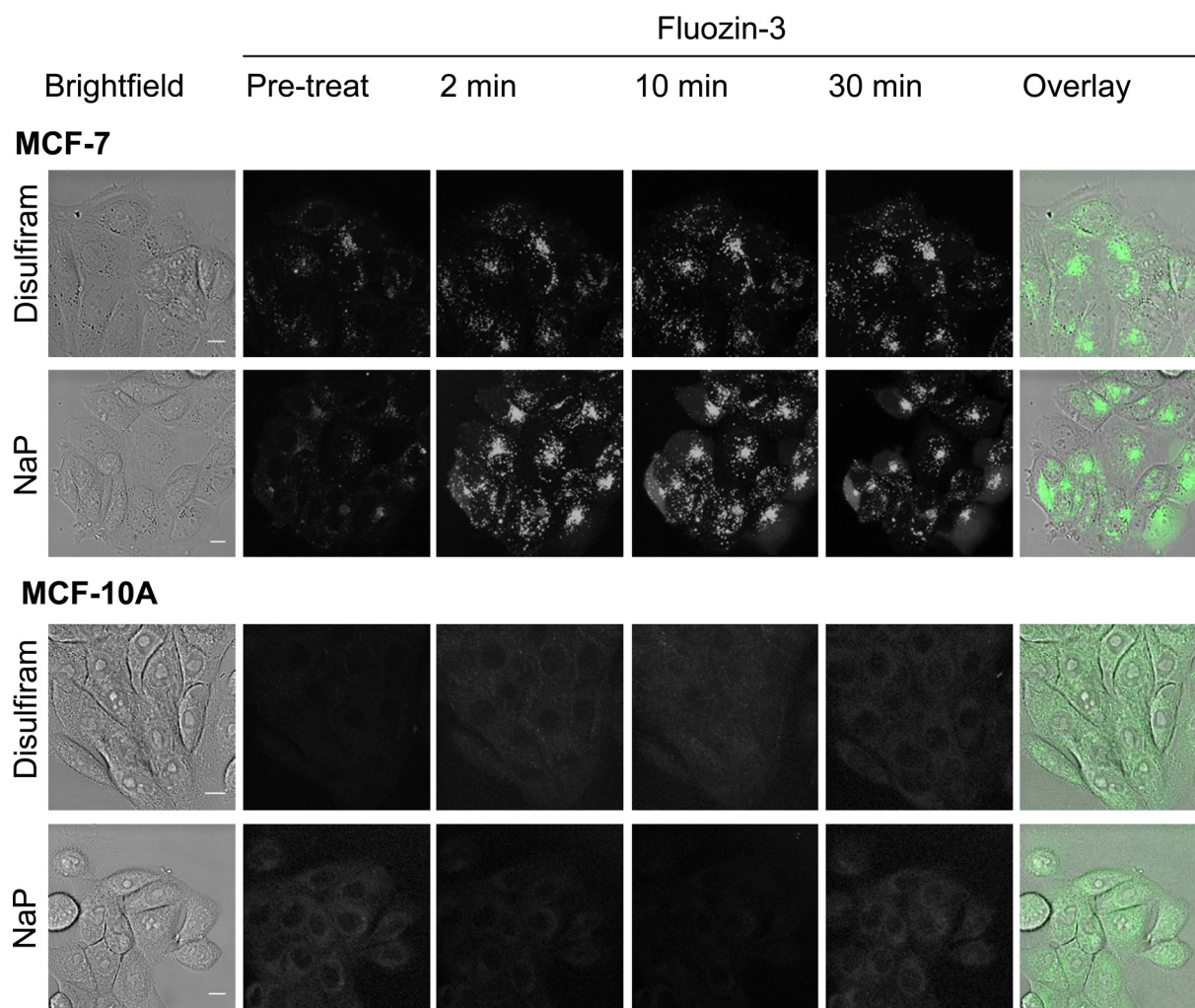

Fig. 3. Disulfiram selectively increases intracellular zinc levels in punctate structures of breast cancer cells. Cells were preloaded with Fluozin-3 for 30 min and imaged before (pre-treat) and subsequent to the addition of 10 μM disulfiram or sodium pyrithione (NaP) in cell imaging media. Images are multiple z-projections from a series of 10 equally spaced, single projections and are representative from three independent experiments. Scale bars show 10 μm.
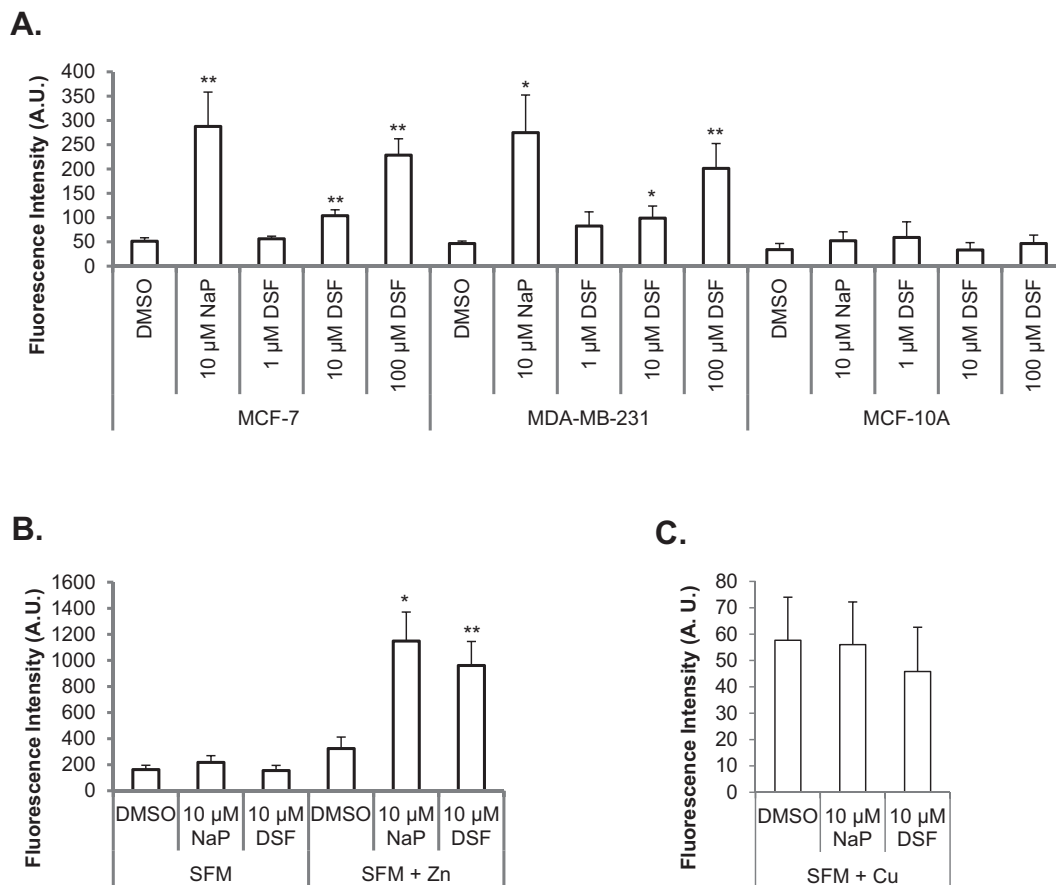
Fig. 4. Disulfiram delivers extracellular zinc into cells rather than releasing intracellular stores. Cells were preloaded with Fluozin-3 and treated with disulfiram (DSF), DMSO or sodium pyrithione for 10 min in complete media (A) or serum free media (SFM) $\pm20\ \mu M$ zinc (B) or copper (C) in MCF-7 cells. Fluozin-3 fluorescence was then determined via flow cytometry. Error bars show standard error. T-tests in (A) were conducted between DMSO and treatment groups and in (B, C) were conducted between SFM and SFM + Zn/Cu for each treatment, $^*p < 0.05$, $^{**}p < 0.001$.

unaffected by the same treatment. To further investigate this, and minimize the effects of extracellular zinc in serum, the flow cytometry experiments were conducted in serum free media- low zinc and copper conditions. Under these conditions, neither sodium pyrithione nor disulfiram evoked a statistically significant increase in intracellular zinc in MCF-7 cells (Fig. 4B). Supplementation of serum free media with $20\ \mu M$ zinc was sufficient to completely restore, and in fact exaggerate, the ionophore ability of both disulfiram and sodium pyrithione, demonstrating that this ionophore activity is dependent on extracellular zinc levels. This effect, with respect to the selectivity of the dye for zinc versus copper which could possibly also provide Fluozin-3 fluorescence, was tested by conducting the experiments in serum free media supplemented with copper. Here copper was unable to significantly restore the fluorescence of Fluozin-3 in disulfiram or sodium pyrithione treated cells (Fig. 4C), demonstrating that the increased fluorescence of Fluozin-3 observed in Figs. 3 and 4 was specifically due to the effects of zinc.

3.3. Disulfiram sequesters intracellular zinc in endo-lysosomal compartments

The observation that disulfiram sequestered zinc in punctate structures lead us to investigate the nature of these compartments. In order to determine whether they were components of the endocytic network, fluorescent dextran was utilized as an endocytic probe for co-localization studies. By conducting a 2 h pulse with dextran-Alexa 647 followed by cell washing and a further 4 h chase, the probe can be trafficked and confined to lysosomes [19]. Dextran pulse-chase experiments were performed and cells were co-stained with Fluozin-3 and treated with disulfiram; the degree of co-localization between dextran-Alexa 647 and Fluozin-3 was then analyzed using live cell confocal microscopy. Fig. 5A demonstrates that a significant portion of dextran labeled lysosomes were also labeled with Fluozin-3 and very few dextran only structures were observed (Pearsons coefficient = 0.49 ± 0.06 for three independent experiments). When the entire fluid phase network was labeled with dextran as a single 4 h pulse (Fig. 5B), a higher degree of co-localization was observed between the two probes (Pearsons coefficient = 0.67 ± 0.04) suggesting that disulfiram was also driving zinc into earlier compartments of the endocytic network.

To investigate whether disulfiram influences the spatial organization of these endocytic structures MCF-7 cells were treated with the drug for 3 h prior to performing immunofluorescence analysis using antibodies recognizing the early endosomal marker, Early Endosome Antigen 1 (EEA1) or the late endosomal/lysosomal marker, Lysosome Associated Membrane Protein 2 (LAMP2) [21]. Disulfiram was observed to have no effect on the localization of early endocytic structures (Fig. 6A), however caused late endosomes and lysosomes to be redistributed from typical perinuclear clusters observed in control cells to more diffuse
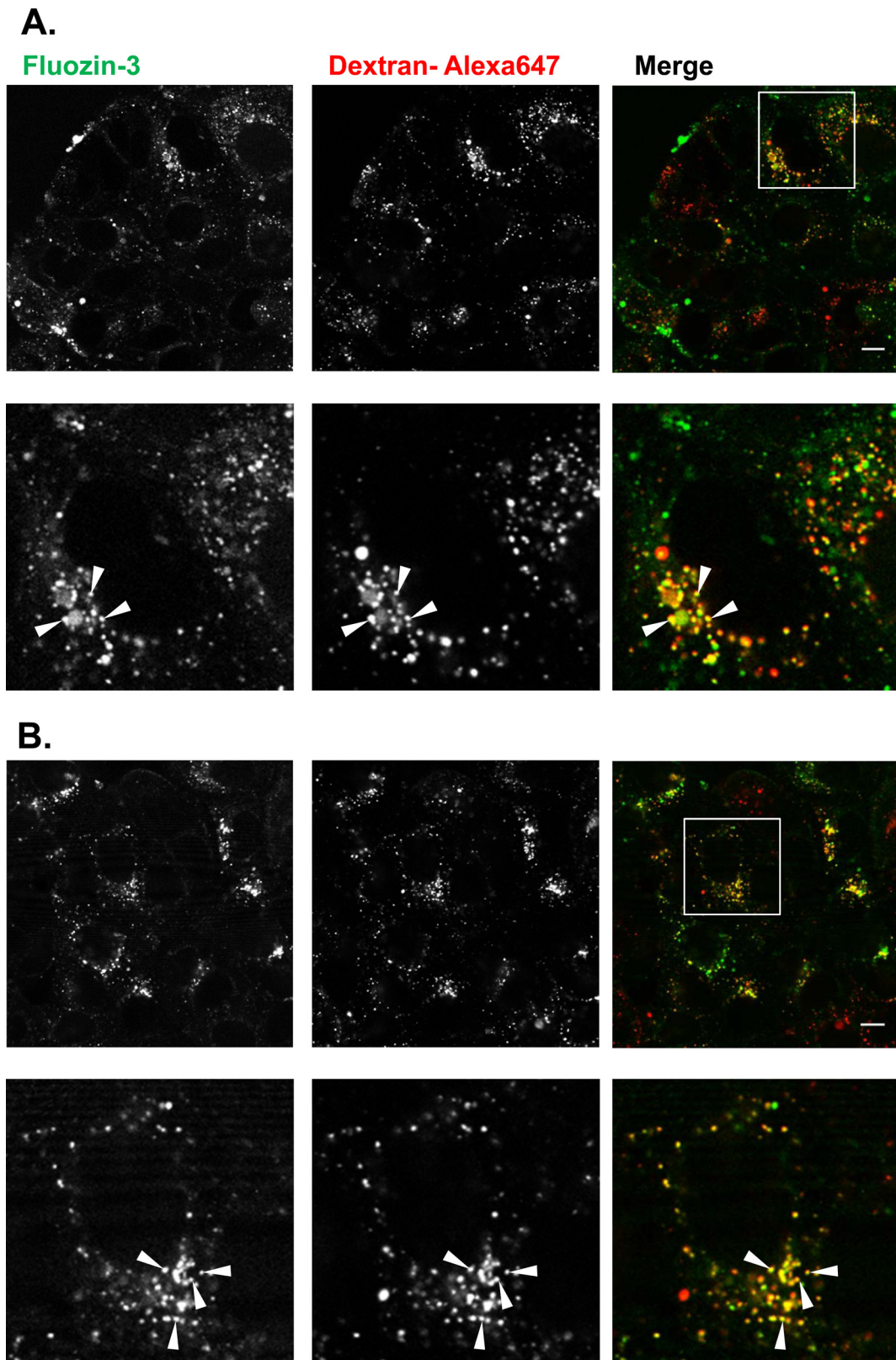
Fig. 5. Disulfiram increases intracellular zinc in endo-lysosomal compartments of breast cancer cells. Dextran-Alexa 647 was used to highlight late endo-lysosomal compartments (A) or the entire fluid phase endocytic network (B) in MCF-7 cells, as described in Section 2. Cells were then incubated with Fluozin-3, treated with 10 μM disulfiram for 10 min and co-localization between Fluozin-3 and dextran-Alexa 647 was analyzed via confocal microscopy. Images show single *z*-projections through the cells and lower panel in (A) and (B) show a zoomed image of an identified cell in upper panel. Images shown are representative from three independent experiments. Co-localization is marked by arrow heads. Scale bars show 10 μm.
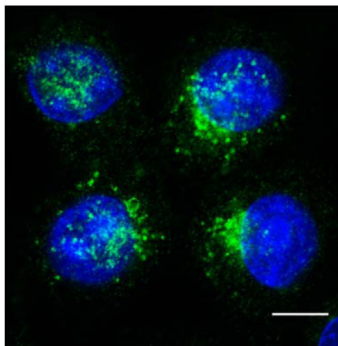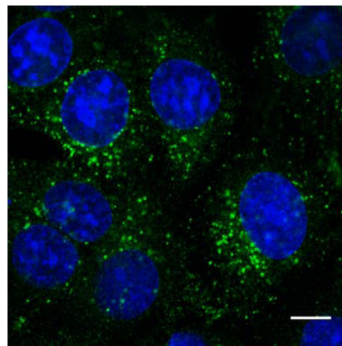
A. EEA1
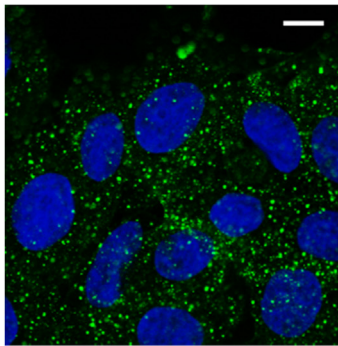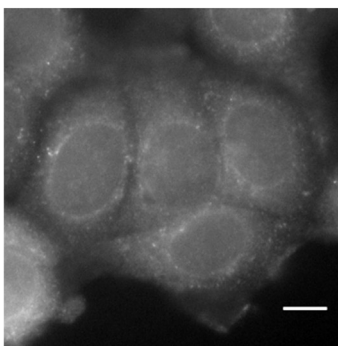
DMSO   Disulfiram
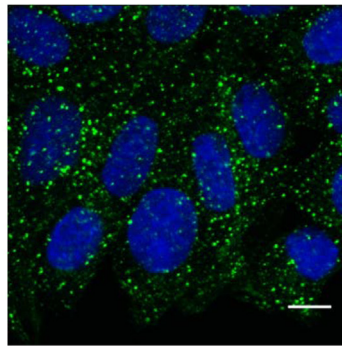
B. LAMP2

DMSO   Disulfiram
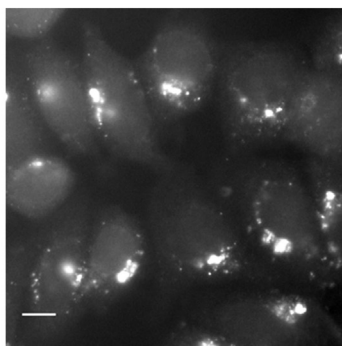

C. LC3B
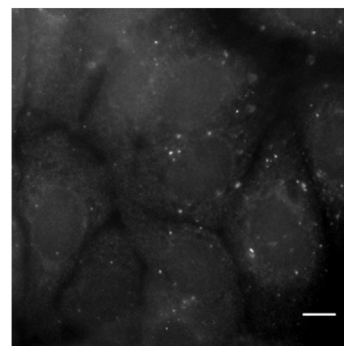
DMSO   Chloroquine   Disulfiram

Fig. 6. Disulfiram causes mislocalization of lysosomes, however does not alter localization of early endosomes or autophagic membranes. MCF-7 cells were treated with 1 μM disulfiram or chloroquine (100 μM, 6 h) and then analyzed via immunofluorescence microscopy using antibodies recognizing EEA1 (A), LAMP2 (B) or LC3B (C). Blue nuclei are labeled with Hoechst 33342. Image shows single projection through the middle of the cell and is representative from three independent experiments. Scale bars show 10 μm.

scattering throughout the cytoplasm (Fig. 6B). The ability of disulfiram to induce autophagy was investigated using antibodies recognizing a marker of autophagic membranes, microtubule-associated Light Chain 3 B (LC3B). For this experiment cells were either treated with disulfiram for 24 h prior to LC3B immunofluo-rescence analysis, or for 6 h with chloroquine, an agent which causes accumulated LC3B via stabilization of autophagosomal membranes [22]. Chloroquine treated cells displayed large LC3B containing structures representing autophagosomes, however this phenotype was absent in cells treated with disulfiram (Fig. 6C).

3.4. Supplementation with zinc or copper increases disulfiram potency

The interaction between disulfiram and zinc observed in our previous results lead us to consider whether enrichment of complete media with zinc or copper could affect the cytotoxicity of the drug in cancerous and non-cancerous breast cells. As control experiments, we initially investigated whether supplementing cell media with increasing concentrations of zinc or copper in the absence of disulfiram had any effect on cell viability. These studies

demonstrated that $\leq 20\,\mu M$ zinc or copper was without effect but toxicity was observed at higher concentrations of both metals with MCF-7 and MCF-10A showing particular sensitivity to copper (Fig. 7A). When a non-toxic dose of zinc or copper ($20\,\mu M$) was given in combination with disulfiram, cytotoxicity was significantly enhanced in all cell lines (Fig. 7B, Table 1). In the case of MCF-7 cells, the disulfiram biphasic response was completely abolished by both zinc and copper supplementation, however cytotoxicity of disulfiram at lower concentrations was reduced by addition of either metal supplement. The minimum concentration of copper and zinc supplement required to influence cell recovery (biphasic peak) in MCF-7 cells was then determined and data in Fig. 7C and D shows that $2.0\,\mu M$ zinc and $0.125\,\mu M$ copper significantly reduced the ability of the cells to recover from disulfiram effects. At higher concentrations both metals completely reversed the biphasic response.
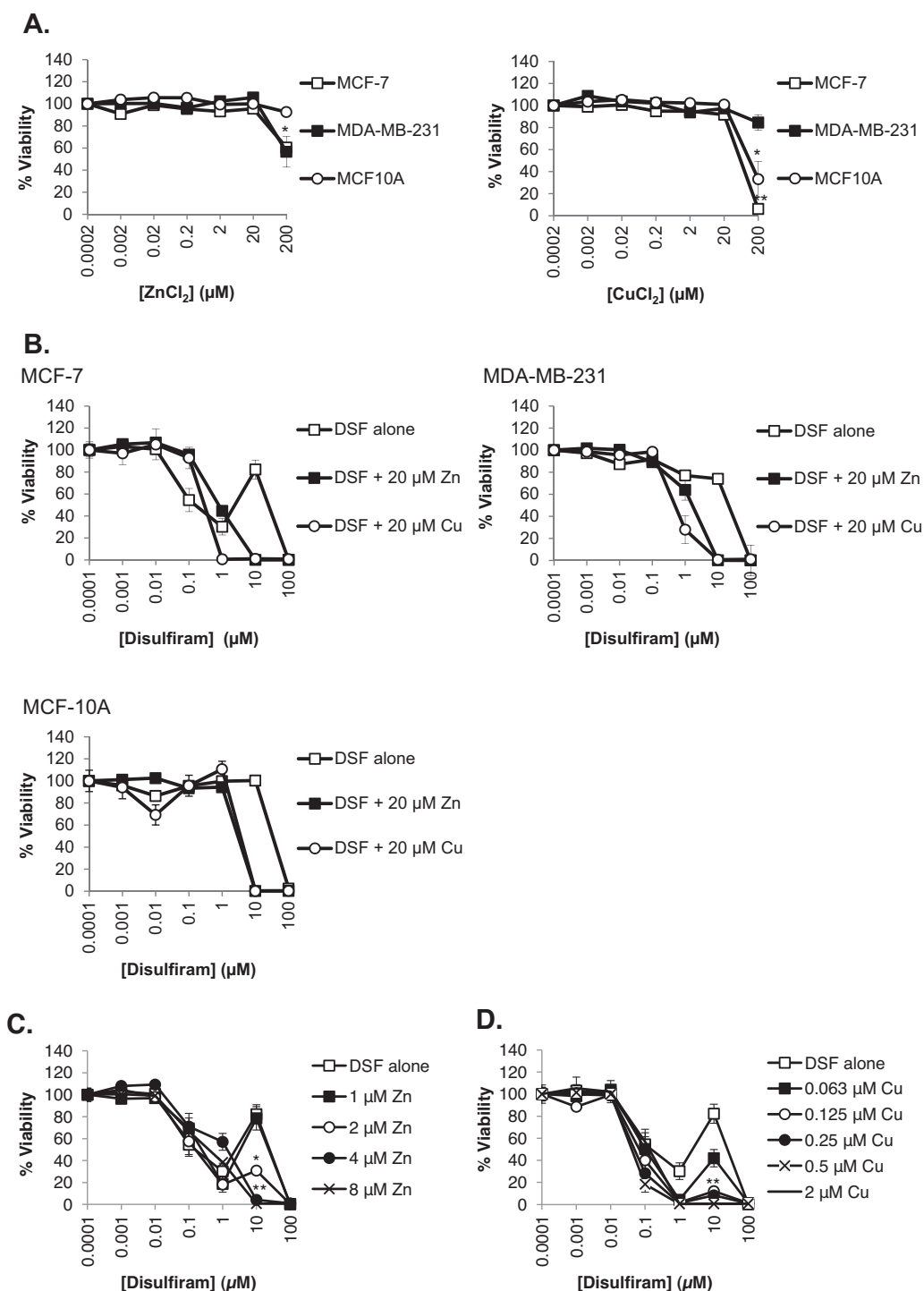

Fig. 7. Zinc and copper enhance the cytotoxicity of disulfiram. (A) Cells were treated with a serial dilution of zinc or copper for 72 h in the presence of complete growth media before cell viability analysis was performed. (B) Cells were treated with disulfiram $\pm 20\,\mu M$ zinc or copper in complete media for 72 h prior to performing viability analysis. (C and D) Viability of MCF-7 cells treated with disulfiram $\pm$ zinc or copper in supplemented in complete media was analyzed after 72 h. Error bars show standard error. p-values for data in Fig. 7B are provided in Table 1.

Table 1
Co-incubation of copper/zinc significantly altered the cytotoxico profile of disulfiram.

[DSF]	MCF-7				MDA-MB-231				MCF-10A			
	0.1 µM	1 µM	10 µM	100 µM	0.1 µM	1 µM	10 µM	100 µM	0.1 µM	1 µM	10 µM	100 µM
DSF alone	54.5 ± 10.5	30.2 ± 7.5	82.2 ± 8.7	0.1 ± 0.2	91.6 ± 2.8	77.0 ± 10.8	74.0 ± 12.3	0.02 ± 0.1	95.5 ± 1.6	99.8 ± 1.6	100.3 ± 2.9	2.4 ± 1.2
DSF + Zn	95.8 ± 4.2**	44.6 ± 3.5*	0.1 ± 0.2**	0.1 ± 0.3	89.1 ± 4.6	63.9 ± 9.3	0.1 ± 0.1**	0.02 ± 0.1	93.3 ± 3.9	94.3 ± 2.9	0.3 ± 0.1**	0.3 ± 0.1
DSF + Cu	92.8 ± 9.8*	0.6 ± 0.2**	1.0 ± 0.4**	0.7 ± 0.2*	98.5 ± 2.2	27.9 ± 12.5*	0.7 ± 0.1**	1.0 ± 0.2*	95.7 ± 9.5	110.7 ± 7.1	0.16 ± 0.1**	0.3 ± 0.1

Breast cells were treated with the indicated concentrations of disulfiram ±20 µM zinc or copper for 72 h prior to performing viability analysis. Values displayed are percentage viability and standard error of the mean. *T*-tests were conducted between disulfiram treatment alone and disulfiram + zinc/copper.

* $p < 0.05$
** $p < 0.001$.

3.5. Cytotoxicity of disulfiram, diethyldithiocarbamate (DDC) and a structural analog correlates with ionophore activity

Disulfiram in vitro and in vivo is rapidly metabolized to give two molecules of DDC [23]. The possibility that this major metabolite was able to induce toxicity and also act as a zinc ionophore was also investigated in MCF-7 cells. DDC displayed a sharp increase in toxicity at concentrations higher than 0.1 µM with evidence of recovery being observed at 100 µM, rather than at 10 µM as in the case of disulfiram (compare Fig. 8A and 2A). Supplementation with copper and zinc completely ablated the DDC biphasic effects (Fig. 8A) and significantly enhanced its toxicity (Table 2). The metabolite was also able to increase intracellular zinc levels (Fig. 8B) but was a less potent zinc ionophore compared with the parent drug (Fig. 4A).

To determine how cytotoxicity may relate to the capacity of disulfiram and DDC to deliver zinc, a close structural analog of disulfiram, FS03EB, was synthesized and viability assays were performed with this compound. FS03EB lacked any significant toxicity at concentrations below 100 µM in complete media and a biphasic response was not observed (Fig. 8C). Here, the core zinc binding thiuram disulfide pharmacophore was retained, but two of the terminal ethyl groups were replaced by the related benzyl group (see Fig. 1B for chemical structure and physical characterization of FS03EB). In complete media, and contrary to the effects observed with disulfiram and DDC, data in Fig. 8D show that FS03EB was unable to significantly increase intracellular zinc levels. However, co-incubation of this compound (>1 µM) with 20 µM zinc or copper was toxic leading to complete loss of viability at 1 µM and 10 µM for copper and zinc respectively (Table 2). When the zinc ionophore activity of FS03EB was investigated in conditions which induced toxicity (complete media + 20 µM zinc), it resulted in a >3-fold increase in Fluozin-3 fluorescence.
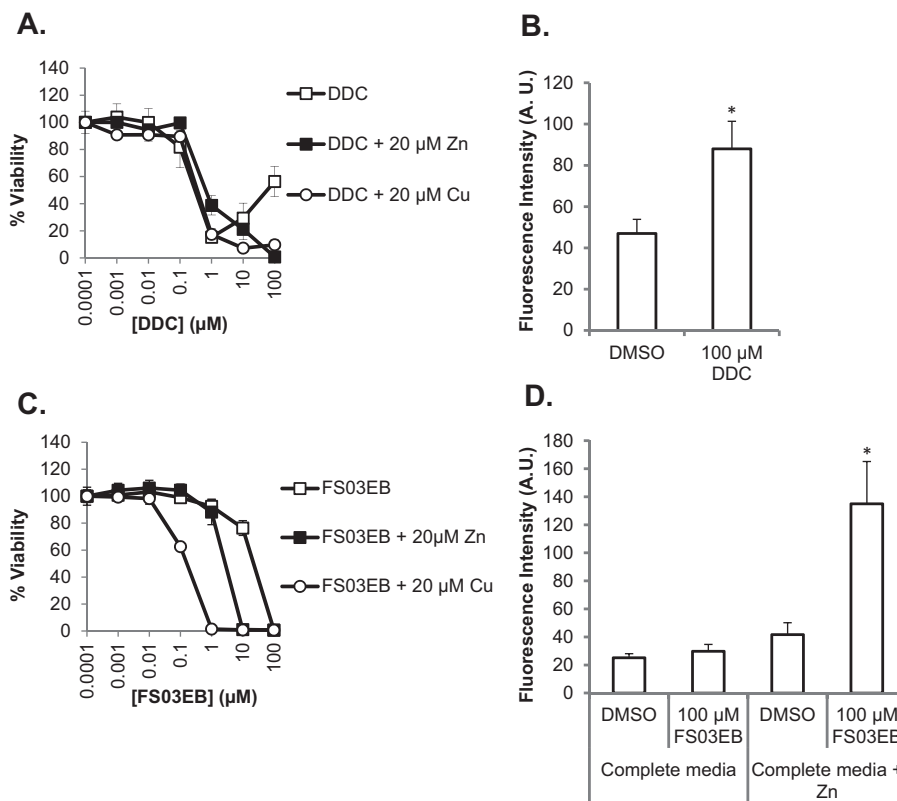

Fig. 8. Toxicity of DDC and FS03EB correlates with zinc ionophore activity. (A, C) MCF-7 cells were treated with DDC (A) or FS03EB (C) ±20 µM copper or zinc in complete media for 72 h prior to performing viability analysis. (B, D) MCF-7 cells were preloaded with Fluozin-3, treated with DDC (B) or FS03EB ±20 µM zinc (D) for 10 min prior to measuring Fluozin-3 fluorescence via flow cytometry. Error bars show standard error. *$p < 0.05$, p-values for data in (A and C) are provided in Table 2.

Table 2
Co-incubation of copper/zinc significantly altered the cytotoxic profile of DDC and FS03EB.

	[DDC]				[FS03EB]			
	0.1 μM	1 μM	10 μM	100 μM	0.1 μM	1 μM	10 μM	100 μM
No supplement	81.7 ± 15.1	15.3 ± 2.1	29.3 ± 11.1	56.4 ± 11.0	98.9 ± 3.1	92.4 ± 5.4	76.4 ± 1.1	0.7 ± 0.4
Zn supplement	99.5 ± 2.4**	38.8 ± 7.1**	21.1 ± 7.6	0.7 ± 0.1**	104.4 ± 4.6	88.2 ± 9.3	1.1 ± 0.2**	0.7 ± 0.2
Cu supplement	89.5 ± 4.4	17.3 ± 4.3	7.2 ± 2.8	9.7 ± 4.1*	63.4 ± 1.9*	1.5 ± 0.2**	0.8 ± 0.2**	0.8 ± 0.1

MCF-7 cells were treated with DDC or FS03EB ± 20 μM zinc or copper for 72 h prior to performing viability analysis. Values displayed are percentage viability and standard error of the mean. Student two-tailed T-tests were conducted between DDC or FS03EB treatment alone and FS03EB or DDC + zinc/copper.

* $p < 0.05$.
** $p < 0.001$.

4. Discussion

Much of the literature surrounding the anti-cancer properties of disulfiram focuses on its interaction with copper, particularly as a disulfiram-copper complex [6,24]. In contrast, the effects of zinc on the drugs toxicity are under-reported, despite knowledge that this metal is dysregulated in breast cancer cells [15]. The aim of this study was to determine the role of intra- and extracellular zinc in the anti-breast cancer properties of disulfiram. We demonstrated that under normal growth conditions the drug is able to selectively kill MCF-7 and BT474 breast cancer cell lines, whilst having no effect at physiologically relevant concentrations on T47D, MDA-MB-231 and the non-cancerous breast epithelial MCF-10A cell line. In disulfiram sensitive cells a biphasic cell viability profile was produced, manifest at concentrations between 5 and 20 μM. The biphasic response has, to varying extents, previously been implied in other studies involving breast [25] and other cancerous cell lines [1], however the underlying cause and its clinical significance remains to be determined. To investigate this further we examined the time dependent toxicity of disulfiram at concentrations within this biphasic range, and demonstrated that the response is due to recovery of initially affected cells. This effect is highly time dependent and may explain why this is frequently reported in the literature at time points greater than 24 h [1,25,26], however to our knowledge, no studies have investigated the sensitivity of cells to disulfiram at shorter (<8 h) time points.

Studies have shown that supplementing media with zinc to increase intracellular levels, presumably through zinc channels, induces oxidative toxicity [14] and inhibits NFκB signaling [27]. Our findings demonstrate that under normal conditions (complete media) disulfiram selectively increases intracellular zinc in breast cancer cells and this may have numerous cellular effects with some leading to toxicity. However, the fact that disulfiram resistant cells (MDA-MB-231) are sensitive to the zinc loading activity of disulfiram suggests a complex link between viability and intracellular zinc. It is also apparent that ionophore-independent mechanisms could contribute to disulfiram cytotoxicity, as 1 μM disulfiram did not show a measurable increase in intracellular zinc levels in MCF-7 cells, however produced >50% decrease in cell viability. Previous studies have demonstrated that disulfiram releases zinc from proteins [28], raising the possibility that the source of this metal which accumulates inside drug treated cells may be from intracellular proteins. However, our studies show that the ability of the drug to increase intracellular zinc is dependent on the availability of extracellular levels of this metal, supporting the hypothesis that the drug is acting as a zinc ionophore. This finding could have far reaching clinical consequences as comparative studies between cancerous and non-cancerous breast tissue from the same patient have shown that the latter has elevated zinc levels [15]. Tumors may therefore provide a more favorable environment for disulfiram to induce zinc-associated toxicity by providing an increased source of zinc for the drug to exert its ionophore action.

The observation that disulfiram is able to increase endo-lysosomal zinc levels is previously unreported, and may have important implications in its selective anti-breast cancer effect. The possibility exists that the cell utilizes certain compartments as an intracellular pool of zinc [29], and we hypothesize that breast cancer cells treated with disulfiram experience a sudden increase in zinc which the cell compartmentalizes to endo-lysosomes in an attempt to buffer the excess. The cytoprotective distribution of excess zinc to lysosomes has recently been reported, however high lysosomal zinc sequestration was also able to induce apoptosis when lysosomal release mechanisms were compromised [30]. Additionally, increased lysosomal storage of zinc has been observed in cancer cells treated with clioquinol, another zinc ionophore [31]. High zinc levels led to lysosomal dysfunction, causing the release of lysosomal enzymes to the cytoplasm and consequently apoptosis. Whether this represents a mechanism underlying disulfiram action here is not yet known but currently under investigation. It has been established that intracellular localization of endo-lysosomal components is integral to their cellular function, for example starvation and altered intracellular pH have been shown to redistribute lysosomes between perinuclear and peripheral regions of the cell [32,33]. Here, we show that disulfiram is able to alter the sub-cellular localization of endo-lysosomal components and by this mechanism may alter their function, providing more evidence that the lysosomal sequestration of zinc may promote lysosomal disruption. Other studies have noted that increased lysosomal zinc is required for inducing autophagy in tamoxifen treated MCF-7 cells [34]. Despite increasing lysosomal zinc levels, we found that disulfiram did not induce autophagy.

It has previously been reported that the addition of copper [5,9,24,25], zinc [9] and other metal ions such as cadmium [35] to the extracellular media increases the potency of disulfiram across a range of cancer cell types. The incubation of copper to remove the biphasic phase has previously been reported [25] but here we demonstrate that zinc supplement has the same effect. Critically the ability of either metal ion to remove the biphasic peak implies that the toxicity of disulfiram at 10 μM is limited by the availability of copper and zinc in the media. When considering the ability of disulfiram to increase intracellular zinc and copper levels, the possibility exists that an increase in extracellular copper and zinc allows disulfiram to transport more of these metal ions into the cell, which accounts for the increased toxicity at this concentration. The low concentrations of either copper and zinc required to increase disulfiram potency, suggest that increasing the availability of either metal ion could be achievable in vivo with oral supplements to enhance the cytotoxic effects of the drug. However, data with the MCF-10A cell line suggests that such supplementation may adversely alter the selectivity of the drug for breast cancer cells and could cause non-specific toxicity.

In vivo disulfiram is rapidly and extensively metabolized in a systemic manner; the first degradation product is DDC and this metabolite is thought to be a major contributor in the clinical effects of the drug [36]. DDC has been shown to have toxicity

against breast cancer cells in vitro and increases intracellular copper in other model systems [7,37]. Additionally, a clinical trial has shown that adjuvant DDC is able to increase survival in patients at high risk of metastatic breast cancer [38]. We show here that DDC, albeit to a lesser extent than disulfiram was also able to increase intracellular zinc levels and this may be a mechanism behind its increased cytotoxicity in the presence of high extracellular levels of these metal ions.

Measurable cytotoxicity $<100 \mu M$, and zinc ionophore activity of the new disulfiram analog, FS03EB, was only observed with zinc supplementation. This provides a direct link between zinc ionophore activity and cytotoxicity, and supports our hypothesis that the observed toxicity profiles for disulfiram, DDC and FS03EB relate to their capacity to increase intracellular zinc. Overall we propose that extracellular zinc levels and ionophore activity should be given higher prominence when discussing the effects of disulfiram on cancer cells.

Acknowledgments

References

[1] Wickstrom M, Danielsson K, Rickardson L, Gullbo J, Nygren P, Isaksson A, et al. Pharmacological profiling of disulfiram using human tumor cell lines and human tumor cells from patients. Biochem Pharmacol 2007;73:25–33.

[2] Marikovsky M, Nevo N, Vadai E, Harris-Cerruti C. Cu/Zn superoxide dismutase plays a role in angiogenesis. Int J Cancer 2002;97:34–41.

[3] Shiah SG, Kao YR, Wu FYH, Wu CW. Inhibition of invasion and angiogenesis by zinc-chelating agent disulfiram. Mol Pharmacol 2003;64:1076–84.

[4] Franklin RB, Costello LC. The important role of the apoptotic effects of zinc in the development of cancers. J Cell Biochem 2009;106:750–7.

[5] Wang F, Zhai S, Liu X, Li L, Wu S, Dou QP, et al. A novel dithiocarbamate analogue with potentially decreased ALDH inhibition has copper-dependent proteasome-inhibitory and apoptosis-inducing activity in human breast cancer cells. Cancer Lett 2011;300:87–95.

[6] Chen D, Cui QC, Yang H, Dou QP. Disulfiram, a clinically used anti-alcoholism drug and copper-binding agent, induces apoptotic cell death in breast cancer cultures and xenografts via inhibition of the proteasome activity. Cancer Res 2006;66:10425–33.

[7] Cvek B, Milacic V, Taraba J, Dou QP. Ni(II), Cu(II), and Zn(II) diethyldithiocarbamate complexes show various activities against the proteasome in breast cancer cells. J Med Chem 2008;51:6256–8.

[8] Guo X, Xu B, Pandey S, Goessl E, Brown J, Armesilla AL, et al. Disulfiram/copper complex inhibiting NF kappa B activity and potentiating cytotoxic effect of gemcitabine on colon and breast cancer cell lines. Cancer Lett 2010;290:104–13.

[9] Brar SS, Grigg C, Wilson KS, Holder WD, Dreau D, Austin C, et al. Disulfiram inhibits activating transcription factor/cyclic AMP-responsive element binding protein and human melanoma growth in a metal-dependent manner in vitro, in mice and in a patient with metastatic disease. Mol Cancer Ther 2004;3:1049–60.

[10] Kagara N, Tanaka N, Noguchi S, Hirano T. Zinc and its transporter ZIP10 are involved in invasive behavior of breast cancer cells. Cancer Sci 2007;98:692–7.

[11] Taylor KM, Vichova P, Jordan N, Hiscox S, Hendley R, Nicholson RI. ZIP7-mediated intracellular zinc transport contributes to aberrant growth factor signaling in antihormone-resistant breast cancer cells. Endocrinology 2008;149:4912–20.

[12] Kim YM, Reed W, Wu WD, Bromberg PA, Graves LM, Samet JM. Zn^{2+}-induced IL-8 expression involves AP-1, JNK, and ERK activities in human airway epithelial cells. Am J Physiol Lung Cell Mol Physiol 2006;290:L1028–35.

[13] Velazquez-Delgado EM, Hardy JA. Zinc-mediated allosteric inhibition of caspase-6. J Biol Chem 2012;287:36000–11.

[14] Bozym RA, Chimienti F, Giblin LJ, Gross GW, Korichneva I, Li Y, et al. Free zinc ions outside a narrow concentration range are toxic to a variety of cells in vitro. Exp Biol Med 2010;235:741–50.

[15] Rizk SL, Skypeck HH. Comparison between concentrations of trace-elements in normal and neoplastic human-breast tissue. Cancer Res 1984;44:5390–4.

[16] Liang F, Tan J, Piao C, Liu Q. Carbon tetrabromide promoted reaction of amines with carbon disulfide: facile and efficient synthesis of thioureas and thiuram disulfides. Synth Stuttg 2008;3579–84.

[17] Brahemi G, Kona FR, Fiasella A, Buac D, Soukupova J, Brancale A, et al. Exploring the structural requirements for inhibition of the ubiquitin E3 ligase breast cancer associated protein 2 (BCA2) as a treatment for breast cancer. J Med Chem 2010;53:2757–65.

[18] Santner SJ, Dawson PJ, Tait L, Soule HD, Eliason J, Mohamed AN, et al. Malignant MCF10CA1 cell lines derived from premalignant human breast epithelial MCF10AT cells. Breast Cancer Res Treat 2001;65:101–10.

[19] Al-Taei S, Penning NA, Simpson JC, Futaki S, Takeuchi T, Nakase I, et al. Intracellular traffic and fate of protein transduction domains HIV-1 TAT peptide and octaarginine. Implications for their utilization as drug delivery vectors. Bioconjug Chem 2006;17:90–100.

[20] Bolte S, Cordelieres FP. A guided tour into subcellular colocalization analysis in light microscopy. J Microsc 2006;224:213–32.

[21] Webber JP, Spary LK, Sanders AJ, Chowdhury R, Jiang WG, Steadman R, et al. Differentiation of tumour-promoting stromal myofibroblasts by cancer exosomes. Oncogene 2014. http://dx.doi.org/10.1038/onc.2013.560.

[22] Geng Y, Kohli L, Klocke BJ, Roth KA. Chloroquine-induced autophagic vacuole accumulation and cell death in glioma cells is p53 independent. Neuro-oncology 2010;12:473–81.

[23] Agarwal RP, McPherson RA, Phillips M. Rapid degradation of disulfiram by serum-albumin. Res Commun Chem Pathol Pharmacol 1983;42:293–310.

[24] Liu P, Brown S, Goktug T, Channathodiyil P, Kannappan V, Hugnot JP, et al. Cytotoxic effect of disulfiram/copper on human glioblastoma cell lines and ALDH-positive cancer-stem-like cells. Br J Cancer 2012;107:1488–97.

[25] Yip NC, Fombon IS, Liu P, Brown S, Kannappan V, Armesilla AL, et al. Disulfiram modulated ROS-MAPK and NF kappa B pathways and targeted breast cancer cells with cancer stem cell-like properties. Br J Cancer 2011;104:1564–74.

[26] Rae C, Tesson M, Babich JW, Boyd M, Sorensen A, Mairs RJ. The role of copper in disulfiram-induced toxicity and radiosensitization of cancer cells. J Nucl Med 2013;54:953–60.

[27] Uzzo RG, Crispen PL, Golovine K, Makhov P, Horwitz EM, Kolenko VM. Diverse effects of zinc on NF-kappa B and AP-1 transcription factors: implications for prostate cancer progression. Carcinogenesis 2006;27:1980–90.

[28] Hao Q, Maret W. Aldehydes release zinc from proteins. A pathway from oxidative stress/lipid peroxidation to cellular functions of zinc. FASEB J 2006;273:4300–10.

[29] Colvin RA, Bush AI, Volitakis I, Fontaine CP, Thomas D, Kikuchi K, et al. Insights into Zn^{2+} homeostasis in neurons from experimental and modeling studies. Am J Physiol Cell Physiol 2008;294:C726–42.

[30] Kukic I, Kelleher SL, Kiselyov K. Zinc efflux through lysosomal exocytosis prevents zinc-induced toxicity. J Cell Sci 2014;127:3094–103.

[31] Yu H, Zhou Y, Lind SE, Ding W-Q. Clioquinol targets zinc to lysosomes in human cancer cells. Biochem J 2009;417:133–9.

[32] Malek M, Guillaumot P, Huber AL, Lebeau J, Petrilli V, Kfoury A, et al. LAMTOR1 depletion induces p53-dependent apoptosis via aberrant lysosomal activation. Cell Death Dis 2012;3:e300.

[33] Korolchuk VI, Saiki S, Lichtenberg M, Siddiqi FH, Roberts EA, Imarisio S, et al. Lysosomal positioning coordinates cellular nutrient responses. Nat Cell Biol 2011;13:453–60.

[34] Hwang JJ, Kim HN, Kim J, Cho D-H, Kim MJ, Kim Y-S, et al. Zinc(II) ion mediates tamoxifen-induced autophagy and cell death in MCF-7 breast cancer cell line. Biometals 2010;23:997–1013.

[35] Li L, Yang H, Chen D, Cui C, Dou QP. Disulfiram promotes the conversion of carcinogenic cadmium to a proteasome inhibitor with pro-apoptotic activity in human cancer cells. Toxicol Appl Pharmacol 2008;229:206–14.

[36] Nagendra SN, Shetty KT, Subhash MN, Guru SC. Role of glutathione-reductase system in disulfiram conversion to diethyldithiocarbamate. Life Sci 1991;49:23–8.

[37] Tonkin EG, Valentine HL, Milatovic DM, Valentine WM. N,N-diethyldithiocarbamate produces copper accumulation, lipid peroxidation, and myelin injury in rat peripheral nerve. Toxicol Sci 2004;81:160–71.

[38] Dufour P, Lang JM, Giron C, Duclos B, Haehnel P, Jaeck D, et al. Sodium ditiocarb as adjuvant immunotherapy for high-risk breast-cancer – a randomized study. Biotherapy 1993;6:9–12.